National University of Ireland, Galway
Ollscoil na hÉireann, Gaillimh

Optimisation of High Frequency Transformer Design with Arbitrary Current and Voltage Waveforms

John Gerard Breslin
B.E., National University of Ireland, Galway

Submitted in Fulfilment of the Requirements
for the Degree of Ph.D.

at the

National University of Ireland

April 2002

Department of Electronic Engineering,
Faculty of Engineering,
National University of Ireland, Galway

Supervisor: Prof. W.G. Hurley

TABLE OF CONTENTS

TABLE OF FIGURES

TABLE OF TABLES

ACKNOWLEDGMENTS

With sincere thanks and gratitude to Professor Ger Hurley, for his unending help, patience and guidance during the period of this work.

In grateful appreciation of funding, support and friendship from the Power Electronics Research Centre and PEI Technologies; I hope that the research carried out during this scholarship was mutually beneficial.

Thanks to friends and colleagues at the Department of Electronic Engineering at the National University of Ireland, Galway for spurring me on. I would also like to thank Professor Javier Uceda and Professor Ger Lyons for serving as my oral examination committee.

With love to my parents – this is for you. Finally, special thanks to Josephine who gave me love, support, and the motivation to finish this thesis.

Typeset in Microsoft Word™ using the Georgia, Verdana and Symbol true type fonts. Figures created using CorelDraw™. Data Flow Diagrams created using Visible Analyst Workbench™.

DECLARATION

I, the undersigned, declare that this thesis is entirely my own work and that it has not been submitted previously, either in part or as a whole, at NUI, Galway or any other university to be examined for a postgraduate degree. The research embodied in this thesis was carried out under the supervision of Prof. W.G. Hurley during the period 1994 to 2001. The library of NUI, Galway has my full consent to lend or copy this thesis so that it may be used by the staff and students of NUI, Galway and other universities for research purposes.

John Breslin

ABSTRACT

Switching circuits, operating at high frequencies, have led to considerable reductions in the size of magnetic components and power supplies. Non-sinusoidal voltage and current waveforms and high frequency skin and proximity effects contribute to transformer losses. Traditionally, transformer design has been based on sinusoidal voltage and current waveforms operating at low frequencies. The physical and electrical properties of the transformer form the basis of a new design methodology while taking full account of the type of current and voltage waveforms and high frequency effects. Core selection is based on the optimum throughput of energy with minimum losses. The optimum core is found directly from the transformer specifications: frequency, power output and temperature rise. The methodology is suitable for use in a computer application in conjunction with a database of core and winding materials.

High frequency AC loss effects must then be taken into account. The AC losses due to non-sinusoidal current waveforms have traditionally been found by calculating the losses at harmonic frequencies when the Fourier coefficients are known. An optimised foil or layer thickness in a winding may be found by applying the Fourier analysis over a range of thickness values. New methodologies have been developed to find the optimum foil or layer thickness for any periodic waveshape, without the need for calculation of AC losses at harmonic frequencies. The first methodology requires the RMS value of the current waveform and the RMS value of its derivative. The second methodology makes use of regression analysis and some harmonic summations.

NOMENCLATURE

A_c	Physical cross-sectional area of magnetic circuit.
A_m	Effective cross-sectional area of magnetic circuit.
A_p	Window area, $W_a \times$ cross-sectional area, A_c.
A_t	Surface area of wound transformer.
A_w	Bare wire conduction area.
B_m	Maximum flux density.
B_o	Optimum flux density.
B_{sat}	Saturation flux density.
d	Thickness of foil or layer.
D	Duty cycle.
f	Frequency in Hz.
h	Coefficient of heat transfer by convection.
I_{dc}	Average value of current.
I_n	RMS value of the nth harmonic.
I_{rms}	RMS value of the current waveform.
I'_{rms}	RMS value of the derivative of the current waveform.
J	Current density.
k_a, k_c, k_w	Dimensionless constants.
k_f	Core stacking factor, A_m/A_c.
k_p	Power factor.
k_{p_n}	Ratio of the AC resistance to DC resistance at n^{th} harmonic frequency.
k_s	Skin effect factor, R_{ac}/R_{dc}.
k_u	Window utilisation factor, W_c/W_a.
k_x	Proximity effect factor, R_{ac}'/R_{dc}
K	Waveform factor.
K_c	Core material parameter.
K_o, K_t, K_j	1.54×10^{-7}, 53.9×10^3, 81.4×10^6.
m	Mass of core.
M	Number of turns per layer.
n	Number of windings (Chapter 3).
n	Harmonic number (Chapter 4).
N	Number of turns (Chapter 3).
N	Number of harmonics (Chapter 4).

P	Number of layers.
P_{cu}	Copper losses.
P_{fe}	Iron losses.
P, P_{tot}	Total losses.
r_o	Radius of bare wire in wire-wound winding.
R_{ac}	AC resistance of a winding.
R_δ	DC resistance of a winding with thickness δ_o.
R_{dc}	DC resistance of a winding.
R_{eff}	Effective AC resistance of a winding carrying arbitrary current waveform.
R_θ	Thermal resistance.
t_r	Rise time (0 - 100%).
T	Period of the current waveform.
T_{max}	Maximum operating temperature.
$<v>$	Average value of voltage over time τ.
V_c	Volume of core.
V_w	Volume of windings.
VA	Volts-ampere rating of winding.
W_a	Window area.
W_c	Electrical conduction area.
α, β	Core material constants.
δ	Skin depth.
δ_o	$\sqrt{\dfrac{2}{\omega\mu_o\sigma}}$, skin depth at fundamental frequency, $\omega = 2\pi f$.
δ_n	Skin depth at the nth harmonic frequency.
Δ	d/δ.
ΔT	Temperature rise.
ρ_c	Mass density of core material.
ρ_w	Electrical resistivity of winding at T_{max}.
η	Porosity factor.
Ψ	$(5p^2 - 1)/15$ for RMS values method, $(2p^2 - 2)/b + 3/a$ for regression analysis method.
τ	Time for flux to go from zero to B_m.
μ_r	Relative permeability of core material.
μ_o	Permeability of free space, $4\pi \times 10^{-7}$ H/m.

Chapter 1

TECHNICAL REVIEW AND OBJECTIVES

1.1   Transformer Design Review

The unrelenting movement to higher density integrated circuits continues unabated. Reductions in the size of magnetic components have been achieved by operating at higher frequencies, mainly in switching circuits. The primary magnetic component in these circuits is the transformer, which must transfer the input voltage waveform of the primary windings to the output or secondary windings.

Traditionally, transformer design has been based on power frequency transformers with sinusoidal excitation. Empirical rules have evolved which generally lead to conservative designs. However, non-sinusoidal excitation at high frequencies introduces new design issues: skin and proximity effects in windings, and increased eddy current and hysteresis losses in cores.

The basic design methodology for transformers at both low and high frequencies involves the area product method by McLyman [72]. This method is most conveniently applied to cores for which McLyman has defined specially developed design parameters called "K factors". However, while an acceptable design results from this methodology, the design is not optimal either in terms of the losses or the size.

The word "optimise" has been used so frequently in the last few years to mean such a variety of conditions that its popular meaning appears to be "something that the author has developed". The accurate meaning is "to achieve the best or most satisfactory balance among several factors". Since we are using mathematical methods to evaluate magnetic

components, we will define optimise as "to seek a maximum or minimum for some parameter or weighted combination of parameters".

The basis for an optimised design is the assumption that the winding losses are approximately equal to the core losses [80]. However, in a typical power frequency transformer the ratio may be as high as 5:1. This is due to the fact that the flux density is limited by its saturation value. At the high end of the frequency scale, the transformer may be operating with a maximum flux density well below its saturation value to achieve an optimum design.

Judd and Kressler [53] reviewed a number of existing design procedures for transformer design. The principle objectives of these methods were to minimise the physical size or mass of a transformer (and hence the cost) and to maximise efficiency (by minimising losses). Some of the methods involved fixing the electrical and magnetic parameters of a design and adjusting the transformer geometry to minimise an objective such as weight, volume, cost or losses. Others worked in reverse, by keeping the core geometry fixed, electrical and magnetic parameters were chosen to minimise the desired objective.

Judd and Kressler opted for the second choice in their proposed mathematical optimisation method. This was chosen because at that time cores were only available in discrete sizes, and even if there were a wider choice of cores, a designer would ultimately have to choose suitable values for the electrical and magnetic parameters. However, while this approach may have been justified when there was only a limited range of manufactured cores available, it is now easier to get a much closer match to a theoretical core size calculated after an optimum flux density has been found.

Consultation of maximum VA capability, optimum flux density, optimum current density, and efficiency versus frequency curves is required in [53] to determine the flux and current densities that will maximise VA output for a particular set of circuit specifications on an assumed core structure. These densities are also constrained so that they do not exceed specified values. While the saturation limit on the value of flux is acknowledged,

Judd and Kressler do not specify exactly what current density is required if the flux density is set to its saturation value, stating that it should be constrained to some value less than the maximum current density.

Undeland et al. [102] presented a design procedure for small, naturally cooled, high-frequency (over 10 kHz) inductors and transformers. Their method, based on a two-winding transformer with sinusoidal excitation, is an extension of the conventional area product approach that includes thermal considerations based on the maximum device temperature and physical height of the device. The winding losses and core losses are inherently assumed to be equal and are given in per unit volume, and the transformer volume (core plus winding) is required to find the power dissipation from the total loss formula.

However, while core selection is made at the beginning of the design, the winding geometry is selected after power loss densities are calculated, and this means that the actual losses can only be evaluated at the end. Skin and proximity effects are also neglected in this method, and optimising the component size and shape cannot be included as part of the design function. The Undeland method also requires that the designer consult tables to find the temperature rise in cores. However, the procedure for deriving the information in these tables is not outlined if, for example, one wanted to use a different type of core than those listed.

Petkov [86] proposed a method to optimise transformers for minimum eddy current and hysteresis losses as a function of temperature rise. He discusses the mechanism by which the combined losses in the windings and core must be dissipated through the surface of the wound transformer.

1.2   High Frequency Effects Review

The increased switching frequencies in magnetic components have resulted in renewed attention to the problem of AC losses in transformer windings.

As a consequence of Lenz's law, a high-frequency AC current flowing in a conductor induces a field that will oppose the penetration of the current into the conductor. The result is a diffusion-type current density profile, where the current distribution decreases exponentially from the edge of the conductor. Current is effectively restricted to an annular shape with a thickness equal to the typical diffusion length. This thickness is called the "skin depth", δ, and the effect is known as the "skin effect" since the current bunches towards the 'skin' of a conductor.

A similar effect occurs when a time-varying flux density field, B, in a conductor is not caused by the current flowing in the conductor, but by a current flowing in another conductor nearby. This is called the "proximity effect". As a result of these two effects, a conductor section will have a non-uniform current density. This will yield a higher effective resistance (and therefore more ohmic losses) than for DC currents.

One of the problems with the McLyman [72] transformer design method is that it uses the DC resistances of the winding wires to design the transformer winding, without making provisions for skin and proximity effects. Switching and resonant circuits in power supplies have non-sinusoidal current waveforms, and the harmonics in these waveforms give rise to the additional skin and proximity effect AC losses. It is important that these effects are included in a design as they can cause the power losses in transformer windings to increase dramatically with frequency. For example, the winding loss at 1 MHz can sometimes be one hundred times that at DC.

The AC resistance effects due to sinusoidal currents in multilayered windings were treated by Bennett and Larson [5]. They stated that eddy current losses in any layer can be thought of as the result of the superposition of skin effect and multilayer effect (or proximity effect) distributions.

Bennett and Larson presented a one-dimensional plate approximation to the field solution for a cylindrical winding, and derived a formula for a sinusoidal current resistance factor which yields an optimum normalised

winding thickness in "skin depth units" for each layer in a layered winding. To the author's knowledge, this was the first time that the concept of a normalised effective resistance and optimum thickness was used, and it was an important development. They define the optimum thickness of a layer as that which occurs when the effective resistance of the layer is at a minimum.

However, Bennett and Larson's method involves choosing an optimum thickness for layer 1, then another optimum thickness for layer 2, and so on for each layer in the multilayered winding. The end result of this "layer-by-layer" approach is that each of the layers in the optimally designed winding may have a different thickness.

Having to choose a different thickness for each layer as proposed by Bennett and Larson (and later on by [85]) can be somewhat tedious, and it is also impractical and expensive for production purposes.

Bennett and Larson also presented several curves for the current density and magnetic field intensity within the conductors.

Dowell [20] expanded Bennett and Larson's work so that it could be specifically applied to modern transformers. Dowell's work used a one-dimensional solution of the fields in the winding space to analytically determine the effect of eddy currents on the transformer windings. Although the problem of magnetic field and eddy current distribution is two-dimensional, one-dimensional analysis gives sufficient accuracy for the practical design of transformers.

For a two-winding transformer under sinusoidal current excitation, Dowell demonstrates how to compute the effective AC resistance and winding leakage inductance associated with each winding from the transformer geometry. However, this method applies only to what Dowell terms "winding portions". When examining the low frequency magnetic field intensity diagram, a winding portion is defined as a part of a winding which extends in either direction along the axis of winding height from a position of zero field intensity to the first peak (positive or negative) of magnetic field intensity. The leakage inductance and winding resistance

are calculated individually for each winding portion, and these are then summed for each winding in the transformer.

Dowell's expressions for the ratios of the AC to DC winding resistances and leakage inductances are given as functions of conductor height, a complex waveform frequency variable and the number of layers in the winding portion. He also presents graphs illustrating the variation of the two ratios with these parameters.

Dowell classifies windings as either optimal or non-optimal. Optimal windings have all zeros of magnetomotive force (MMF) either in the regions between layers or exactly in the middle of a layer; non-optimal satisfy neither condition. Dowell derives results for the optimal case only, stating that the windings of a transformer should always be arranged in the optimal configuration in order to reduce leakage inductance.

Dowell also assumes that the transformer is wound with circular conductors where each layer fills the breadth of the winding space. His results are easily extended to foil or layered windings, despite not being explicitly mentioned in his paper.

Dowell's formula has been found to reliably predict the increased resistance in cylindrical windings where the foil or layer thickness is less than 10% of the radius of curvature. However, his work does not feature any method for minimising the winding losses.

Jongsma [51] adapted Dowell's analysis to provide an algorithm for designing transformer windings with minimum losses. The paper begins with a theoretical development of the necessary equations, along with an overview of issues related to the design of minimum loss transformers. The lowest loss winding combination to fit into a particular window height is found using a design chart method.

Jongsma's analysis focuses mainly on round wire windings with sinusoidal excitation in two-winding transformers, but other winding types are also discussed. Optimal winding configurations as defined by Dowell are also assumed. Jongsma later showed [52] that partial layers, those that do not

extend the full window breadth, can also be accommodated as an extension to Dowell's method.

The next most significant paper in this area was produced by Perry [85]. In this, he deals with multilayer windings with variable layer thickness, and like Dowell, Perry's one-dimensional model refers to sinusoidal waveforms. In a significant departure from Dowell, Perry's analysis refers to winding layers instead of winding portions, and he also places a large emphasis on the minimisation of winding losses. While Perry only relates his method to air core inductors, it can also be applied to multiwinding transformers.

Perry's analysis is based on field solutions for the current density distribution in layers of a cylindrical current sheet of infinite length, and is performed in both the cylindrical and rectangular coordinate systems. He uses the results he obtains for the current density in each winding layer to calculate the power dissipation per unit area of a layer based on its height, the frequency, and magnetic field boundary conditions for the layer. Perry then utilises these high frequency power dissipation predictions to determine the normalised optimum thickness for each layer of the inductor winding. This critical conductor thickness occurs at the point of minimum power dissipation. As the optimum thickness becomes smaller with increasing layer number, he shows that the corresponding minimum power dissipation also becomes more sharply defined.

Like Bennett and Larson, Perry begins with a layer-by-layer approach, whereby each of the layers in the optimally designed winding will have a different thickness. However, he also introduces a constant layer thickness design method whereby a single thickness conductor is chosen for every layer. He states that the layer-by-layer approach yields 12% less loss for windings with more than three layers, but even so it is still slightly impractical and expensive for most manufacturing purposes.

With the advent of switch mode power supplies, attention switched to non-sinusoidal current waveforms. These currents were decomposed into Fourier components; the harmonic components are orthogonal so that the

total loss is equal to the sum of the losses calculated by Dowell's formula for the amplitude and frequency of each harmonic in turn.

Venkatraman [112] derived expressions and plotted curves for both the effective resistance and leakage inductance of a duty cycle varying pulsed or rectangular waveform typical of a forward converter transformer winding. Venkatraman uses Fourier analysis to determine the harmonic content of the rectangular waveform, and then sums the losses for each harmonic. Venkatraman presents graphical plots from which total loss values can be estimated for varying layer thickness. These plots are given for five fixed duty cycle values only.

Venkatraman noted that the eddy current losses due to rectangular wave currents were considerably different from losses due to the sinusoidal waveforms considered by the other authors thus far, even for rectangular and sinusoidal waveforms with similar RMS values. Using experimental data, he also showed that the eddy current losses for waveforms with the same frequency and RMS current varied greatly with both the waveform duty cycle and the number of winding layers.

Since Venkatraman's work is largely based on Dowell's analysis, most of Dowell's restrictions hold, including the use of the optimal winding configuration. Unlike Dowell, Venkatraman shows that the analysis also applies to foil windings.

However, Venkatraman only considers rectangular-type wave currents, ignoring the other types of current waveforms encountered in modern switch mode power converters. Venkatraman also does not go into detail about how to minimise the winding conductor losses.

Venkatraman mentioned that while he found Litz wire design to be effective under sinusoidal conditions, its effectiveness considerably decreased when using rectangular waveforms at high frequencies. Carsten [8] confirms this result, noting that while some modest reductions in loss were possible with Litz wire, if not used with care the losses could substantially increase.

Carsten [8] focuses on the calculation and minimisation of eddy current losses due to skin and proximity effects. He extends the Venkatraman pulsed waveform analysis to include square waveforms, which are encountered in full bridge converters, and triangular waveforms, which occur in filter chokes. He deals with pulsed, triangular and square waveshapes with either 50% or 100% duty cycle.

Carsten uses the effective winding resistance to calculate a normalised effective resistance factor. This factor is the ratio of the effective resistance of the winding for the non-sinusoidal current waveform to the DC resistance of a similar winding with a height of one skin depth at the fundamental frequency. Since the DC resistance is normalised, no recalculations are required to compare losses for different size wires.

Carsten presents graphical results for the normalised effective resistance factor for various non-sinusoidal current waveforms with varying rise times, duty cycles and numbers of layers. The optimum winding thickness is then read from the point where the resistance factor, proportional to winding loss, is a minimum. Two unverified formulas are given to estimate the optimum thicknesses for pulsed and square waveforms with fast rise and fall times.

Vandelac and Ziogas [104] took the most important aspects from Dowell and Perry and extended these aspects into a single unified analysis which can be applied to various topologies, including flyback converters. The paper also incorporates the Fourier analysis method from Venkatraman, and the normalisation to DC resistance of a conductor with a height of one skin depth which was introduced by Bennett and Larson and later utilised by Carsten. They show that a transformer field distribution, as described by Dowell using winding portions, can be viewed as a combination of Perry's layer-by-layer field solutions.

Vandelac and Ziogas state that there are times when non-optimal winding transformers (as classified by Dowell) are necessary, perhaps due to physical design constraints. The advantage of their method is that it is based on Perry's infinite length current sheet analysis and is not limited to Dowell's optimal windings. Copper losses can therefore be calculated

for a larger variety of winding arrangements once the winding excitation conditions and winding structure geometry are known.

Vandelac and Ziogas also introduced an alternative graphical approach based on low frequency magnetomotive force (MMF) diagrams to determine losses due to non-sinusoidal winding currents. This "field harmonic analysis" technique utilises field intensity diagrams corresponding to each of the conducting time intervals for a switch mode circuit. These diagrams can be combined to yield a periodic non-sinusoidal waveform representing the magnetic field between each of the winding layers.

Snelling [97] provides a useful reference on soft ferrite materials and their applications. He also gives an approximation to Dowell's AC resistance factor in his discussions on power transformers and the properties of windings.

Ferreira [26], [29] tackled the problem of analysing eddy currents in Litz wire and thin foils in flat structures. He contrived the decoupling of skin and proximity effect losses by recognition of orthogonality between the two, a significant advance in eddy current analysis.

Dowell's original formula has also been adopted by several other authors and utilised in many applications such as planar magnetics by Kassakian and Schlecht [54] and Sullivan and Sanders [99], matrix transformers by Williams et al. [117], toroidal inductors by Cheng and Evans [10], distributed air-gaps by Evans and Chew [23], and slot bound conductors by Hanselman and Peake [43].

Sullivan [101] also recently introduced the "square field derivative" method for calculating eddy current proximity effect losses in round and Litz wire windings of transformers or inductors. He states that his method is not intended to address foil windings.

1.3   Research Hypothesis

One major disadvantage with traditional design methodologies is that they do not take into account the unequal core to winding losses ratio encountered in some topologies, assuming optimal efficiency must occur when the core and winding losses are set to be equal. This is not always the case, and indeed at some frequencies the winding losses must often be set much greater than the core losses so as to avoid core saturation. Methodologies are usually developed to design transformers for applications operating at either high or low frequencies, but not both.

Both [80] and [102] assume that the losses are equal, and their methods will sometimes yield a flux saturated design. The suitability of [102] at high frequencies is questionable since neither skin nor proximity effects are taken into account. [53] is also targeted towards power transformers operating at low frequencies (under 10 kHz) and involves reading values from pre-requisite design curves; the latter does not lend itself well to an automated transformer design process.

A new mathematical optimisation methodology for designing transformers with either high frequency switching-type waveforms or conventional low frequency sinusoids is necessary. Once the physical properties of the core and winding are established in the methodology, detailed thermal and electrical models can then be evaluated. The method should also be inclusive of high frequency skin and proximity effects encountered in designs for switching power supply circuits.

Our approach will be to optimise a figure of merit in a magnetic design. We will derive a general expression for the total transformer loss; this is the parameter in our design that we wish to optimise (by minimising it). Minimum losses will yield maximum energy transfer efficiency. Usually the functions we deal with have a single minimum, so the decision-making process will be clear-cut. We recognise that the factors to which we wish to optimise our design must be included in the initial specification. When the lowest loss for a given set of specifications is the object, then a

mathematical statement of the losses must be formulated as a function of frequency, flux density, etc.

By designing a winding at an optimum thickness value corresponding to the lowest possible resistance value, the losses are minimised thus producing more efficient operation and a monetary saving through an initially correct design.

While a number of authors have shown how to optimise a winding design by plotting losses for a range of winding thickness values and designing at the minimum loss thickness, no formulas have been published for the actual specific thickness value required for minimum winding losses for any waveform (except for pure sine waves and rough approximations for square waves). Such a formula would reduce the number of calculations from hundreds to a single formula that might even be used on paper to find the optimum thickness.

The traditional graphical approach involves the calculation of the AC resistance for each thickness in a range of X thickness values where the summation of Y harmonic calculations is required for each of the X thicknesses. For example, if X = 100 and Y = 13, over 1300 calculations would be required. Each resistance value would be graphed against its corresponding thickness value, and the optimum thickness could then be read from the point of minimum resistance on the plotted curve. The problem with this method, apart from the obvious time consuming plotting issue (constructing these graphs 20 years ago would have taken weeks with a programmable calculator), was that reading the exact optimum thickness value from such a graph could often prove inaccurate if the curve minimum was not sharply defined.

More recently, the resistance-thickness combinations would instead be stored in a 2-by-X matrix, and the minimum resistance value in this matrix could then be found through some mathematical iteration. The time required to perform this analysis has dropped from 20 minutes to 2 minutes in the past five years, but even so it cannot be incorporated in a transformer design methodology without significant time delays if either a winding or waveshape parameter is changed.

The advantage of a single formula is that even if the above method only took less than a minute to yield an optimum thickness value, the single calculation of the formula could be done in less time and also by hand on paper, and it could easily be implemented as part of a spreadsheet solution without the need for matrix minimisation routines. The graphical or mathematical approaches must be repeated from scratch for any change in waveform duty cycle/rise time or number of winding layers, whereas it is much easier to insert new values into a formula.

Approximate formulas for the optimum thickness of a layered or foil winding have been given by [5] (for sinusoids using the layer-by-layer design method), [85] (for sinusoids using both the layer-by-layer and constant layer methods), and [8] (unverified formulas for pulsed and square waveforms with fast rise and fall times); however accurate formulas for rectified and bipolar sinusoidal, rectangular or triangular current waveshapes have not been published previously. Limited sets of graphical results are available for rectangular current waveshapes with fixed duty cycles [8], [112] (for example, 50% or 100% duty cycle). One of the contributions of this thesis is the extension of the previous work for rectangular waveforms with fixed duty cycles to sinusoidal, rectangular and triangular waveforms with variable duty cycles.

From the above proposals it was noted that both the transformer design methodology and the winding loss minimisation technique could be incorporated in a software system for high frequency magnetic design. An added advantage is that such a system could incorporate both core and winding data previously obtained by consulting catalogues. Not only would such a system save on the time previously required either designing by hand or working with spreadsheets and consulting catalogues, but the accuracy of designs could be improved by avoiding errors commonly encountered when writing on paper or when reading from design graphs.

The motivations for this research can therefore be summarised as follows:

- To extend the applicability of a revised transformer design methodology to both low and high frequencies and any current or voltage waveforms.

- To automate such a robust metholodology using computing methods.
- To improve upon previous work on optimum winding thickness formulas and to extend the analysis to other waveforms with variable duty cycles.
- By improving on formulas for the optimum thickness, to make automation of this calculation easier for incorporation into the proposed automated design metholodogy.

1.4   Objectives

As the trend to increase the switching frequencies of power converters continues, better tools need to be developed to evaluate the high-frequency effects on the induced losses in magnetic components. Many design techniques, often coinciding with CAD software development, make assumptions regarding choices of magnetic flux densities and current densities without regard to thermal consequences [30], [11]. Density formulas that take component temperature rise into account are therefore an essential part of a design system.

Another problem with traditional design methodologies is that they do not take the unequal core to winding losses ratio mentioned earlier into account. This needs to be incorporated into a new design algorithm and implemented in a computer design package.

We have also mentioned with regards to proximity effect losses that the ideal situation is to design at the point of minimum AC winding resistance in order to minimise these losses, and traditionally to do this one had to plot computationally demanding graphs and then read values from these graphs. Separate graphs were required for each type of waveform or for variations of the same waveform. For example, the graph plotted for a rectified sinusoidal waveform is very different from that for a square waveform. To incorporate such a method in a computer algorithm, quick formulas for the optimum design point are necessary.

The objectives of this thesis are outlined below:

- To produce a robust method which leads to optimised core selection and winding selection from the design specifications: power output, frequency and temperature rise.
- To find the critical design frequency, above which the losses can be minimised by selecting a flux density which is less than the saturation flux density, and below which the limitation is that the flux density cannot be greater than the saturation value corresponding to the core material.
- To provide a unified approach that gives exact AC resistance formulas for sinusoidal, rectangular and triangular waveforms, with variable duty cycles.
- To derive optimum thickness formulas for non-sinusoidal current waveforms in order to avoid the protracted plotting and reading from graphs.
- To develop a new design package for the Windows environment to implement the techniques proposed here for the first time.

In Chapter 2, we will present an elegant derivation of Dowell's AC resistance formula from Maxwell's equations that makes use of the Poynting vector. This will form the basis for our analysis of the optimum thickness of layer in a multilayered transformer winding later on.

Chapter 3 will demonstrate a methodology that yields optimised core selection and winding selection from a set of design specifications. This method is expressed in flow chart form for use in a software package. Examples from rectifiers and PWM switched mode power supplies are given. Particular emphasis is placed on modern circuits where non-sinusoidal waveforms are encountered.

Chapter 4 will deal with proximity losses and their effect on the design of magnetic components at high frequencies. General rules are established for optimising the design of windings under various excitation and operating conditions; in particular, the waveform types encountered in switching circuits are treated in detail. The traditional method for

calculating the optimum winding layer thickness will be compared with two new methods. Comparison results will be analysed.

Chapter 5 presents a high level overview of a computer aided design program that implements the combined methodologies of Chapter 3 and Chapter 4. This includes a description of the software design processes used and the main aspects that had to be incorporated into the system.

Finally, in Chapter 6, we will present sets of experimental results to verify the efficiency of design examples from Chapter 3. We will show the existence of the optimum design point, and give loss plots for various cores and winding arrangements.

Chapter 2

MAXWELL'S EQUATIONS

2.1   Introduction

I
n order to determine the effect of AC eddy currents on the losses in a shell-type winding, a one-dimensional field solution for the transformer winding space can be performed if some simple assumptions are made.

Firstly, we assume that the curvature of the transformer winding can be neglected when calculating the field distribution across a single layer in a multilayered winding. This holds true if the layer height is less than 10% of the radius of curvature. Secondly, we assume that the breadth of a layer in a cylindrical winding is much greater than the height (radial thickness) of the layer.

The combination of these assumptions means that we can model the winding as a set of infinite current sheets that have the same height as the equivalent winding layers, but that extend to infinity in the directions of breadth and depth. We can thus reduce our analysis to a one-dimensional case.

One-dimensional solutions of the fields in a shell winding configuration have been performed by both Dowell and Perry. However, this chapter will present a complete solution uniquely solved using the Poynting vector.

Beginning with Maxwell's equations, we will derive equations for the power dissipated from the inside and from the outside of a winding layer. The asymptotic expansion of the Bessel functions in the power dissipation expressions leads to Dowell's formula for the AC resistance of a coil with p layers, under sinusoidal excitation.
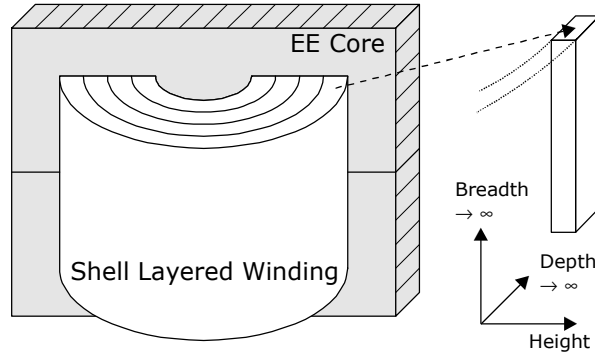
Figure 2.1. Typical transformer with shell winding configuration.

2.2   AC Resistance in a Cylindrical Conductor

For a magnetoquasistatic system, Maxwell's equations in a linear homogeneous isotropic medium take the following form:

$$\nabla \times \mathbf{H} = \sigma \mathbf{E}, \tag{2.1}$$

$$\nabla \times \mathbf{E} = -\mu_o \frac{\partial \mathbf{H}}{\partial t}. \tag{2.2}$$
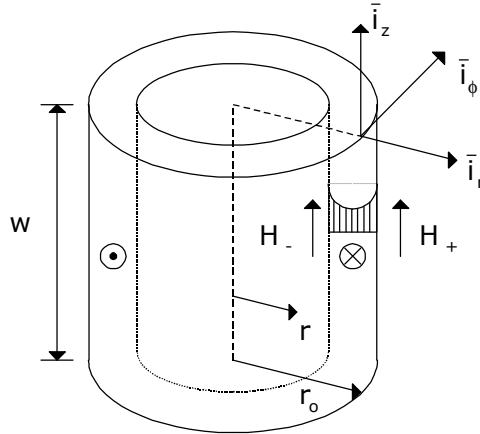
Figure 2.2. Conducting cylinder.

The annular cylindrical conducting layer shown in Figure 2.2 carries a sinusoidal current $i_\phi(t) = I_\phi e^{j\omega t}$. The conductivity of the conducting medium is σ and the physical dimensions are shown in Figure 2.2. H_- and H_+ are the magnetic fields parallel to the inside and outside surfaces of

the cylinder, respectively. We shall see later that H_- and H_+ are independent of z.

Assuming cylindrical symmetry, the various components of the electric field intensity **E** and the magnetic field intensity **H** inside the cylinder, in cylindrical co-ordinates (r, ϕ, z), satisfy the following identities:

$$E_r = 0, \ E_z = 0, \ \frac{\partial E_\phi}{\partial z} = 0 \,, \tag{2.3}$$

$$H_r = 0, H_\phi = 0, \frac{\partial H_z}{\partial \phi} = 0 \,. \tag{2.4}$$

The two Maxwell's equations above then reduce to

$$-\frac{\partial H_z}{\partial r} = \sigma E_\phi \,, \tag{2.5}$$

$$\frac{1}{r}\frac{\partial}{\partial r}(rE_\phi) = -j\omega\mu_o H_z \,. \tag{2.6}$$

Since **H** has only a z-component and **E** has only a ϕ-component, we drop the subscripts without ambiguity. Furthermore, the electric and magnetic field intensities are divergence-free and so it follows that E and H are functions of r only. Substituting the expression for E given by (2.5) into (2.6) then yields the ordinary differential equation

$$\frac{d^2H}{dr^2} + \frac{1}{r}\frac{dH}{dr} - j\omega\mu_o\sigma H = 0 \,. \tag{2.7}$$

This is a *modified Bessel's equation* [71]. The general solution is

$$H(r) = AI_o(mr) + BK_o(mr) \,. \tag{2.8}$$

where I_o and K_o are modified Bessel functions of the first and second kind, of order o, and $m = \sqrt{j\omega\mu_o\sigma}$, so that the argument of I_o and K_o is complex. We take the principal value of the square root, that is $\sqrt{j} = e^{j\pi/4}$.

The coefficients A and B are determined from the boundary conditions and will be complex. It is worth noting that the solutions of (2.7) are in fact combinations of the Kelvin functions with real argument, *viz*

$$\mathrm{ber}(r\sqrt{\omega\mu_o\sigma}),\, \mathrm{bei}(r\sqrt{\omega\mu_o\sigma}),\, \mathrm{ker}(r\sqrt{\omega\mu_o\sigma}),\, \mathrm{kei}(r\sqrt{\omega\mu_o\sigma}),$$

though in our analysis we find it more convenient to use the modified Bessel functions with complex argument.
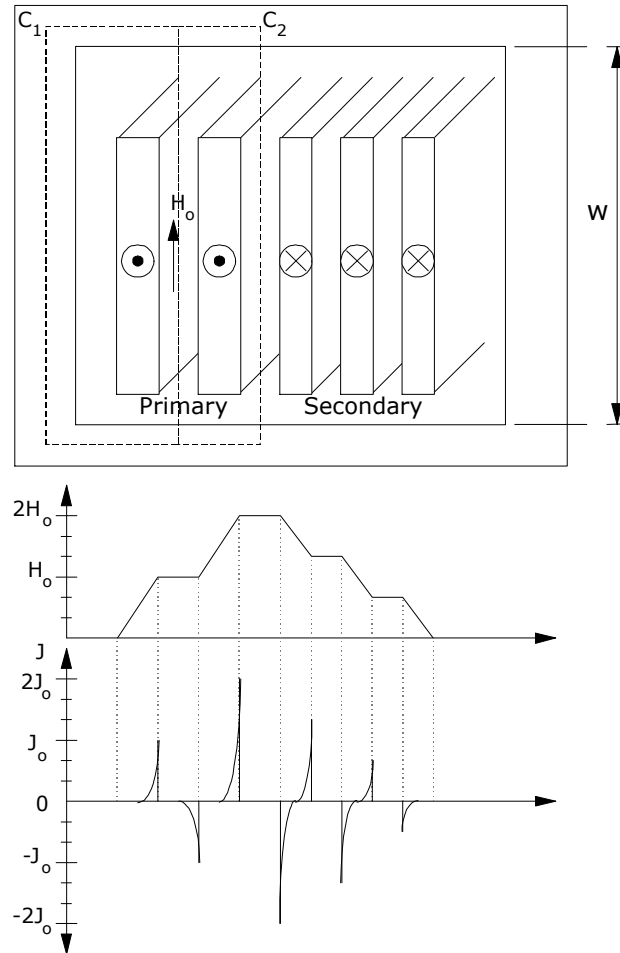
Figure 2.3. Transformer cross section with associated MMF diagram and current density at high frequency.

A typical transformer cross-section is shown in Figure 2.3 with associated MMF diagram and current density distribution for a two-turn primary and a three-turn secondary winding. The physical dimensions of a generalised n^{th} layer are shown in Figure 2.4 (the innermost layer is counted as layer 1). We assume that the magnetic material in the core is ideal ($\mu_r \rightarrow \infty$, $\sigma \rightarrow 0$) so that the magnetic field intensity goes to zero inside the core. We also assume that the dimension w is much greater than the radial dimensions so that end effects are taken as negligible.
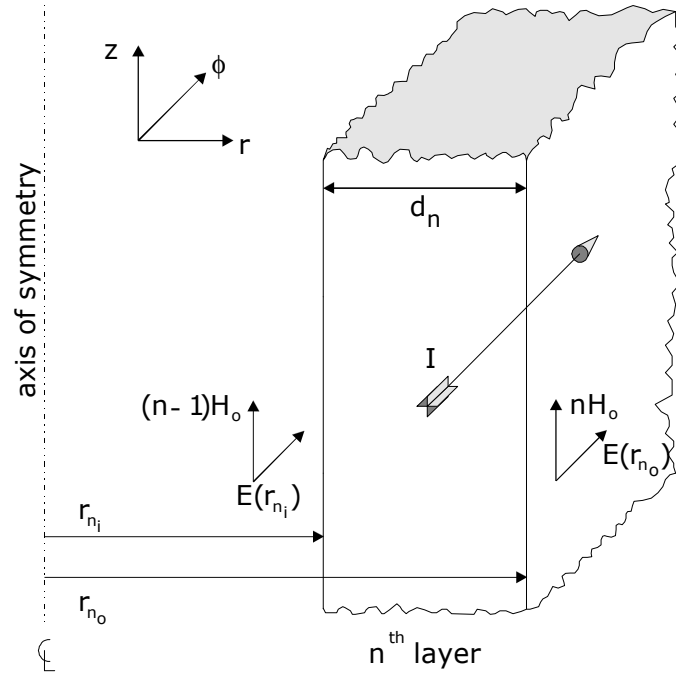
Figure 2.4. Generalised n^{th} layer.

Invoking Ampere's law for the closed loops C_1 and C_2 (Figure 2.3) in a high permeability core ($\mu_r \gg 1$),

$$H_o = \frac{NI}{w},$$

(2.9)

where N is the number of turns in layer n, each carrying constant current I. n here refers to the layer number. Applying the inner and outer boundary conditions for layer n, i.e. $H(r_{n_i}) = (n-1)H_o$ and $H(r_{n_o}) = nH_o$ to the general solution (2.8), we obtain the coefficients

$$A = \frac{[(nK_0(mr_{n_i}) - (n-1)K_0(mr_{n_o})]H_o}{I_0(mr_{n_o})K_0(mr_{n_i}) - K_0(mr_{n_o})I_0(mr_{n_i})},$$ (2.10)

$$B = \frac{[(-nI_0(mr_{n_i}) + (n-1)I_0(mr_{n_o})]H_o}{I_0(mr_{n_o})K_0(mr_{n_i}) - K_0(mr_{n_o})I_0(mr_{n_i})}.$$ (2.11)

The corresponding value of E(r) is found from (2.5), that is

$$E(r) = -\frac{1}{\sigma}\frac{dH(r)}{dr}$$
$$= -\frac{1}{\sigma}\left[A\frac{d}{dr}I_0(mr) + B\frac{d}{dr}K_0(mr)\right].$$ (2.12)

Using the modified Bessel function identities

$$\frac{d}{dr}I_x(mr) = mI_x^{'}(mr),$$ (2.13)

$$mrI_x^{'}(mr) = xI_x(mr) + mrI_{x+1}(mr),$$ (2.14)

we can express the first part of (2.12) as

$$\frac{d}{dr}I_0(mr) = mI_0^{'}(mr) = \frac{o}{r}\cancel{I_0}(mr) + mI_1(mr)$$
$$= mI_1(mr)$$ (2.15)

Similarly, using the identities

$$\frac{d}{dr}K_x(mr) = mK_x^{'}(mr),$$ (2.16)

$$mrK_x^{'}(mr) = xK_x(mr) - mrK_{x+1}(mr),$$ (2.17)

we can express the second half of (2.12) as

$$\frac{d}{dr}K_o(mr) = mK_o{}'(mr) = \frac{o}{r}K_o(mr) - mK_1(mr)$$
$$= -mK_1(mr)$$
(2.18)

The electric field intensity is then given by

$$E(r) = -\frac{m}{\sigma}[AI_1(mr) - BK_1(mr)].$$
(2.19)

The Poynting vector $\mathbf{E} \times \mathbf{H}$ [26] represents the energy flux density per unit area crossing the surface per unit time. In the cylindrical coordinate system illustrated in Figure 2.2, the power per unit area into the cylinder is given by $\mathbf{E} \times \mathbf{H}$ on the inside surface and $-\mathbf{E} \times \mathbf{H}$ on the outside surface. Since $\mathbf{E}$ and $\mathbf{H}$ are orthogonal, the magnitude of the Poynting vector is simply the product $E(r)H(r)$ and its direction is radially outwards.

The power per unit length (around the core) of the inside surface of layer n is

$$P_{n_i} = E(r_{n_i})H(r_{n_i})w$$
$$= -\frac{m}{\sigma}(n-1)H_o w[AI_1(mr_{n_i}) - BK_1(mr_{n_i})]$$
(2.20)

A and B are given by (2.10) and (2.11) respectively, and H_o is given by (2.9) so

$$P_{n_i} = \frac{N^2 I^2 m}{\sigma w \psi}\{(n-1)^2[I_o(mr_{n_o})K_1(mr_{n_i}) +$$
$$K_o(mr_{n_o})I_1(mr_{n_i})] - n(n-1)[I_o(mr_{n_i})K_1(mr_{n_i}) +,$$
$$K_o(mr_{n_i})I_1(mr_{n_i})]\}$$
(2.21)

where we define:

$$\psi = I_o(mr_{n_o})K_o(mr_{n_i}) - K_o(mr_{n_o})I_o(mr_{n_i}).$$
(2.22)

In a similar fashion, we find the power per unit length (around the core) of the outside surface of layer n is

$$P_{n_o} = -E(r_{n_o})H(r_{n_o})w$$

$$= \frac{m}{\sigma}nH_o w[AI_1(mr_{n_o}) - BK_1(mr_{n_o})]$$

$$= \frac{N^2I^2m}{\sigma w\psi}\{n^2[I_0(mr_{n_i})K_1(mr_{n_o}) + K_0(mr_{n_i})I_1(mr_{n_o})]$$

$$-n(n-1)[I_0(mr_{n_o})K_1(mr_{n_o}) + K_0(mr_{n_o})I_1(mr_{n_o})]\} \qquad . \ (2.23)$$

The minus sign is required to find the power into the outer surface.

We now assume that mr >> 1 and use the leading terms in the asymptotic approximations for the modified Bessel functions in (2.21) and (2.23) (noting for purposes of validity $\arg(mr) = \frac{\pi}{4} < \frac{\pi}{2}$):

$$I_0(mr) \approx \frac{1}{\sqrt{2\pi mr}}e^{mr}, \quad I_1(mr) \approx \frac{1}{\sqrt{2\pi mr}}e^{mr},$$

$$K_0(mr) \approx \sqrt{\frac{\pi}{2mr}}e^{-mr}, \quad K_1(mr) \approx \sqrt{\frac{\pi}{2mr}}e^{-mr}. \qquad (2.24)$$

Substituting these into (2.21) and rearranging,

$$P_{n_i} = \frac{N^2I^2m}{\sigma w}\left\{\begin{array}{l}(n-1)^2\dfrac{I_0(mr_{n_o})K_1(mr_{n_i}) + K_0(mr_{n_o})I_1(mr_{n_i})}{I_0(mr_{n_o})K_0(mr_{n_i}) - K_0(mr_{n_o})I_0(mr_{n_i})} \\[2mm] -n(n-1)\dfrac{I_0(mr_{n_i})K_1(mr_{n_i}) + K_0(mr_{n_i})I_1(mr_{n_i})}{I_0(mr_{n_o})K_0(mr_{n_i}) - K_0(mr_{n_o})I_0(mr_{n_i})}\end{array}\right\}$$

$$= \frac{N^2I^2m}{\sigma w}\left\{\begin{array}{l}(n-1)^2\dfrac{\dfrac{1}{2m\sqrt{r_{n_o}}\sqrt{r_{n_i}}}e^{md_n} + \dfrac{1}{2m\sqrt{r_{n_o}}\sqrt{r_{n_i}}}e^{-md_n}}{\dfrac{1}{2m\sqrt{r_{n_o}}\sqrt{r_{n_i}}}e^{md_n} - \dfrac{1}{2m\sqrt{r_{n_o}}\sqrt{r_{n_i}}}e^{-md_n}} \\[6mm] -n(n-1)\dfrac{\dfrac{1}{2m\sqrt{r_{n_i}}\sqrt{r_{n_i}}} + \dfrac{1}{2m\sqrt{r_{n_i}}\sqrt{r_{n_i}}}}{\dfrac{1}{2m\sqrt{r_{n_o}}\sqrt{r_{n_i}}}e^{md_n} - \dfrac{1}{2m\sqrt{r_{n_o}}\sqrt{r_{n_i}}}e^{-md_n}}\end{array}\right\}$$

$$= \frac{N^2I^2m}{\sigma w}\left\{(n-1)^2\frac{(e^{md_n})^2 + 1}{(e^{md_n})^2 - 1} - n(n-1)\frac{\sqrt{r_{n_i}}\sqrt{r_{n_o}}}{\sqrt{r_{n_i}}\sqrt{r_{n_i}}}\frac{2}{e^{md_n} - e^{-md_n}}\right\}$$

$$= \frac{N^2I^2m}{\sigma w}\left\{(n-1)^2\mathrm{Coth}(md_n) - n(n-1)\frac{\sqrt{r_{n_o}}}{\sqrt{r_{n_i}}}\frac{1}{\mathrm{Sinh}(md_n)}\right\} \qquad (2.25)$$

,

where $d_n \equiv r_{n_o} - r_{n_i}$ is the thickness of layer n.

Substituting the (2.24) expressions into (2.23) and rearranging,

$$P_{n_o} = \frac{N^2 I^2 m}{\sigma w} \left\{ n^2 \frac{I_0(mr_{n_i})K_1(mr_{n_o}) + K_0(mr_{n_i})I_1(mr_{n_o})}{I_0(mr_{n_o})K_0(mr_{n_i}) - K_0(mr_{n_o})I_0(mr_{n_i})} - n(n-1) \frac{I_0(mr_{n_o})K_1(mr_{n_o}) + K_0(mr_{n_o})I_1(mr_{n_o})}{I_0(mr_{n_o})K_0(mr_{n_i}) - K_0(mr_{n_o})I_0(mr_{n_i})} \right\}$$

$$= \frac{N^2 I^2 m}{\sigma w} \left\{ n^2 \frac{\dfrac{1}{2m\sqrt{r_{n_i}}\sqrt{r_{n_{oi}}}}e^{-md_n} + \dfrac{1}{2m\sqrt{r_{n_i}}\sqrt{r_{n_o}}}e^{md_n}}{\dfrac{1}{2m\sqrt{r_{n_o}}\sqrt{r_{n_i}}}e^{md_n} - \dfrac{1}{2m\sqrt{r_{n_o}}\sqrt{r_{n_i}}}e^{-md_n}} - n(n-1) \frac{\dfrac{1}{2m\sqrt{r_{n_o}}\sqrt{r_{n_o}}} + \dfrac{1}{2m\sqrt{r_{n_o}}\sqrt{r_{n_o}}}}{\dfrac{1}{2m\sqrt{r_{n_o}}\sqrt{r_{n_i}}}e^{md_n} - \dfrac{1}{2m\sqrt{r_{n_o}}\sqrt{r_{n_i}}}e^{-md_n}} \right\}$$

$$= \frac{N^2 I^2 m}{\sigma w} \left\{ n^2 \frac{(e^{md_n})^2 + 1}{(e^{md_n})^2 - 1} - n(n-1) \frac{\sqrt{r_{n_i}}}{\sqrt{r_{n_o}}} \frac{\sqrt{r_{n_o}}}{\sqrt{r_{n_o}}} \frac{2}{e^{md_n} - e^{-md_n}} \right\}$$

$$= \frac{N^2 I^2 m}{\sigma w} \left\{ n^2 \text{Coth}(md_n) - n(n-1) \frac{\sqrt{r_{n_i}}}{\sqrt{r_{n_o}}} \frac{1}{\text{Sinh}(md_n)} \right\} \qquad (2.26)$$

.

Combining (2.25) and (2.26) yields the total power dissipation for layer n as

$$P_{n_i} + P_{n_o} = \frac{N^2 I^2 m}{\sigma w} \left[(2n^2 - 2n + 1)\text{Coth}(md_n) - \frac{n^2 - n}{\text{Sinh}(md_n)} \left(\sqrt{\frac{r_{n_o}}{r_{n_i}}} + \sqrt{\frac{r_{n_i}}{r_{n_o}}} \right) \right]. \qquad (2.27)$$

This result was obtained from the Poynting vector for the complex field intensities, so the real part represents the actual power dissipation.

We now assume that each layer has constant thickness d, so that $d_n = d$ (independent of n). Furthermore we assume that $d \ll r_{n_i}$. Then, using the Taylor expansion with $r_{n_o} = d + r_{n_i}$ (or $\varepsilon = d/r_{n_i}$),

$$\sqrt{1+\varepsilon} + \frac{1}{\sqrt{1+\varepsilon}} = 2 + \frac{\varepsilon^2}{4} + O(\varepsilon^3), \qquad (2.28)$$

and it follows that if $\varepsilon < 10\%$, the error incurred by approximating the sum of the square roots in (2.27) by 2 is in the order of 0.1%.

Also, the part of (2.27) in square brackets can be reduced as follows:

$$
\begin{aligned}
[\ldots] &= (2n^2 - 2n + 1)\mathrm{Coth}(md) - \frac{2(n^2 - n)}{\mathrm{Sinh}(md)} \\
&= \mathrm{Coth}(md) + 2(n^2 - n)\left(\mathrm{Coth}(md) - \frac{1}{\mathrm{Sinh}(md)}\right) \\
&= \mathrm{Coth}(md) + 2(n^2 - n)\left(\frac{\mathrm{Cosh}(md) - 1}{\mathrm{Sinh}(md)}\right) \\
&= \mathrm{Coth}(md) + 2(n^2 - n)\mathrm{Tanh}\left(\frac{md}{2}\right)
\end{aligned} \tag{2.29}
$$

Then, the total power dissipation in layer n becomes

$$
\begin{aligned}
\Re(P_{n_i} + P_{n_o}) &\approx \Re\left(\frac{N^2 I^2 m}{\sigma w}\left[\begin{array}{c}(2n^2 - 2n + 1)\mathrm{Coth}(md) \\ -\dfrac{2(n^2 - n)}{\mathrm{Sinh}(md)}\end{array}\right]\right), \\
&= \Re\left(\frac{N^2 I^2 m}{\sigma w}\left[\begin{array}{c}\mathrm{Coth}(md) \\ + 2(n^2 - n)\mathrm{Tanh}\left(\dfrac{md}{2}\right)\end{array}\right]\right)
\end{aligned} \tag{2.30}
$$

$$
P_{dc} = R_{dc}(NI)^2 = \frac{(NI)^2}{\sigma w d}. \tag{2.31}
$$

The AC resistance factor is the ratio of the AC resistance to the DC resistance:

$$
\begin{aligned}
\frac{R_{ac}}{R_{dc}} &= \frac{\Re(P_{n_i} + P_{n_o})}{P_{dc}} \\
&= \Re\left(md\left[\mathrm{Coth}(md) + 2(n^2 - n)\mathrm{Tanh}\left(\frac{md}{2}\right)\right]\right).
\end{aligned} \tag{2.32}
$$

Finally, the general result for p layers is

$$\frac{R_{ac}}{R_{dc}} = \frac{\Re \sum_{n=1}^{p} (P_{n_i} + P_{n_o})}{\sum_{n=1}^{p} P_{dc}}$$

$$= \frac{1}{p} \Re \left(md \sum_{n=1}^{p} \left[Coth(md) + 2(n^2 - n) Tanh\left(\frac{md}{2}\right) \right] \right), \qquad (2.33)$$

$$= \Re \left(md \left[Coth(md) + \frac{2(p^2 - 1)}{3} Tanh\left(\frac{md}{2}\right) \right] \right)$$

since

$$\sum_{n=1}^{p} 2(n^2 - n) = \frac{2(p^3 - p)}{3}. \qquad (2.34)$$

From the definition of m,

$$md = \sqrt{\omega \mu_o \sigma} \left(\frac{1+j}{\sqrt{2}}\right) d = (1+j)\Delta, \qquad (2.35)$$

where $\Delta = d/\delta_o$ and δ_o is the skin depth.
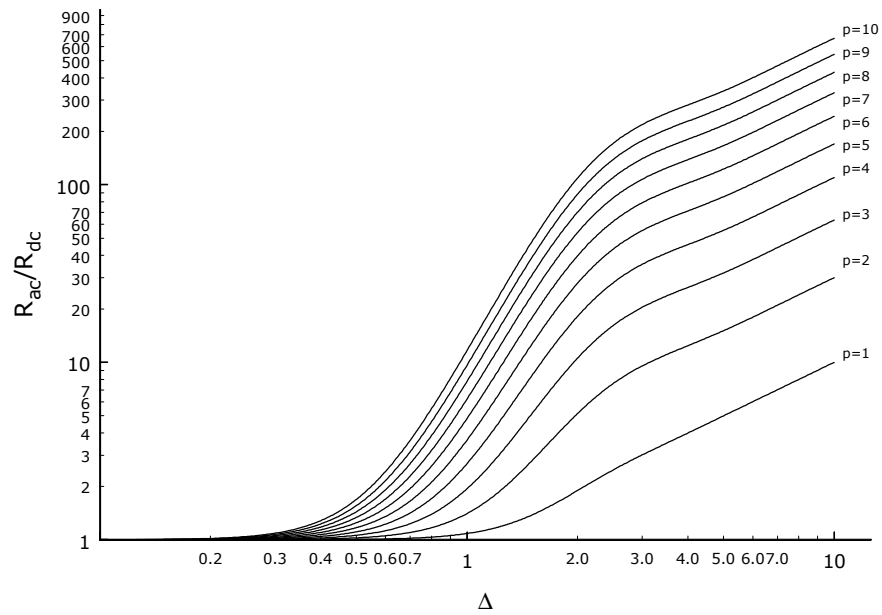
Figure 2.5. AC to DC resistance ratio versus normalised thickness.

The AC resistance factor for p layers (as plotted in Figure 2.5) is then

$$\frac{R_{ac}}{R_{dc}} = \Re\left(\Delta(1+j)\left[\text{Coth}(\Delta(1+j)) + \frac{2(p^2-1)}{3}\text{Tanh}(\frac{\Delta}{2}(1+j))\right]\right). \quad (2.36)$$

The real and imaginary parts of the complex expression $\Delta(1+j)[\text{Coth}(\Delta(1+j)) + (2(p^2-1)/3)\text{Tanh}(\Delta(1+j)/2)]$ are equivalent in magnitude and are both given by

$$\Delta\frac{\text{Sinh}\Delta\text{Cosh}\Delta + \text{Sin}\Delta\text{Cos}\Delta}{\text{Sinh}^2(\Delta) + \text{Sin}^2(\Delta)}$$
$$+ \Delta\frac{2(p^2-1)}{3}\frac{\text{Sinh}\left(\frac{1}{2}\Delta\right)\text{Cosh}\left(\frac{1}{2}\Delta\right) - \text{Sin}\left(\frac{1}{2}\Delta\right)\text{Cos}\left(\frac{1}{2}\Delta\right)}{\text{Sinh}^2\left(\frac{1}{2}\Delta\right) + \text{Cos}^2\left(\frac{1}{2}\Delta\right)}. \quad (2.37)$$

With some simplification, we can rewrite the AC resistance factor as [85]

$$\frac{R_{ac}}{R_{dc}} = \Delta\left(\frac{2\left(p^2+\frac{1}{2}\right)}{3}\left[\frac{\text{Sinh}2\Delta + \text{Sin}2\Delta}{\text{Cosh}2\Delta - \text{Cos}2\Delta}\right] - \frac{4(p^2-1)}{3}\left[\frac{\text{Cosh}\Delta\text{Sin}\Delta + \text{Cos}\Delta\text{Sinh}\Delta}{\text{Cosh}2\Delta - \text{Cos}2\Delta}\right]\right), \quad (2.38)$$

or $\quad\dfrac{R_{ac}}{R_{dc}} = \Delta\left[\dfrac{\text{Sinh}2\Delta + \text{Sin}2\Delta}{\text{Cosh}2\Delta - \text{Cos}2\Delta} + \dfrac{2(p^2-1)}{3}\dfrac{\text{Sinh}\Delta - \text{Sin}\Delta}{\text{Cosh}\Delta + \text{Cos}\Delta}\right].$ $\quad$ (2.39)

This is Dowell's formula.

2.3   Summary

A unique one-dimensional field solution of the diffusion equation for shell-type transformer windings is detailed in this chapter. A layered winding is modelled as a set of infinite current sheets. Each sheet has the

same height as the corresponding winding layer, but extends to infinity in the directions of breadth and depth.

Starting from Maxwell's equations for a linear homogeneous isotropic medium, the end result is the derivation of Dowell's formula for the AC resistance of a layered winding. This formula is the basis for our analysis in Chapter 4.

The derivation in this chapter is particularly elegant for its use of the Poynting vector, a measure of the energy flux density per unit area crossing the surface of a conducting layer per unit time.

Chapter 3

OPTIMISING CORE AND WINDING DESIGN

3.1   Introduction

T he purpose of a transformer is to transfer energy from the input to the output through the magnetic field. The aim of a magnetic designer is to make this energy transfer as efficient as possible for a given application. The amount of energy transferred in a transformer is determined by the operating temperature, the frequency and the flux density.

Our approach will be to derive a general expression for the total transformer loss; this is the parameter in our design that we wish to optimise (minimise). Minimum losses will yield maximum energy transfer efficiency. We use known design relationships to reduce the number of variables so that the loss expression can be given in terms of one variable parameter and other fixed parameters. We then take the first derivative of that expression with respect to our variable parameter and set it equal to zero. This will locate a point of zero slope on our loss expression, which is a minimum point.

It will be shown that for any transformer core there is a critical frequency. Above this critical frequency, the total transformer losses can be optimised by selecting a certain flux density value which must also be less than the saturation flux density. Below the critical frequency, the throughput of energy is restricted by the limitation that the flux density cannot be greater than the saturation value for the core material in question.

Failure mechanisms in magnetic components are almost always due to excessive temperature rise which means that the design must satisfy electrical and thermal criteria. A robust design must be based on sound

knowledge of circuit analysis, electromagnetism and heat transfer. We will show that familiar transformer equations, based on sinusoidal excitation conditions, may be restated to include the types of non-sinusoidal waveforms found in switching circuits. The analysis is based on fundamental principles. Approximations based on dimensional analysis are introduced to simplify calculations without compromising the generality of the design methodology or the underlying fundamental principles; a proliferation of design factors is avoided to retain clarity.

The primary objective of this chapter is to establish a robust method which leads to optimised core selection and winding selection from the design specifications: power output, frequency and temperature rise. Once the physical properties of the core and winding are established, detailed thermal and electrical models can be evaluated. High frequency effects can also be taken into account.

Three design examples will be presented at the end of this chapter to illustrate the new design methodology: a rectifier circuit, a forward converter and a push-pull converter. Each example illustrates an important aspect of the design methodology while underlining the generality of the approach. The optimisation of core and winding losses is discussed in detail. Further optimisation of the winding design at high frequencies is described.

3.2 Minimising the Losses

3.2.1 The Voltage Equation

Faraday's law of electromagnetic induction states that the electromotive force (EMF) induced in an electric circuit is equal to the rate of change of flux linking that circuit. Lenz's law shows that the polarity of the induced EMF is found by noting that the induced EMF opposes the flux creating it.

A combination of these laws can be used to relate the impressed voltage on a winding, v, to the rate of change of flux density, B:

$$v = -\frac{d\lambda}{dt} = -N\frac{d\phi}{dt},$$
$$= -NA_m \frac{dB}{dt}$$

(3.1)

where λ is the total flux linkage, ϕ is the flux linked by each turn, N is the number of turns, and A_m is the effective cross-sectional area of the magnetic core. In the case of laminated and tape-wound cores, A_m is less than the physical cross-sectional area, A_c, due to interlamination space and insulation.
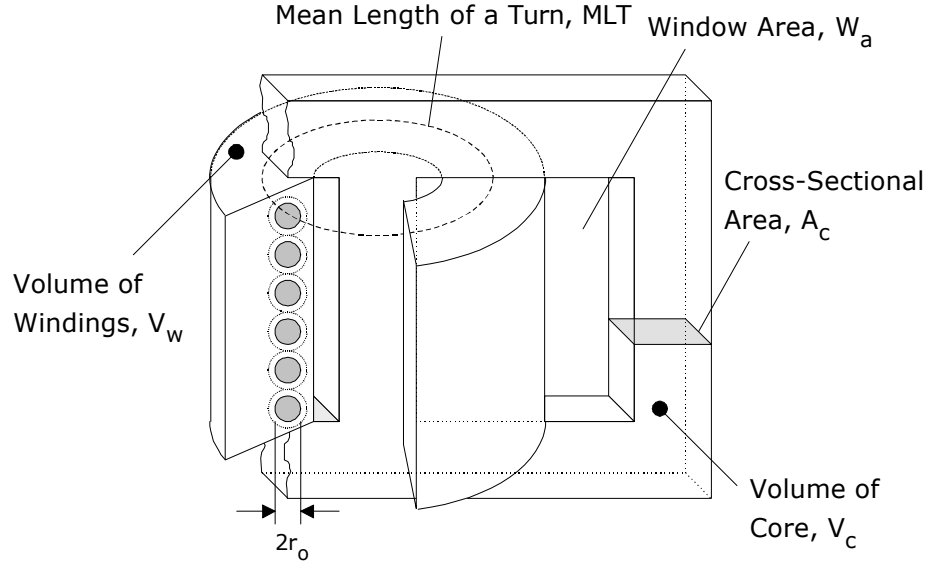
Figure 3.1. Typical layout of a transformer.

The layout of a typical transformer is shown in Figure 3.1 and the physical parameters are illustrated. The two areas, A_m and A_c, are related by the core stacking factor, k_f ($A_m = k_f A_c$). Typically, k_f is 0.95 for laminated cores.

Integrating (3.1) between the point where the flux density is zero and its maximum value (B_m) gives

$$\langle v \rangle = \frac{1}{\tau} \int_{o}^{\tau} v \, dt = \frac{1}{\tau} NA_m \int_{o}^{\tau} \frac{dB}{dt} \, dt = \frac{1}{\tau} NA_m B \big|_{t=\tau} \, ,$$

$$= \frac{1}{\tau} NB_m A_m$$

(3.2)

where <v> is the average value of the impressed voltage of a winding in the time period τ.

The form factor, k, is defined as the ratio of the RMS value of the applied voltage waveform to <v>:

$$k = \frac{V_{rms}}{\langle v \rangle} \, .$$

(3.3)

Combining (3.2) and (3.3) yields

$$V_{rms} = k \langle v \rangle = \frac{k}{\tau} N B_m A_m$$

$$= \frac{k}{\tau/T} f N B_m A_m \, ,$$

$$= K f N B_m A_m$$

(3.4)

where $f = \frac{1}{T}$ is the frequency of v, and T is the period of v.

Equation (3.4) is the classic equation for voltage in a transformer winding, with K, the waveform factor, defined by k, τ and T. Evidently, for a sinusoidal waveform,

$$K = \frac{k}{\tau/T} = \frac{V_{rms}/\langle v \rangle}{\tau/T}$$

$$= \frac{\left(V_{pk}/\sqrt{2}\right)/\left(2V_{pk}/\pi\right)}{(T/4)/T} = 4.44 \, ,$$

and for a square waveform,

$$K = \frac{k}{\tau/T} = \frac{V_{rms}/\langle v \rangle}{\tau/T}$$
$$= \frac{(V_{pk})/(V_{pk})}{(T/4)/T} = 4$$

The calculation of K for the push-pull converter is illustrated in section 3.4.1.

3.2.2   The Power Equation

Equation (3.4) applies to each winding of the transformer. Taking the sum of the VA products for each winding of an n winding transformer,

$$\sum VA = \sum_{i=1}^{n} V_i I_i$$
$$= K f B_m A_m \sum_{i=1}^{n} N_i I_i \qquad (3.5)$$

where N_i is the number of turns in the ith winding carrying current I_i. The current density in each winding is $J_i = I_i/A_{wi}$, where A_{wi} is the wire conduction area of the ith winding.
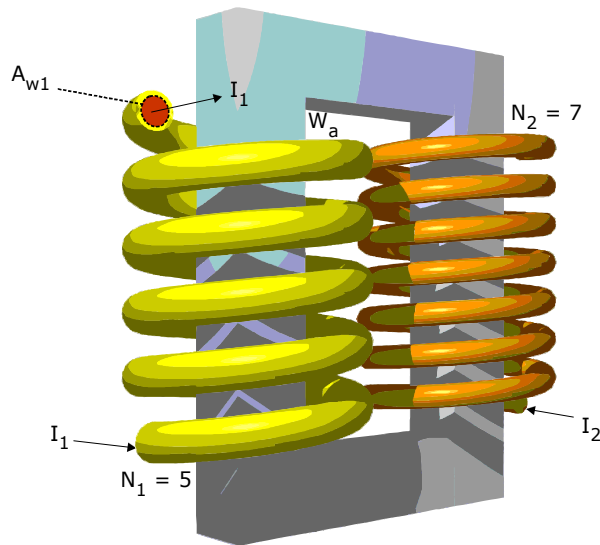
Figure 3.2. Transformer with n = 2 windings.

Figure 3.2 shows a two-winding transformer with different bare wire sizes for the insulated primary and secondary windings (high frequency effects would lead to a further reduction in the wire conduction areas A_{wi} shown).

The total area occupied by conducting windings is equal to the sum of the products of the number of turns with the wire conduction area for each of n windings. If we set a window utilisation factor, k_u, equal to the ratio of the total winding conduction area, W_c, to the total core window area, W_a, then we can say that

$$\sum_{i=1}^{n} N_i A_{wi} = k_u W_a. \qquad (3.6)$$

A cross-section of the Figure 3.2 transformer is given in Figure 3.3 showing the total winding conduction area.
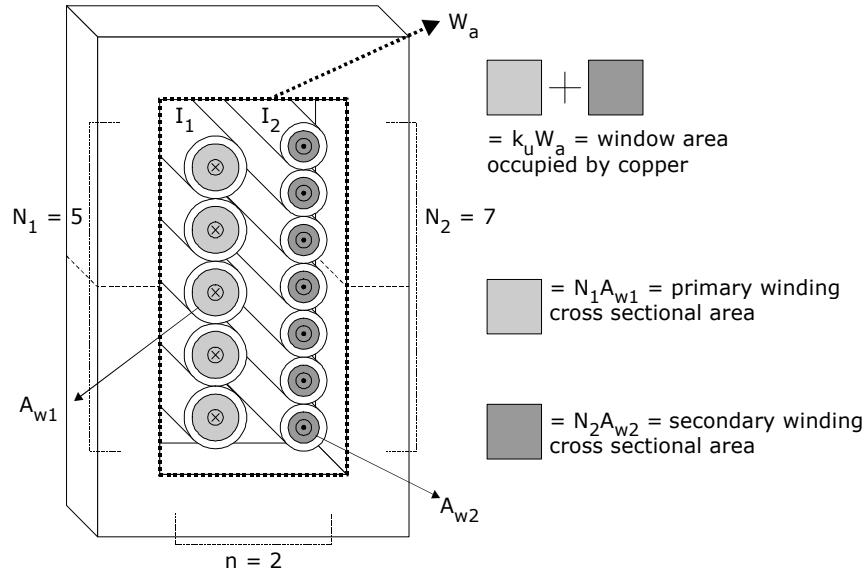
Figure 3.3. Section of previous transformer showing window utilisation.

Normally the wire area and the conduction area are taken as the area of bare conductor, however, we can account for skin effect in a conductor and proximity effect between conductors by noting that the increase in resistance due to these effects is manifested by reducing the effective conduction area. The skin effect factor, k_s, is the increase in resistance (or decrease in conduction area) due to skin effect, and likewise for the proximity effect factor, k_x:

$$k_s = \frac{R_{ac}}{R_{dc}}, \quad k_x = \frac{R_{ac}'}{R_{dc}}. \tag{3.7}$$

We can combine the scaling factors k_b (ratio of the total bare wire area to the total window area, accounting for winding insulation and interwinding spaces) and $1/k_s k_x$ (ratio of the total conduction area to the total bare wire area, accounting for skin and proximity effects) into the single factor k_u:

$$k_u = \frac{k_b}{k_s k_x}, \quad W_c = k_u W_a. \tag{3.8}$$

Typically, $k_b = 0.7$, $k_s = 1.3$ and $k_x = 1.3$ giving $k_u = 0.4$.

Combining (3.5) and (3.6) with the same current density, J, in each winding, the sum of the VA products is thus given by

$$\begin{aligned}
\sum VA &= KfB_m A_m \sum_{i=1}^{n} N_i J_i A_{wi} \\
&= KfB_m A_m J \sum_{i=1}^{n} N_i A_{wi} \quad . \\
&= KfB_m k_f A_c J k_u W_a
\end{aligned} \tag{3.9}$$

The product $A_c W_a$ appearing in (3.9) is an indication of the core size, and is designated A_p for area product. Rewriting (3.9) yields

$$\sum VA = KfB_m J k_f k_u A_p. \tag{3.10}$$

3.2.3 Winding Losses

The total resistive losses for all the windings are

$$P_{cu} = \sum RI^2 = \rho_w \sum_{i=1}^{n} \frac{N_i MLT (J A_{wi})^2}{A_{wi}}, \tag{3.11}$$

where ρ_w is the resistivity of the winding conductor, and MLT is the mean length of a turn in the windings. Incorporating the definition of window utilisation factor, k_u (3.8), and noting that the volume of the windings is $V_w = MLT \times W_a$ and the conduction volume is $V_w \times k_u$, then

$$
\begin{aligned}
P_{cu} &= \rho_w J^2 MLT \sum_{i=1}^{n} N_i A_{wi} \\
&= \rho_w J^2 MLT \times W_a k_u \quad . \\
&= \rho_w V_w k_u J^2
\end{aligned}
\tag{3.12}
$$

3.2.4 Core Losses

In general, core losses are given in W/kg so that for a core of mass m (m = $\rho_c V_c$),

$$
P_{fe} = m K_c f^{\alpha} B_m{}^{\beta} = \rho_c V_c K_c f^{\alpha} B_m{}^{\beta} ,
\tag{3.13}
$$

where ρ_c is the mass density of the core material, V_c is the core volume, and K_c, α, β are constants which can be established from manufacturer's data.

Typical values for different magnetic materials are given in Table 3.1 below.

MATERIAL	SAT. FLUX DENS. (T)	RELATIVE PERMEABILITY	RESISTIVITY (Ω-m)	ρ_c (kg/m³)	K_c	α	β
Powder Iron	2.1	4500	0.01	6000	0.1 $\rightarrow$ 10	1.1	2.0
Si-Steel	2.0	10000	0.01	7650	0.5×10^{-3}	1.7	1.9
Ni-Mo Alloy	0.8	250	0.01	13000	5.0×10^{-3}	1.2	2.2
Ferrite (Mn-Zn)	0.4	2000	1.0	4800	1.9×10^{-3}	1.24	2.0
Ferrite (Ni-Zn)	0.3	400	1000	4800	2.5×10^{-5}	1.6	2.3
Metallic Glass	1.6	10000	10^{10}	60000			
Values are typical and are given for comparison purposes only. Specific values should be established from manufacturer's data sheets for specific cores.							

Table 3.1. Typical core data.

The losses include hysteresis and eddy current losses. However, the manufacturer's data is normally measured for sinusoidal excitation. Furthermore, the test specimen size may be different from the designed component. Losses are dependent on the size of the core. In the absence of test data on the design core, the manufacturer's data must be used in establishing the constants in (3.13). Variations in core loss data will be examined in section 6.3.

3.2.5   The Thermal Equation

The combined losses in the windings and core must be dissipated through the surface of the wound transformer. This topic is discussed in detail in [86]. The dominant heat transfer mechanism is by convection from the transformer surface. Newton's equation of convection relates heat flow to temperature rise (ΔT), surface area (A_t) and the coefficient of heat transfer, h, by

$$P = hA_t \Delta T,$$ (3.14)

where P is the sum of the winding losses and the core losses.

[86] separates the contributions from the winding and the core to give a more detailed model. This may be useful after the initial design is completed as a refinement.

The thermal resistance R_θ is the inverse of the product (hA_t) given by

$$\Delta T = R_\theta P.$$ (3.15)

The thermal resistance path for the winding losses, $R_{\theta cu}$, is in parallel with the resistance path of the core losses, $R_{\theta fe}$. Using the electrical analogy, the equivalent thermal resistance is

$$\frac{1}{R_\theta} = \frac{1}{R_{\theta cu}} + \frac{1}{R_{\theta fe}} = hA_t,$$ (3.16)

where h and A_t are the equivalent values for the transformer treated as a single unit. For natural heat convection, h is a function of the height, H, of the transformer, and the empirical result has been proposed by [70]:

$$h = 1.42\left[\frac{\Delta T}{H}\right]^{0.25}.$$

(3.17)

For an ETD44 core, H = 0.045 m and h = 8.2 W/m²°C for a 50 °C temperature rise. Evidently, the position of the transformer relative to other components will have a profound effect on the value of h. In fact, the value of h is probably the most uncertain parameter in the entire design. However, the typical value of h = 10 W/m²°C is confirmed by test results in [53] and [79] for cores encountered in switching power supplies under natural convection. A higher value of h applies for forced convection with fan cooling.

3.2.6 Optimisation

Eliminating the current density in (3.12) using (3.10) yields

$$P_{cu} = \rho_w V_w k_u \left[\frac{\sum VA}{KfB_m k_f k_u A_p}\right]^2 = \frac{a}{f^2 B_m^{\ 2}}.$$

(3.18)

Rewriting (3.13),

$$P_{fe} = \rho_c V_c K_c f^\alpha B_m^{\ \beta} = bf^\alpha B_m^{\ \beta}.$$

(3.19)

The total losses are

$$P = \frac{a}{f^2 B_m^{\ 2}} + bf^\alpha B_m^{\ \beta}.$$

(3.20)

The domain of P is in the first quadrant of the f-B_m plane. P is everywhere positive and it is singular along the axes. If $\alpha = \beta$, P has a global minimum $\left\{ \dfrac{dP}{d(fB_m)} = 0 \right\} = \dfrac{-2a}{f^3 B_m{}^3} + b\beta f^{\beta-1} B_m{}^{\beta-1}$ at

$$f_o B_o = \left[\frac{2a}{\beta b} \right]^{\frac{1}{\beta+2}}. \tag{3.21}$$

For $\alpha = \beta = 2$, with (3.18) and (3.19),

$$f_o B_o = \sqrt[4]{\frac{\rho_w V_w k_u}{\rho_c V_c K_c}} \sqrt{\frac{\sum VA}{K k_f k_u A_p}}. \tag{3.22}$$

Given that B_o must be less the saturation flux density B_{sat}, there is a critical frequency, given by (3.22), above which the losses may be minimised by selecting an optimum value of flux density which is less than the saturation value ($B_o < B_{sat}$). Equation (3.22) shows that $f_o B_o$ is related to power density since A_p is related to core size.

In the more general case ($\alpha \neq \beta$), there is no global minimum. The minimum of P at any given frequency is obtained by taking the partial derivative w.r.t. B_m and setting it to zero:

$$\begin{aligned} \frac{\partial P}{\partial B_m} &= -\frac{2a}{f^2 B_m{}^3} + \beta b f^\alpha B_m{}^{\beta-1} \\ &= -\frac{2P_{cu}}{B_m} + \beta \frac{P_{fe}}{B_m} = 0 \end{aligned}.$$

The minimum losses occur *for a fixed frequency f* when:

$$P_{cu} = \frac{\beta}{2} P_{fe}. \tag{3.23}$$

The minimum of P at any given flux density is obtained by taking the partial derivative w.r.t. f and setting it to zero:

$$\frac{\partial P}{\partial f} = -\frac{2a}{f^3 B_m{}^2} + \alpha b f^{\alpha-1} B_m{}^{\beta}$$

$$= -\frac{2P_{cu}}{f} + \alpha \frac{P_{fe}}{f} = 0$$

The minimum losses occur *for a fixed flux density B_m* when:

$$P_{cu} = \frac{\alpha}{2} P_{fe} \,. \tag{3.24}$$

Evaluation of (3.24) with (3.18) and (3.19) at $B_o = B_{sat}$ gives the critical frequency above which the total losses are minimised by operating at an optimum value of flux density which is less than the saturation value ($B_o < B_{sat}$):

$$f_o{}^{\alpha+2} B_o{}^{\beta+2} = \left[\frac{\alpha}{2} b\right]^{-1} a$$

$$= \frac{2}{\alpha} \frac{\rho_w V_w k_u}{\rho_c V_c K_c} \left[\frac{\sum VA}{Kk_f k_u A_p}\right]^2 , \tag{3.25}$$

The nature of (3.20) is illustrated in Figure 3.4. The two sets of curves shown are for low frequency (50 Hz) and high frequency (50 kHz).
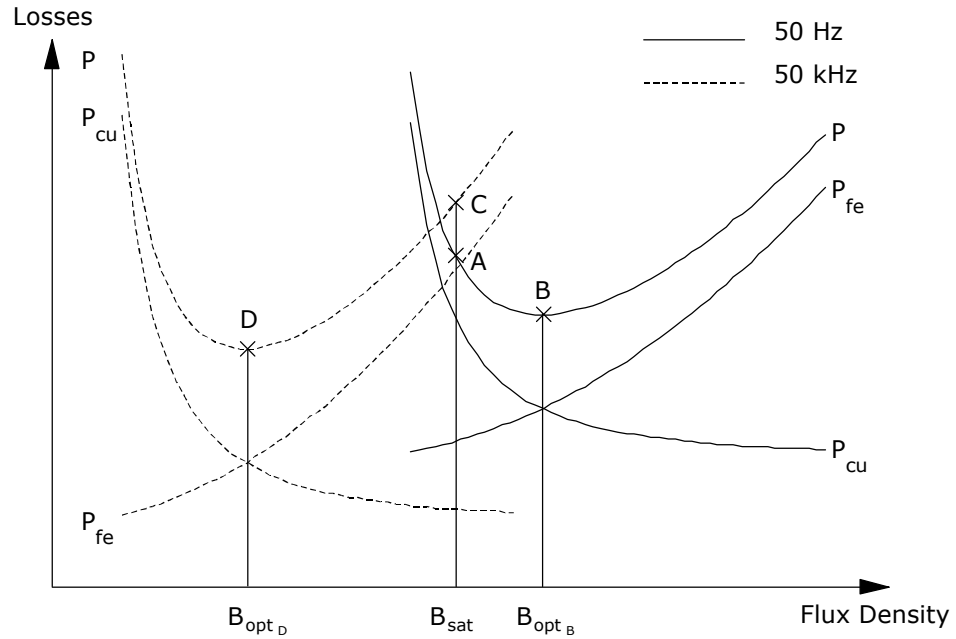
Figure 3.4. Winding, core, and total losses at different frequencies.

At 50 Hz, the optimum flux density (at point B) is greater than the saturation flux density and therefore the minimum total losses achievable are at point A. However, the winding and core losses are not equal. At 50 kHz, the optimum flux density is less than the saturation flux density and the core and winding losses are equal. The first step in a design is to establish whether the optimum flux density given by the optimisation criterion in (3.23) is greater or less than the saturation flux density; this will be described in section 3.3.

3.2.6.1   Critical Frequency

A three dimensional version of the total loss curve is shown in Figure 3.5; this has been plotted for the specifications of the design example we will encounter in section 3.4.1. The dark line is the optimum curve, corresponding to the minimum loss points at each frequency.
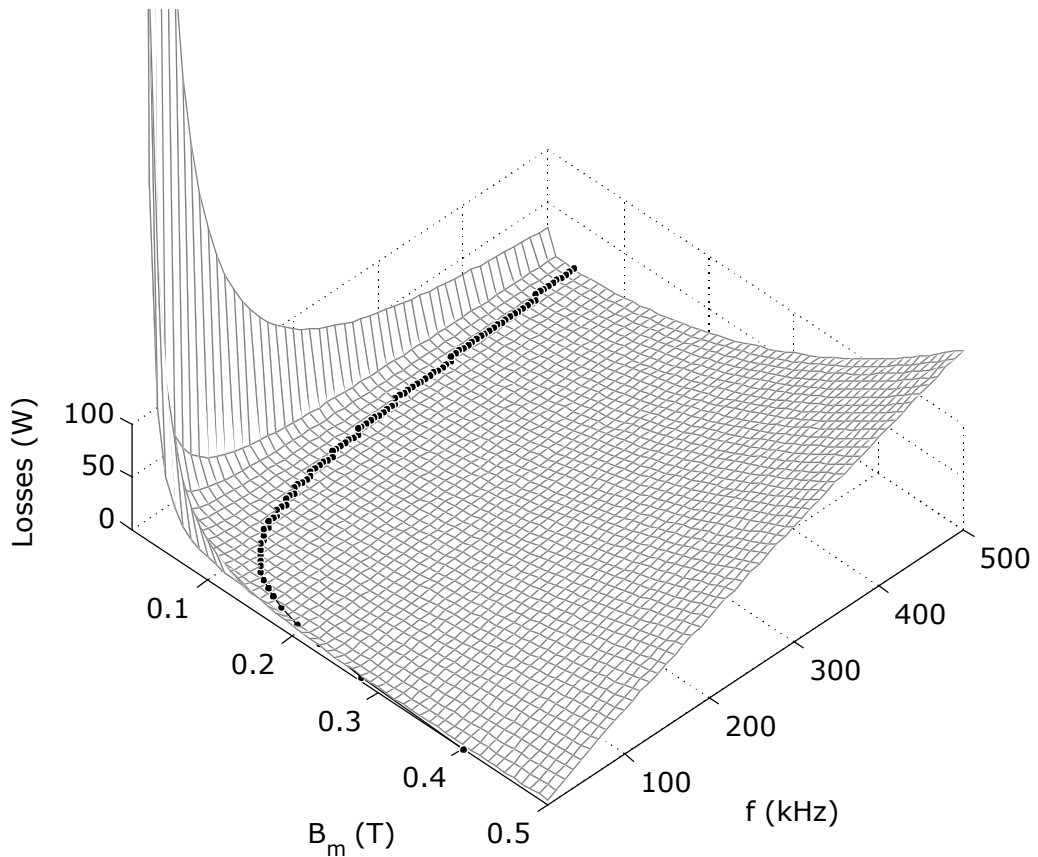
Figure 3.5. Three dimensional plot of total core and winding losses.

At low frequencies, the total losses are large at low flux density levels due to the dominance of the inverse squared frequency term in the winding losses equation (3.18). The core loss component accounts for the majority of the total losses at higher frequency and flux density levels.

The plot starts at 5 kHz with a corresponding optimum flux density of 0.4 T. This is equal to the saturation flux density, B_{sat}, of the core material used for this design, and thus marks the critical frequency, f_c, for this particular case.

Total loss values (core and winding) along the optimum line increase with increasing flux density, and decrease with increasing frequency, as shown in Figure 3.6. This will be verified with experimental results later on.
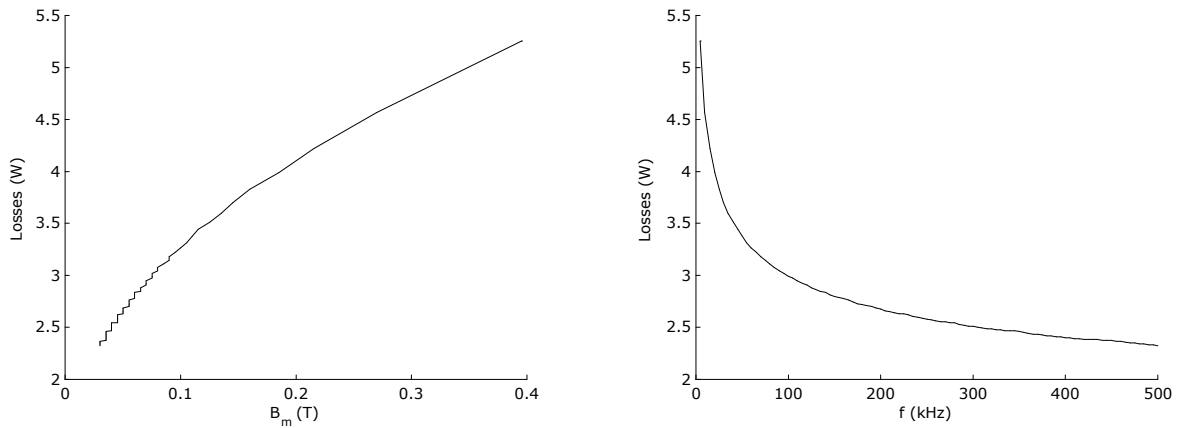
Figure 3.6. Optimum curve as a function of flux density and frequency.

Figure 3.7 is a 2-D flux versus frequency plot of the optimum curve, and shows the saturation flux density and corresponding critical frequency. Some sample values from this plot are given in Table 3.2. The critical value can also be confirmed using (3.34).

f_o (kHz)	4	5	6	10	20	50	100	200	500
B_o (mT)	450	397	359	270	184	110	75	51	31

Table 3.2. Sample optimum points.
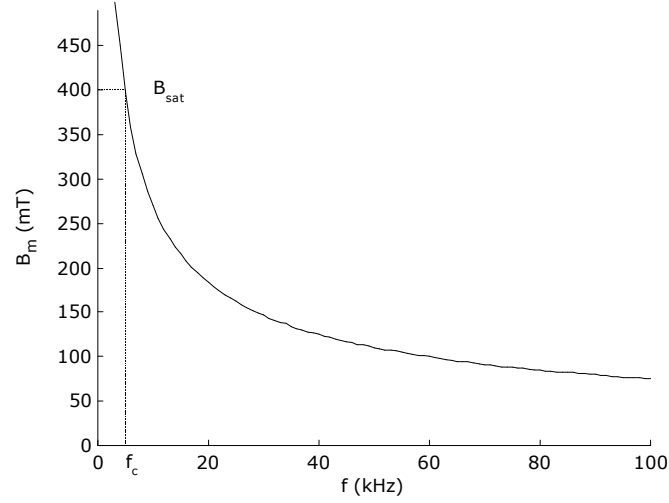
Figure 3.7. The critical frequency.

3.3 The Design Equations

3.3.1 Dimensional Analysis

The physical quantities V_c, V_w and A_t may be related to core size A_p by dimensional analysis:

$$V_c = k_c A_p^{3/4}, \; V_w = k_w A_p^{3/4}, \; A_t = k_a A_p^{1/2}. \tag{3.26}$$

All the coefficients are dimensionless. The values of k_c, k_w, and k_a vary for different types of cores [80], [72]. However, the combinations that are required for the transformer design are approximately constant.

For instance, using the surface area method proposed by McLyman [72] and also utilised by Katane et al. [55], we have estimated the k_a constant for three commonly used sets of manufacturer's cores: Linton and Hirst EI cores, Siemens Matsushita EE cores and Siemens Matsushita UU cores. This method plots both the exposed core and winding surface areas for each core in a group against the root of the area product, and then uses the combined slopes to find k_a.

Core Surface Area
= 2((A + 2B + 2C)A
+ (E + 2D)A
+ (E + 2D)(A + 2B + 2C)
- E(A + 2B))

Winding Surface Area
= 2((A + 2B + 2C)2B
- 4BC + (E + 2D)2B
- 4BD + E(A + 2B))
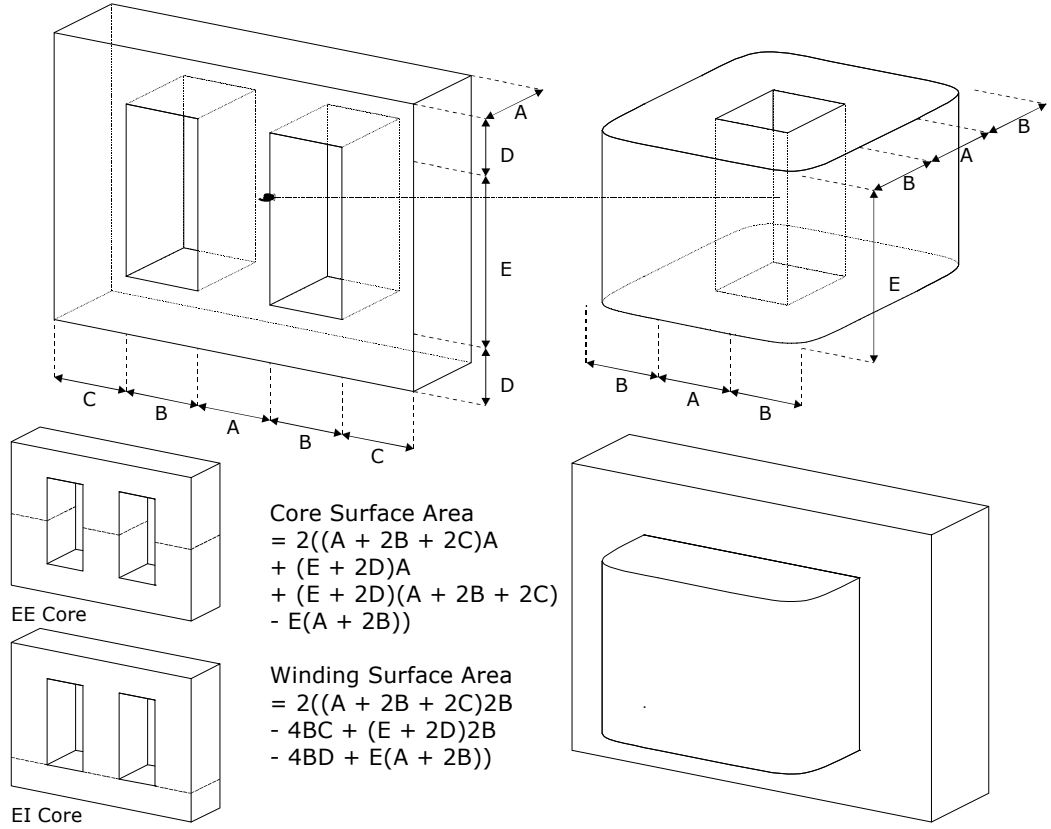
EE Core

EI Core

Figure 3.8. Core and winding surface areas for EE and EI core shapes.

For the EE, EI and UU shape cores, k_a was calculated to be 39, 38 and 38.5 respectively.

Similarly, the constants that relate the volume of a transformer winding or core to the area product are calculated from data for sets of different shape cores. The k_c or k_w constants are found by calculating the slope of plots of the core volume V_c or winding volume V_w (derived from dimensions as shown in Figure 3.8 or Figure 3.9 for example) versus $A_p^{3/4}$.

Alternatively, k_w can be calculated by combining the slopes of plots of the mean length of a turn MLT versus $A_p^{1/2}$ and of the window area W_a versus $A_p^{1/2}$, since $V_w = MLT \times W_a$.

McLyman [72] treats the transformer core and winding as a single solid quantity with no subtraction for the core window to yield a single constant that is effectively the sum of k_c and k_w.

63
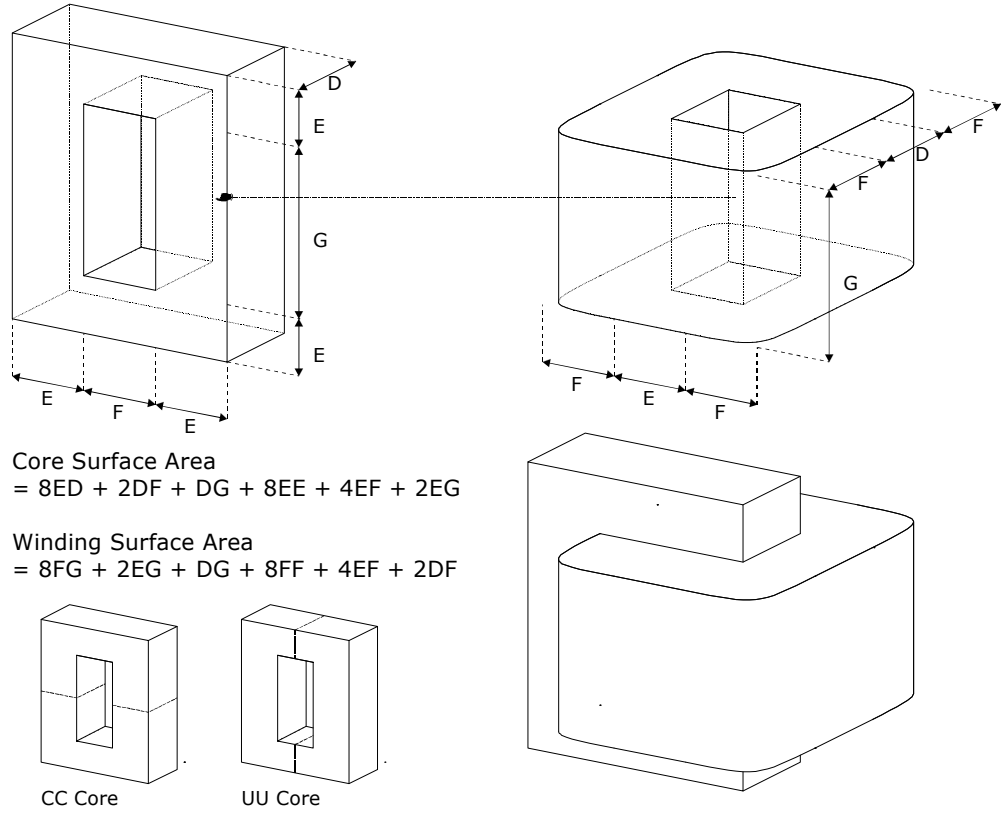
Figure 3.9. Core and winding surface areas for CC and UU core shapes.

It may be stated that $k_a = 40$, $k_c = 5.6$ and $k_w = 10$. Further refinement of the dimensionless constants in (3.26) is somewhat redundant since the value of the heat transfer coefficient h is not always well known. The pot core is sufficiently different in construction such that k_w is 5. The calculation of A_p is described in the next section.

3.3.2 $B_o < B_{sat}$

When the flux density B_o given by (3.34) is less than the saturation flux density, the optimum design is at point D in Figure 3.4.

The optimum conditions established by (3.23) can be exploited to establish a formula for A_p in terms of the design specifications: output power, frequency and temperature rise:

$$P_{cu} = \frac{\beta}{2} P_{fe} = P - \frac{2}{\beta} P_{cu} \Rightarrow P_{cu} = \frac{P}{1 + 2/\beta} = \frac{\beta P}{\beta + 2},$$

$$P_{fe} = \frac{2}{\beta}P_{cu} = P - \frac{\beta}{2}P_{fe} \Rightarrow P_{fe} = \frac{P}{1+\beta/2} = \frac{2P}{\beta+2},$$

$$\therefore P_{cu}P_{fe} = \frac{2\beta}{(\beta+2)^2}P^2. \tag{3.27}$$

P_{cu}, P_{fe} and P are given by (3.18), (3.13) and (3.14) respectively. Taking β = 2 and invoking the dimensional analysis of (3.26),

$$P_{cu}P_{fe} = \rho_w V_w k_u \left[\frac{\sum VA}{KfB_m k_f k_u A_p}\right]^2 \rho_c V_c K_c f^\alpha B_m^2 = \frac{4}{16}(hA_t \Delta T)^2$$

$$= \rho_w k_w A_p^{3/4} \frac{\sum VA^2}{K^2 f^2 k_f^2 k_u A_p^2} \rho_c k_c A_p^{3/4} K_c f^\alpha = \frac{1}{4}h^2 k_a^2 A_p \Delta T^2,$$

$$\Rightarrow \left[\frac{4\rho_w}{k_f^2 k_u h^2}\frac{k_c k_w}{k_a^2}\right]\left[\frac{\sum VA}{Kf\Delta T}\right]^2[\rho_c K_c f^\alpha] = \frac{A_p A_p^2}{A_p^{3/4} A_p^{3/4}} = A_p^{3/2}$$

which with rearrangement yields

$$A_p = K_o \left[\frac{\sum VA}{Kf\Delta T}\right]^{4/3}[\rho_c K_c f^\alpha]^{2/3}, \tag{3.28}$$

where

$$K_o = \left[\frac{4\rho_w}{k_f^2 k_u h^2}\frac{k_c k_w}{k_a^2}\right]^{2/3}. \tag{3.29}$$

Taking typical values: $\rho_w = 1.72 \times 10^{-8}$ Ω-m, h = 10 W/m²°C, k_a = 40, k_c = 5.6, k_w = 10, k_f = 1.0, and k_u = 0.4 yields K_o = 1.54 × 10⁻⁷. SI units have been used and A_p is in m⁴.

The optimum value of current density in the windings may be found from the optimum criterion (3.23) using the equations for copper losses (3.12) and thermal heat transfer (3.14):

$$J_o = \sqrt{\frac{P_{cu}}{\rho_w V_w k_u}}$$
$$= \sqrt{\frac{\beta}{\beta+2} \frac{hA_t \Delta T}{\rho_w V_w k_u}} \, . \tag{3.30}$$

Employing the dimensional analysis equations (3.26) with $\beta = 2$ in (3.30) yields

$$J_o = \sqrt{\frac{2}{2+2} \frac{hk_a A_p^{1/2} \Delta T}{\rho_w k_w A_p^{3/4} k_u}} \, ,$$
$$= K_t \sqrt{\frac{\Delta T}{A_p^{1/4}}} \tag{3.31}$$

where

$$K_t = \sqrt{\frac{h}{2\rho_w k_u} \frac{k_a}{k_w}} \, . \tag{3.32}$$

Taking typical values: $\rho_w = 1.72 \times 10^{-8}$ Ω-m, $h = 10$ W/m²°C, $k_a = 40$, $k_w = 10$ and $k_u = 0.4$ gives $K_t = 53.9 \times 10^3$.

The flux density is found from the power equation (3.10):

$$B_m = \frac{\sum VA}{Kfk_f k_u J A_p} \, . \tag{3.33}$$

Substituting the optimum value of J given by (3.31) and A_p given by (3.28) into (3.33), results in an expression for the optimum flux density:

$$B_o = \frac{\sum VA}{Kfk_f k_u A_p} \sqrt{\frac{k_w k_u 2\rho_w}{hk_a}} \sqrt{\frac{A_p^{1/4}}{\Delta T}}$$

$$= \frac{\sum VA}{Kfk_f k_u} \sqrt{\frac{k_w k_u 2\rho_w}{hk_a}} \frac{1}{\sqrt{\Delta T}} \frac{1}{A_p^{7/8}} \quad ,$$

$$= \frac{\sum VA}{Kfk_f k_u} \sqrt{\frac{k_w k_u 2\rho_w}{hk_a}} \frac{1}{\sqrt{\Delta T}} \frac{1}{K_o^{7/8}} \frac{1}{[\rho_c K_c f^\alpha]^{7/12}} \left[\frac{Kf\Delta T}{\sum VA} \right]^{7/6}$$

which can be rearranged as

$$B_o = \frac{1}{K_o^{7/8} K_t} \frac{\sqrt{\Delta T}}{k_f k_u} \left[\frac{Kf\Delta T}{\sum VA} \right]^{1/6} \frac{1}{[\rho_c K_c f^\alpha]^{7/12}} . \tag{3.34}$$

Evidently, (3.28) and (3.34) may be evaluated from the specifications of the application and the material constants.

3.3.3 $B_o > B_{sat}$

In this case, the saturation of the magnetic material dictates that the design is at point A in Figure 3.4. The value of B_m in the voltage equation is fixed by B_{sat}. The current density is found by combining the winding losses (3.12) and the core losses (3.13) and using the thermal equation (3.14):

$$J^2 = \frac{P_{cu}}{\rho_w V_w k_u} = \frac{P - P_{fe}}{\rho_w V_w k_u}$$

$$= \frac{hA_t \Delta T}{\rho_w V_w k_u} - \frac{\rho_c V_c K_c f^\alpha B_m^{\,\beta}}{\rho_w V_w k_u} . \tag{3.35}$$

Despite the unwieldy nature of (3.35), J may be expressed in terms of the transformer specifications with the aid of dimensional analysis equations as follows:

$$J = \sqrt{\frac{hk_a A_p^{1/2}\Delta T}{\rho_w k_w A_p^{3/4} k_u} - \frac{\rho_c k_c A_p^{3/4} K_c f^\alpha B_m^{\ \beta}}{\rho_w k_w A_p^{3/4} k_u}}$$

$$= \sqrt{2\left[\frac{hk_a}{2\rho_w k_u k_w}\right]\frac{\Delta T}{A_p^{1/4}} - \left[\frac{k_c}{\rho_w k_u k_w}\right]\rho_c K_c f^\alpha B_m^{\ \beta}}, \qquad (3.36)$$

$$= \sqrt{\frac{2K_t^{\ 2}\Delta T}{A_p^{1/4}} - K_j \rho_c K_c f^\alpha B_m^{\ \beta}}$$

where

$$K_j = \frac{k_c}{\rho_w k_u k_w}. \qquad (3.37)$$

Taking typical values: $\rho_w = 1.72 \times 10^{-8}$ Ω-m, $k_c = 5.6$, $k_w = 10$ and $k_u = 0.4$ gives $K_j = 81.4 \times 10^6$.

J is a function of A_p in (3.36) which has yet to be calculated, and therefore some iteration is required. Evidently, substituting for J given by (3.10) in (3.36),

$$\frac{\sum VA}{KfB_m A_p k_f k_u} = \sqrt{\frac{2K_t^{\ 2}\Delta T}{A_p^{1/4}} - K_j \rho_c K_c f^\alpha B_m^{\ \beta}}$$

$$\Rightarrow \left[\frac{\sum VA}{KfB_m k_f k_u}\right]^2 \frac{1}{A_p^{\ 2}} = [2K_t^{\ 2}\Delta T]\frac{1}{A_p^{1/4}} - [K_j \rho_c K_c f^\alpha B_m^{\ \beta}]$$

yields a second order polynomial in A_p where

$$f(A_p) = a_o A_p^{\ 2} - a_1 A_p^{\ 7/4} + a_2 = 0, \qquad (3.38)$$

and

$$a_o = K_j \rho_c K_c f^\alpha B_m^{\ \beta},$$

$$a_1 = 2K_t^{\ 2}\Delta T,$$

68

$$a_2 = \left[\frac{\Sigma VA}{KfB_m k_f k_u} \right]^2 .$$

The roots of $f(A_p)$ are found numerically using the Newton Raphson method:

$$
\begin{aligned}
A_{p_{i+1}} &= A_{p_i} - \frac{f(A_{p_i})}{f'(A_{p_i})} \\
&= A_{p_i} - \frac{a_o A_{p_i}^{\,2} - a_1 A_{p_i}^{\,7/4} + a_2}{2a_o A_{p_i} - \frac{7}{4} a_1 A_{p_i}^{\,3/4}} .
\end{aligned}
\tag{3.39}
$$

Normally, one iteration is sufficient.

The initial estimate of A_p is found by assuming the total losses are equal to twice the copper losses (at point A in Figure 3.4, the total losses are less than twice the copper losses). In this case, J is given by (3.31) and may be substituted into the power equation (3.10) to give

$$A_{p_i} = \frac{\sum VA}{KfB_m J k_f k_u} = \frac{\sum VA}{KfB_m k_f k_u K_t \sqrt{\Delta T} / A_{p_i}^{\,1/8}} ,$$

or rearranging in terms of the area product,

$$A_{p_i} = \left[\frac{\sum VA}{KfB_m k_f k_u K_t \sqrt{\Delta T}} \right]^{8/7} .
\tag{3.40}$$

3.3.4   Design Methodology

The overall design methodology is shown in flow chart form in Figure 3.10. The process begins with entry of the transformer specifications (power output, frequency, temperature rise, etc.) and selection of the desired core and winding materials.
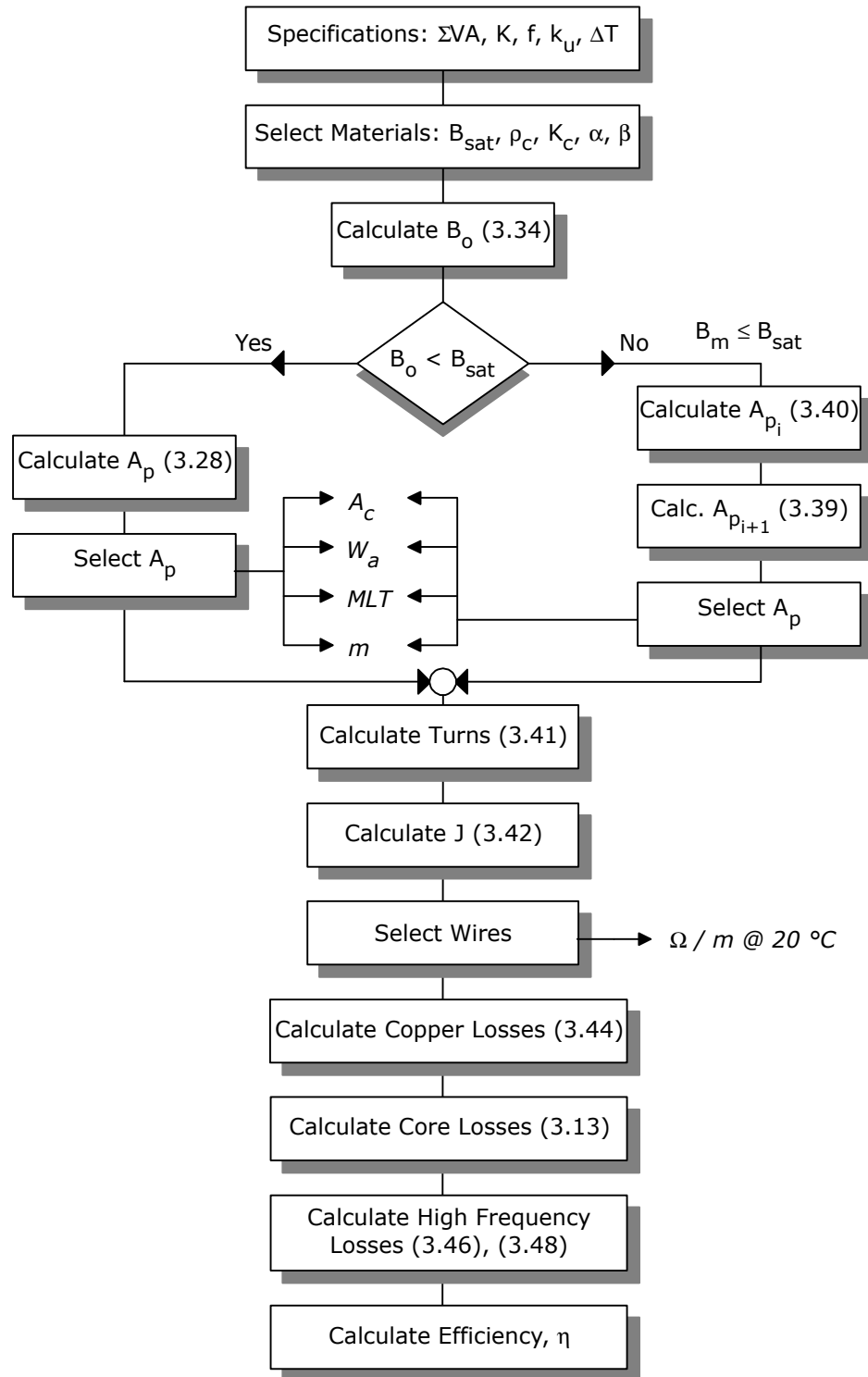
Figure 3.10. Flow chart of design process.

The optimum flux density, B_o, for the input specifications is then calculated. The diagonal choice symbol in Figure 3.10 shows the comparison of B_o with B_{sat}, the saturation flux density. This is a critical point in the design.

If this optimum flux density is less than the saturation flux density for the core material being used in the design, the maximum flux density B_m allowed is set to the optimum value. This will lead to a particular size of core (based on the calculated area product value, A_p). But if the optimum flux density is greater than the saturation flux density, the maximum flux density is set to the saturation value, and thus a different route is taken which may lead to a different size core.

The core manufacturer normally supplies sets of core data for different shapes and materials, but a core with an area product equal to the calculated value may not be available in a particular set. In this case, a core with an area product slightly greater than the calculated value is selected from the set. The manufacturer's catalogues are consulted to obtain the rest of the data corresponding to the selected core: the physical cross-section A_c (yielding the effective cross-section A_m), the window area W_a, the mean length of a turn MLT ($V_w = \text{MLT} \times W_a$), and the core mass m ($m = \rho_c V_c$).

Once the core has been selected, the parameters of the core are used to find the number of turns for each winding from (3.4):

$$N = \frac{V_{rms}}{KfB_m A_m}. \tag{3.41}$$

As detailed above, B_m in this equation is interpreted as B_o or B_{sat}, depending on which is lower. Since the selected core from standard designs may not correspond exactly to the optimum selection, the current density may therefore be calculated using (3.35). With $h = 10$ W/m^2°C and $k_a = 40$, then

$$
\begin{aligned}
J &= \sqrt{\frac{hA_t\Delta T - \rho_c V_c K_c f^\alpha B_m{}^\beta}{\rho_w k_u V_w}} \\
&= \sqrt{\frac{hk_a\sqrt{A_p}\Delta T - \rho_c V_c K_c f^\alpha B_m{}^\beta}{\rho_w k_u V_w}} \ . \\
&= \sqrt{\frac{400\sqrt{A_p}\Delta T - mK_c f^\alpha B_m{}^\beta}{\rho_w k_u V_w}}
\end{aligned}
\tag{3.42}
$$

The resistivity of the conductor at the maximum operating temperature is given by

$$\rho_w = \rho_{20}[1 + \alpha_{20}(T_{max} - 20\,^\circ C)],\tag{3.43}$$

where T_{max} is the maximum temperature, ρ_{20} is the resistivity at 20 °C, and α_{20} is the temperature coefficient of resistivity at 20 °C. The wire sizes are selected from standard wire tables, which normally specify resistance in Ω/m at 20 °C. The DC winding loss is then equal to

$$P_{cu} = MLT \times N \times (\Omega/m) \times [1 + \alpha_{20}(T_{max} - 20\,^\circ C)] \times I^2.\tag{3.44}$$

High frequency AC winding losses can be accounted for using the equations detailed in section 3.3.5.

Finally, the core losses, P_{fe}, and the total losses, P or P_{tot}, are established. The efficiency is found from $\eta = P_o/(P_o + P_{tot})$, and if an unsatisfactory level is achieved, refinement of the design may be necessary.

3.3.5   Skin and Proximity Effects

An isolated round conductor carrying AC current generates a concentric alternating magnetic field which, in turn, induces eddy currents (Faraday's law). Figure 3.12 shows the distribution of the magnetic field in a round conductor at low frequencies.

Eddy currents oppose the flux and the resulting distribution of current means that eddy currents cancel some of the current at the centre of the conductor while increasing the current near the surface as shown in Figure 3.12. The overall effect is that the current flows in a smaller annular area. At high frequencies, it can be shown that the current flows in an equivalent annular cylinder at the surface with thickness δ (called the skin depth), as shown in Figure 3.11.

Solid Conductor with Skin Effect   Equivalent Hollow Conductor
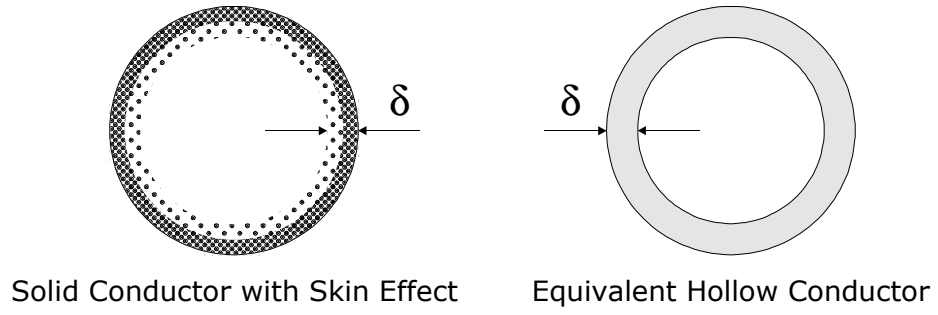
Figure 3.11. Surface bunching of current due to skin effect.

This field problem can be solved from Maxwell's equations giving the internal impedance of the conductor as:

$$Z_i = R_{dc} \frac{mr_o I_o(mr_o)}{2 I_1(mr_o)},$$ (3.45)

where

$$m = (1+j)/\delta.$$
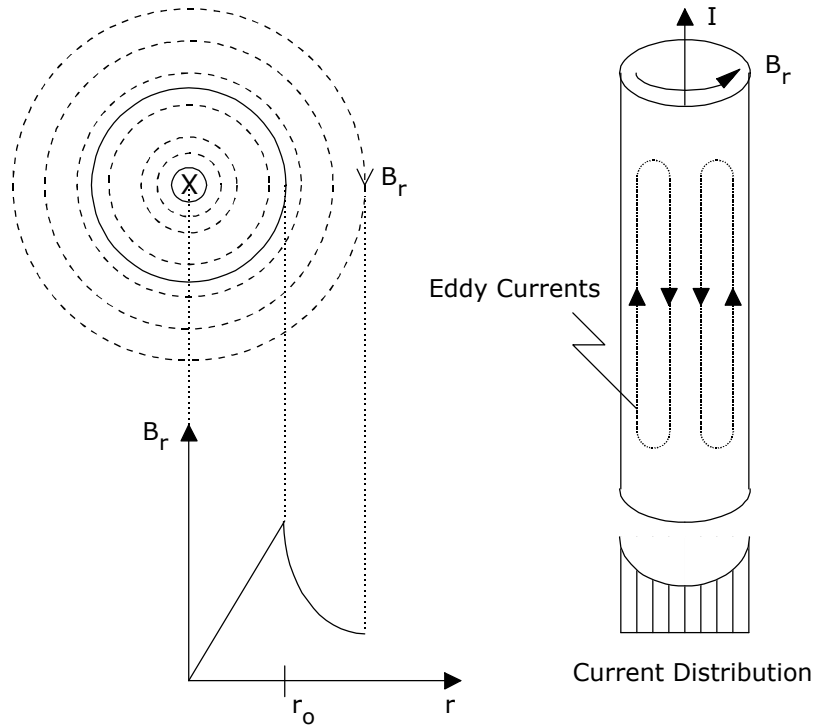
Figure 3.12. Eddy currents in a circular conductor.
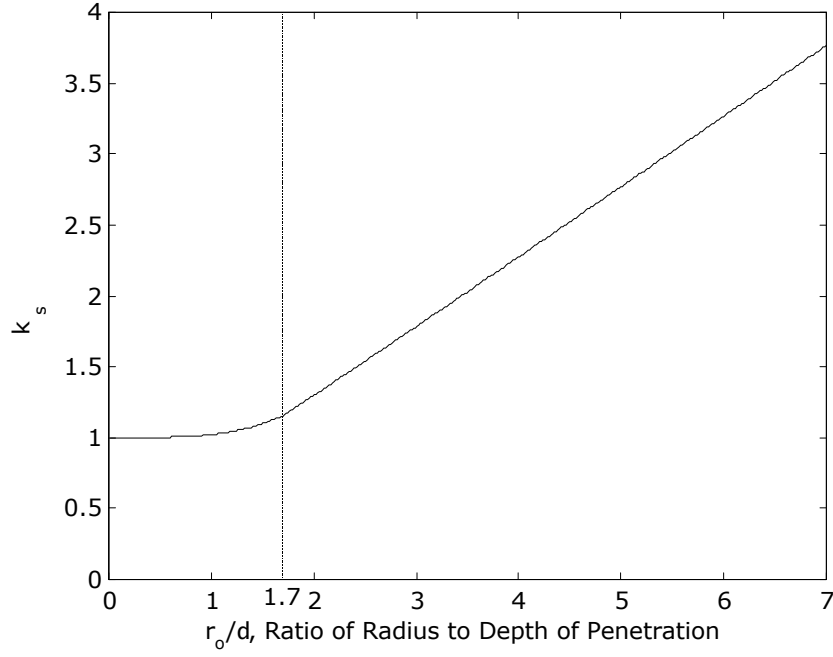
Figure 3.13. AC resistance due to skin effect.

δ is called the skin depth, $\delta = \sqrt{\rho_w / \pi f \mu_o}$, I_0 and I_1 are modified Bessel functions of the first kind, and j is the complex operator, $j = \sqrt{-1}$. The AC resistance of a round conductor is given by the real part of Z_i and internal inductive reactance is given by the imaginary part of Z_i. This expression is too cumbersome to use and the following approximations are useful. Recalling $k_s = R_{ac}/R_{dc}$,

$$
\begin{aligned}
k_s &= 1 + \frac{(r_o / \delta)^4}{48 + 0.8(r_o / \delta)^4} \quad \dots r_o / \delta < 1.7 \\
&= 0.25 + 0.5\left(\frac{r_o}{\delta}\right) + \frac{3}{32}\left(\frac{\delta}{r_o}\right) \dots r_o / \delta > 1.7
\end{aligned}
\tag{3.46}
$$

A plot of k_s is shown in Figure 3.13.

The proximity effect factor for a sinusoidal waveform in a winding with p layers was derived in Chapter 2, as (2.39):

$$
k_x = \Delta\left\{ \frac{\text{Sinh}2\Delta + \text{Sin}2\Delta}{\text{Cosh}2\Delta - \text{Cos}2\Delta} + \frac{2(p^2 - 1)}{3} \frac{\text{Sinh}\Delta - \text{Sin}\Delta}{\text{Cosh}\Delta + \text{Cos}\Delta} \right\}.
\tag{3.47}
$$

74

A simple approximation is [97]

$$k_x = 1 + \frac{5p^2 - 1}{45} \Delta^4,$$

(3.48)

where Δ is the ratio of the thickness of a layer of foil, d, to the skin depth, δ (see Figure 3.14). We will focus on the proximity effect for other non-sinusoidal waveforms in more detail in Chapter 4.
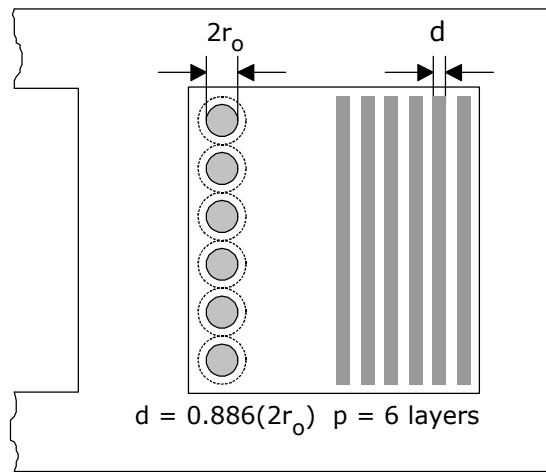
Figure 3.14. Winding layout.

3.4   Design Examples

In the following examples, we will be analysing a number of transformer applications utilising some of the waveforms listed in Table 3.3.

The waveform factor, K, for a particular waveform can be established from the form factor, k, in Table 3.3, the period, T, and the time for the flux density to go from zero to its maximum value, τ, using (3.4). If the form factor is unknown, it can also be found from the RMS value of the waveform and the average DC value in the time period τ. The power factor is calculated using the average power and the RMS values (applied to either current or voltage waveforms) in Table 3.3.
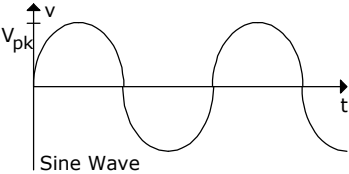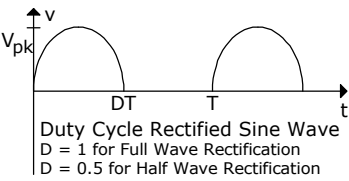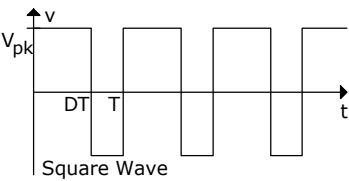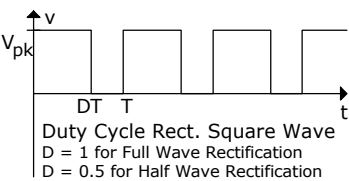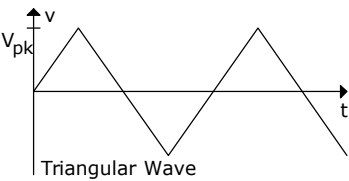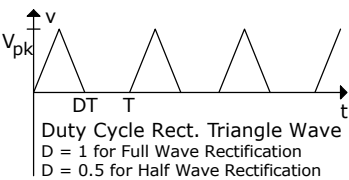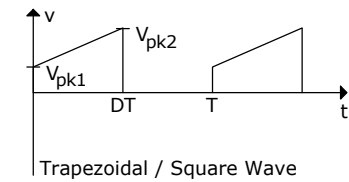
VOLTAGE PATTERN	RMS VALUE	AVG. VALUE / FORM FACTOR	RMS OF FUNDAMENTAL
Sine Wave	$\dfrac{V_{pk}}{\sqrt{2}}$	0 / ∞	$\dfrac{V_{pk}}{\sqrt{2}}$
Duty Cycle Rectified Sine Wave D = 1 for Full Wave Rectification D = 0.5 for Half Wave Rectification	$V_{pk}\sqrt{\dfrac{D}{2}}$	$V_{pk}\dfrac{2D}{\pi}$ / $\dfrac{\pi}{2\sqrt{2}D}$	$D = 0.5 \rightarrow \dfrac{V_{pk}}{2\sqrt{2}}$ $D \neq 0.5 \rightarrow$ $\dfrac{V_{pk}\,2\sqrt{2}D}{p(1-4D^2)}CospD$
Square Wave	V_{pk}	$V_{pk}\times(2D-1)$ / ∞	$\dfrac{2V_{pk}}{\pi}\sqrt{1-Cos(2\pi D)}$
Duty Cycle Rect. Square Wave D = 1 for Full Wave Rectification D = 0.5 for Half Wave Rectification	$V_{pk}\sqrt{D}$	$V_{pk}D$ / $\dfrac{1}{\sqrt{D}}$	$V_{pk}\dfrac{\sqrt{2}}{\pi}Sin\pi D$
Triangular Wave	$\dfrac{V_{pk}}{\sqrt{3}}$	0 / ∞	$V_{pk}\dfrac{4\sqrt{2}}{\pi^2}$
Duty Cycle Rect. Triangle Wave D = 1 for Full Wave Rectification D = 0.5 for Half Wave Rectification	$V_{pk}\sqrt{\dfrac{D}{3}}$	$V_{pk}\dfrac{D}{2}$ / $\dfrac{2}{\sqrt{3D}}$	$V_{pk}\dfrac{2\sqrt{2}}{D\pi^2}Sin^2\dfrac{D\pi}{2}$
Trapezoidal / Square Wave	$\sqrt{\dfrac{D}{3}}\sqrt{(V_{pk1}-V_{pk2})^2-V_{pk1}V_{pk2}}$	$\dfrac{D}{2}\left(V_{pk1}+V_{pk2}\right)$	

Table 3.3. Waveshape parameters.

3.4.1   Push-Pull Converter

The example which follows is based on a push-pull converter with the specifications given in Table 3.4.

SPECIFICATION	VALUE
Output	24 V, 12.5 A
Input	$36 \rightarrow 72$ V
Frequency, f	50 kHz
Temperature Rise, ΔT	30 °C
Ambient Temperature, T_a	45 °C
Efficiency, η	90%

Table 3.4. Push-pull converter specifications.

The push-pull converter circuit and its associated voltage and current waveforms are shown in Figure 3.15 and Figure 3.16.
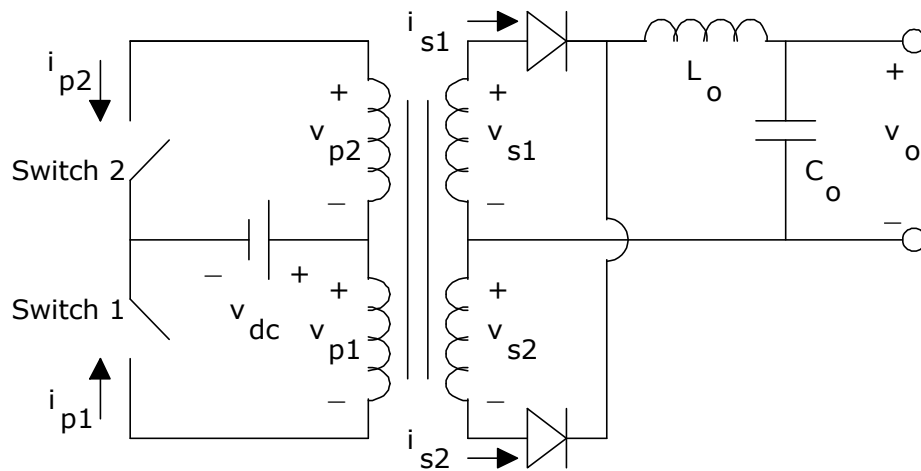
Figure 3.15. Push-pull converter circuit.

We assume for simplicity that the turns ratio is 1:1.
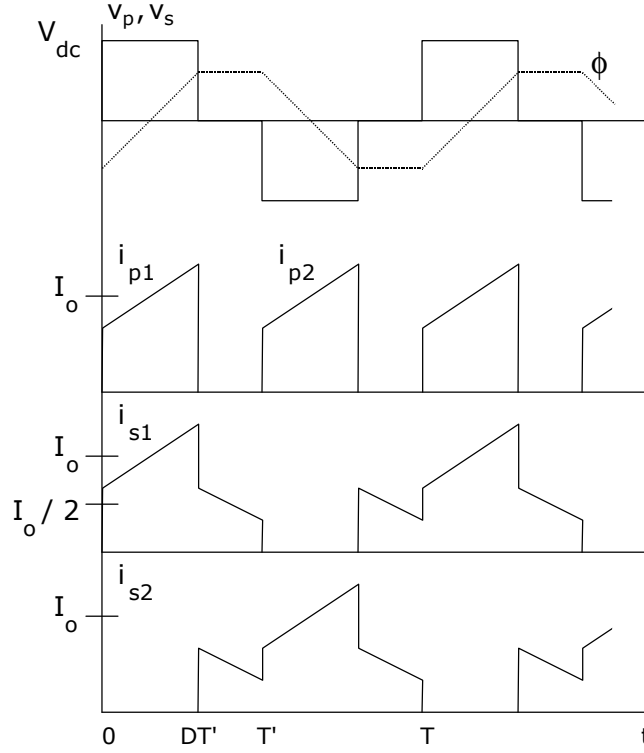
Figure 3.16. Push-pull converter waveforms.

In Figure 3.16, switch 1 turns on at t = 0 and turns off at time DT'. By defining the duty cycle in this manner, the combined on time of the two switches is DT and the output voltage is DV_{dc}. The RMS value of the applied voltage waveform on each winding is $\sqrt{D}V_{dc}$. The DC value over the time period when the flux is being established is V_{dc}. The switching period is T and each switch controls the voltage waveform for T' = T/2. From section 3.2.1,

$$k = \frac{V_{rms}}{\langle v \rangle} = \frac{\sqrt{D}V_{dc}}{V_{dc}} = \sqrt{D}, \tag{3.49}$$

$$\frac{\tau}{T} = \frac{DT'/2}{T} = \frac{D}{4}, \tag{3.50}$$

$$K = \frac{k}{\tau/T} = \frac{\sqrt{D}}{D/4} = \frac{4}{\sqrt{D}}. \tag{3.51}$$

For D = 1.0, K = 4.0 as expected for a square waveform.

78

An interesting feature of the push-pull circuit is that when both switches are off, the current circulates in the secondary windings. This circulating current contributes to heating but there is no transfer of power through the transformer. Our definition of power factor must take this into account.

The RMS value of the secondary current (neglecting the ripple), as shown in Figure 3.16, is given by

$$I_s = \frac{I_o}{2}\sqrt{(1+D)}. \tag{3.52}$$

The RMS value of the secondary voltage is

$$V_s = \sqrt{D}V_{dc} = V_o/\sqrt{D}. \tag{3.53}$$

The VA rating of each secondary winding is now

$$V_s I_s = \frac{1}{2}\frac{\sqrt{1+D}}{\sqrt{D}}V_o I_o = \frac{1}{2}\frac{\sqrt{1+D}}{\sqrt{D}}P_o. \tag{3.54}$$

Recalling the definition of power factor and noting that for each winding the average power $\langle p\rangle = P_o/2$ where P_o is the total output power, the power factor of each secondary winding is

$$k_{ps} = \frac{\langle p\rangle}{V_{rms}I_{rms}} = \sqrt{\frac{D}{1+D}}. \tag{3.55}$$

For $D = 1$, $k_{ps} = 1/\sqrt{2}$ as expected. The RMS values of the input voltage and current are

$$V_p = \sqrt{D}V_{dc}, \quad I_p = \sqrt{(D/2)}I_{dc}. \tag{3.56}$$

For 1:1 turns ratio, $I_{dc} = I_o$ and the power factor in each primary winding is then given by $k_{pp} = 1/\sqrt{2}$.

We can now sum the VA ratings over the two input windings and the two output windings. The average power through each secondary winding is $P_o/2$ and the average power through each primary winding is $P_o/(2\eta)$. Thus we have

$$\sum VA = \left(\frac{1}{\eta k_{pp}} \left(\frac{P_o}{2} + \frac{P_o}{2} \right) + \frac{1}{k_{ps}} \left(\frac{P_o}{2} + \frac{P_o}{2} \right) \right)$$
$$= \left(\frac{\sqrt{2}}{\eta} + \sqrt{\frac{1+D}{D}} \right) P_o . \qquad (3.57)$$

For the input voltage range, the duty cycle can vary between 33% and 67%. For an input voltage of 36 V, the duty cycle is 24/36 = 67%. The waveform factor $K = 4/\sqrt{D} = 4.88$.

3.4.1.1   Core Selection

Ferrite would normally be used for this type of application at the specified frequency. The material specifications for Siemens N67 Mn-Zn ferrite are listed in Table 3.5.

SPECIFICATION	VALUE
K_c	1.9×10^{-3}
α	1.24
β	2.0
ρ_m	4800 kg/m³
B_{sat}	0.4 T

Table 3.5. Siemens N67 material specifications.

The output power of the transformer is P_o = (24 + 1.5) × 12.5 = 318.8 W, assuming a forward voltage drop of 1.5 V for the diode. The power factor and VA ratings of the winding are established above. In terms of core selection, the worst case occurs at maximum duty cycle, i.e. D = 0.67, K = 4.88 and $\sum VA = 1005\ VA$.

The optimum flux density (3.34) is $B_o = 0.112\,\text{T}$. The optimum flux density is less than B_{sat} and A_p from equation (3.28) is 3.644 cm⁴. The Siemens ETD44 EE core with A_p = 4.81 cm⁴ is suitable. The core specifications are given in Table 3.6.

SPECIFICATION	VALUE
A_c	1.73 cm²
W_a	2.78 cm²
A_p	4.81 cm⁴
m	0.094 kg
k_f	1.0
k_u	0.4
MLT	7.77 cm
ρ_{20}	1.72 μΩ-cm
α_{20}	0.00393

Table 3.6. Push-pull core and winding specifications.

It is important to note here that because we are choosing a different A_p value, we are moving away slightly from the optimum point. This is more clearly illustrated by the following two plots, which show the loss conditions for the calculated A_p (Figure 3.17) and for the actual A_p of the chosen ETD44 core (Figure 3.18).
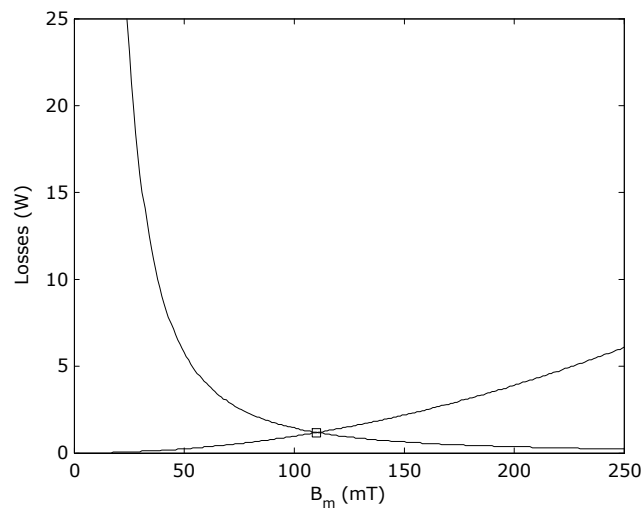
Figure 3.17. Loss conditions for optimum A_p.

Figure 3.17 is plotted for $A_p = 3.644$ cm^4 (with $W_a = 2A_p^{0.5} = 3.82$ cm^2 and scaled m = 0.0763 kg), with the left curve representing the winding losses and the right one representing the core losses. From this, we can see that the minimum total losses occur around 0.11 T (as calculated).
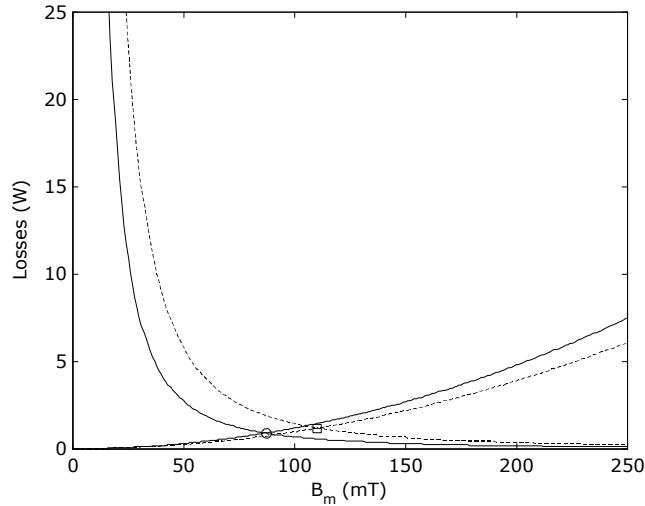
Figure 3.18. Loss conditions for available core A_p.

When we select the ETD 44 core with an $A_p = 4.81$ cm^4 (and m = 0.094 kg), both curves move to the left as shown in Figure 3.18, and we can see a shift in the optimum point to around 0.09 T. Since the winding losses are inversely proportional to the square of the area product, an increase in area product will result in a decrease in the copper losses (the left curve). Conversely, the core losses are proportional to the mass and hence the area product of a core, resulting in increased core losses for increased area product (the right curve). However, the change in winding loss is dominant in this particular case, and the overall effect is that the total losses are reduced when the A_p value is increased slightly.

3.4.1.2 Turns

The ratio V_{rms}/K is evidently $V_o/4$ from the above analysis and therefore independent of D. The number of turns (3.41) in each primary is $N_p = 6.2$. Choose $N_p = 6$ turns and $N_s = 6$ turns.

3.4.1.3   Wire Sizes

The maximum temperature is $T_{max} = T_a + \Delta T = 45 + 30 = 75 \,°C$. The current density (3.42) for the chosen core is $J = 2.644 \times 10^6 \, A/m^2$, based on the core and winding specifications in Table 3.6.

For the primary windings with D = 0.67, the RMS value of the voltage is $V_p = \sqrt{D} V_{dc} = \sqrt{0.67}(36) = 29.5$ V. The current and wire size are

$$I_p = \frac{P_o/2}{\eta k_{pp} V_p} = \frac{318.8/2}{(0.9)(0.707)(29.5)} = 8.5 \text{ A},$$

$$A_w = I_p / J = 3.215 \text{ mm}^2.$$

Standard 0.1×30 mm copper foil with a DC resistance of 5.8 mΩ/m @ 20 °C meets this requirement. For the secondary windings,

$$I_s = \frac{I_o}{2}\sqrt{1+D} = \frac{12.5}{2}\sqrt{1+0.67} = 8.08 \text{ A},$$

$$A_w = I_s / J = 3.056 \text{ mm}^2.$$

Again, standard 0.1×30 mm copper foil meets this requirement.

3.4.1.4   Copper Losses

For the primary windings, the losses are calculated with (3.44). R_p = 3.3 mΩ, and the copper losses in the two primary windings are $R_p I_p^2 \times 2$ = 0.477 W.

The secondary winding resistance is R_s = 3.3 mΩ. The copper losses in the two secondary windings are $R_s I_s^2 \times 2$ = 0.431 W.

3.4.1.5 High Frequency Effects

The skin depth in copper at 50 kHz is 0.295 mm which is greater than the thickness of the foil and therefore does not present a problem. For Δ = 0.1/0.295 and p = 6, k_x given by (3.47) is 1.05. With foil windings, the total copper losses become $0.908 \times 1.05 = 0.953$ W.

A 0.1×30 mm foil is equivalent in area to a number 11 AWG round wire with r_o = 1.154 mm, and k_s given by (3.46) is 2.2 (see Figure 3.13). The total copper losses using round wire windings are therefore $0.908 \times 2.2 = 1.998$ W. Evidently in this case, the choice of a foil is vastly superior.

3.4.1.6 Core Losses

The core losses (3.13) are $P_{fe} = 1.503$ W.

3.4.1.7 Efficiency

The total losses are 2.456 W and the efficiency η is 99.3%. Using round wire windings instead of foil, the efficiency drops to 98.9%.

3.4.2 Forward Converter

SPECIFICATION	VALUE
Output	9 V, 7.5 A
Input	$12 \rightarrow 36$ V
Frequency, f	25 kHz
Temperature Rise, ΔT	50 ^{o}C
Ambient Temperature, T_a	25 ^{o}C
Efficiency, η	90%

Table 3.7. Forward converter specifications.

In a forward converter, the transformer provides electrical isolation and adjusts the input/output voltage ratio for correct component stresses.

When switch Q in Figure 3.19 turns on, flux builds up in the core as shown in Figure 3.20. When the switch is turned off, this core flux must be reset, otherwise core creep takes place and eventually the core will saturate.
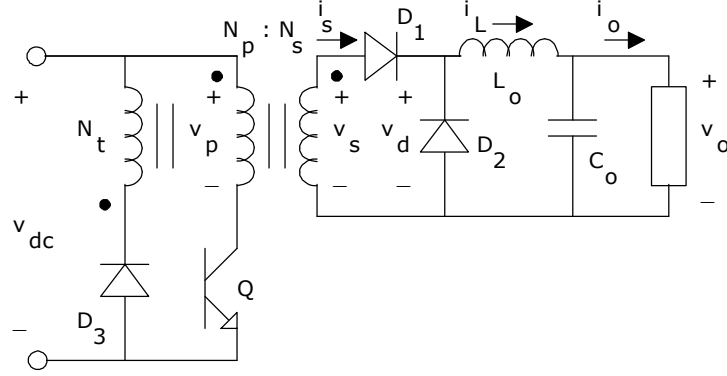
Figure 3.19. Forward converter circuit.
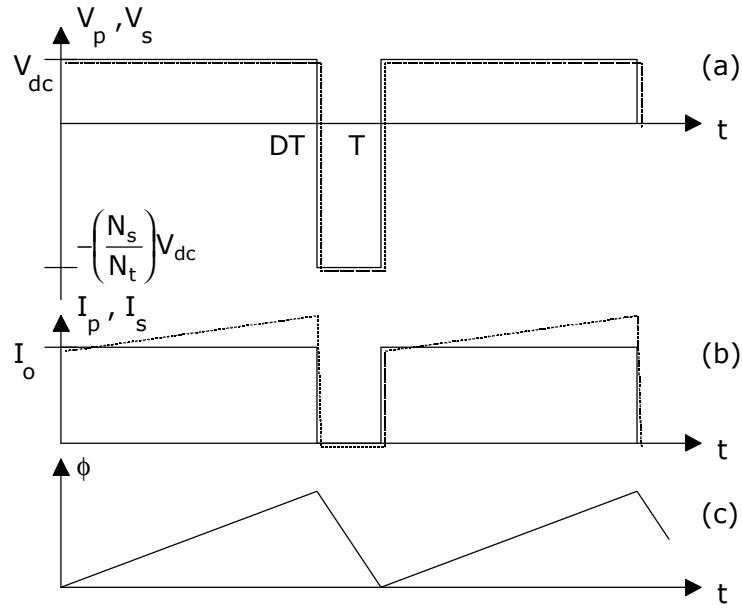
Figure 3.20. Forward converter waveforms.

Assume at t = 0, the core flux is 0, so that at the end of the switching period, DT, the flux is ϕ_{max}:

$$V_{dc} = N_p \frac{d\phi}{dt},$$ (3.58)

$$\phi = \frac{1}{N_p} \int V_{dc} dt = \frac{V_{dc}}{N_p} t, \tag{3.59}$$

$$\phi_{max} = \frac{V_{dc}}{N_p} DT \dots 0 < t < DT. \tag{3.60}$$

At t = DT, the core is reset through the action of the reset winding; this must be achieved in the time (1 - D)T. During this time period, the flux in the core is

$$\phi = \phi_{max} - \frac{V_{dc}}{N_t} (t - DT) \dots DT < t < (1 - D)T. \tag{3.61}$$

Evidently, if the flux is to reset to zero at the end of this period, then

$$\frac{N_p}{N_t} = \frac{D}{1-D}. \tag{3.62}$$

For a duty cycle of 75%, the ratio of primary turns to reset turns is 3.

For the purposes of this example, we shall assume equal turns in the primary and secondary windings; then the maximum duty cycle is $D = 9\,V/12\,V = 0.75$. The waveform factor, K, for a forward converter is found as follows. The volts-seconds of the primary winding indicate that

$$\tau = DT, \tag{3.63}$$

$$\begin{aligned} V_{rms} &= \sqrt{\frac{\int_0^{DT} V_{dc}^2 dt + \int_{DT}^{T} \left(-\frac{N_s}{N_t} V_{dc}\right)^2 dt}{T}} \\ &= \sqrt{\frac{V_{dc}^2 DT + (T - DT)\left(\frac{D}{1-D} V_{dc}\right)^2}{T}}, \\ &= \sqrt{\frac{D}{1-D}} V_{dc} \end{aligned} \tag{3.64}$$

$$\langle v \rangle = V_{dc} \,, \tag{3.65}$$

and thus

$$K = \frac{k}{\tau/T} = \frac{k}{D} = \frac{1}{\sqrt{D(1-D)}} \,. \tag{3.66}$$

For example, if the duty cycle is 50% (corresponding to $\tau = 0.5 \times T$), the waveform factor is equal to 2 as expected. For D = 0.75, K = 2.31.

The power factor, k_p of the input and output windings can be found from the voltage and current waveforms in Figure 3.20, with reference to Table 3.3:

$$V_{rms} = \sqrt{\frac{D}{1-D}} V_{dc} \,, \tag{3.67}$$

$$I_{rms} = \sqrt{D} I_o \,, \tag{3.68}$$

$$\begin{aligned} P_{av} &= V_{av} I_{av} \\ &= \left(\frac{N_s}{N_p} D V_{dc} \right) (I_o), \\ &= D V_{dc} I_o \end{aligned} \tag{3.69}$$

$$k_p = \frac{P_{av}}{V_{rms} I_{rms}} = \frac{D V_{dc} I_o}{\sqrt{\frac{D}{1-D}} V_{dc} \sqrt{D} I_o} = \sqrt{1-D} \,, \tag{3.70}$$

where P_{av} is the average power delivered, and V_{rms} and I_{rms} are the RMS values of input voltage and current respectively.

With 75% duty cycle, the power factor k_p is $\sqrt{(1 - D)} = \sqrt{(1 - 0.75)} = 0.5$ for both the primary and secondary windings.

The window utilisation factor, k_u, is assumed to be 0.4.

3.4.2.1 Core Selection

Ferrite would normally be used for this type of application at the specified frequency. The material specifications for TDK Mn-Zn are listed in Table 3.8.

SPECIFICATION	VALUE
K_c	6.2×10^{-3}
α	1.13
β	2.07
ρ_m	6000 kg/m^3
B_{sat}	0.4 T

Table 3.8. TDK Mn-Zn material specifications.

The output power of the transformer is $P_o = (9 + 1) \times 7.5 = 75$ W, assuming a forward voltage drop of 1 V for the diode.

The power factor and VA ratings of the windings are established above giving

$$\sum VA = \left(\frac{1}{\eta k_{pp}} + \frac{1}{k_{ps}} \right) P_o = \left(\frac{2}{0.9} + 2 \right)(75) = 317 \text{ VA}.$$

Adding 5% for the reset winding gives $\sum VA = 333 \text{ VA}$.

The optimum flux density (3.34) is 0.208 T. $B_m = B_o$.

The optimum flux density is less than B_{sat} and A_p from (3.28) is 1.976 cm^4.

The TDK pot core P36/22, with dimensions as shown in Figure 3.21, is suitable. The core specifications are given in Table 3.1.
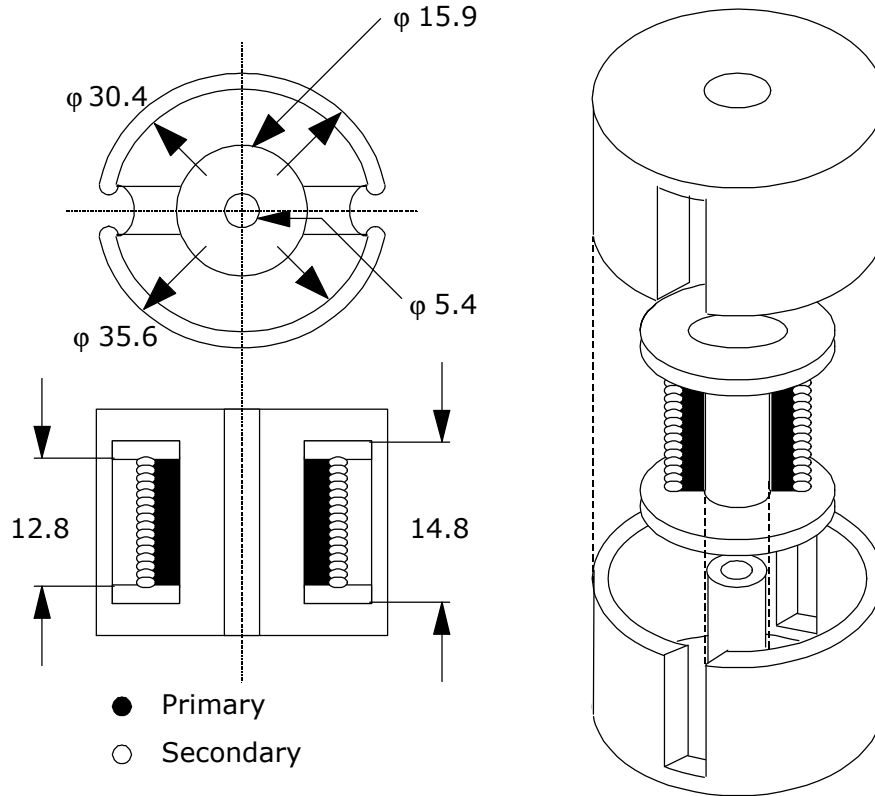
Figure 3.21. Pot core, dimensions in mm.

SPECIFICATION	VALUE
A_c	2.02 cm²
W_a	1.07 cm²
A_p	2.161 cm⁴
m	0.0604 kg
k_f	1.0
k_u	0.4
MLT	7.5 cm
ρ_{20}	1.72 μΩ-cm
α_{20}	0.00393

Table 3.9. Forward converter core and winding specifications.

3.4.2.2 Turns

The ratio V_{rms}/K is given by DV_{dc} from the analysis above. Thus in calculating the number of turns, take D at its maximum value, i.e. D = 0.75. The number of turns (3.41) is N_p = 9 turns, N_s = 9 turns.

The number of turns in the reset winding is

$$N_t = \frac{1-D}{D} N_p = \frac{1-0.75}{0.75}(9) = 3 \,.$$

3.4.2.3   Wire Sizes

The maximum temperature is $T_{max} = T_a + \Delta T = 25 + 50 = 75\,^\circ C$ where the ambient temperature T_a is assumed to be 25 °C. The current density (3.42) for the chosen core is $J = 4.862 \times 10^6 \, A/m^2$, based on the core and winding specifications in Table 3.9.

For the primary windings with D = 0.75, the RMS value of the voltage is $V_p = \sqrt{\frac{D}{1-D}} V_{dc} = \sqrt{3} \times 12$ V. The primary current and wire size are

$$I_p = \frac{P_o}{\eta k_{pp} V_p} = \frac{75}{(0.9)(0.5)\sqrt{3}(12)} = 8.02 \, A \,,$$

$$A_w = I_p / J = 8.02 / 4.862 = 1.65 \, mm^2 \ldots 1.45 \, mm \, diameter \,.$$

Select #15 AWG wire, with a 1.45 mm diameter and a DC resistance of 10.42 mΩ/m @ 20 °C (Table A.1). The secondary current and wire size are

$$I_s = \sqrt{D} I_o = \sqrt{0.75}(7.5) = 6.49 \, A \,,$$

$$A_w = I_s / J = 6.49 / 4.862 = 1.335 \, mm^2 \ldots 1.3 \, mm \, diameter \,.$$

Select #15 AWG wire, with a 1.45 mm diameter and a DC resistance of 10.42 mΩ/m @ 20 °C.

3.4.2.4   Copper Losses

For the primary winding, the losses are given by

$$R_p = MLT \times N \times [m\Omega / m @ 20\,°C \times 10^{-3}][1 + \alpha_{20}(T_{max} - 20)]$$
$$= (7.5 \times 10^{-2})(9)(10.42 \times 10^{-3})[1 + (0.00393)(75 - 20)] \times 10^3 \,,$$
$$= 8.55\,m\Omega$$

$$I_p{}^2 R_p = (8.02)^2(8.55 \times 10^{-3}) = 0.550\,W\,.$$

And for the secondary winding, we have

$$R_s = MLT \times N \times [m\Omega / m @ 20\,°C \times 10^{-3}][1 + \alpha_{20}(T_{max} - 20)]$$
$$= (7.5 \times 10^{-2})(9)(10.42 \times 10^{-3})[1 + (0.00393)(75 - 20)] \times 10^3 \,,$$
$$= 8.55\,m\Omega$$

$$I_s{}^2 R_s = (6.49)^2(8.55 \times 10^{-3}) = 0.360\,W\,.$$

3.4.2.5   High Frequency Effects

The losses given in 3.4.2.4 are DC values. At 25 kHz, the skin depth $\delta = 66\sqrt{25000} = 0.42$ mm; this is less than the radius of either the primary or secondary conductors so it increases the resistance. k_s is the correction factor for DC resistance to account for skin effect and is given by (3.46) as

$$R_{ac} = R_{dc}k_s = R_{dc}\left[1 + \frac{(r_o / \delta)^4}{48 + 0.8(r_o / \delta)}\right],$$

where r_o is the radius of a round conductor. For the primary winding, the losses are increased to

$$R_{P_{ac}} = R_{P_{dc}}k_s = 8.55\left[1 + \frac{(0.725 / 0.42)^4}{48 + 0.8(0.725 / 0.42)^4}\right],$$
$$= 9.93\,m\Omega$$

$$I_p^2 R_{p_{ac}} = (8.02^2)(9.93 \times 10^{-3}) = 0.638 \text{ W}.$$

And for the secondary,

$$R_{s_{ac}} = R_{s_{dc}} k_s = 9.93 \text{ m}\Omega,$$

$$I_s^2 R_{s_{ac}} = (6.49^2)(9.93 \times 10^{-3}) = 0.418 \text{ W}.$$

3.4.2.6   Core Losses

The core losses are (3.13)

$$\begin{aligned} P_{fe} &= m K_c f^\alpha B_m^\beta \\ &= (0.0604)(6.2 \times 10^{-3})(25 \times 10^3)^{1.13}(0.208)^{2.07}. \\ &= 1.353 \text{ W} \end{aligned}$$

This gives a total loss of

$$\begin{aligned} P_{tot} &= (P_{cu})_p + (P_{cu})_s + P_{fe} \\ &= 0.638 + 0.418 + 1.353. \\ &= 2.409 \text{ W} \end{aligned}$$

3.4.2.7   Efficiency

Finally, the efficiency of our design is now

$$\text{Efficiency} = \eta = \frac{75}{75 + 2.409} = 96.9\,\%.$$

Our initial specification included a desired efficiency of at least 90%; the predicted design value exceeds this specification value significantly.

3.4.3 Centre-Tapped Rectifier

We will now perform a low frequency design for a rectifier application that incorporates a centre-tapped transformer. Unlike the previous examples that operated in the kHz frequency range, this transformer operates at just 50 Hz. At lower frequencies, the optimum flux density will be limited by the saturation flux density of the core material, and we must therefore follow the path shown on the right of the Figure 3.10 flow chart.

SPECIFICATION	VALUE
Output	100 V_{rms}, 10 A_{rms}
Input	230 V_{rms}, Sinewave
Frequency, f	50 Hz
Temperature Rise, ΔT	50 ^{o}C
Ambient Temperature, T_a	25 ^{o}C
Efficiency, η	90%

Table 3.10. Centre-tapped rectifier specifications.

The centre-tapped rectifier transformer is shown in Figure 3.22. The waveform factor K = 4.44 for sinewave excitation.
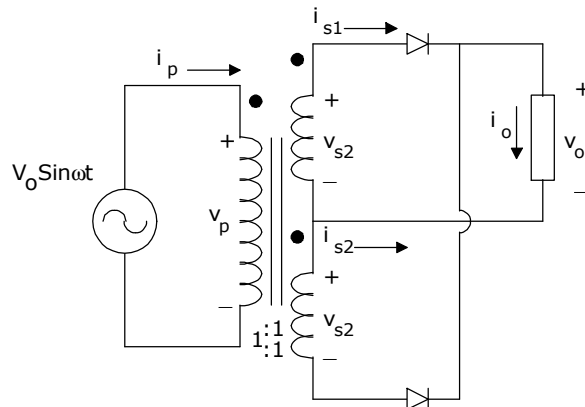
Figure 3.22. Centre-tapped rectifier circuit.
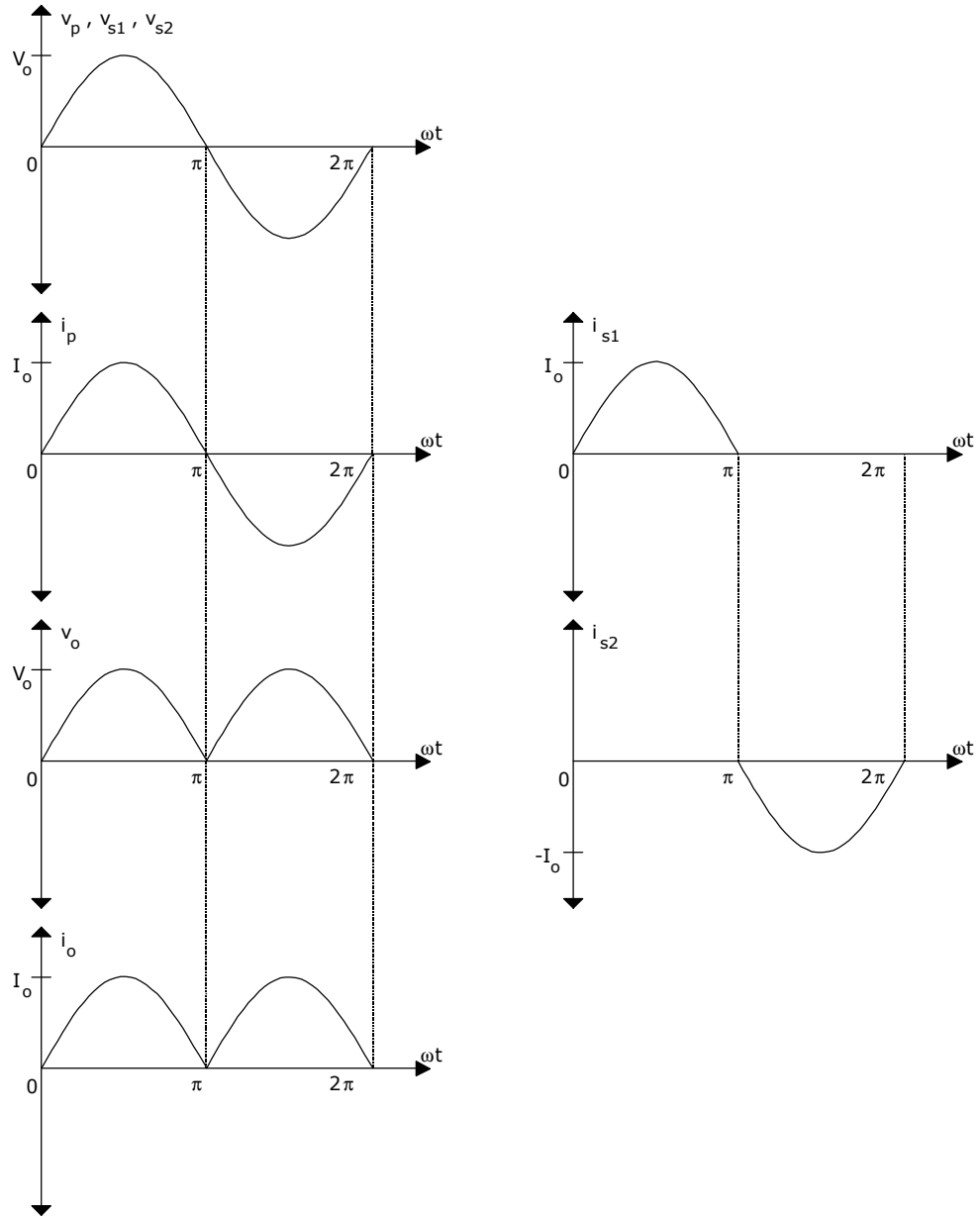
Figure 3.23. Centre-tapped rectifier waveforms.

The average power delivered through each winding is $\langle p \rangle = \dfrac{P_o}{2}$. For the secondary winding, the power for each winding is found from

$$V_{s1} = V_{s2} = \frac{V_o}{\sqrt{2}}, \; I_{s1} = I_{s2} = \frac{I_o}{2}, \tag{3.71}$$

$$\langle p \rangle = \frac{V_o I_o}{2\pi} \int_0^\pi \mathrm{Sin}^2(\omega t) d(\omega t)$$
$$= \frac{V_o I_o}{4}$$

(3.72)

We can then calculate the power factor and VA rating for each secondary winding as

$$k_p = \frac{\langle p \rangle}{V_s I_s} = \frac{1}{\sqrt{2}} \, ,$$

(3.73)

$$VA_s = \frac{\langle p \rangle}{k_p} = \sqrt{2}\langle p \rangle = \frac{P_o}{\sqrt{2}} \, .$$

(3.74)

For the primary windings, the power is given by

$$V_p = \frac{V_o}{\sqrt{2}}, \quad I_p = \frac{I_o}{\sqrt{2}}, \quad P_o = \frac{V_o I_o}{2} \, ,$$

(3.75)

yielding a power factor of

$$k_p = \frac{P_o}{V_p I_p} = 1 \, .$$

(3.76)

The total VA rating is then given by

$$\sum VA = \left(\frac{1}{\eta} + \frac{1}{\sqrt{2}} + \frac{1}{\sqrt{2}} \right) P_o$$
$$= \left(\frac{1}{\eta} + \sqrt{2} \right) P_o$$

(3.77)

3.4.3.1 Core Selection

Laminated grain oriented steel would normally be used for this type of application. The material specifications for 27 MOH laminated grain oriented steel are listed in Table 3.11.

SPECIFICATION	VALUE
K_c	0.5×10^{-3}
α	1.7
β	1.9
ρ_m	7650 kg/m³
B_{sat}	1.5 T

Table 3.11. 27 MOH grain oriented steel material specifications.

The output power of the transformer is $P_o = (100 + 1) \times 10 = 1010$ W, assuming a forward voltage drop of 1 V for each diode. The power factor and VA ratings of the windings were established in (3.77) giving

$$\sum VA = \left(\frac{1}{\eta k_{pp}} + \frac{1}{k_{ps}} \right) P_o = \left(\frac{1}{0.9} + 1.414 \right) 1010 = 2550 \text{ VA} .$$

The optimum flux density (3.34) is 3.6 T. Since $B_o > B_{sat}$, the design is saturation limited. On the 1st iteration, $B_m = 1.5$ T, and from (3.40) $A_{pi} = 1221$ cm⁴. On the 2nd iteration, from (3.38), $a_o = 5.201 \times 10^{11}$, $a_1 = 2.905 \times 10^{11}$, $a_2 = 366.498$ and from (3.39) $A_p = 908$ cm⁴.

A tape wound toroidal core, 0.27 mm BS grain oriented 27 MOH steel with 11 mils laminations, is suitable. The core data is given in Table 3.12.

SPECIFICATION	VALUE
A_c	19.5 cm²
W_a	50.2 cm²
A_p	979 cm⁴
M	5.3 kg
k_f	1.0
k_u	0.4
MLT	28 cm
ρ_{20}	1.72 μΩ-cm
α_{20}	0.00393

Table 3.12. Centre-tapped rectifier core and winding specifications.

3.4.3.2 Turns

From (3.41), the primary turns are found to be

$$N_p = \frac{V_p}{KB_m A_c f} = \frac{230}{(4.44)(1.5)(19.5 \times 10^{-4})(50)} = 354 \text{ turns}.$$

The RMS value of each secondary voltage is (100 + 1) = 101 V, which includes a 1 V forward voltage drop in the diode. The secondary turns are then

$$N_s = N_p \frac{V_s}{V_p} = 354 \frac{101}{230} = 155 \text{ turns}.$$

3.4.3.3 Wire Sizes

The maximum temperature is $T_{max} = T_a + \Delta T = 25 + 50 = 75\,^\circ C$ where the ambient temperature T_a is assumed to be 25 °C. The current density (3.42) for the chosen core is $J = 2.224 \times 10^6 \text{ A/m}^2$, based on the core and winding specifications in Table 3.12.

The primary wire sizes are found as follows:

$$I_p = \frac{P_o}{\eta k_{pp} V_p} = \frac{1010}{(0.9)(1)(230)} = 4.88 \text{ A},$$

$$A_w = I_p / J = 4.88 / 2.224 = 2.194 \text{ mm}^2 \dots 1.67 \text{ mm diameter}.$$

Select #13 AWG wire, with a 1.83 mm diameter and a DC resistance of 6.54 mΩ/m @ 20 °C (Table A.1).

The RMS value of the load current, which is a full wave rectified sinewave, is 10 A. The current appears in each secondary winding as a half wave

rectified sinewave as shown in Figure 3.23. From Table 3.3 (D = 0.5), $I_{s1rms} = I_{s2rms} = 10/2 = 5$ A. The secondary wire sizes are then given by

$$I_s = 5\,A\,,$$

$$A_w = I_s / J = 5 / 2.224 = 2.248\,mm^2 \ldots 1.69\,mm\,diameter\,.$$

This is a rather large conductor (#13 AWG). Such a large conductor may be difficult to wind. An alternative is to use two parallel conductors with the same combined areas:

$$A_w = 2.248 / 2 = 1.124\,mm^2 \ldots 1.2\,mm\,diameter\,.$$

Select #16 AWG wire, with a 1.29 mm diameter and a DC resistance of 13.16 mΩ/m @ 20 °C.

3.4.3.4 Copper Losses

The primary copper losses are given by

$$\begin{aligned}
R_p &= MLT \times N \times [m\Omega / m\ @\ 20\,°C \times 10^{-3}][1 + \alpha_{20}(T_{max} - 20)] \\
&= (28 \times 10^{-2})(354)(6.54 \times 10^{-3})[1 + (0.00393)(75 - 20)] \quad, \\
&= 0.788\,\Omega
\end{aligned}$$

$$I_p{}^2 R_p = (4.88)^2(0.788) = 18.8\,W\,.$$

The secondary copper losses are given by

$$\begin{aligned}
R_s &= MLT \times N \times [m\Omega / m\ @\ 20\,°C \times 10^{-3}][1 + \alpha_{20}(T_{max} - 20)] \\
&= (28 \times 10^{-2})(155)(13.16 \times 10^{-3} / 2)[1 + (0.00393)(75 - 20)], \\
&= 0.348\,\Omega
\end{aligned}$$

$$I_s{}^2 R_s = (5)^2(0.348 \times 2) = 17.4\,W\,.$$

Recall the secondary is two #16 AWG wires in parallel, but there are two secondary windings.

3.4.3.5 High Frequency Effects

The skin depth at 50 Hz in copper is $\delta = 66\sqrt{50} = 9.3$ mm, and therefore does not create additional losses.

3.4.3.6 Core Losses

The core losses are (3.13)

$$\begin{aligned}
P_{fe} &= mK_c f^{\alpha} B_m{}^{\beta} \\
&= (5.3)(0.5\times 10^{-3})(50)^{1.7}(1.5)^{1.9} = 4.43 \text{ W}
\end{aligned}$$

This gives a total loss of

$$\begin{aligned}
P_{tot} &= (P_{cu})_p + (P_{cu})_s + P_{fe} \\
&= 18.8 + 17.4 + 4.4 \\
&= 40.6 \text{ W}
\end{aligned}$$

3.4.3.7 Efficiency

The efficiency is therefore

$$\text{Efficiency} = \eta = \frac{1010}{1010 + 40.6} = 96.1\,\%.$$

From the above example, it is particularly evident that the assumption of copper losses and core losses being roughly equal does not hold for cases where the flux density is limited by its saturation value. In this design, the ratio of copper to core losses is actually around 8:1.

3.5   Summary

A new methodology for designing transformers has been described. The model takes account of switching type waveforms encountered in switching mode power supplies, inclusive of high frequency skin and proximity effects. The selection of the core has been optimised to minimise the core and winding losses. Accurate approximations have been provided to facilitate calculations.

The design procedure has been illustrated with the full design of a push-pull converter, a forward converter, and a centre-tapped rectifier, thus underlining the generality of the approach. The high frequency push-pull converter incorporates an EE core and foil windings, and proximity effect losses are taken into account. The forward converter design example utilises a pot core with round wire windings, and includes high frequency AC losses due to the skin effect. These first two examples are designed for minimised total losses at an optimum flux density, with the winding losses approximately equal to the core losses. The 50 Hz centre-tapped transformer does not suffer from high frequency losses, but its winding losses are much larger than the core losses due to the fact that the optimum design point is limited by the saturation flux density of the core material.

The methodology is eminently suitable for use in a computer application in conjunction with a database of core materials. We will demonstrate this in Chapter 5.

Chapter 4

OPTIMISING THE WINDING

4.1   Introduction

T he optimum thickness of a layer in a constant thickness multilayered transformer winding with non-sinusoidal excitation was traditionally found using the following method:

- Calculate the Fourier coefficients of the waveform.
- Calculate the AC winding losses at each harmonic frequency component.
- Calculate the total losses for each thickness in a range of values.
- Read the optimum layer thickness from a graph of AC winding loss versus layer thickness.

Typically this might involve loss calculations at up to 30 harmonics for up to 100 thickness values in order to find the optimum value. Furthermore, Fourier coefficients are only available for a few waveforms, and these are generally only approximations to the waveforms encountered in practice.

In this chapter, we will show how the traditional Fourier analysis method can be used to calculate the optimum thickness of a winding for a particular waveform.

We will then present formulas for the AC resistance (proportional to AC loss) and the optimum layer thickness for any current waveform using two new methods, and we will show that the results are just as accurate as the cumbersome method based on Fourier analysis.

In the first new method, referred to as the RMS values method, the optimum thickness formulas presented only require knowledge of the RMS value of the current waveform and the RMS value of its derivative.

Both these quantities can be easily measured or calculated with simulation programs such as PSPICE.

The second new method, based on regression analysis, presents more complicated optimum thickness formulas involving harmonic summations. These formulas may not be as elegant as those derived using the RMS values method, but they can be as accurate.

We will conclude with a comparison of values obtained using the three methods outlined in this chapter: the traditional method and the two new methods.

4.2   Fourier Analysis

Appendix B contains a Fourier analysis of the current waveforms we will be considering:

1. *Sine Wave*
2. *Duty Cycle Varying Rectified Sine Wave*
3. *Duty Cycle Varying Bipolar Sine Wave*
4. *Duty Cycle Varying Square Wave*
5. *Duty Cycle Varying Rectified Square Wave*
6. *Duty Cycle Varying Bipolar Square Wave*
7. *Duty Cycle Varying Triangle Wave*
8. *Duty Cycle Varying Rectified Triangle Wave*
9. *Duty Cycle Varying Bipolar Triangle Wave*

Sinusoidal waveforms (numbers 1, 2) are traditionally found in centre-tapped transformers and other rectifiers. The rectified square (number 5) is typically found in single ended or half-wave DC-DC converters, for example in the windings of forward, flyback or Weinberg converters. Bipolar square waves (number 6) are sometimes used in full or half bridge converters. Triangular current waveforms (numbers 7, 8) are commonly found in filter chokes, and buck, boost and buck-boost regulators.

To calculate the AC resistance for a particular waveform, we need to find expressions for the average value of current, I_{dc}, the RMS value of the waveform, I_{rms}, and the RMS value of the nth harmonic, I_n. These are related to the Fourier coefficients, which are derived for each of the waveforms in Appendix B. We then minimise the R_{eff}/R_δ AC resistance factor (4.1) to yield the optimum winding thickness Δ for the waveform under analysis. These terms will be explained in more detail in section 4.3.1. For now, it is enough to know that R_{eff}/R_δ is the ratio of the effective AC resistance of the winding with normalised layer thickness Δ and p layers to the DC resistance of a similar winding having a layer thickness of skin depth δ:

$$\frac{R_{eff}}{R_\delta} = \frac{I_{dc}^2 + \sum_{n=1}^{\infty} \sqrt{n}\Delta \left[\frac{Sinh(2\sqrt{n}\Delta)+Sin(2\sqrt{n}\Delta)}{Cosh(2\sqrt{n}\Delta)-Cos(2\sqrt{n}\Delta)} + \frac{2(p^2-1)}{3}\frac{Sinh(\sqrt{n}\Delta)-Sin(\sqrt{n}\Delta)}{Cosh(\sqrt{n}\Delta)+Cos(\sqrt{n}\Delta)} \right] I_n^2}{\Delta I_{rms}^2} . \quad (4.1)$$

After substituting the expressions for I_{dc}, I_n and I_{rms} corresponding to a particular waveform, R_{eff}/R_δ must be calculated for a range of thicknesses Δ. To find the optimum Δ, we then plot R_{eff}/R_δ and read off its minimum point. This method has been performed for each waveform in Appendix B, and the results are given in Table 4.1.

WAVEFORM NO.	OPTIMUM THICKNESS
1	0.539
2	0.490
3	0.348
4 I	0.381
5 I	0.435
6 I	0.358
4 II	0.429
5 II	0.416
6 II	0.328
7	0.515
8	0.469
9	0.333

Table 4.1. Optimum thicknesses using Fourier, p = 6, D = 0.4, t_r/T = 4%.

4.3   RMS Values Method

We will now present a unified approach which gives optimum thickness formulas for bipolar rectangular, triangular and sinusoidal waveforms and their rectified equivalents, with variable duty cycle, as illustrated in Table 4.2.

4.3.1   The AC Resistance

Normalisation, a concept new to most electronic engineers, but familiar to mathematicians and physicists, is introduced in order to analyse magnetic components of varying characteristics and sizes. This is a keystone of the optimisation analysis.

Triangles are said to be similar if they have equal angles, even if some are larger or smaller than others. Let us say that we wish to discuss the general class of all similar right-angled triangles. We take the larger triangles and scale them down to the size of a standard triangle of unit height. We also take the smaller triangles and scale them up to the size of our standard triangle. The standard unit height triangle is said to be the normalised size; all our different triangles have been normalised, and the process is called *normalisation*. We keep track of the scaling factor by which we multiplied each of our original triangles in order to normalise them, so that when we have finished studying the different triangles we can return them to their original sizes. The dimensions of each triangle are multiplied by the reciprocal of its corresponding scaling factor. This is called *denormalisation*, and marks a return to the original, real-world size. The reciprocal of the scaling factor is called the denormalisation factor.

This is an extremely powerful mathematical tool. It allows us to easily obtain a much deeper understanding of how to go about designing a magnetic component, and why some designs are better than others.

In our case, we wish to normalise the thickness of a transformer winding so that we can see the effect of varying the thickness on the resistance of a winding, without having to worry about the particular frequency we are operating at.

Δ is a normalised variable, and is equal to the ratio of the actual layer thickness d (in metres) to the skin depth δ_o (a variable related to the operating frequency). Our scaling factor is therefore the reciprocal of skin depth. On denormalisation, we multiply Δ by the skin depth and return to a winding that is measured in metres.

$$d = \sqrt{\frac{\pi}{4}}D \qquad \eta_1 = \frac{Md}{w} \qquad \eta_2 = \frac{w_f}{w}$$

$$\sigma_w = \eta_i \sigma$$
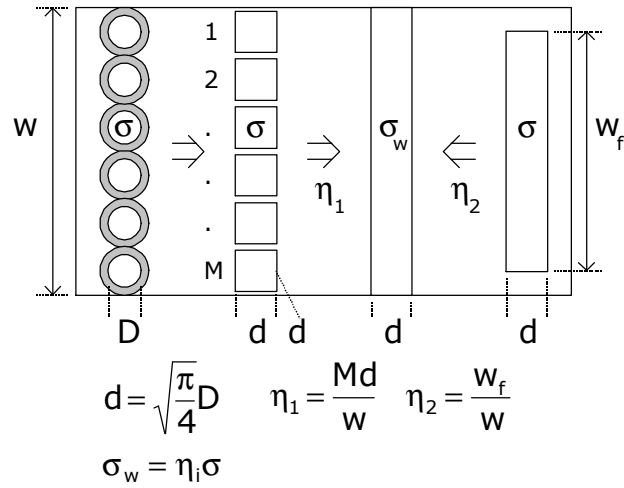
Figure 4.1. Porosity factor for foils and round conductors.

The solution of the diffusion equation for cylindrical windings has already been detailed in Chapter 2. The asymptotic expansion of the Bessel functions in the solution leads to the AC resistance of a coil with p layers, under sinusoidal excitation. The real part of (2.36) gives the AC to DC resistance factor (2.39):

$$\frac{R_{ac}}{R_{dc}} = \Delta \left[\frac{\text{Sinh}(2\Delta) + \text{Sin}(2\Delta)}{\text{Cosh}(2\Delta) - \text{Cos}(2\Delta)} + \frac{2(p^2 - 1)}{3} \frac{\text{Sinh}(\Delta) - \text{Sin}(\Delta)}{\text{Cosh}(\Delta) + \text{Cos}(\Delta)} \right]. \quad (4.2)$$

Equation (4.2) is a very good approximation to the original cylindrical solution, particularly if the layer thickness is less than 10% of the radius of curvature. Windings which consist of round conductors, or foils which do not extend the full winding window, may be treated as foils with equivalent thickness d and effective conductivity $\sigma_w = \eta\sigma$. This

105

calculation is shown graphically in Figure 4.1; a detailed treatment of wire conductors is given by [29] and [51]. The orthogonality of skin and proximity effects in wire windings is described by [29].

The trigonometric and hyperbolic functions in (4.2) can be approximated using Taylor series. Let us define the two halves of (4.2) as y_1 and y_2,

$$
\begin{aligned}
y_1 &= \frac{\mathrm{Sinh}(2\Delta) + \mathrm{Sin}(2\Delta)}{\mathrm{Cosh}(2\Delta) - \mathrm{Cos}(2\Delta)} \\
y_2 &= \frac{\mathrm{Sinh}(\Delta) - \mathrm{Sin}(\Delta)}{\mathrm{Cosh}(\Delta) + \mathrm{Cos}(\Delta)}
\end{aligned} \qquad (4.3)
$$

Firstly, we shall state the Taylor series expansions for the trigonometric functions below:

$$
\begin{aligned}
\mathrm{Cos}(\Delta) &\approx 1 - \frac{\Delta^2}{2!} + \frac{\Delta^4}{4!} - \frac{\Delta^6}{6!} + \frac{\Delta^8}{8!} - \frac{\Delta^{10}}{10!} \\
\mathrm{Cosh}(\Delta) &\approx 1 + \frac{\Delta^2}{2!} + \frac{\Delta^4}{4!} + \frac{\Delta^6}{6!} + \frac{\Delta^8}{8!} + \frac{\Delta^{10}}{10!} \\
\mathrm{Sin}(\Delta) &\approx \Delta - \frac{\Delta^3}{3!} + \frac{\Delta^5}{5!} - \frac{\Delta^7}{7!} + \frac{\Delta^9}{9!} - \frac{\Delta^{11}}{11!} \\
\mathrm{Sinh}(\Delta) &\approx \Delta + \frac{\Delta^3}{3!} + \frac{\Delta^5}{5!} + \frac{\Delta^7}{7!} + \frac{\Delta^9}{9!} + \frac{\Delta^{11}}{11!}
\end{aligned} \qquad (4.4)
$$

Using these expressions in y_1 yields

$$
\begin{aligned}
y_1 &= \frac{\mathrm{Sinh}(2\Delta) + \mathrm{Sin}(2\Delta)}{\mathrm{Cosh}(2\Delta) - \mathrm{Cos}(2\Delta)} \\
&\approx \frac{\left[\begin{array}{l} 2\Delta + \dfrac{(2\Delta)^3}{3!} + \dfrac{(2\Delta)^5}{5!} + \dfrac{(2\Delta)^7}{7!} + \dfrac{(2\Delta)^9}{9!} + \dfrac{(2\Delta)^{11}}{11!} \\[2mm] + 2\Delta - \dfrac{(2\Delta)^3}{3!} + \dfrac{(2\Delta)^5}{5!} - \dfrac{(2\Delta)^7}{7!} + \dfrac{(2\Delta)^9}{9!} - \dfrac{(2\Delta)^{11}}{11!} \end{array}\right]}{\left[\begin{array}{l} 1 + \dfrac{(2\Delta)^2}{2!} + \dfrac{(2\Delta)^4}{4!} + \dfrac{(2\Delta)^6}{6!} + \dfrac{(2\Delta)^8}{8!} + \dfrac{(2\Delta)^{10}}{10!} \\[2mm] -1 + \dfrac{(2\Delta)^2}{2!} - \dfrac{(2\Delta)^4}{4!} + \dfrac{(2\Delta)^6}{6!} - \dfrac{(2\Delta)^8}{8!} + \dfrac{(2\Delta)^{10}}{10!} \end{array}\right]} \\[3mm]
&= \frac{4\Delta + \dfrac{2^6\,\Delta^5}{5!} + \dfrac{2^{10}\,\Delta^9}{9!}}{2^3\,\Delta^2\big/2! + 2^7\,\Delta^6\big/6! + 2^{11}\,\Delta^{10}\big/10!}
\end{aligned} \qquad (4.5)
$$

106

Similarly, we can apply the same method to the expression for y_2,

$$y_2 = \frac{\text{Sinh}(\Delta) - \text{Sin}(\Delta)}{\text{Cosh}(\Delta) + \text{Cos}(\Delta)}$$

$$\approx \frac{\left[\begin{array}{l} \Delta + \dfrac{\Delta^3}{3!} + \dfrac{\Delta^5}{5!} + \dfrac{\Delta^7}{7!} + \dfrac{\Delta^9}{9!} + \dfrac{\Delta^{11}}{11!} \\[2mm] -\Delta + \dfrac{\Delta^3}{3!} - \dfrac{\Delta^5}{5!} + \dfrac{\Delta^7}{7!} - \dfrac{\Delta^9}{9!} + \dfrac{\Delta^{11}}{11!} \end{array}\right]}{\left[\begin{array}{l} 1 + \dfrac{\Delta^2}{2!} + \dfrac{\Delta^4}{4!} + \dfrac{\Delta^6}{6!} + \dfrac{\Delta^8}{8!} + \dfrac{\Delta^{10}}{10!} \\[2mm] +1 - \dfrac{\Delta^2}{2!} + \dfrac{\Delta^4}{4!} - \dfrac{\Delta^6}{6!} + \dfrac{\Delta^8}{8!} - \dfrac{\Delta^{10}}{10!} \end{array}\right]}$$

$$= \frac{\dfrac{2\Delta^3}{3!} + \dfrac{2\Delta^7}{7!} + \dfrac{2\Delta^{11}}{11!}}{2 + \dfrac{2\Delta^4}{4!} + \dfrac{2\Delta^8}{8!}} \qquad . \tag{4.6}$$

After division of the numerators by the denominators in (4.5) and (4.6), the trigonometric and hyperbolic functions in (4.2) may therefore be represented by the series expansions:

$$\frac{\text{Sinh}2\Delta + \text{Sin}2\Delta}{\text{Cosh}2\Delta - \text{Cos}2\Delta} \approx \frac{1}{\Delta} + \frac{4}{45}\Delta^3 - \frac{16}{4725}\Delta^7 + O(\Delta^{11}), \tag{4.7}$$

$$\frac{\text{Sinh}\Delta - \text{Sin}\Delta}{\text{Cosh}\Delta + \text{Cos}\Delta} \approx \frac{1}{6}\Delta^3 - \frac{17}{2520}\Delta^7 + O(\Delta^{11}). \tag{4.8}$$

If only terms up to the order of Δ^3 are used, the relative error incurred in (4.7) is less than 1.2% for $\Delta < 1.2$, and the relative error in (4.8) is less than 4.1% for $\Delta < 1.0$ and is less than 8.4% if $\Delta < 1.2$. The asymptotic values of the functions on the left hand side of (4.7) and (4.8) are 1 for $\Delta > 2.5$. Terms up to the order of Δ^3 are sufficiently accurate to account for the Fourier harmonics which are used to predict the optimum value of Δ (which is normally in the range 0.3 to 1.0).

Thus (4.2) becomes [97]

$$\frac{R_{ac}}{R_{dc}} = 1 + \frac{\Psi}{3}\Delta^4, \tag{4.9}$$

where

$$\Psi = \frac{5p^2 - 1}{15}. \tag{4.10}$$

An arbitrary periodic current waveform may be represented by its Fourier Series

$$i(t) = I_{dc} + \sum_{n=1}^{\infty} a_n \mathrm{Cos}(n\omega t) + b_n \mathrm{Sin}(n\omega t). \tag{4.11}$$

The sine and cosine terms may be combined to give an alternative form:

$$i(t) = I_{dc} + \sum_{n=1}^{\infty} c_n \mathrm{Cos}(n\omega t + \varphi_n), \tag{4.12}$$

where I_{dc} is the DC value of i(t) and c_n is the amplitude of the nth harmonic with corresponding phase φ_n. The RMS value of the nth harmonic is $I_n = c_n/\sqrt{2}$. The total power loss due to all the harmonics is

$$P = R_{dc}I_{dc}{}^2 + R_{dc}\sum_{n=1}^{\infty} k_{p_n} I_n{}^2, \tag{4.13}$$

where R_{dc} is the DC resistance of a foil winding of thickness d, and k_{p_n} is the AC resistance factor at the nth harmonic frequency, which may be found from (4.2):

$$k_{p_n} = \sqrt{n}\Delta\left[\frac{\mathrm{Sinh}(2\sqrt{n}\Delta) + \mathrm{Sin}(2\sqrt{n}\Delta)}{\mathrm{Cosh}(2\sqrt{n}\Delta) - \mathrm{Cos}(2\sqrt{n}\Delta)} + \frac{2(p^2 - 1)}{3}\frac{\mathrm{Sinh}(\sqrt{n}\Delta) - \mathrm{Sin}(\sqrt{n}\Delta)}{\mathrm{Cosh}(\sqrt{n}\Delta) + \mathrm{Cos}(\sqrt{n}\Delta)}\right]. \tag{4.14}$$

R_{eff} is the AC resistance due to i(t) so that $P = R_{eff}I_{rms}^2$, I_{rms} being the RMS value of i(t). Thus the ratio of effective AC resistance to DC resistance is

$$\frac{R_{eff}}{R_{dc}} = \frac{I_{dc}^2 + \sum_{n=1}^{\infty} k_{p_n} I_n^2}{I_{rms}^2} . \qquad (4.15)$$

The skin depth at the nth harmonic is $\delta_n = \delta_o/\sqrt{n}$ and, from (4.9), the AC resistance factor at the nth harmonic frequency is

$$k_{p_n} = 1 + \frac{\Psi}{3} n^2 \Delta^4 . \qquad (4.16)$$

Substituting (4.16) into (4.15) yields

$$\frac{R_{eff}}{R_{dc}} = \frac{I_{dc}^2 + \sum_{n=1}^{\infty} I_n^2 + \frac{\Psi}{3} \Delta^4 \sum_{n=1}^{\infty} n^2 I_n^2}{I_{rms}^2} . \qquad (4.17)$$

The RMS value of the current in terms of its harmonics is

$$I_{rms}^2 = I_{dc}^2 + \sum_{n=1}^{\infty} I_n^2 . \qquad (4.18)$$

The derivative of i(t) in (4.12) is

$$\frac{di}{dt} = -\omega \sum_{n=1}^{\infty} n c_n \mathrm{Sin}(n\omega t + \phi_n) , \qquad (4.19)$$

and the RMS value of the derivative of the current is [100]

$$I'_{rms}^2 = \omega^2 \sum_{n=1}^{\infty} \frac{n^2 c_n^2}{2} = \omega^2 \sum_{n=1}^{\infty} n^2 I_n^2 , \qquad (4.20)$$

which, upon substitution into (4.17) using (4.18), yields

$$\frac{R_{eff}}{R_{dc}} = 1 + \frac{\Psi}{3}\Delta^4 \left[\frac{I'_{rms}}{\omega I_{rms}}\right]^2.$$ (4.21)

This is a straightforward expression for the effective resistance of a winding with an arbitrary current waveform and it may be evaluated without knowledge of the Fourier coefficients of the waveform.

4.3.2   The Optimum Conditions

There is an optimum value of d which gives a minimum value of effective AC resistance. Define R_δ as the resistance of a foil of thickness δ_o such that

$$\frac{R_\delta}{R_{dc}} = \frac{d}{\delta_o} = \Delta,$$ (4.22)

which implies that

$$\frac{R_{eff}}{R_{dc}} = \Delta\frac{R_{eff}}{R_\delta}.$$ (4.23)

Evidently, a plot of R_{eff}/R_δ versus Δ has the same shape as a plot of R_{eff} versus d at a given frequency. A typical 3-D plot of R_{eff}/R_δ versus Δ with p, the number of winding layers, on the third axis is shown in Figure 4.2.

For each value of p there is an optimum value of Δ where the AC resistance of the winding is minimum. These optimum points lie on the line marked minima in the graph of Figure 4.2, and the corresponding value of the optimum layer thickness is

$$d_{opt} = \Delta_{opt}\delta_o.$$ (4.24)
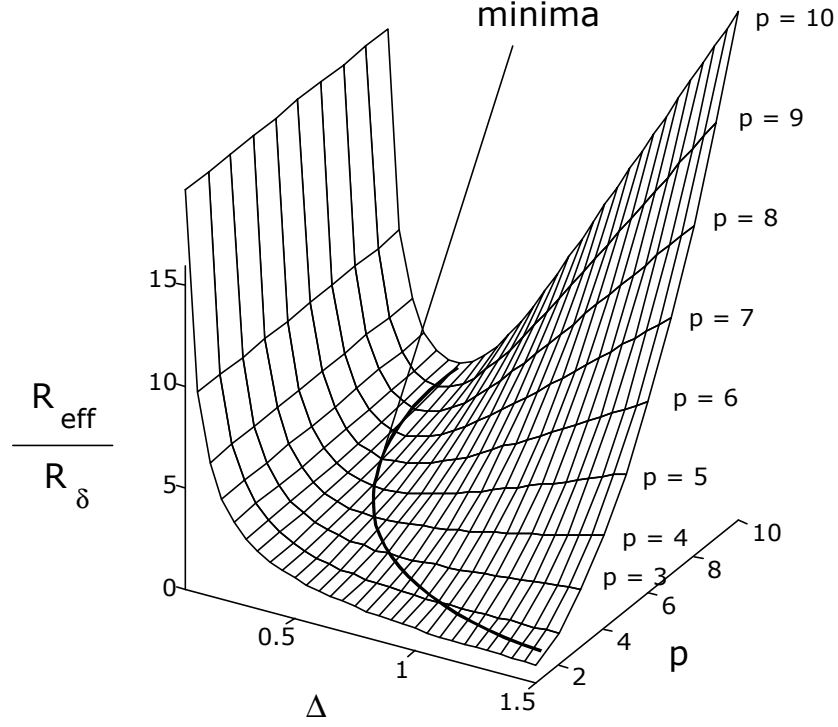
Figure 4.2. Plot of AC resistance versus Δ and number of layers p.

From (4.23), using (4.21) [15],

$$\frac{R_{eff}}{R_{\delta}} = \frac{1}{\Delta} + \frac{\Psi}{3}\Delta^3 \left[\frac{I'_{rms}}{\omega I_{rms}}\right]^2 .$$

(4.25)

The optimum value of Δ is found by taking the derivative of (4.25) and setting it to zero.

$$\frac{d}{d\Delta}\left(\frac{R_{eff}}{R_{\delta}}\right) = -\frac{1}{\Delta^2} + \Psi\Delta^2\left[\frac{I'_{rms}}{\omega I_{rms}}\right]^2 = 0 .$$

(4.26)

The optimum value of Δ is

$$\Delta_{opt} = \frac{1}{\sqrt[4]{\Psi}}\sqrt{\frac{\omega I_{rms}}{I'_{rms}}} .$$

(4.27)

A variation on this formula is given by [34]. For a sinusoidal current waveform,

111

$$I'_{rms}{}^2 = \omega^2 \sum_{n=1}^{\infty} n^2 I_n{}^2 = \omega^2 1^2 \left(\frac{I_o}{\sqrt{2}}\right)^2 ,$$

$$I_{rms}{}^2 = \left(\frac{I_o}{\sqrt{2}}\right)^2$$

(4.28)

and with large p (so that $5p^2 >> 1$), we get [85]

$$\Delta_{opt} = \frac{1}{\sqrt[4]{p^2/3}} = \frac{3^{1/4}}{\sqrt{p}} .$$

(4.29)

Substituting (4.27) into (4.21) yields the optimum value of the effective AC resistance with an arbitrary periodic current waveform:

$$\left(\frac{R_{eff}}{R_{dc}}\right)_{opt} = \frac{4}{3} .$$

(4.30)

[51] and [97] have already established this result for sinusoidal excitation. The corresponding value for wire conductors with sinusoidal excitation is 3/2.

We may also write (4.21) in term of Δ_{opt} as follows ($R_{eff}/R_{dc} \propto f^2$):

$$\frac{R_{eff}}{R_{dc}} = 1 + \frac{1}{3}\left(\frac{\Delta}{\Delta_{opt}}\right)^4 .$$

(4.31)

We now have a set of simple formulas with which to find the optimum value of the foil or layer thickness of a winding and its effective AC resistance; these formulas are based on the RMS value of the current waveform and the RMS value of its derivative.

4.3.3   Validation

Consider the pulsed current waveform in Figure 4.3 along with its derivative, which is typical of a forward converter.
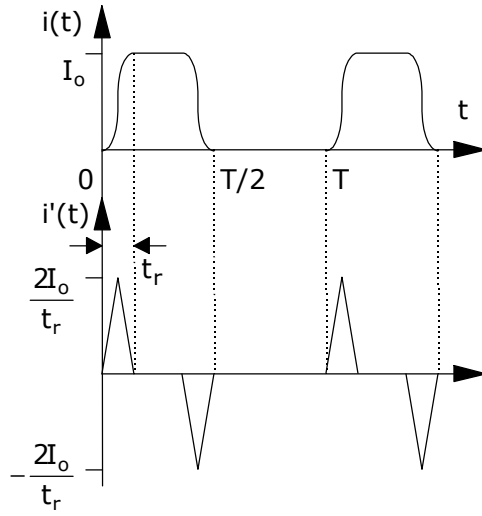
Figure 4.3. Pulsed wave and its derivative.

This waveform has a Fourier series

$$
\begin{aligned}
i(t) = I_o\left(\frac{1}{2} - \frac{t_r}{T}\right) + \sum_{n=1}^{\infty} \frac{4I_o}{n^3\pi^3\left(\dfrac{t_r}{T}\right)^2}\left[1 - Cos\left(\frac{n\pi t_r}{T}\right)\right] \\
\times Sin\left(n\pi\left(\frac{1}{2} - \frac{t_r}{T}\right)\right)Cos\left(n\left(\omega t - \frac{\pi}{2}\right)\right)
\end{aligned}
$$
. (4.32)

The RMS value of i(t) and the the RMS value of its derivative are

$$
I_{rms} = I_o\sqrt{0.5 - \frac{37 t_r}{30 T}}
$$
. (4.33)
$$
I'_{rms} = I_o\sqrt{\frac{8}{3 t_r T}}
$$

The optimum value of Δ given by the Fourier series (4.32) along with (4.14), (4.15) and (4.23), for p = 6 and t_r/T = 4% is 0.418. The value given by the proposed formula (4.27)

$$\Delta_{opt} = \frac{1}{\sqrt[4]{\frac{5p^2 - 1}{15}}} \sqrt{\frac{\left(\frac{2\pi}{T}\right) I_o \sqrt{0.5 - \frac{37t_r}{30T}}}{I_o \sqrt{\frac{8}{3t_r T}}}} \, , \tag{4.34}$$

is 0.387 which represents an error of

$$\varepsilon = \frac{0.418 - 0.387}{0.418} = 7.4\% \, . \tag{4.35}$$

Waveform 5 in Table 4.2 is an approximation to the pulse in Figure 4.3 and the optimum value of Δ using Fourier analysis is 0.448 which represents an error of

$$\varepsilon = \frac{0.418 - 0.448}{0.418} = -7.2\% \, , \tag{4.36}$$

when compared to the Fourier analysis of the waveform given by (4.32). Evidently waveforms with known Fourier series are often approximations to the actual waveform and can give rise to errors which are of the same order as the proposed formula, which is simpler to evaluate.

At 50 kHz, the skin depth in copper is 0.295 mm. With $\Delta_{opt} = 0.418$, $d_{opt} = 0.295 \times 0.418 = 0.123$ mm.

The proposed formula may be validated by comparing the value of Δ_{opt} obtained from (4.27) with the value obtained in section 4.2 from Fourier analysis (found by plotting R_{eff}/R_δ, using (4.23) along with (4.14) and (4.15), over a range of values of Δ and finding the optimum value). The results are shown in Table 4.3 for the waveforms in Table 4.2. In general the agreement is within 3%, with the exception of waveform 5 where the error is 6.5%. For the Fourier analysis, 19 harmonics were evaluated and R_{eff}/R_δ was calculated for 20 values of Δ. This means that (4.14) was computed 380 times for each waveform in order to find the optimum layer thickness, whereas (4.27) was computed once for the same result. For 1 to 3 layers the accuracy of the proposed formula is not very good, however,

as evidenced by Figure 4.2, the plot of R_{eff}/R_δ is almost flat in the region of the optimum value of Δ, and therefore the error in the AC resistance is negligible.
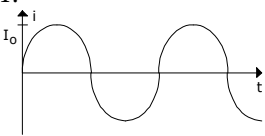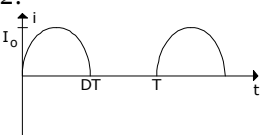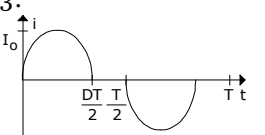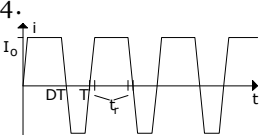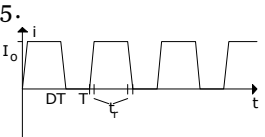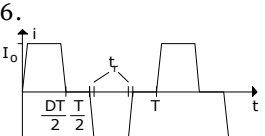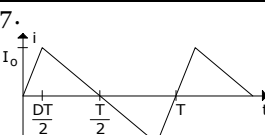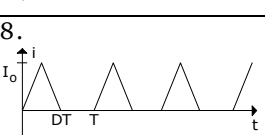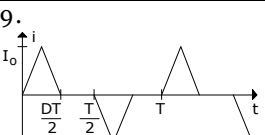
CURRENT WAVEFORM	I_{rms} AND I_{rms}'	FOURIER SERIES, i(t)	Δ_{opt}
1.	$I_{rms} = \dfrac{I_o}{\sqrt{2}}$ $I_{rms}' = \dfrac{2\pi}{T\sqrt{2}}I_o$	$I_o \mathrm{Sin}(\omega t)$	$\Delta_{opt} = \sqrt[4]{\dfrac{1}{\Psi}}$
2.	$I_{rms} = I_o\sqrt{\dfrac{D}{2}}$ $I_{rms}' = I_o\dfrac{\pi}{DT}\sqrt{\dfrac{D}{2}}$	$\dfrac{2DI_o}{\pi} + \sum_{n=1}^{\infty}\dfrac{4DI_o}{\pi}\left\{\dfrac{\mathrm{Cos}(n\pi D)}{\left(1-4n^2D^2\right)}\right\}\mathrm{Cos}(n\omega t)$ ♦	$\Delta_{opt} = \sqrt[4]{\dfrac{4D^2}{\Psi}}$
3.	$I_{rms} = I_o\sqrt{\dfrac{D}{2}}$ $I_{rms}' = I_o\dfrac{2\pi}{DT}\sqrt{\dfrac{D}{2}}$	$\sum_{n=1,odd}^{\infty}\dfrac{4DI_o}{\pi}\left\{\dfrac{\mathrm{Cos}(n\pi D/2)}{\left(1-n^2D^2\right)}\right\}\mathrm{Cos}(n\omega t)$ ♦	$\Delta_{opt} = \sqrt[4]{\dfrac{D^2}{\Psi}}$
4.	$I_{rms} = I_o\sqrt{1-\dfrac{8t_r}{3T}}$ $I_{rms}' = I_o\sqrt{\dfrac{4}{t_rT}}$	$I_o(2D-1)+\sum_{n=1}^{\infty}\dfrac{4I_o}{n\pi}\mathrm{Sin}(n\pi D)$ $\times\mathrm{Sinc}\left(n\pi\dfrac{2t_r}{T}\right)\mathrm{Cos}(n\omega t)$	$\Delta_{opt} = \sqrt[4]{\dfrac{\left[1-\dfrac{8t_r}{3T}\right]\pi^2\dfrac{t_r}{T}}{\Psi}}$
5.	$I_{rms} = I_o\sqrt{D-\dfrac{4t_r}{3T}}$ $I_{rms}' = I_o\sqrt{\dfrac{2}{t_rT}}$	$I_o\left(D-\dfrac{t_r}{T}\right)+\sum_{n=1}^{\infty}\dfrac{2I_o}{n\pi}\mathrm{Sin}\left(n\pi\left(D-\dfrac{t_r}{T}\right)\right)$ $\times\mathrm{Sinc}\left(n\pi\dfrac{t_r}{T}\right)\mathrm{Cos}(n\omega t)$	$\Delta_{opt} = \sqrt[4]{\dfrac{\left[D-\dfrac{4t_r}{3T}\right]2\pi^2\dfrac{t_r}{T}}{\Psi}}$
6.	$I_{rms} = I_o\sqrt{D-\dfrac{8t_r}{3T}}$ $I_{rms}' = I_o\sqrt{\dfrac{4}{t_rT}}$	$\sum_{n=1,odd}^{\infty}\dfrac{4I_o}{n\pi}\mathrm{Sin}\left(n\pi\left(\dfrac{D}{2}-\dfrac{t_r}{T}\right)\right)$ $\times\mathrm{Sinc}\left(n\pi\dfrac{t_r}{T}\right)\mathrm{Cos}(n\omega t)$	$\Delta_{opt} = \sqrt[4]{\dfrac{\left[D-\dfrac{8t_r}{3T}\right]\pi^2\dfrac{t_r}{T}}{\Psi}}$
7.	$I_{rms} = I_o\sqrt{\dfrac{1}{3}}$ $I_{rms}' = \dfrac{2I_o}{T\sqrt{D(1-D)}}$	$\sum_{n=1}^{\infty}\dfrac{2I_o\mathrm{Sin}(n\pi D)}{\pi^2n^2D(1-D)}\mathrm{Sin}(n\omega t)$	$\Delta_{opt} = \sqrt[4]{\dfrac{\pi^2D(1-D)}{3\Psi}}$
8.	$I_{rms} = I_o\sqrt{\dfrac{D}{3}}$ $I_{rms}' = \dfrac{2I_o}{\sqrt{DT}}$	$\dfrac{I_oD}{2} + \sum_{n=1}^{\infty}\dfrac{4I_o}{\pi^2n^2D}\mathrm{Sin}^2\left(\dfrac{n\pi D}{2}\right)\mathrm{Cos}(n\omega t)$	$\Delta_{opt} = \sqrt[4]{\dfrac{\pi^2D^2}{3\Psi}}$
9.	$I_{rms} = I_o\sqrt{\dfrac{D}{3}}$ $I_{rms}' = \dfrac{4I_o}{\sqrt{DT}}$	$\sum_{n=1,odd}^{\infty}\dfrac{16I_o}{\pi^2n^2D}\mathrm{Sin}^2\left(\dfrac{n\pi D}{4}\right)\mathrm{Cos}(n\omega t)$	$\Delta_{opt} = \sqrt[4]{\dfrac{\pi^2D^2}{12\Psi}}$
♦ In waveform 2 for n = k = 1/2D ∈ **N** (the set of natural numbers), and in waveform 3 for n = k = 1/D ∈ **N**, the {expression in curly brackets} is replaced by $\pi/4$.			

Table 4.2. Formulas for the optimum thickness of a winding using the RMS values method, $\Psi = (5p^2 - 1)/15$, p = number of layers.

WAVEFORM NO.	FOURIER ANALYSIS	RMS VALUES
1	0.539	0.538
2	0.490	0.481
3	0.348	0.340
4 II	0.429	0.415
5 II	0.416	0.389
6 II	0.328	0.314
7	0.515	0.507
8	0.469	0.458
9	0.333	0.324

Table 4.3. Optimum thickness validation, $p = 6$, $D = 0.4$, $t_r/T = 4\%$.

4.4   Regression Analysis Method

We will now take a look at the regression analysis method for minimising AC winding losses. For each of the nine basic waveforms, an approximation to the AC resistance versus layer thickness curve has been derived and the optimum point can be expressed using a straightforward formula. As with the RMS values method, these formulas are given in terms of the duty cycle, number of layers and harmonics (related to rise time). The time previously required to plot an endless supply of resistance-thickness graphs, for cases where these variables are changing, is eliminated. This section also gives an example of a push-pull converter and shows that a multilayer foil winding is superior to a round conductor configuration.

4.4.1   Least Squares

We will begin by showing how the two trigonometric parts of the AC resistance factor at the nth harmonic frequency (4.14) can be approximated using regression analysis.

Non-linear regression, also called non-linear curve fitting, uses an iterative algorithm to fit a user-defined mathematical model to data points. Initial values are specified for every parameter in the model, and the values of the parameters are adjusted with each iteration until the curve that "best" fits the data is found. It is generally used when the model is non-linear in the parameters. Otherwise, linear regression would be used as it is much faster computationally. A model is linear in its parameters if the parameters are all added or multiplied times a variable.

One of the most commonly used non-linear estimation methods is the non-linear least squares algorithm developed by Marquadt (using an idea by Levenberg) [69]. The least squares method finds the values of the model parameters that generate the curve that comes closest to the data points by minimising the sum of the squares of the vertical distances between the data points and the curve.

Non-linear models all have the general form [21] and [93]

$$y = f(x,a,b,...) + \varepsilon \, , \qquad\qquad (4.37)$$

where y is the dependent variable, x is one or more independent variables, a, b, ... are the unknown parameters to be estimated, f() is the non-linear function of the unknown parameters and independent variables, and ε is the error term.

Marquadt's method can be used to estimate the parameters a, b, ... of the non-linear model using given data points. The residual sum of squares formula for the model given above can be written as

$$\sum e^2 = \sum_{u=1}^{n} \left(y_u - f(x_u, a, b, ...) \right)^2 \, , \qquad\qquad (4.38)$$

where (x_u, y_u) are the corresponding data point pairs (independent variable, dependent variable) for u from 1 to n, the total number of data points, and $f(x_u, a, b, ...)$ is the non-linear function evaluated at its corresponding x_u value.

The unknowns a, b, ... are to be chosen to make $\sum e^2$ a minimum, so that the derivatives of $\sum e^2$ with respect to a, b, ... must vanish. Therefore,

$$\frac{\partial\left(\sum e^2\right)}{\partial a} = 2\sum\left(\frac{\partial e}{\partial a}e\right) = 0$$

$$\frac{\partial\left(\sum e^2\right)}{\partial b} = 2\sum\left(\frac{\partial e}{\partial b}e\right) = 0$$

$$\begin{matrix} . & & . \\ . & & \\ . & & \end{matrix} \tag{4.39}$$

Normal equations for the unknown parameters are then derived from these equations.

For example, Figure 4.4 shows a sum of squared errors graph for a typical two-parameter model. The x and y axes correspond to the two parameters to be fit by non-linear regression, a and b. The z axis is $\sum e^2$. Each point on the surface corresponds to one possible curve fit. The goal of non-linear regression is to find the values of a and b that make the sum of squared errors as small as possible (to find the bottom of the valley).
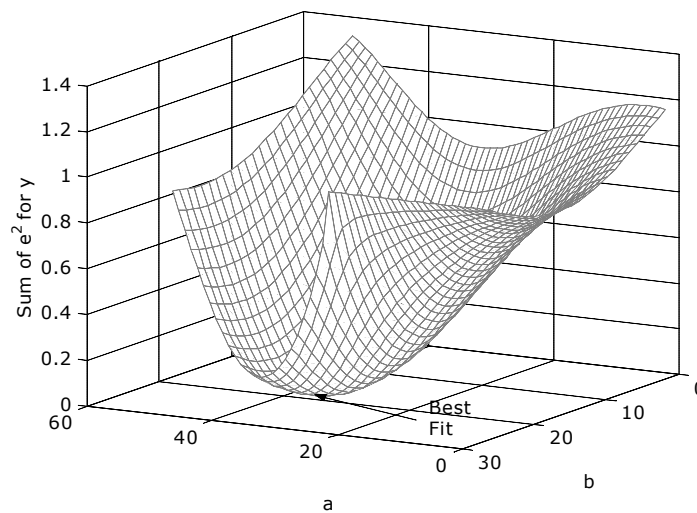
Figure 4.4. Minimising the sum of squared errors by varying parameters.

The least squares method will now be applied to the two trigonometric cases of interest, and the corresponding independent and dependent variable data is given in Table 4.4. The variable x corresponds to the normalised thickness Δ. For each case, we will have a single adjustable parameter.

Looking back to the graph in Figure 4.2, we see that the minima for $p > 3$ occur somewhere in the regions of maximum curvature ranging between $\Delta = 0.1$ and 1.0. These minima correspond to the optimum normalised thicknesses, Δ_{opt}, and we can therefore restrict our independent variable x to this range since this is where we ultimately wish to operate[1].

x	y_1	y_2
0.1	10.0001	0.0002
0.2	5.0007	0.0013
0.3	3.3357	0.0045
0.4	2.5057	0.0107
0.5	2.0111	0.0208
0.6	1.6858	0.0358
0.7	1.4588	0.0566
0.8	1.2948	0.0839
0.9	1.1743	0.1184
1.0	1.0856	0.1602

Table 4.4. Independent and dependent variable data.

4.4.1.1   Part 1

We will apply the least squares method to the formula

$$y_1 = \frac{\text{Sinh}(2x) + \text{Sin}(2x)}{\text{Cosh}(2x) - \text{Cos}(2x)} . \qquad (4.40)$$

It was postulated that a non-linear model of the form

---

[1] In fact, averaging the optimum thickness for each of the current waveforms listed in section 4.2 and over $p = 1 \dots 10$ yields a value of around 0.55, i.e. midway in the range 0.1 to 1.0.

$$y_1 = \frac{1}{x} + \frac{x^3}{a} + \varepsilon, \qquad (4.41)$$

would suitably account for the variation in y_1 values over a limited range of x. The problem is to estimate the parameter a of the non-linear model using the data given in Table 4.4. The residual sum of squares is given by

$$\sum e^2 = \sum_{u=1}^{n} \left(y_{1u} - \frac{1}{x_u} - \frac{x_u^3}{a} \right)^2. \qquad (4.42)$$

Differentiating this with respect to a and setting the results equal to zero yields

$$\frac{\partial \left(\sum e^2 \right)}{\partial a} = 2 \sum \left(\frac{\partial e}{\partial a} e \right) = 0$$
$$= 2 \sum_{u=1}^{n} \left(\frac{x_u^3}{a^2} \left(y_{1u} - \frac{1}{x_u} - \frac{x_u^3}{a} \right) \right) \qquad (4.43)$$

Rearranging the above gives a normal equation for the unknown parameter a,

$$a = \frac{\displaystyle\sum_{u=1}^{n} x_u^6}{\displaystyle\sum_{u=1}^{n} \left(y_{1u} x_u^3 - x_u^2 \right)}. \qquad (4.44)$$

For x ranging between 0.1 and 1.0 and using the data given in Table 4.4 for the dependent variable y_1, a is found to be 11.571 from (4.44).

Marquadt's method is implemented in many data analysis packages. Using the Axum package, the a parameter converges over 7 iterations from an initial estimate of 1 to 1.914 $\rightarrow$ 3.512 $\rightarrow$ 5.961 $\rightarrow$ 8.854 $\rightarrow$ 10.936 $\rightarrow$ 11.537 $\rightarrow$ 11.571. This curve fitting is illustrated in Figure 4.5.
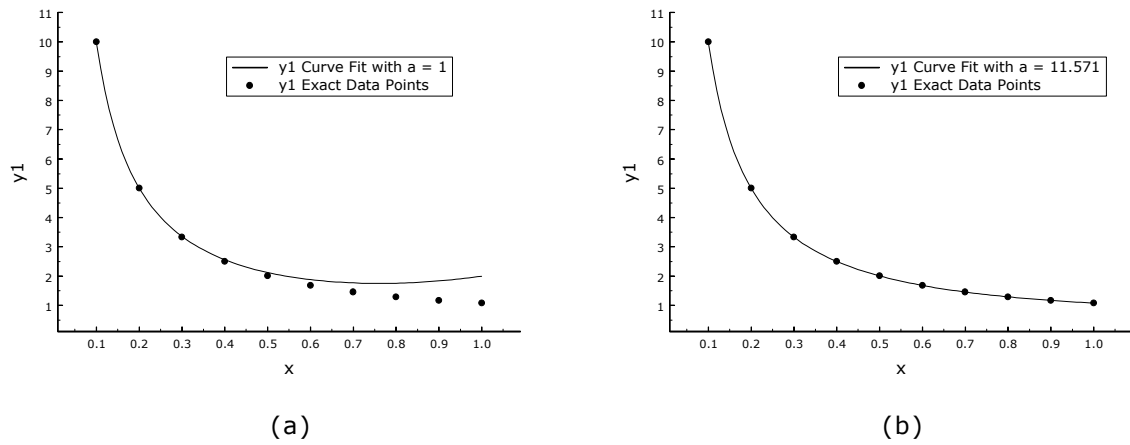
Figure 4.5. Curve fits for y_1 with (a) a = 1, (b) a = 11.571.
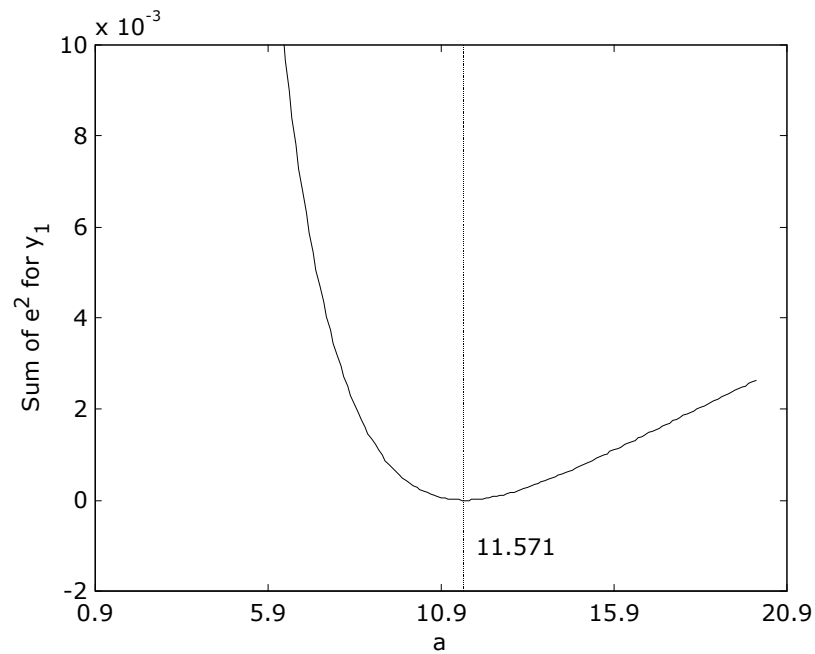
Figure 4.6. Sum of squared errors minimisation for y_1 curve fit.

4.4.1.2 Part 2

The least squares methods will now be applied to the formula

$$y_2 = \frac{\mathrm{Sinh}(x) - \mathrm{Sin}(x)}{\mathrm{Cosh}(x) + \mathrm{Cos}(x)} \,. \tag{4.45}$$

A non-linear model of the form

121

$$y_2 = \frac{x^3}{b} + \varepsilon, \tag{4.46}$$

is used where y_2 varies over a limited range of x. This time, the parameter b must be estimated using the data given in Table 4.4. The residual sum of squares is given by

$$\sum e^2 = \sum_{u=1}^{n} \left(y_{2u} - \frac{x_u^3}{b} \right)^2. \tag{4.47}$$

Differentiating this with respect to b and setting to zero yields

$$\begin{aligned}
\frac{\partial \left(\sum e^2 \right)}{\partial a} &= 2 \sum \left(\frac{\partial e}{\partial b} e \right) = 0 \\
&= 2 \sum_{u=1}^{n} \left(\frac{x_u^3}{b^2} \left(y_{2u} - \frac{x_u^3}{b} \right) \right)
\end{aligned} \tag{4.48}$$

A normal equation for the unknown parameter b can then be obtained,

$$b = \frac{\sum_{u=1}^{n} x_u^6}{\sum_{u=1}^{n} y_{2u} x_u^3}. \tag{4.49}$$

For x ranging between 0.1 and 1.0 and using the data given in Table 4.4 for the dependent variable y_2, b is equal to 6.182 from (4.49).

Using the Marquadt algorithm in the data analysis package Axum, the b parameter converges over 6 iterations from an initial estimate of 1 to $1.838 \rightarrow 3.131 \rightarrow 4.678 \rightarrow 5.817 \rightarrow 6.161 \rightarrow 6.182$, as shown in Figure 4.7.
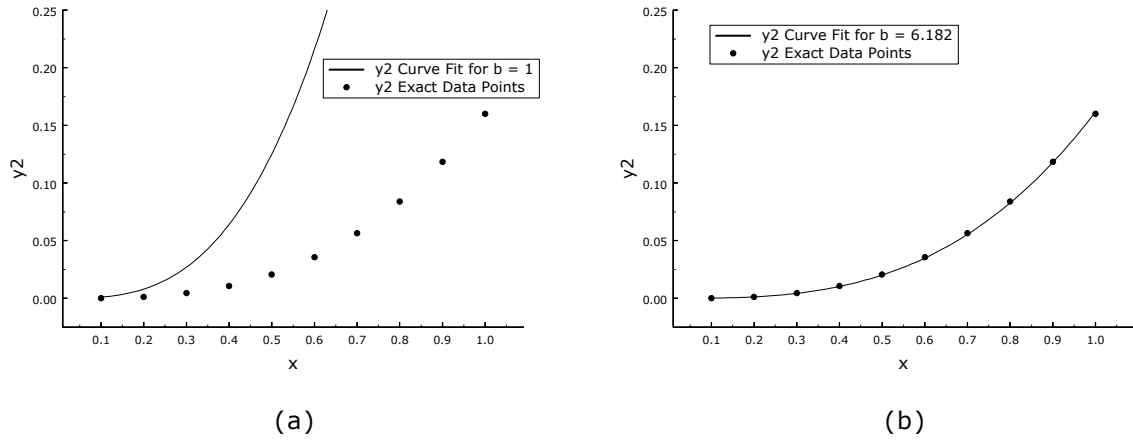
Figure 4.7. Curve fits for y_2 with (a) b = 1, (b) b = 6.182.
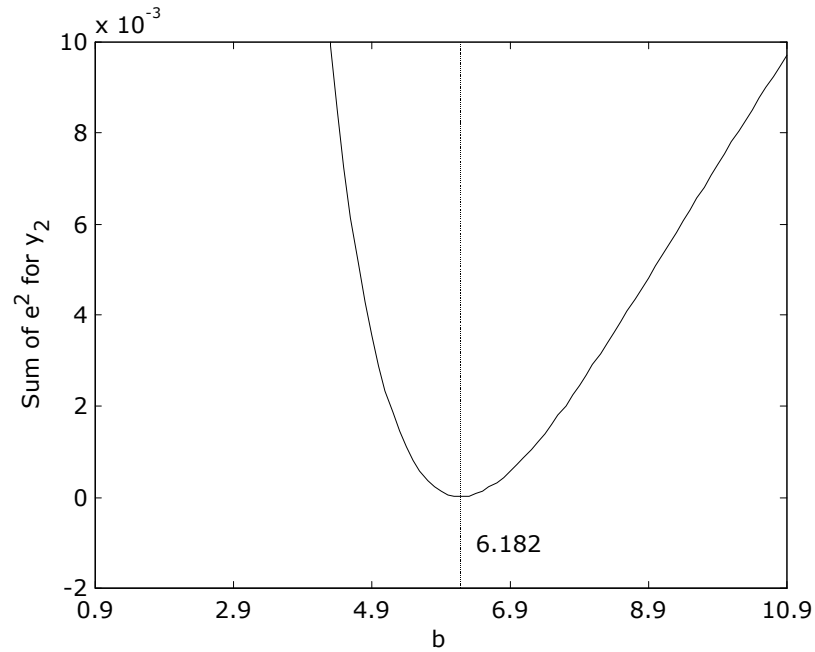
Figure 4.8. Sum of squared errors minimisation for y_2 curve fit.

4.4.2   Duty Cycle Varying Pulsed Wave

Formulas for the optimum winding or layer thickness are unique to each current waveform illustrated in Table 4.5, but the same method is followed in each case.   A pulsed (or rectified square) waveform with variable duty cycle, as encountered in a push-pull converter, is again analysed to illustrate the regression analysis methodology.   The Fourier

123

coefficients for this waveform are given in Appendix B, and the Fourier series is given by

$$i(t) = I_o D + \sum_{n=1}^{\infty} \frac{2I_o}{n\pi} Sin(n\pi D) Cos\left(\frac{2n\pi}{T} t\right). \qquad (4.50)$$
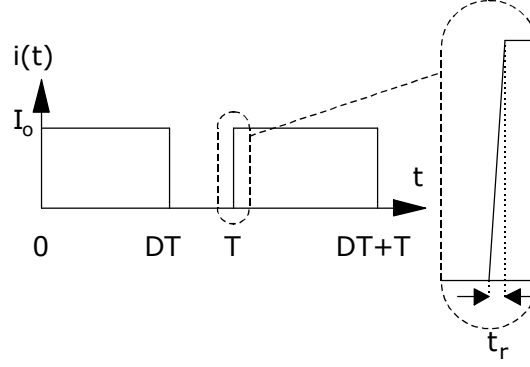
Figure 4.9. Pulsed wave with duty cycle D and rise time t_r.

The average value of current is $I_{dc} = I_o D$. The RMS value of current is $I_{rms} = I_o \sqrt{D}$. The RMS value of the nth harmonic is

$$I_n = \frac{1}{\sqrt{2}}\left[\frac{2I_o}{n\pi} Sin(n\pi D)\right] = \frac{\sqrt{2}I_o}{n\pi} Sin(n\pi D). \qquad (4.51)$$

The pulsed waveform in Figure 4.9 is not an ideal case as there is a rise time and fall time associated with it so that a finite number of harmonics are required. Typically, the upper limit on the number of harmonics is

$$N = \frac{35}{t_r \%}, \qquad (4.52)$$

where t_r is the rise time percentage of T as shown in Figure 4.9, and N is odd. For example, a 2.5% rise time would give N = 13.

The ratio of effective AC resistance to DC resistance is given by (4.15), and substituting the expressions for I_{dc}, I_n and I_{rms} from Appendix B yields

$$\frac{R_{eff}}{R_{dc}} = \frac{I_{dc}^2 + \sum_{n=1}^{\infty} k_{p_n} I_n^2}{I_{rms}^2}$$

$$= \frac{I_o^2 D^2 + \frac{2I_o^2}{\pi^2} \sum_{n=1}^{\infty} \frac{1}{n^2} \text{Sin}^2(n\pi D) k_{p_n}}{I_o^2 D} \quad . \tag{4.53}$$

$$= D + \frac{2}{\pi^2 D} \sum_{n=1}^{\infty} \frac{1}{n^2} \text{Sin}^2(n\pi D) k_{p_n}$$

Substituting for k_{p_n} given by (4.14) into (4.53) yields an expression for R_{eff}/R_{dc}:

$$\frac{R_{eff}}{R_{dc}} = D + \frac{2\Delta}{\pi^2 D} \sum_{n=1}^{N} \frac{\text{Sin}^2(n\pi D)}{n^{\frac{3}{2}}}$$

$$\times \left[\begin{array}{l} \dfrac{\text{Sinh}(2\sqrt{n}\Delta) + \text{Sin}(2\sqrt{n}\Delta)}{\text{Cosh}(2\sqrt{n}\Delta) - \text{Cos}(2\sqrt{n}\Delta)} + \\[2mm] \dfrac{2(p^2-1)}{3} \dfrac{\text{Sinh}(\sqrt{n}\Delta) - \text{Sin}(\sqrt{n}\Delta)}{\text{Cosh}(\sqrt{n}\Delta) + \text{Cos}(\sqrt{n}\Delta)} \end{array} \right] . \tag{4.54}$$

We can approximate the two trigonometric parts of (4.14) using the least squares method as described in section 4.4.1,

$$y_1 = \frac{\text{Sinh}(2\Delta) + \text{Sin}(2\Delta)}{\text{Cosh}(2\Delta) - \text{Cos}(2\Delta)} \approx \frac{1}{\Delta} + \frac{\Delta^3}{a}, \tag{4.55}$$

$$y_2 = \frac{\text{Sinh}(\Delta) - \text{Sin}(\Delta)}{\text{Cosh}(\Delta) + \text{Cos}(\Delta)} \approx \frac{\Delta^3}{b} . \tag{4.56}$$

Therefore, the proximity effect factor k_{p_n} in (4.14) may be approximated using (4.55) and (4.56) as

$$k_{p_n} \approx 1 + \frac{\left(\sqrt{n}\Delta\right)^4}{a} + \frac{2(p^2-1)}{3} \frac{\left(\sqrt{n}\Delta\right)^4}{b}$$

$$= 1 + \frac{1}{3}\left[\frac{2p^2-2}{b} + \frac{3}{a}\right]\left(\sqrt{n}\Delta\right)^4 . \tag{4.57}$$

Substituting this expression into (4.53) using (4.23) yields

$$\frac{R_{eff}}{R_\delta} = \frac{D}{\Delta} + \frac{2}{\pi^2 D}\sum_{n=1}^{N}\frac{Sin^2(n\pi D)}{n^2\Delta} \times$$

$$\left(1 + \left[\frac{2p^2-2}{3b} + \frac{1}{a}\right](\sqrt{n}\Delta)^4\right)$$

$$= \frac{D + \frac{2}{\pi^2 D}\sum_{n=1}^{N}\frac{Sin^2(n\pi D)}{n^2}}{\Delta}$$

$$+ \frac{2}{\pi^2 D}\sum_{n=1}^{N}Sin^2(n\pi D)\left[\frac{2p^2-2}{3b} + \frac{1}{a}\right]\Delta^3$$

(4.58)

The derivative of (4.58) with respect to Δ is used to calculate the optimum value of Δ:

$$\frac{d\left(\frac{R_{eff}}{R_\delta}\right)}{d\Delta} = -\frac{\left[D + \frac{2}{\pi^2 D}\sum_{n=1}^{N}\frac{Sin^2(n\pi D)}{n^2}\right]}{\Delta^2}$$

$$+ \left(\frac{2}{\pi^2 D}\sum_{n=1}^{N}Sin^2(n\pi D)\left[\frac{2p^2-2}{b} + \frac{3}{a}\right]\right)\Delta^2$$

(4.59)

Setting this equal to zero gives

$$\Delta_{opt} = \sqrt[4]{\frac{D + \frac{2}{\pi^2 D}\sum_{n=1}^{N}\frac{Sin^2(n\pi D)}{n^2}}{\left[\frac{2p^2-2}{b} + \frac{3}{a}\right]\frac{2}{\pi^2 D}\sum_{n=1}^{N}Sin^2(n\pi D)}}.$$

(4.60)

If D = 0.5, $Sin^2(n\pi D)$ is 1 for odd n and 0 for even n, and also $\sum_{n=1,\,odd}^{N}1 = \frac{N+1}{2}$.

Then the formula for Δ_{opt} is given by

$$\Delta_{opt} = \sqrt[4]{\dfrac{0.5 + \dfrac{4}{\pi^2} \displaystyle\sum_{n=1,\,odd}^{N} \dfrac{1}{n^2}}{\left[\dfrac{2p^2 - 2}{b} + \dfrac{3}{a}\right]\dfrac{4}{\pi^2}\left(\dfrac{N+1}{2}\right)}} \ . \qquad\qquad (4.61)$$

For large N (short rise time), $\displaystyle\sum_{n=1,\,odd}^{N} \dfrac{1}{n^2} = \dfrac{\pi^2}{8}$, and with a = 11.571, b = 6.182, Δ_{opt} is given by

$$\Delta_{opt} = \dfrac{1}{\sqrt[4]{(0.1312p^2 - 0.0261)\left(\dfrac{N+1}{2}\right)}} \ . \qquad\qquad (4.62)$$

Formulas for other waveshapes have been derived in a similar fashion, and the general forms are given in Table 4.5.

Substituting (4.60) in (4.58) and then in (4.23) yields an approximation for the optimum value of R_{eff}/R_{dc}:

$$\left[\dfrac{R_{eff}}{R_{dc}}\right]_{opt} = \dfrac{4D}{3} + \dfrac{8}{3\pi^2 D}\left\{\sum_{n=1}^{N} \dfrac{1}{n^2}\operatorname{Sin}^2(n\pi D)\right\}$$
$$= \dfrac{4D}{3} + \dfrac{8}{3\pi^2 D}\left\{\dfrac{\pi^2}{2}D(1-D)\right\} \ \dots \ N \to \infty \ . \qquad (4.63)$$
$$= \dfrac{4}{3}$$

In general, R_{eff}/R_{dc} is found to be around 4/3 at the optimum point for all waveshapes with large N (as with the RMS values method).
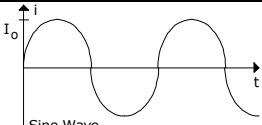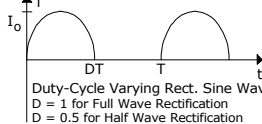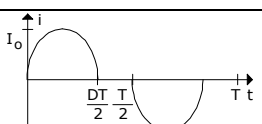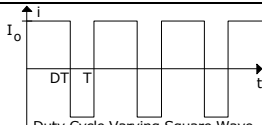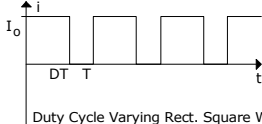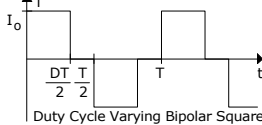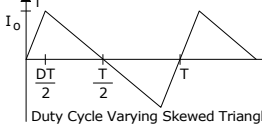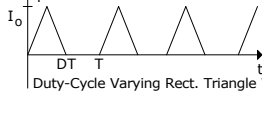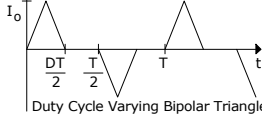
CURRENT WAVEFORM	CORRESPONDING FOURIER SERIES	FORMULAS FOR Δ_{opt}
1. I_o / i / t — Sine Wave	$i(t) = I_o Sin(\omega t)$	$\Delta_{opt} = \sqrt[4]{\dfrac{1}{\Psi}}$
2. I_o / i / DT / T / t — Duty-Cycle Varying Rect. Sine Wave. D = 1 for Full Wave Rectification. D = 0.5 for Half Wave Rectification	$i(t) = \dfrac{2DI_o}{\pi} + \sum_{n=1}^{\infty} \dfrac{4DI_o}{\pi}\left\{\dfrac{Cos(n\pi D)}{(1-4n^2D^2)}\right\}Cos(n\omega t)$ ♦	$\Delta_{opt} = \sqrt[4]{\dfrac{\dfrac{1}{2} + \sum_{n=1}^{N}\left\{\dfrac{Cos(n\pi D)}{(1-4n^2D^2)}\right\}^2}{\Psi \sum_{n=1}^{N}\left\{\dfrac{Cos(n\pi D)}{(1-4n^2D^2)}\right\}^2 n^2}}$ ♦
3. I_o / i / $\frac{DT}{2}$ / $\frac{T}{2}$ / T / t — Duty-Cycle Varying Bipolar Sine Wave	$i(t) = \sum_{n=1,odd}^{\infty} \dfrac{4DI_o}{\pi}\left\{\dfrac{Cos\left(\frac{n\pi D}{2}\right)}{(1-n^2D^2)}\right\}Cos(n\omega t)$ ♦	$\Delta_{opt} = \sqrt[4]{\dfrac{\sum_{n=1,odd}^{N}\left\{\dfrac{Cos\left(\frac{n\pi D}{2}\right)}{(1-n^2D^2)}\right\}^2}{\Psi \sum_{n=1,odd}^{N}\left\{\dfrac{Cos\left(\frac{n\pi D}{2}\right)}{(1-n^2D^2)}\right\}^2 n^2}}$ ♦
4. I_o / i / DT / T / t — Duty Cycle Varying Square Wave	$i(t) = I_o(2D-1) + \sum_{n=1}^{\infty}\dfrac{4I_o}{n\pi}Sin(n\pi D)Cos(n\omega t)$	$\Delta_{opt} = \sqrt[4]{\dfrac{(2D-1)^2 + \dfrac{8}{\pi^2}\sum_{n=1}^{N}\dfrac{Sin^2(n\pi D)}{n^2}}{\Psi \dfrac{8}{\pi^2}\sum_{n=1}^{N}Sin^2(n\pi D)}}$
5. I_o / i / DT / T / t — Duty Cycle Varying Rect. Square Wave	$i(t) = I_o D + \sum_{n=1}^{\infty}\dfrac{2I_o}{n\pi}Sin(n\pi D)Cos(n\omega t)$	$\Delta_{opt} = \sqrt[4]{\dfrac{D + \dfrac{2}{\pi^2 D}\sum_{n=1}^{N}\dfrac{Sin^2(n\pi D)}{n^2}}{\Psi \dfrac{2}{\pi^2 D}\sum_{n=1}^{N}Sin^2(n\pi D)}}$
6. I_o / i / $\frac{DT}{2}$ / $\frac{T}{2}$ / T / t — Duty Cycle Varying Bipolar Square Wave	$i(t) = \sum_{n=1,odd}^{\infty}\dfrac{4I_o}{n\pi}Sin\left(\dfrac{n\pi D}{2}\right)Cos(n\omega t)$	$\Delta_{opt} = \sqrt[4]{\dfrac{\sum_{n=1,odd}^{N}Sin^2\left(\frac{n\pi D}{2}\right)\dfrac{1}{n^2}}{\Psi \sum_{n=1,odd}^{N}Sin^2\left(\frac{n\pi D}{2}\right)}}$
7. I_o / i / $\frac{DT}{2}$ / $\frac{T}{2}$ / T / t — Duty Cycle Varying Skewed Triangle Wave	$i(t) = \sum_{n=1}^{\infty}\dfrac{2I_o Sin(n\pi D)}{\pi^2 n^2 D(1-D)}Sin(n\omega t)$	$\Delta_{opt} = \sqrt[4]{\dfrac{\sum_{n=1}^{N}\dfrac{Sin^2(n\pi D)}{n^4}}{\Psi \sum_{n=1}^{N}\dfrac{Sin^2(n\pi D)}{n^2}}}$
8. I_o / i / DT / T / t — Duty-Cycle Varying Rect. Triangle Wave	$i(t) = \dfrac{I_o D}{2} + \sum_{n=1}^{\infty}\dfrac{4I_o}{\pi^2 n^2 D}Sin^2\left(\dfrac{n\pi D}{2}\right)Cos(n\omega t)$	$\Delta_{opt} = \sqrt[4]{\dfrac{1 + \dfrac{32}{\pi^4 D^4}\sum_{n=1}^{N}\dfrac{1}{n^4}Sin^4\left(\frac{n\pi D}{2}\right)}{\Psi \dfrac{32}{\pi^4 D^4}\sum_{n=1}^{N}\dfrac{1}{n^2}Sin^4\left(\frac{n\pi D}{2}\right)}}$
9. I_o / i / $\frac{DT}{2}$ / $\frac{T}{2}$ / T / t — Duty Cycle Varying Bipolar Triangle Wave	$i(t) = \sum_{n=1,odd}^{\infty}\dfrac{8I_o}{\pi^2 n^2 D}\left(1-Cos\left(\dfrac{nD\pi}{2}\right)\right)Cos(n\omega t)$	$\Delta_{opt} = \sqrt[4]{\dfrac{\sum_{n=1,odd}^{N}\left(1-Cos\left(\frac{n\pi D}{2}\right)\right)^2\dfrac{1}{n^4}}{\Psi \sum_{n=1,odd}^{N}\left(1-Cos\left(\frac{n\pi D}{2}\right)\right)^2\dfrac{1}{n^2}}}$

♦ In waveform 2 for n = k = 1/2D ∈ **N** (the set of natural numbers), and in waveform 3 for n = k = 1/D ∈ **N**, the {expression in curly brackets} is replaced by $\pi/4$.

Table 4.5. Formulas for the optimum thickness of a winding using the regression analysis method, a = 11.571, b = 6.182, $\Psi = (2p^2 - 2)/b + 3/a$.

4.4.3   Push-Pull Converter

The current waveform in each primary winding of a push-pull converter may be approximated by the pulsed waveform of Figure 4.9, with the ripple neglected. Take D = 0.5, p (number of foil layers) = 6, t_r (rise time) = 2.5%, and f = 50 kHz. For t_r = 2.5%, take 13 harmonics (4.52). The optimum thickness and skin depth are given by

$$\Delta_{opt} = \frac{1}{\sqrt[4]{([13+1]/2)(0.1312\times 6^2 - 0.0261)}} = 0.42 \,, \qquad (4.64)$$

$$\delta_o = \frac{66}{\sqrt{f}} = \frac{66}{\sqrt{50\times 10^3}} = 0.295 \text{ mm} \,. \qquad (4.65)$$

The optimum foil thickness is $d_{opt} = \Delta_{opt}\delta_o = 0.42 \times 0.295 = 0.12$ mm. The AC to DC resistance ratio is found from (4.63) to be $R_{eff}/R_{dc} = 1.314$.
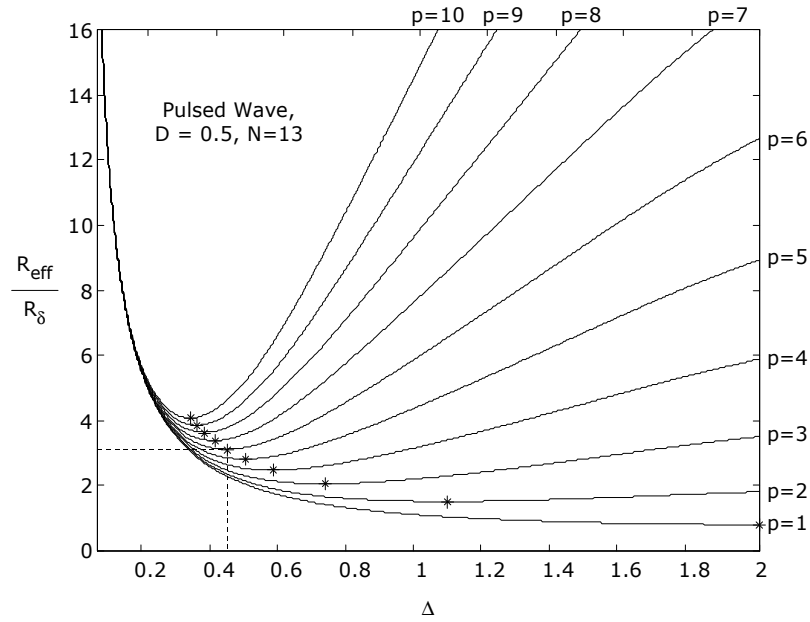
Figure 4.10. Plot of AC resistance versus Δ for D = 0.5, N = 13.

Alternatively, the winding could be constructed with a single layer of round conductors; assuming a window height of 30 mm, a 2.14 mm diameter of bare copper wire has the same copper area as a 0.12 × 30 mm foil. In this case p = 1, d = 0.886(2.14) = 1.896, Δ = 1.896/0.295 = 6.427,

and R_{eff}/R_{dc} = 4.203. Evidently in this case, the choice of a foil is vastly superior.

The value Δ_{opt} calculated in (4.64) can be matched against that found using the Fourier analysis method. Figure 4.10 shows a plot of R_{eff}/R_δ versus Δ for the pulsed wave with D = 0.5, N = 13 and p = 1 … 10. For p = 6, Δ = 0.43, and this represents an error of 2%.

4.5   Comparison of Methods

Table 4.6 shows a comparison between optimum thickness values obtained using both of the new methods presented in this chapter and those obtained using exact Fourier analysis calculations.

WAVEFORM NO.	FOURIER ANALYSIS METHOD	RMS VALUES METHOD	REGR. ANALYSIS METHOD
1	0.539	0.538	0.538
2	0.490	0.481	0.485
3	0.348	0.340	0.345
4 I	0.381	-	0.375
5 I	0.435	-	0.424
6 I	0.358	-	0.354
4 II	0.429	0.415	-
5 II	0.416	0.389	-
6 II	0.328	0.314	-
7	0.515	0.507	0.501
8	0.469	0.458	0.463
9	0.333	0.324	0.330

Table 4.6. Comparison of optimum thicknesses, p = 6, D = 0.4, t_r/T = 4%.

The following tables represent sample data for all waveforms analysed with 40% duty cycle and 4% rise time where applicable. Fourier analysis was carried out over 19 harmonics. The average error is calculated with p > 3 for reasons mentioned earlier (section 4.3.3).

WAVEFORM	1 FOU	1 RMS	2 FOU	2 RMS	3 FOU	3 RMS	4 II FOU	4 II RMS	5 II FOU	5 II RMS
p = 1	1.571	1.392	1.000	1.245	1.464	0.880	1.578	1.072	1.000	1.007
p = 2	0.961	0.943	0.917	0.843	0.648	0.596	0.834	0.726	0.931	0.682
p = 3	0.770	0.764	0.715	0.683	0.506	0.483	0.636	0.589	0.658	0.553
p = 4	0.663	0.660	0.609	0.590	0.431	0.418	0.536	0.509	0.535	0.478
p = 5	0.591	0.590	0.540	0.528	0.383	0.373	0.473	0.455	0.464	0.427
p = 6	0.539	0.538	0.490	0.481	0.348	0.340	0.429	0.415	0.416	0.389
p = 7	0.499	0.498	0.453	0.445	0.321	0.315	0.395	0.384	0.381	0.360
p = 8	0.466	0.466	0.422	0.417	0.300	0.295	0.368	0.359	0.354	0.337
p = 9	0.439	0.439	0.398	0.393	0.282	0.278	0.347	0.338	0.332	0.318
p = 10	0.417	0.416	0.377	0.372	0.268	0.263	0.328	0.321	0.314	0.301
Av. Error	-	0.2%	-	1.8%	-	2.1%	-	3.2%	-	6.3%

WAVEFORM	6 II FOU	6 II RMS	7 FOU	7 RMS	8 FOU	8 RMS	9 FOU	9 RMS		
p = 1	1.485	0.812	1.563	1.312	1.000	1.185	1.450	0.838		
p = 2	0.651	0.550	0.937	0.889	0.879	0.803	0.621	0.568		
p = 3	0.490	0.446	0.744	0.720	0.685	0.651	0.485	0.460		
p = 4	0.411	0.385	0.637	0.622	0.583	0.562	0.413	0.398		
p = 5	0.363	0.344	0.566	0.556	0.517	0.502	0.367	0.355		
p = 6	0.328	0.314	0.515	0.507	0.469	0.458	0.333	0.324		
p = 7	0.303	0.291	0.476	0.469	0.433	0.424	0.308	0.300		
p = 8	0.282	0.272	0.444	0.439	0.404	0.397	0.287	0.281		
p = 9	0.265	0.256	0.418	0.414	0.380	0.374	0.271	0.264		
p = 10	0.251	0.243	0.396	0.393	0.360	0.355	0.257	0.251		
Av. Error	-	4.3%	-	1.4%	-	2.2%	-	2.8%		

Table 4.7. Average error between Fourier analysis and RMS values methods for N = 19, D = 0.4, t_r/T = 4%.

The waveform 1 results correspond to those presented by Perry [85] in his analysis for sine waves.

While the average error between the RMS values method and the Fourier analysis method (Table 4.7) is slightly higher than that between the regression analysis method and the Fourier analysis method (Table 4.8), the harmonic summations involved in calculating the optimum formulas using the regression analysis method make it preferable to use the RMS values method in a quick design or on paper.

WAVEFORM	1 FOU	1 REG	2 FOU	2 REG	3 FOU	3 REG	4 I FOU	4 I REG	5 I FOU	5 I REG
p = 1	1.571	1.392	1.000	1.253	1.464	0.892	1.575	0.971	1.000	1.096
p = 2	0.961	0.943	0.917	0.849	0.648	0.604	0.772	0.658	0.961	0.742
p = 3	0.770	0.764	0.715	0.688	0.506	0.490	0.570	0.533	0.673	0.602
p = 4	0.663	0.660	0.609	0.594	0.431	0.423	0.477	0.461	0.552	0.520
p = 5	0.591	0.590	0.540	0.531	0.383	0.378	0.421	0.411	0.482	0.465
p = 6	0.539	0.538	0.490	0.485	0.348	0.345	0.381	0.375	0.435	0.424
p = 7	0.499	0.498	0.453	0.448	0.321	0.319	0.351	0.347	0.400	0.392
p = 8	0.466	0.466	0.422	0.419	0.300	0.298	0.328	0.325	0.372	0.367
p = 9	0.439	0.439	0.398	0.395	0.282	0.281	0.308	0.306	0.350	0.346
p = 10	0.417	0.416	0.377	0.375	0.268	0.267	0.292	0.291	0.331	0.328
Av. Error	-	0.2%	-	1.1%	-	0.8%	-	1.5%	-	2.5%

WAVEFORM	6 I FOU	6 I REG	7 FOU	7 REG	8 FOU	8 REG	9 FOU	9 REG		
p = 1	1.524	0.916	1.563	1.319	1.000	1.197	1.450	0.855		
p = 2	0.702	0.620	0.937	0.893	0.879	0.811	0.621	0.579		
p = 3	0.529	0.503	0.744	0.724	0.685	0.657	0.485	0.469		
p = 4	0.447	0.434	0.637	0.626	0.583	0.568	0.413	0.405		
p = 5	0.395	0.388	0.566	0.559	0.517	0.507	0.367	0.362		
p = 6	0.358	0.354	0.515	0.510	0.469	0.463	0.333	0.330		
p = 7	0.331	0.328	0.476	0.472	0.433	0.428	0.308	0.306		
p = 8	0.309	0.306	0.444	0.441	0.404	0.401	0.287	0.286		
p = 9	0.290	0.289	0.418	0.416	0.380	0.378	0.271	0.270		
p = 10	0.275	0.274	0.396	0.395	0.360	0.358	0.257	0.256		
Av. Error	-	1.2%	-	0.9%	-	1.3%	-	0.9%		

Table 4.8. Average error between Fourier analysis and regression analysis methods for N = 19, D = 0.4, t_r/T = 4%.

There is also a discrepancy between the optimum thicknesses for the different versions of waveforms 4, 5 and 6 used in the RMS values and regression analysis methods of around 10%. This is due to the fact that we used the approximation given in (4.52) to estimate a rise time of t_r/T = 4%, or N = 35/4 = 8.75 ≈ 9 odd harmonics, for the version I waveforms.

A graph of Δ using the Fourier analysis, regression analysis and RMS values methods for waveform 7 shows good correlation for p = 2 … 10, as illustrated in Figure 4.11. If we denormalise the optimum thicknesses using the skin depth factor for copper, we will see that the difference

between the RMS values and regression analysis thicknesses is only in the order of 0.001 mm.
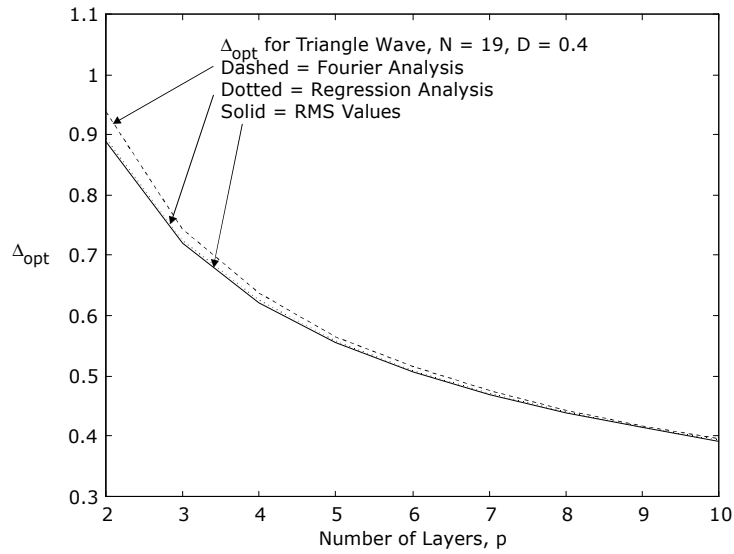
Figure 4.11. Optimum thickness plots for waveform 7 using each method.

However, the main advantage of the RMS values method over the regression analysis method is the ease with which an optimum thickness formula can be found, since the regression analysis method requires that the Fourier coefficients be derived for each new waveshape.

It was also noted that waveforms with known Fourier series are often in themselves only approximations to the actual waveforms encountered in transformer windings, and it was shown by example in section 4.3.3 that using such approximations in the Fourier analysis method can give rise to optimum thickness errors which are of the same order as those obtained when the RMS values method is applied to the actual waveforms.

4.6   Summary

We began this chapter by looking at the traditional Fourier analysis method for evaluating AC resistance over a range of winding thicknesses. A general procedure to calculate the AC resistance of multilayer windings for general waveshapes encountered in switching mode power supplies was described.

133

Two new methods were presented that enable the optimum foil or layer thickness at minimum AC resistance to be found from knowledge of the number of layers, number of harmonics (related to rise time) and duty cycle in any arbitrary periodic current waveform. Variable duty cycle is an integral part of both procedures.

The first method, using RMS values, establishes a simple and accurate approximation so that optimum thickness formulas can be derived from the AC resistance for arbitrary waveshapes. It was shown that this method is computationally easier to use than Fourier analysis while enjoying the same level of accuracy.

The second method, using regression analysis, requires that the Fourier coefficients be derived for each new waveshape. The optimum thickness formulas derived in this method incorporate harmonic summations, but are closer in accuracy to the Fourier analysis method.

Finally, a comparison of the various methods was carried out illustrating that the RMS values method has a wider range of application than the Fourier analysis method by virtue of its simplicity.

Chapter 5

SOFTWARE DEVELOPMENT

5.1   Introduction

The chapter begins with an overview of the engineering design process, concentrating on how a design was developed for our system.

Section 5.3 discusses traditional software and analytical tools used in the domain followed by a discussion on each of the software and analytical tools used in our system. These are: a database management system; a graphical user interface; optimisation techniques; and a repository of relevant knowledge.

Finally, section 5.4 gives a high level overview and some screenshots of the system which implements the methodologies described in Chapter 3 and Chapter 4.

5.2   Design Process

The engineering design process is a decision-based process where the creative skills of the designer are combined with their acquired engineering knowledge to produce the concrete definition of an engineering product or system. If a computer aided design (CAD) system is to be used to aid this process, then it must evidently provide interfaces between person and computer. An input interface is necessary to define design concepts to the computer, and an output interface is needed to present calculation results to the designer. The organisation of these interfaces, not just with respect to communication method, but also

regarding the design information content, is a primary task in designing a CAD system.

The basic design process implemented by CAD packages is shown in Figure 5.1 [83], [76], where three main process stages are distinguished.
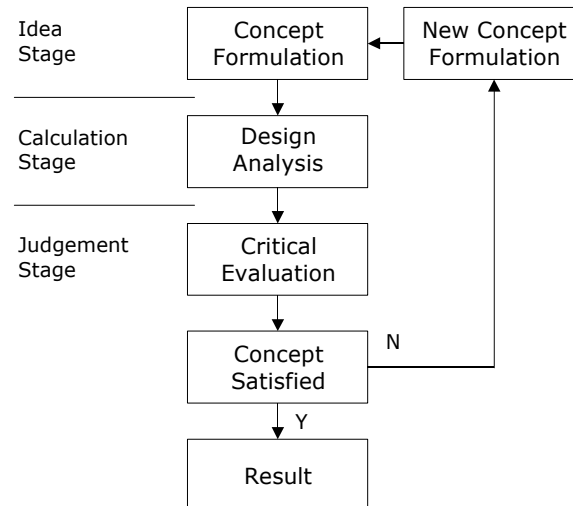
Figure 5.1. Basic CAD structure.

The first is the idea stage, in which the designer formulates a concept. This is followed by the calculation stage, where the proposed designs are analysed; the computer can predominantly perform this part. The third stage is the critical judgement stage, which is the designer's ultimate responsibility, although some more routine evaluations may be delegated to computer programs. The evaluation stage will often lead to new concepts being proposed so that the process is generally highly iterative and interactive.

This type of process is acceptable if, for example, you are designing a football, and your initial concept is that it will be round and made from glass. You may encounter problems in the analysis and evaluation phases that will lead you to conclude a new concept needs to be formulated, perhaps trying rubber or leather as the material. It is a one-way system; if you are not satisfied with the result you receive, you must go back to the beginning, revise the concept and start again.

Our transformer design process was initially programmed in this fashion. Application specifications were entered (concept formulation), geometric

136

definitions of transformer cores and then windings were made subject to manufacturing details and constraints (design analysis), and predicted performance data - losses, efficiency, temperature rise etc. - were examined (critical evaluation).

If the result was not satisfactory, you had to go back and enter your specifications again (with some modifications if required), choose a different core or winding geometry, etc. The screen changed to display each new step in the process. Once the specifications data entry or geometry selection step was completed, that particular window would disappear never to be seen again unless the process was started from scratch - there was no backtracking allowed through steps. Also, any previous calculations made in the calculation and judgement stages were lost after restarting the process.
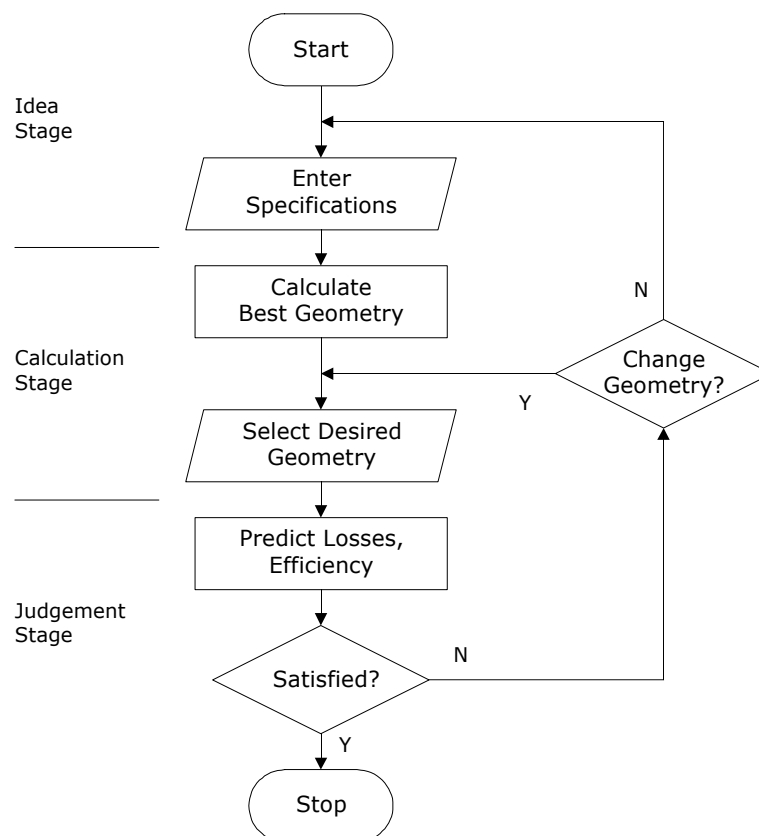
Figure 5.2. Revised flow chart.

It quickly became apparent that sometimes you would not want to change the specifications at all, but merely return midway to either the core or winding geometry steps and select a new shape or type there. Our design

process had to be revised to accommodate this (Figure 5.2). The flow chart may not seem significantly different from the basic structure of Figure 5.1, but this extra choice meant that we would need to be able to hop back and forth through steps in a manner that would not be confusing to a user of the software.

The easiest way to display the steps was to represent each one with a folder in a group of folders, each one accessible by clicking on a named folder tab. With such an interface, however, some checks would have to be put in place so that for example a user would not complete steps 1 to 3 and skip forward to 5 without finishing 4.

This was a small price to pay in comparison with the other changes the user could make with this new flexible design process, for example:

- Since the initial specifications no longer disappear, a user can modify any of the input values and then view its effect on the geometry or losses.
- The user can hop back and manually override turns numbers and ratios to calculate new geometries based on these revised values.
- A custom core or winding can be entered into the database using an extra folder, without losing the entered specifications, and this new item can then be used in the design by moving back to the geometry selection area and reloading the database.

It is clear that a flow chart showing the above proposed design paths becomes a lot more complicated than that shown in Figure 5.2. It would be very difficult to illustrate a flow chart incorporating all of the choices the user can now make in our design process (the three choices listed are just a few of many eventually programmed).

Therefore a data flow diagram (DFD) approach was preferable [32] so that the functionality of the various folders could be shown independently of each other whilst still being able to see the inputs from other folders. This reduces the amount of information that a person has to assimilate at any one time and makes the system design easier to understand.

Data flow diagrams are often used to show the flow of data into, out of, and within a software system. A legend of the symbols used in Gane and Sarson convention data flow diagrams [32] is given in Figure 5.3.

- "External entities" are a source or destination of data and are external to the software-based part of the system.

- "Data flows" show the movement of data from one point to another and point to the destination.

- "Processes" refer to main functions being performed by the system and may denote a change in or transformation of data. PID is a unique ID for each process.

- "Data stores" show depositories for data or databases that allow addition and retrieval of data. SID is a unique ID number for each store.
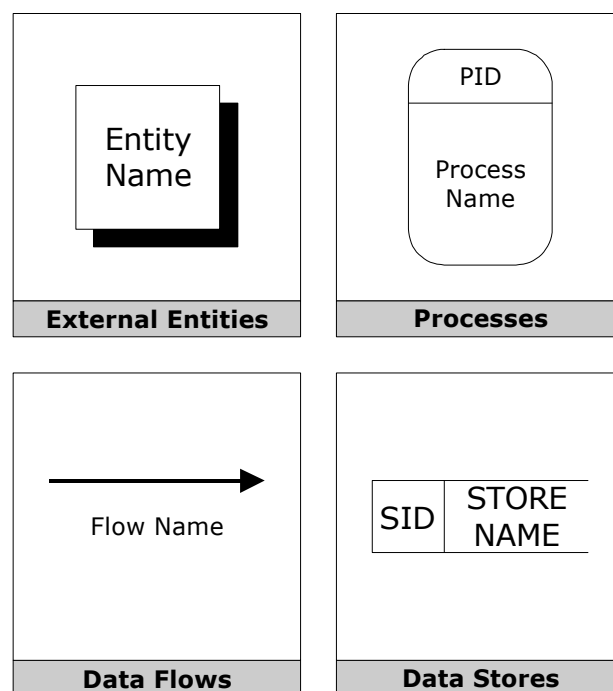
Figure 5.3. Data flow diagram conventions.

We will be using data flow diagrams to describe the system in section 5.4.

5.3   Software and Analytical Tools

Designers from many domains have been using pen and paper as the means to carry out designs for centuries. From the conceptual stage to the final drafting stage, the ideas are expressed on paper, and this is the medium for the exchange of information from one design stage to the next. As paper is a passive medium, it just retains what is written on it and cannot respond to the material on it. Therefore, the conventional design process becomes a passive activity whereby the designer must complete the whole job, with pen and paper acting as a passive design medium.

Computer aided design uses the computer primarily as a design medium. Once it is programmed to act as a medium for design, it can be made to respond to whatever has been input by the designer. Thus, the computer becomes an active medium for carrying out an engineering design. This in itself is a major step towards improving the design process. Making use of the many other capabilities of computers gives many additional advantages for computer aided design over conventional methods.

Many magnetic design companies have developed computer spreadsheets to satisfy their own needs and requirements. They thus tend to be solely related to a company and its products, and remain unpublished as their content is only of interest to their direct users and competitors. Some of the limitations of these spreadsheets are as follows:

- It is difficult to incorporate previous designer expertise due to limited decision or case statements.
- Accessing manufacturer's component information from a spreadsheet table can be difficult, as it does not conform to professional database formats.
- Spreadsheets are unable to implement most optimisation routines due to slow iterative capabilities and a reduced set of mathematical functions.
- Spreadsheet input mechanisms are very basic and lack the features possible with a customised graphical user interface (GUI).

To address these issues, a GUI-based software package was developed that would include a database management system, a repository of knowledge and optimisation techniques to aid in analytical modelling and effective handling of data during analysis. We will now describe the combination of these four major aspects in our package:

1. Database Management System
2. Graphical User Interface
3. Optimisation Techniques
4. Repository of Knowledge

5.3.1   Database Management System

Depending on the type and complexity of the magnetic component being designed, the amount of data that has to be handled during the design process can vary. In transformer design, huge amounts of core and winding data have to be managed for effective exchange of information between various design stages.

In addition, the magnetic designer should not get lost in the data management process as a result of which their concentration on the real design problem may be affected. The large data storage capabilities of modern personal computers can be properly exploited with an efficient data management system, which will relieve designers from searching through books with manufacturer's data or from manipulating data themselves with lower level external programs.

Database management systems (DBMS) provide designers with the facilities for effective use of computer memory, proper organisation of data without losing its physical significance, and also effective manipulation of data stored in databases.

Relational databases are the most widespread DBMS for Windows operating systems. The relational model was first proposed by Codd in 1972 [13] and has been widely and successfully adapted, representing the

dominant trend in the marketplace today. Data in the relational model is stored in set of tables (or relations) consisting of columns (fields or attributes) and rows (records or tuples).

All transformer core and winding data is accessible using the sophisticated database storage and retrieval capabilities of a relational database engine incorporated into the design application.

There are four separate databases used in our system: standard cores, standard windings, custom cores and custom windings. The structure of each database is similar. In each database, there is a table of data corresponding to each core or winding group. There can be as many of these groups as necessary. Each group will be made from a particular material, one of many listed in a common materials table.

A sample core materials table is given in Table 5.1, and a sample table for a particular core group is shown in Table 5.2. Tables for winding materials or groups will have different fields (see section C.15).

While some of the fields are optional and provided for informational reasons only, certain fields in the core group table must be filled as they are required for calculations in the package. These are the core cross-sectional area A_c, the window area W_a (and hence the area product A_p), the material type, and the weight in kg. If the area values are not given directly, they must be calculated from other core dimensions or diagrams so that they can be entered into the database. A unique name for each individual core should also be entered (e.g. E17 AG, E17 AH etc.) for use as a primary key.

NAME	MANUFACTURER	SAT. FLUX DENS. (T)	β	K_c	α	DENSITY (kg/m^3)
27MOH	BS Unisil	1.5	1.9	0.0005	1.7	7650
H5A	TDK	0.4	2.07	0.0062	1.13	6000
N27	Siemens	0.45	2.19	0.00135	1.39	4800
N67	Siemens	0.4	2	0.0019	1.24	4800

Table 5.1. Sample core materials table.

NAME	A_c (cm²)	W_a (cm²)	A_p (cm⁴)	WINDOW WIDTH (mm)	WINDOW HEIGHT (mm)	A_L VALUE (nH)
25/13/A	0.58	0.6789	0.393762	3.65	18.6	2000±20%
25/13/B	0.58	0.6789	0.393762	3.65	18.6	160±10%
25/13/C	0.58	0.6789	0.393762	3.65	18.6	250±10%
25/13/D	0.58	0.6789	0.393762	3.65	18.6	315±10%
30/15/A	0.69	0.8736	0.602784	3.9	22.4	2050±20%
30/15/B	0.69	0.8736	0.602784	3.9	22.4	160±10%
30/15/C	0.69	0.8736	0.602784	3.9	22.4	250±10%
30/15/D	0.69	0.8736	0.602784	3.9	22.4	315±10%

μ_e VALUE	MATERIAL	g VALUE (mm)	MPL (cm)	CORE WEIGHT (kg)	MANUFACTURER	MLT (cm)
1560	N67	0	5.7	0.0166	Siemens	5
125	N67	0.55	5.7	0.0166	Siemens	5
195	N67	0.30	5.7	0.0166	Siemens	5
246	N67	0.22	5.7	0.0166	Siemens	5
1610	N67	0	6.8	0.024	Siemens	5.67
125	N67	0.71	6.8	0.024	Siemens	5.67
196	N67	0.38	6.8	0.024	Siemens	5.67
246	N67	0.27	6.8	0.024	Siemens	5.67

Table 5.2. Sample core type or group table.

5.3.2   Graphical User Interface

The aim of any user interface is to make the underlying technology more usable to people by mediating between a person and a system, allowing the person to interact with the system in a way that is meaningful, natural, flexible and consistent.

Command line interfaces (CLIs) were the first interactive dialogue style interfaces to be commonly used. A user interacts with the system via textual commands and function keys thus requiring users to learn commands for any particular system. Graphical User Interfaces (GUIs), and in particular WIMP interfaces (windows, icons, menus, pointers) are now the default style for the majority of computer systems. A GUI allows

consistent and relatively meaningful interaction with a system, without the need to memorise commands and instructions.

There are a number of features in the system GUI that should be tailored towards the opposite ends of the user spectrum. For novices, the following are important:

- The package should be easy to follow.
- The user should be able to use default values.
- It should be possible to see results quickly, and to be able to go back and change values and see how the results are affected. This promotes a good learning environment.

For the expert user, a different set of conditions is necessary:

- The package should also be easy to follow.
- There should be default values available, but the expert user should be able to change these if they want to.
- Experts would be more interested in looking at databases of underlying information, and this should be easy to do with the GUI. They should also be able to supplement these databases with updated information.
- Experts would also be more interested in the optimisation routines implemented in the software, and if they are easy to use, it is much quicker (and reliable) for them than using pen and paper.

As computer aided design is an interactive process, the exchange of information between the designer and the computer should be made as effective as possible. The expression "less is more" certainly holds with computer aided design as there is nothing more daunting for a first time designer than to be confronted with a seemingly endless display of query prompts or input boxes. For experienced designers, too many empty blanks to be filled in may seem to be as much trouble as doing it by hand on paper.

In our package, we require over 250 objects for interaction with the user; these include text boxes for both inputs and calculated outputs, labels

describing each text box, option groups, grids or tables of data, graphs, etc. To display them all at once to a prospective user would most likely ensure that their first time using the program would be their last. Proper organisation and presentation of data in stages is our solution to the problem, whereby distinct steps in the design process are identified, and only information related to a particular step is shown at any given time.

Here are some of the GUI features we will be discussing in the following sections:

1. Folders for Each Step
   o Folders are used to distinguish stages in the design process from each other.
2. Screen Size Options
   o The size of the design area on screen should be suitable for all users.
3. Organising Data in Each Step
   o Related data needs to be contained in distinct framed areas within each folder.
4. Software Navigation
   o It should be obvious how to progress through the design process.
5. Input and Output Boxes
   o Text boxes that allow input (or not) should be clearly identifiable, e.g. by colour.
6. High Precision Numbers
   o A decision must be made on how to display numbers with many decimal places.
7. Drop Down Menus
   o A method should be provided for choosing a single item from a long list of data.
8. Grid Areas
   o It is sometimes necessary to display large tables of data in a small area of the screen.
9. Message Boxes
   o The system should inform users of possible errors and also make recommendations to solve these errors.

10. Option Groups
    o Multiple options should be grouped together to allow fast selection of discrete variables.
11. Check Boxes
    o An on/off box can be used to show the status of a Boolean variable.

5.3.2.1   Folders for Each Step

In Chapter 3, we illustrated a flow chart for the transformer design process, and detailed a number of general stages in each design example. These are summarised in Table 5.3.

DESIGN EXAMPLE STAGES	FLOW CHART STEPS
Core Selection	Enter Specifications Select Material Calculate B_o Calculate A_p
Turns	Calculate Turns
Wire Sizes	Calculate J Calculate Wires
Copper Losses	Calculate Copper Losses
High Frequency Effects	Calculate High Frequency Losses
Core Losses	Calculate Core Losses
Efficiency	Calculate Efficiency

Table 5.3. Transformer design example stages.

We have endeavoured to transform these stages into a software package as faithfully as possible, but often the data involved in a particular stage will either be too little or too much to be displayed at any one time, and the result is that a stage will either have to be split up or combined with another smaller stage (in terms of information displayed). For example, the high frequency effects stage now spans two steps of our software package.

While in the design examples of Chapter 3 it is implicit that the specifications are known, in our package we must include a step in the

design process during which the designer will input the desired specifications to the computer program. This first step is circuit dependent, for example, if a centre-tapped rectifier is to be designed, the data input section is simplified to accept specifications applicable to that circuit only. Advanced designs are also possible by customising values in the expert options area.

The rest of the steps follow on from the specifications entry:

1. *Enter Specifications*
2. *Choose Core Data*
3. *Calculate Turns Information*
4. *Choose Winding Data*
5. *Calculate Winding Losses*
6. *Calculate Core Losses*
7. *Calculate Total Losses*
8. *Calculate Optimum Winding Thickness*
9. *Calculate Leakage Inductance*
10. *Allow Custom Addition*

Each of these steps is represented by a folder which can be selected at any time by clicking on its corresponding tab. The user can click on a particular tab to hop back and forth through the design steps with ease. This GUI gives us a cyclic process, and one that is not limited to a strict set of steps that must always be carried out from beginning to end each time in a new application.

One step which can lie outside the normal design process but is essential to the package is "Allow Custom Addition" which enables the designer to input their own data (either core or winding) for use in steps 2 and 4. While this function is closely related to steps 2 and 4, the amount of extra input boxes and command buttons required to implement this utility in the existing steps would have made the screen look too cluttered.

We will describe these processes further in the program overview of section 5.4.

5.3.2.2   Screen Size Options

The screen size available for displaying input and output information at any time is usually governed by the computer user's own desired settings in the operating system setup. It is possible for a software application to change these settings "on the fly" (for example, multimedia applications such as computer games or DVD viewers often change the screen size to suit their own needs), but this can sometimes lead to screen lockups or operating system crashes when improperly coded.

Other applications, web browsers and word processors among them, get around a limited screen size by adding scroll bars to the display. For a design package such as ours, it was considered that it would be confusing to have users scrolling up and down through screens of data for each step. It is better to have all (or as much as possible) of the data relating to a particular step on the screen at once, and thus the folder approach outlined earlier was adopted.

The size of a single folder displayed on screen for each step needed to be calculated. Computer screens are capable of displaying a number of different "resolutions" or levels of detail, where these resolutions are measured in units called "pixels". The pixels themselves have no fixed size, but are usually square in shape and each can take on any one of millions of colours. For example, a 17 inch monitor and graphics card hardware may be capable of the following resolutions: 640×480, 800×600, and 1024×768. The first number refers to the horizontal number of pixels, the second to the vertical. The higher the resolution, the more pixels have to fit into the same physical area on a computer screen.

For the Windows operating system (on which our software runs), the lowest possible resolution is usually 640×480 pixels. It follows logically that if you can manage to fit all of the necessary data for a step on a folder that will be less than or equal to this lower limit of resolution, then you will be catering for users with screen sizes from 640×480 upwards. At higher resolutions the same folder may only occupy half the total screen area.

Of course, some other aspects of the package will be on screen at all times and this is why the folder cannot use the full 640×480 screen size. These include the title bar, menu bar, tool bar for buttons, status bar and the tabs for the folders corresponding to the other steps in a transformer design. The operating system task bar has to be accounted for as well. Taking all these into consideration, we are left with a size of 560×325 for the folder itself.

5.3.2.3 Software Navigation

When designing a system such as the one proposed here, the navigation methods should be as clear as possible, and a number of them should exist for people who are used to different interfaces. As well as providing tabs on folders for each step in the design process, each of the tabs is clearly identifiable with both the order number and name of the step, for example "1. Specifications". Thus, by clicking on the tabs in numerical order, a user of the package can step through a design easily.

However, many computer users may be more familiar with "wizards" (for example, as used when setting up printers or other hardware in Windows), where "Next" and "Back" buttons provide access to each step in order. The advantage of the tabs over the wizard-type buttons is that the user can hop back directly from step 6 to 2 to check values entered there and then back again, whereas in the latter method each intermediary step would have to be viewed.

One must also take into account users who prefer to navigate using the keyboard instead of the mouse. This is usually achieved with what is called "tabbing", where a user will type a value in an input box, and by pressing the tab key, they will automatically move the focus on to the next input box, enter a value, press tab again and so on. The package has to be designed with a tab order that will allow users to move in a preferred sequence through the input stages. The tab key can also be used to select other controls like option groups, grids, and the navigation buttons for access to the other design steps.

5.3.2.4   Input and Output Boxes

One of the most difficult aspects of creating a GUI is that of making clear to a user which areas are for inputting data and which ones are for outputting data, especially when these can be in a state of flux from one design to the next.

For example, our package normally calculates turn values and displays the resulting value in a read only box. But there is an option in the program to enter a custom number of turns and override the suggested value(s). We could have created a separate input box especially for this scenario, but as well as being confusing, space is precious and there are a number of similar options in our package that could also require new boxes.

Instead, it was decided to colour code all boxes that allow input as white, and informational or read only output boxes as light yellow. Thus, the same box can be recycled from input to output by a simple change of background colour. Boxes are changed from input to output mode either by the software when it decides that a particular input is necessary or unnecessary, or by the user through the use of an option button related to that box.

For example, in the turns scenario just mentioned, there is an option group with two states, "use precalculated turns" or "use custom number of turns". Selecting the first option causes the turns text box to stay in output mode. Even though the user can select yellow output boxes, all key presses are ignored while the focus is on a box in output mode. Selecting the second option changes the background colour of the turns text box to white, and this means that it will allow user input (key presses are no longer ignored). The value input by the user can then be stored in a variable for use in later calculations.

5.3.2.5   Organising Data in Each Step

Even though the design process is broken into a number of distinct steps, it can also be necessary to group related sets of data together in separate

areas which could be considered sub-steps. These areas are contained within objects called "frames" – these are boxes with text at the top giving a general description of the contents.

Input boxes or option buttons or other controls then lie within the frame's boxed border. With proper descriptions, these frames can make the task of locating desired data much easier and faster for new users. They also serve to avoid a cluttered look by ensuring that every data input or output box is contained in some frame.

For example, in the core selection folder, we have three frames for the main sub-steps – choose a core shape, choose a core type, and select appropriate core.

5.3.2.6   High Precision Numbers

Another issue encountered was that of numbers in the expert options frame (which uses slightly smaller text boxes) with high precision that extended beyond the end of the text box (in fact this could happen to any box containing a number with a large number of relevant decimal places).

While a user can always click on a box, and either move through the digits using the arrow keys or copy the number and paste it into another application, another option has been added to our GUI - when the mouse is moved over one of these boxes with a cropped value, the full number is shown in a status bar at the bottom of the screen.

5.3.2.7   Drop Down Menus

Given a finite set of options from which a user can choose, these options can best be stored in a drop down menu. This has the advantage of hiding a potentially long list of values, while at the same time allowing a user to easily view the values and select one at any stage rather than having to remember valid options. If screen space is not an issue, a long list box that will show multiple available values at once can be used.

5.3.2.8   Grid Areas

Grid areas are a compact method for displaying and choosing from large tables of data. Since all of the data does not have to be displayed at once, the tables can vary in size, and the user still has the ability through scroll bars to access any data in the table. This is particularly useful for tables of core data which can have many fields or columns, and possibly hundreds of entries or rows.

5.3.2.9   Message Boxes

A user interface should provide adequate and meaningful status feedback, particularly if an error occurs. Message boxes are used to signal errors to users and recommend solutions to problems.

5.3.2.10 Option Groups

Option groups allow fast selection of discrete variables, that is, variables that are limited to discrete states and can be represented in programming terms by integer values (for example in our application option group, the possible states are "forward converter", "push-pull converter" and "centre-tapped transformer").

5.3.2.11 Check Boxes

Check boxes with unambiguous labels clearly show the status of a Boolean variable, that is, a variable with only two states that may be used to confirm the presence or absence of a particular design feature (for example, if the output is rectified or not for a centre-tapped transformer).

5.3.3 Optimisation Techniques

The performance level of an engineering design is a very important criterion in evaluating the design. The search for better and better designs means improvement in the performance level at every stage. It can be said that design, after an initial concept formulation, goes through a decision stage whose objective, from a general vantage point, is the following:

> "Given the functional requirements (technical, physical, regulatory etc.) for a product or technical system. Among the proposed design alternatives meeting these requirements, find the best solution in terms of some selection criterion." [83]

Mathematical optimisation in its general scope deals with a completely analogous type of problem to the decision stages of an engineering design so that we may model these stages of the design process according to the format of mathematical optimisation (with constraints). Magnetic design problems can also be mathematically formulated (as we have seen in Chapter 3) so that mathematical programming techniques can be used to arrive at designs with optimum performance. Optimisation techniques based on mathematical programming provide the magnetic designer with robust analytical tools, which help them in their quest for a better design. The basic elements of a mathematical optimisation problem, applied to a system or product to be designed, can be defined as follows [83]:

1. Design Variables, X
2. Parameters, P
3. Constraints, C
4. Measures of Merit, M

In terms of these elements, the mathematical optimisation problem can thus be formulated as follows (omitting the parameters P for brevity):

> "Find the set of design variables X that will minimise or maximise the measure of merit function M(X) subject to the constraints C(X)."
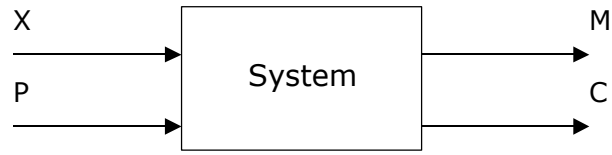
Figure 5.4. Elements of the optimisation problem.

For an algorithmic optimal design like ours, separation of the "problem model" and "problem independent strategy" is necessary. The model provides evaluations of M and C for any given X, and the strategy in response to this information directs the change in the design variables X (Figure 5.5). Thus we have a cyclic process. For example, unacceptable loss levels in our measure of merit M(X) may dictate a change in our desired efficiency level η or temperature rise ΔT, both of which are design variables in X.
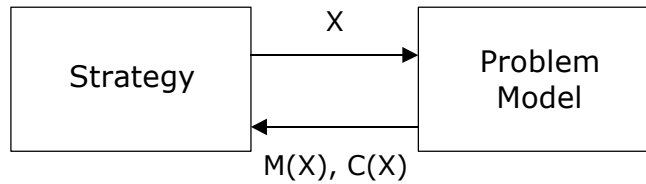
Figure 5.5. Interaction between strategy and model.

5.3.3.1 Design Variables

The design of the system or product can assume many different states characterised by variables. These variables which are under the designer's control are called design variables, and are denoted by the vector X:

$$X = (x_1, \ldots\ldots, x_n).$$ (5.1)

For our magnetic components, X consists of the transformer design specifications (power output, frequency, temperature rise etc.) and user modifiable design factors (window utilisation factor etc.).

5.3.3.2   Parameters

These are variables which influence the state of the system design, but cannot be controlled by the designer (for example, the permeability of free space, $4\pi \times 10^{-7}$ H/m).

5.3.3.3   Constraints

These are conditions which limit the free variation of the design variables, and are expressed by the constraint function C(X, P). These functional relationships can be derived from functional and other requirements which the design must meet.

They can assume the form of equality (5.2) or inequality (5.3) constraints:

$$h_j(X, P) = 0, j = 1, ..., J ,$$
(5.2)

$$g_k(X, P) \geq 0, k = 1, ..., K .$$
(5.3)

For a well-posed problem, J must be less than n (the size of X) but K can be arbitrary.

For example, the duty cycle of a current waveform in a transformer winding should lie in the range from 0 to 1. This is expressed by two inequality constraints:

$$D \geq 0 \text{ and } 1 - D \geq 0 .$$
(5.4)

An important constraint which magnetic designers will be informed of is that the flux density must be less than the saturation value as proscribed by the core manufacturer:

$$B_{sat} - B_m \geq 0 .$$
(5.5)

5.3.3.4   Measures of Merit

The merits of a design are judged on the basis of a criterion called the measure of merit function M(X, P). For a design with a single measure of merit, this is sometimes called the figure of merit. We have already demonstrated methods for optimising total transformer loss (Chapter 3) and AC resistance for foil windings (Chapter 4). These will be our measures of merit.

A measure of merit function is called unimodal if it has only one optimum (a minimum in terms of losses or AC resistance) in its feasible range, that is, the range where no constraint is violated. Figure 5.6 (a) and (c) illustrate this situation. The function is multimodal, as shown in (b) and (d), if more than one local minimum exists, and the lowest of these is the global minimum.
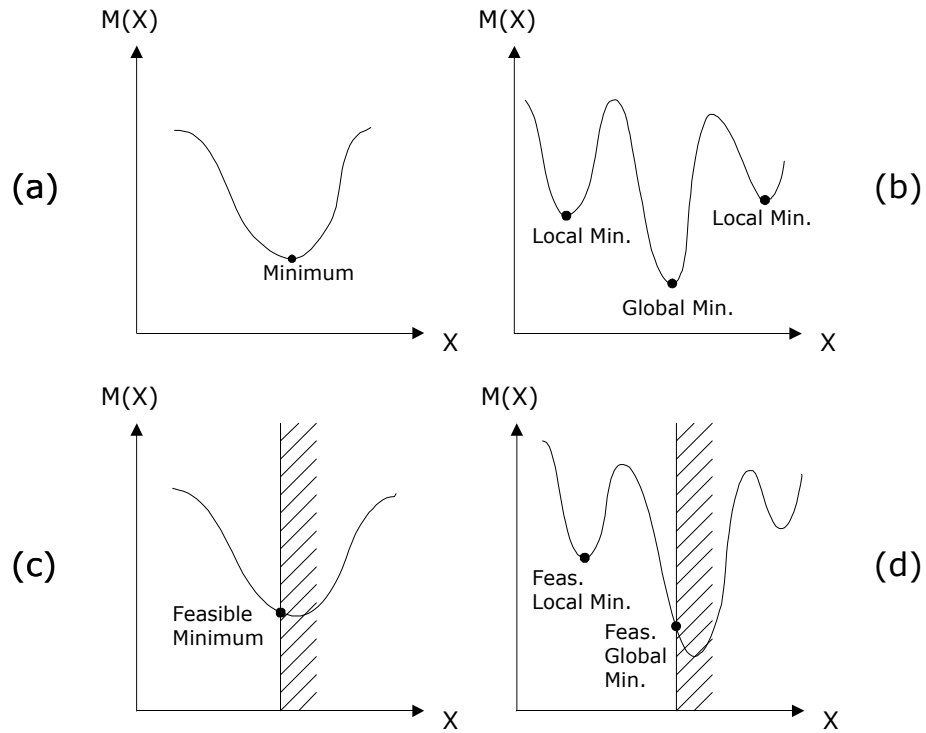
Figure 5.6. Types of optimisation problems for univariate case.

The measure of merit function for minimising total transformer loss is of the constrained-unimodal type (Figure 5.6 (c)) since we are limited by the saturation flux density of the core material. The measure of merit

function for minimising AC resistance is of the unconstrained-unimodal type (Figure 5.6 (a)) since there is a single minimum value.

5.3.4   Repository of Knowledge

In the early design stages, the designer generates the functional requirements of the magnetic component to be designed. The expertise, both engineering knowledge and creative skill, of the designer plays a very important role at this stage and can make a significant difference to the proposed design.

When a novice designer is asked to carry out a design, they cannot generally have access to the expert knowledge in the possession of the experienced designer. Since computers can store large amounts of information, expert knowledge of experienced designers can be stored in the computer's memory so that it can be used to guide the novice designers in taking better design decisions.

For example, an experienced magnetic designer will know that a particular turns ratio or set of input and output voltages will result in an unrealisable duty cycle. This knowledge is incorporated in the system and a designer will be notified if such an issue arises with a message box informing them that a design error is imminent.

Another example is that an experienced designer will know that the use of a plastic bobbin for a winding will reduce the height of the winding by at least 10%. The software will suggest these recommended "expert" values for certain variables. These values are default values only and can be overwritten if the designer wishes.

A "repository of knowledge" is incorporated into our system, and this gives us a program where an algorithmic formulation of the design problem is supplemented by rules of thumb and other designer experience. Although such a system is useful for novices, it can also be used by expert designers who may already know of certain recommended values and want to save time setting them up in the first place.

5.4   Program Overview

Visual Basic was chosen as the programming language for the software as it combines an easy-to-use environment for designing GUI-intensive packages with the power to integrate and distribute the standard libraries required for opening Access-format relational databases.

A top level data flow diagram (DFD) of the system is shown in Figure 5.8. Each of the main processes corresponds to one of the steps mentioned in the section dealing with the folders necessary for each step, 5.3.2.1.

The main processes numbered 1 to 12 in the top level DFD can contain many subprocesses. We will now describe each of these under headings corresponding to the main process stages, and we will also show "exploded" or lower level DFD diagrams for each design step. Generalised structured English code for the important processes is included in Appendix C.

The system is called MaCoDe, or Magnetic Component Designer.
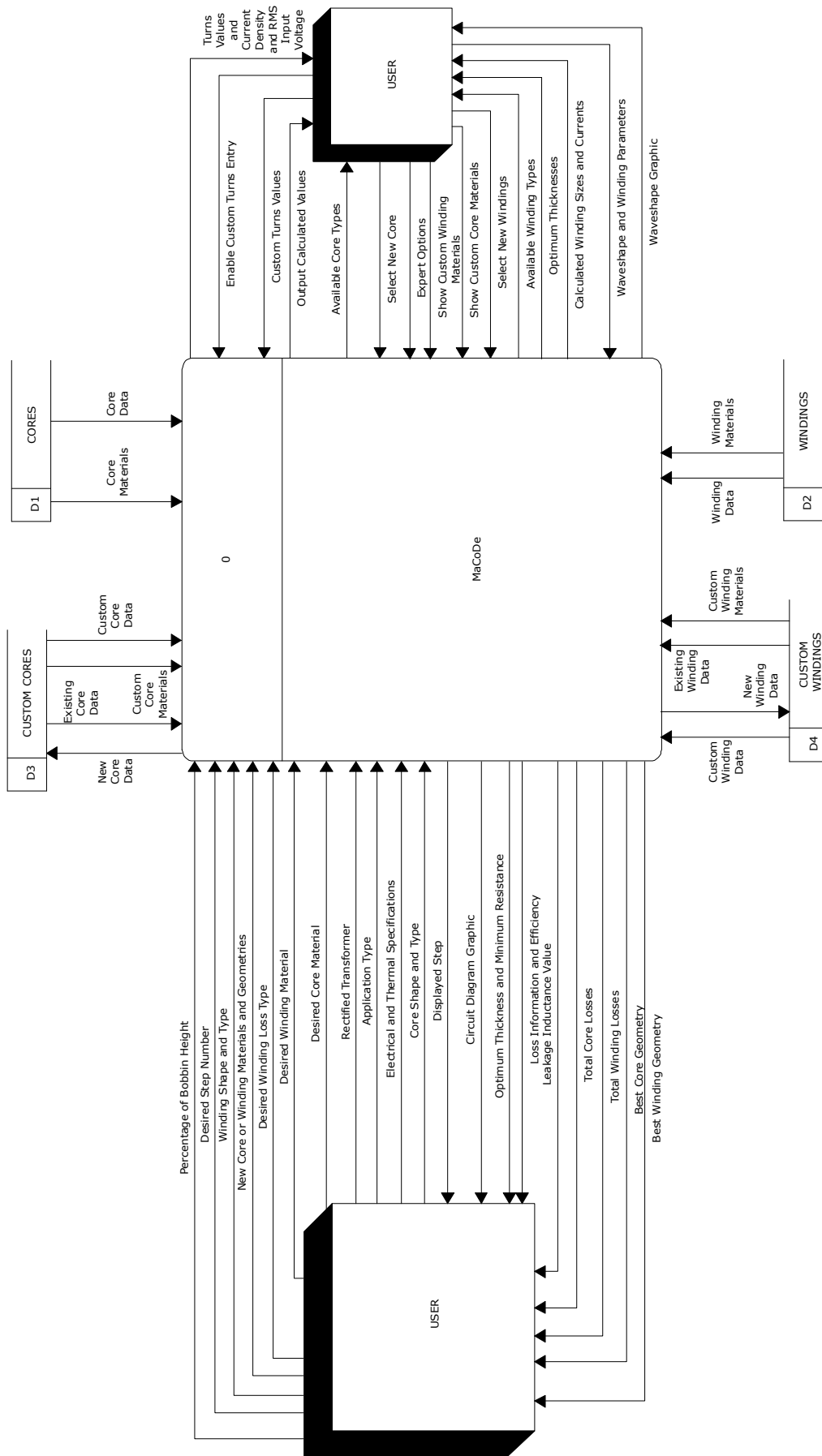
Figure 5.7. Context diagram.
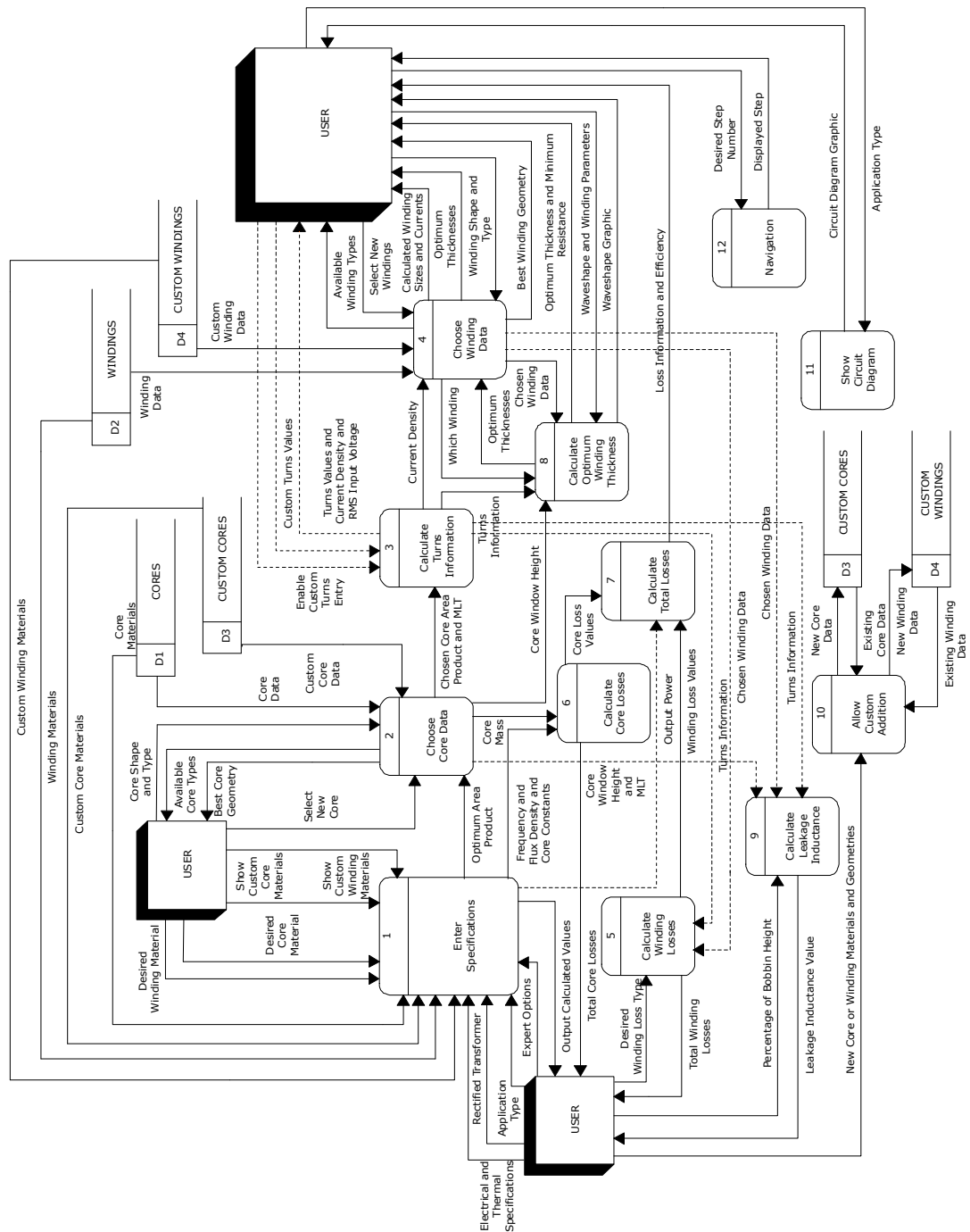
Figure 5.8. Top level process DFD 0.

5.4.1 Enter Specifications

To begin, the user chooses one of the applications available: centre-tapped transformer, forward converter or push-pull converter.

The user is then required to enter the following specifications (Figure 5.9), common to each application:

- Output voltage
- Output current
- Input voltage range (upper and lower)
- Frequency
- Temperature rise
- Ambient temperature
- Desired efficiency

An "Expert Options" section allows the user to view more detailed information on constants/other factors used in calculations and to change some of these default values.

Once the specifications and materials are set, optimum area product and flux density values are calculated. As specifications, materials or expert options are varied, these A_p and B_o values are updated accordingly.

Figure 5.9. Initial screen where specifications are input.

The "Enter Specifications" step is made up of a number of subprocesses as shown in the data flow diagram of Figure 5.10.
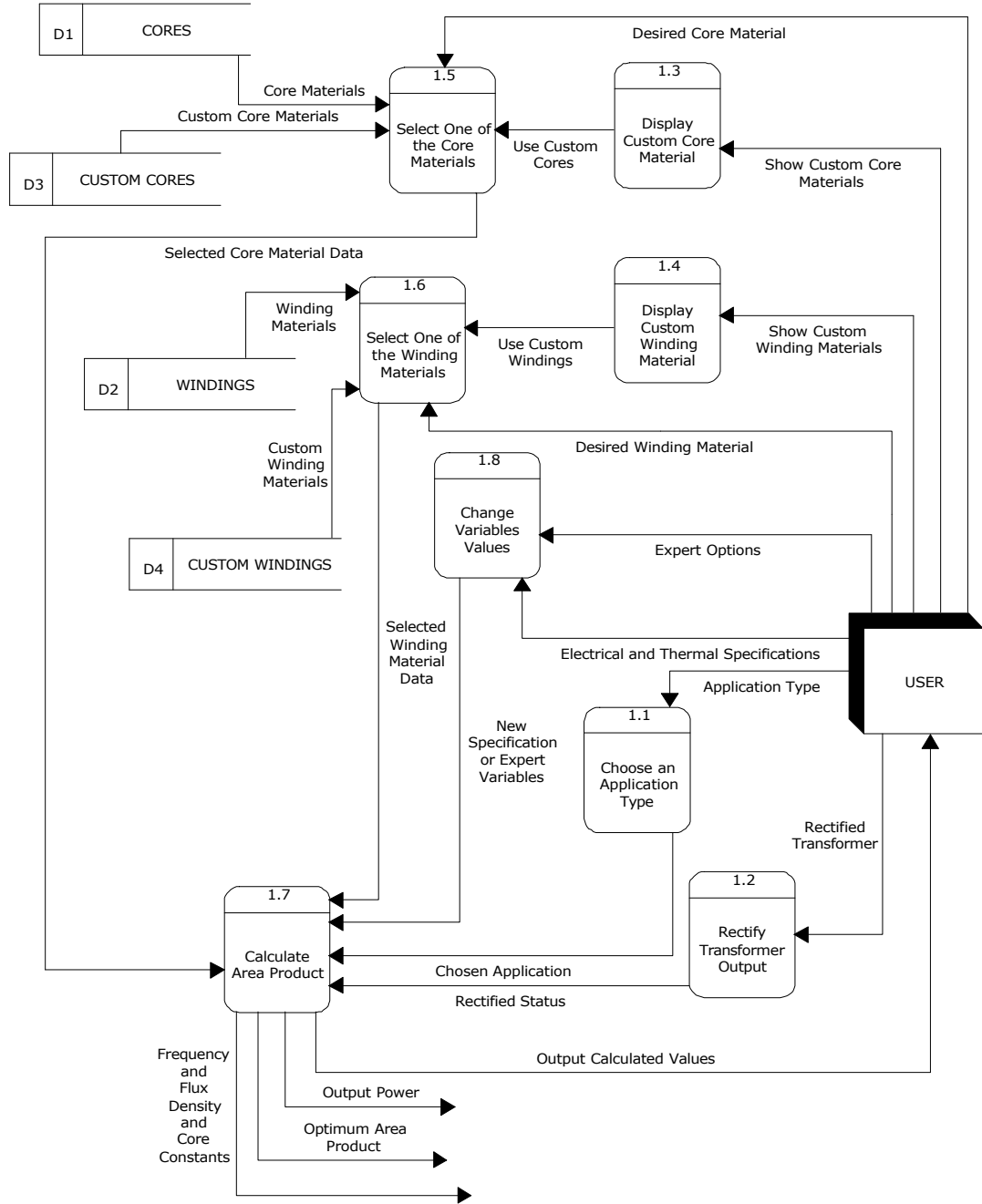
Figure 5.10. "Enter Specifications" process DFD 1.

We will now describe the subprocesses in order of PID or process number, as shown at the top of the rounded process boxes in Figure 5.10.

5.4.1.1   Choose an Application Type

The user must choose the application type for the proposed design. This is the very first step in the design. At the moment, the available choices are: centre-tapped transformer, forward converter and push-pull converter.

Depending on the application chosen, the equations used to calculate certain transformer characteristics (for example, output power, waveform factor, power factor etc.) during the "Calculate Area Product" subprocess will vary as illustrated in the design examples of section 3.4.

5.4.1.2   Rectify Transformer Output

The user can choose to rectify the output of the centre-tapped transformer application. For all other applications, this facility is disabled, and the process is not run. If the transformer is rectified, a 1 V diode drop is assumed in the output, so that $P_o = (V_o + 1)I_o$, and $k_{ps} = 1/\sqrt{(2)}$ (see equation (3.73)). Otherwise, $P_o = V_o I_o$ and $k_{ps} = 1$.

5.4.1.3   Display Custom Core Materials

This process allows the user to choose materials from the custom cores database if they so desire. Turning the "Display Custom Core Materials" option on and off alternates between displaying the custom and standard core material tables to the user.

5.4.1.4   Display Custom Winding Materials

Similar to the previous process, the user can choose to select their application winding material from the custom or standard databases.

5.4.1.5 Select One of the Core Materials

The user must select a core material suitable for the current application. If custom cores are enabled, they can choose from a database of materials they themselves have created. When a new core material is chosen, the area product must be recalculated.

5.4.1.6 Select One of the Winding Materials

Similar to the previous process, the user must choose a standard or custom winding material, after which the area product is recalculated using the process described in section 5.4.1.7.

5.4.1.7 Calculate Area Product

This is a key subprocess in the "Enter Specifications" step. The input specifications are stored as variables; the output power, waveform and power factors are calculated to yield the VA rating of the design. K_o is found from (3.29), K_t from (3.32), K_j from (3.37), and the optimum flux density B_o can then be calculated using (3.34).

B_o is checked against the maximum flux density B_{sat}. If it is less than B_{sat}, A_p is calculated with (3.28), otherwise A_p is found using the Newton Raphson equations of (3.40) and (3.39). All calculated results are then displayed to the user.

5.4.1.8 Change Variable Values

This process allows modification of the following specifications and other variables: ambient temperature, core volume constant, efficiency, frequency, heat transfer coefficient, input voltage range, output current, output voltage, stacking factor, surface area constant, temperature factor, temperature rise, turns ratio, winding volume constant, and window utilisation factor. Only numeric values can be input.

5.4.2 Choose Core Data

After finding the optimum A_p value, the next step in the design process is to select an actual core with a size close to that calculated. A screenshot from this step is shown in Figure 5.11. First the user selects the shape of core from the following - CC, EE, EI, UU, pot, or toroidal. Core types with a matching shape and material (as chosen in the first step) are displayed.
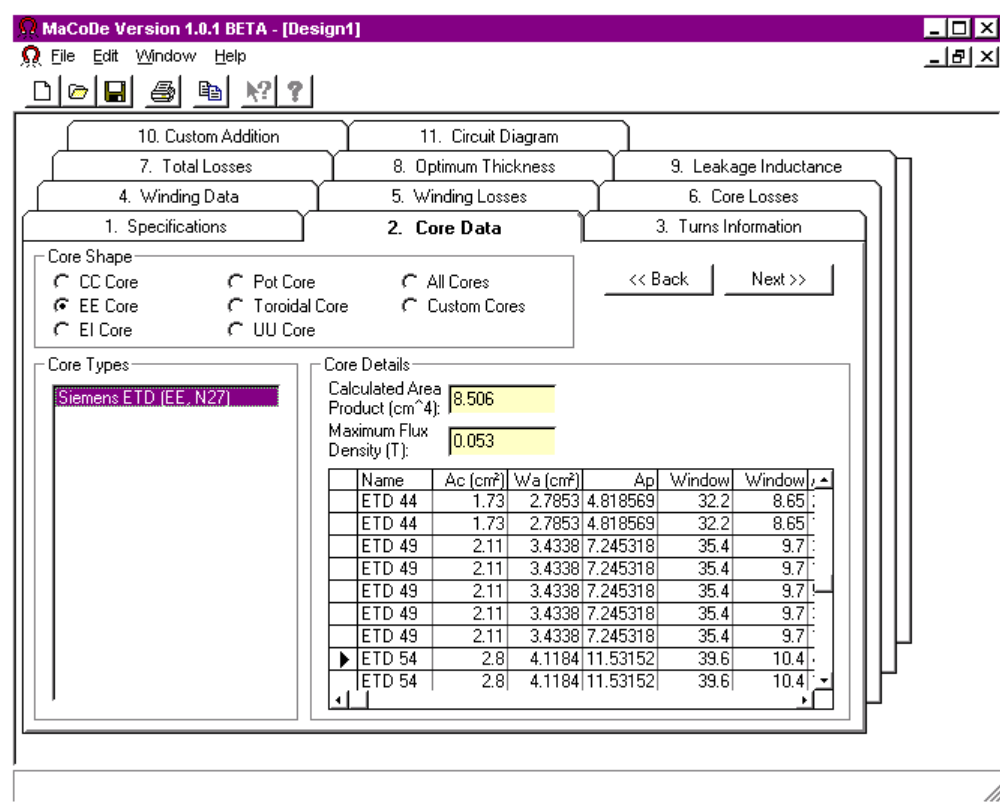
Figure 5.11. Selection of core shapes and types.

The user must then select one of those core types to continue with the design procedure. Once the core type has been chosen, the software selects the core from that category with the most appropriate area product value (if one is available).

A core with an A_p value greater than or equal to that calculated in step 1 is automatically selected. An important feature of the software is that the user is not constrained to accept the core size (or the winding size in step

165

4) that is automatically suggested, a larger or smaller size can be chosen if necessary.
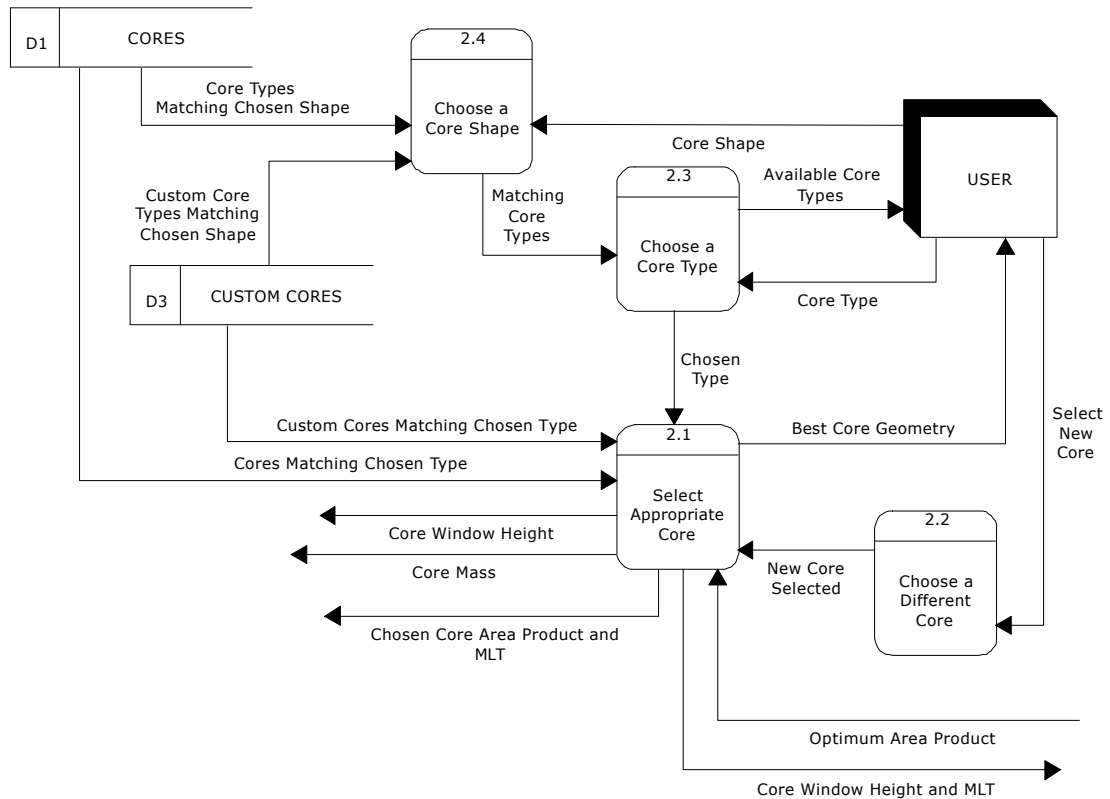
Figure 5.12. "Choose Core Data" process DFD 2.

The "Choose Core Data" step is composed of the subprocesses shown in the data flow diagram of Figure 5.12 and detailed below.

5.4.2.1 Select Appropriate Core

This process attempts to choose a core with an A_p value greater than or equal to that calculated in the first step. The procedure searches through the currently highlighted group of cores, and automatically selects the most suitable. Values for the following core specifications are stored as variables for use in later calculations: mass, MLT, A_p, W_a, A_c, window height and width. If no suitable core is found, the largest core in the group is chosen and the user is informed of this fact.

5.4.2.2   Choose a Different Core

The user can choose to override the automatically selected core from the previous process by simply selecting another core. New values for the core specification variables are then set.

5.4.2.3   Choose a Core Type

This is the second action taken by the user chronologically. After selecting the desired core shape, a list of available core groups is then displayed (i.e. those types of core matching the chosen shape), from which the user must choose one.

After selecting one of these core types, the process to select an appropriate core is then called.

5.4.2.4   Choose a Core Shape

This is the first chronological action that must be taken. A core shape is chosen from the available list: EE, EI, CC, pot, toroidal or UU. By choosing one of these shapes, the process displays all of the available core groups or types that match both this shape and the core material selected in the "Enter Specifications" step.

If the "All Cores" option is selected, all core types matching the core material are displayed regardless of core shape. Another option is "Custom Cores", which will switch to the custom cores database and display all core types created previously by local users of the system.

5.4.3   Calculate Turns Information

The turns information is displayed in step 3, based on the chosen (not automatically calculated) area product value from the previous step.

Users also have the capability to override the calculated turns data and enter their own values.
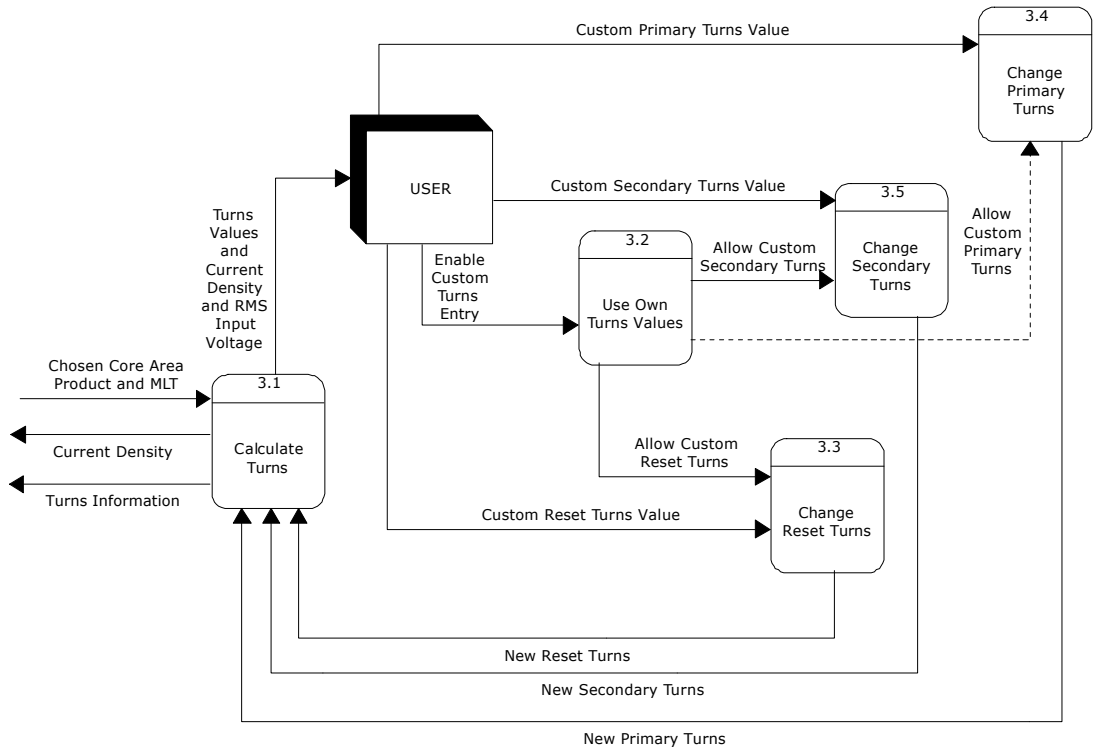
Figure 5.13. "Calculate Turns Information" process DFD 3.

This step consists of the subprocesses detailed below and illustrated in the data flow diagram of Figure 5.13.

5.4.3.1 Calculate Turns

This subprocess begins with a rule of thumb check to see if the core is too large for applications with high switching frequencies. If P_{fe} estimated by (3.13) is greater than P predicted by (3.14), then we clearly have a problem and the user is informed that a smaller core is preferable.

The process continues by calculating the appropriate N_p, N_s (and N_t for the forward converter) values for the chosen application (3.41). ρ_w is then calculated using (3.43) and J is found using (3.42). Finally, the calculated turns information is displayed to the user.

5.4.3.2   Use Own Turns Values

The user can choose to use their own values for N_p, N_s (and N_t for the forward converter) if they are unhappy with the values suggested by the software. Each time this option is disabled, the turns information is automatically calculated again using the previous process.

5.4.3.3   Change Reset Turns

This process is described in section 5.4.3.5.

5.4.3.4   Change Primary Turns

This process is described in section 5.4.3.5.

5.4.3.5   Change Secondary Turns

If the "Use Own Turns Values" option has been enabled, then entry of values for the reset, primary or secondary winding turns value is allowed. The only condition is that values entered must be numeric. These custom values will then be used instead of the automatically generated values in subsequent steps.

5.4.4   Choose Winding Data

As with the cores, the user first chooses the shape of winding required to display a list of matching types for that shape. The user then chooses one of the types of winding to display a full list of windings in that group (one of which will be automatically selected).

Figure 5.14. Data for primary and secondary windings.
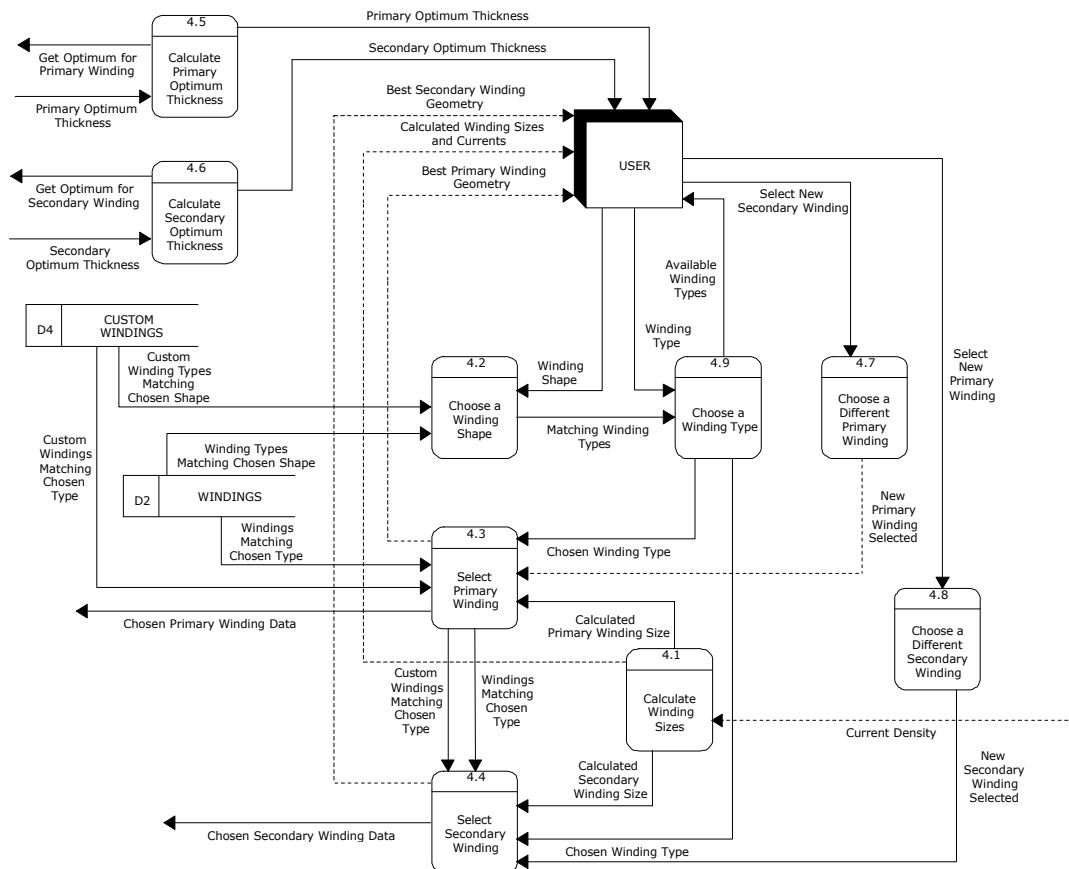
Figure 5.15. "Choose Winding Data" process DFD 4.

For example, the shape might be "Round Wire", the type "AWG Wire", and then "AWG 13" might be the size automatically picked by the software for a particular winding (Figure 5.14).

The subprocesses shown in the data flow diagram of Figure 5.15 are detailed below.

5.4.4.1   Calculate Winding Sizes

The primary and secondary currents are calculated for the different applications as demonstrated in the examples of section 3.4. The primary and secondary winding areas (A_w) can then be found by taking the corresponding current value and dividing this by the current density (as calculated in the "Calculate Turns Information" step). The diameters can then be found using $A_w = \pi r^2$, i.e. $d = 2\sqrt{(A_w/\pi)}$. All calculated values are displayed to the user, and then the processes to select the actual primary and secondary winding sizes from databases are called.

5.4.4.2   Choose a Winding Shape

Similar to the "Choose a Core Shape" process, this procedure allows the user to choose one of the available winding shapes (round or layered) in order to display a list of winding types or groups matching both this chosen shape and the winding material selected in the "Enter Specifications" step. Alternatively, the user can display all standard or custom winding types available in the databases.

5.4.4.3   Select Primary Winding

This procedure opens the windings table corresponding to the currently chosen winding group, and iterates through the records in the table until a winding with bare diameter greater than the calculated primary winding diameter is found. This choice for the primary winding is then

automatically selected in the full table of winding data, as shown in Figure 5.14.

5.4.4.4 Select Secondary Winding

Similar to the process described in section 5.4.4.3, this procedure iterates through all windings in the currently selected winding group until a suitable secondary winding is found.

5.4.4.5 Calculate Primary Optimum Thickness

This process is described in section 5.4.4.6.

5.4.4.6 Calculate Secondary Optimum Thickness

The user can choose to calculate the optimum thickness of a single layer in a layered winding with the current turns specifications by choosing this option. The "Calculate Proximity Effects" routine is called for each winding, and the number of layers and corresponding optimum thickness values are displayed. This is for informational purposes only, and can be used to aid the user in selecting an appropriate winding size.

5.4.4.7 Choose a Different Primary Winding

This process is described in section 5.4.4.8.

5.4.4.8 Choose a Different Secondary Winding

The user can choose to override the primary or secondary winding sizes suggested by the program by manually selecting different windings from the group currently displayed. If a winding shape or type has not yet been chosen, this function is not available.

5.4.4.9   Choose a Winding Type

This procedure is carried out after the selection of a winding shape, which lists all suitable winding types. By selecting one of these winding types, two areas of corresponding core data are displayed for the primary and secondary windings. The most appropriate winding sizes will automatically be selected in these two areas (see sections 5.4.4.3 and 5.4.4.4).

5.4.5   Calculate Winding Losses

The user can choose to display DC winding losses, AC winding losses, or all of the DC and AC losses combined, as shown in Figure 5.16.

Figure 5.16. Display of DC and AC winding losses.

For the AC winding losses calculation, the skin and proximity effect factors are multiplied by the DC losses to account for these high frequency effects.
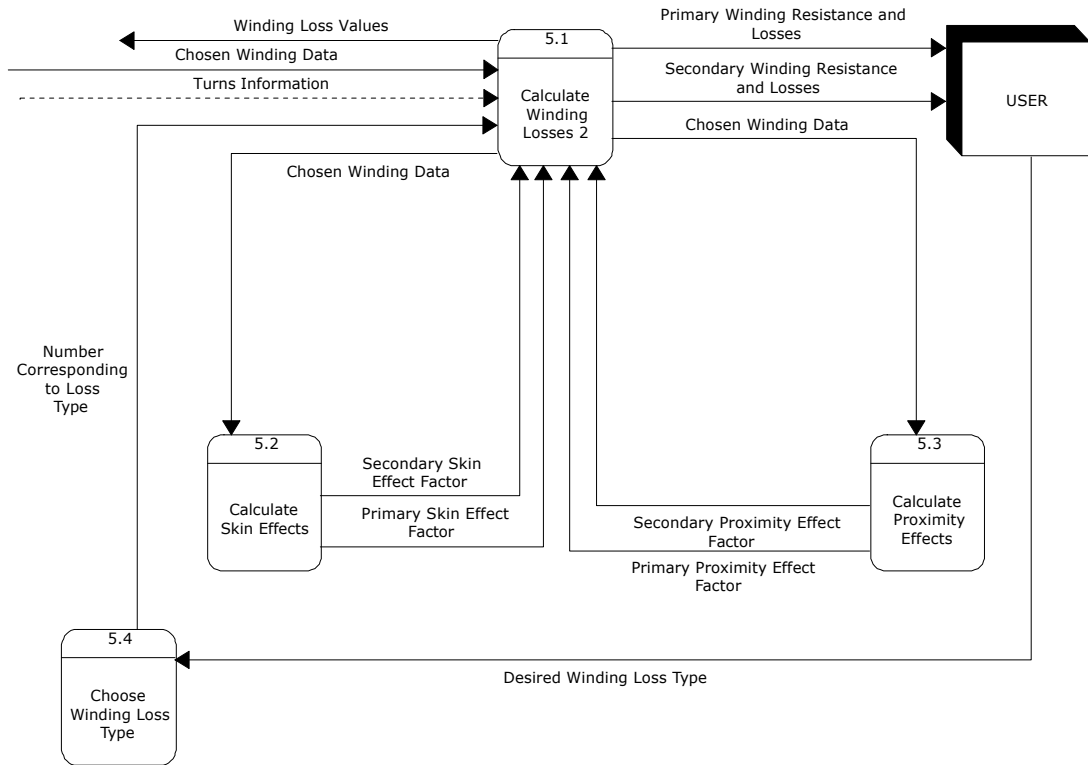
Figure 5.17. "Calculate Winding Losses" process DFD 5.

The subprocesses for the "Calculate Winding Losses" step are shown in Figure 5.17 and will now be described.

5.4.5.1 Calculate Winding Losses

Depending on whether the user chooses to include AC skin and proximity effects or not in the calculated winding loss values, the losses (3.44) will be multiplied by the appropriate AC loss factors. These factors are calculated by calling the "Calculate Skin Effects" and "Calculate Proximity Effects" processes for both the primary and secondary windings. All winding resistances and losses are then displayed.

5.4.5.2   Calculate Skin Effects

Firstly, the skin depth in mm is obtained from $\delta = \sqrt{\rho_w / \pi f \mu_o}$ (see section 3.3.5).   Then, separate skin effect factors for each of the primary and secondary windings are calculated using the appropriate case in equation (3.46), depending on whether r/δ is greater than or less than 1.7.

5.4.5.3   Calculate Proximity Effects

This process spans two steps ("Calculate Winding Losses" and "Calculate Optimum Winding Thickness"), and is detailed later in section 5.4.8.1.

5.4.5.4   Choose Winding Loss Type

When changing the types of effects we wish to include in our winding loss calculations (DC, AC skin effect, AC proximity effect, all AC and DC losses), the "Calculate Winding Losses" process needs to be called again.

5.4.6   Calculate Core Losses

The core losses are calculated automatically, based on the core loss equation with core weight, frequency, maximum flux density and K_c, α, β constants as variables.   There is only one subprocess as shown in Figure 5.18.
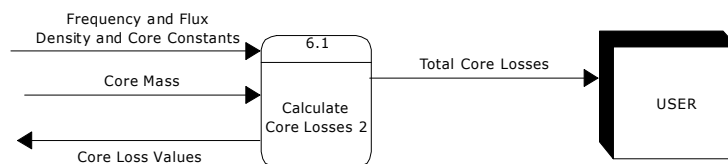
Figure 5.18. "Calculate Core Losses" process DFD 6.

5.4.6.1 Calculate Core Losses

The core losses (3.13) are calculated using the constants associated with the core material selected during the "Enter Specifications" stage, the core specifications from the "Choose Core Data" step, the maximum flux density and the operating frequency.

5.4.7 Calculate Total Losses

Total losses are simply the sum of the winding and core losses previously calculated. The efficiency is then calculated from the output power and these losses. The process is illustrated in Figure 5.19.
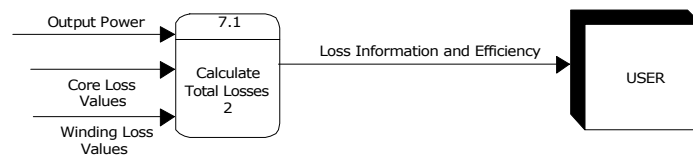
Figure 5.19. "Calculate Total Losses" process DFD 7.

5.4.7.1 Calculate Total Losses

The total losses are found from $P_{tot} = P_{fe} + P_{cup} + P_{cus}$, and the efficiency is then found from $\eta = P_o/(P_o + P_{tot})$.

5.4.8 Calculate Optimum Winding Thickness

Another important feature of the software is the step that performs the optimum winding thickness calculation. This is based on theory presented in Chapter 4.
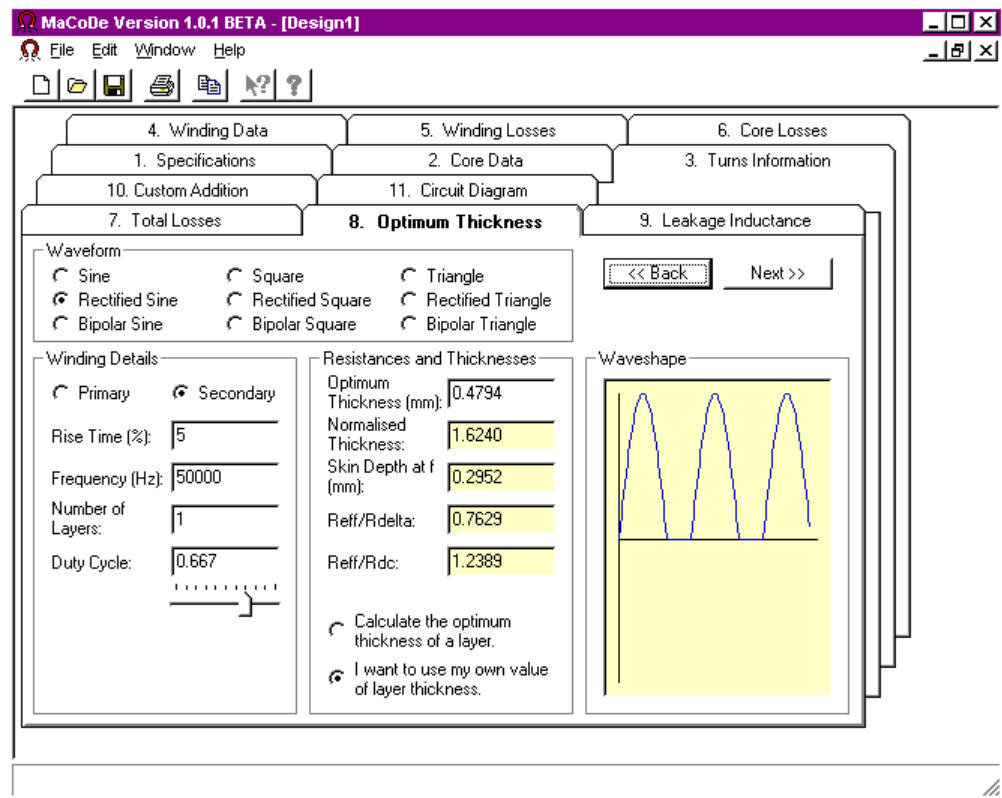
Figure 5.20. Optimum winding thickness for various waveshapes.
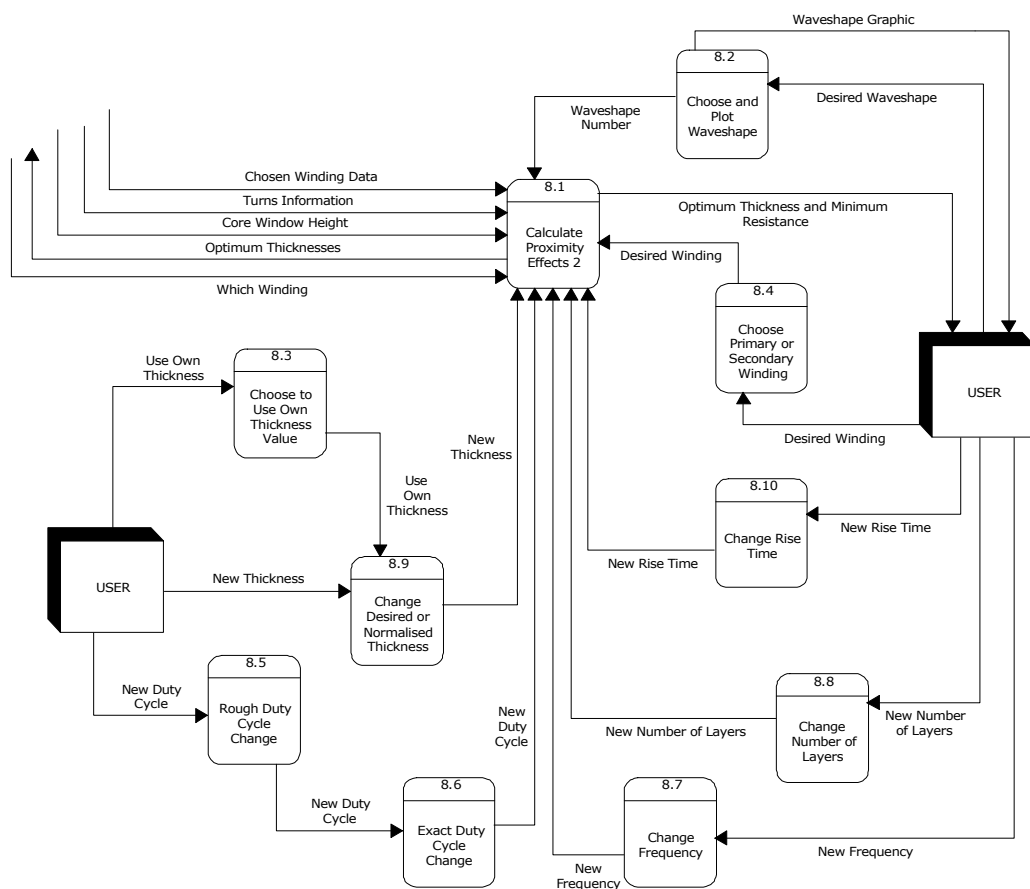
Figure 5.21. "Calculate Optimum Winding Thickness" process DFD 8.

By default, the frequency, duty cycle, number of layers and current waveforms for the application under design are displayed. The user can modify these values or the waveform type to view optimum thicknesses and minimum AC to DC resistance ratio values for multiple configurations if so desired. The user can also choose to try a different value of layer thickness and view its effects on the AC to DC resistance ratio.

This step consists of the subprocesses shown in Figure 5.21 and outlined below.

5.4.8.1   Calculate Proximity Effects

The "Calculate Proximity Effects" process is called after the selection of the current waveshape for the primary or secondary winding. The optimum normalised thickness Δ_{opt} is calculated using the appropriate formulas from Table 4.5 and R_{eff}/R_δ is found from (4.58). The user can choose to override values for the frequency, duty cycle, rise time and number of layers displayed by default (from the application currently being designed). If the user has enabled the "Choose to Use Own Thickness Value" option, the normalised thickness is set to the value entered by the user, and R_{eff}/R_δ is calculated using this value for Δ instead of Δ_{opt}. The process also uses the skin depth to calculate and display values for R_{eff}/R_{dc} and d, the optimum thickness in mm.

5.4.8.2   Choose and Draw Waveshape

The available waveshapes in this step are shown in Figure 5.20. On choosing one of these, this process draws the current waveshape using the specified duty cycle value where applicable. After choosing a new waveshape, the "Calculate Proximity Effects" process is called again since the normalised thickness and AC resistance ratio formulas are unique for each waveshape.

5.4.8.3 Choose to Use Own Thickness Value

This subprocess enables the user to override the optimum normalised thickness value suggested by the software to see the effect of varying the normalised thickness on the AC losses (proportional to AC resistance). This can be a useful tool for fine-tuning the suggested optimum normalised thickness value.

5.4.8.4 Choose Primary or Secondary Winding

The user can choose to calculate the optimum thickness for either the primary or secondary winding using this option. By selecting either the primary or secondary winding, the number of layers must be recalculated for the "Calculate Proximity Effects" process using the core window height, the number of turns and the winding diameter values found in earlier steps of the design process.

5.4.8.5 Rough Duty Cycle Change

The user can choose to either enter a duty cycle value manually, or to vary the duty cycle in steps of 0.1 and view the effect on the optimum thickness and AC resistance. This particular process makes use of a sliding bar which increments the duty cycle by 0.1 in the range 0 to 1. After modifying the duty cycle, the waveshape is redrawn.

5.4.8.6 Exact Duty Cycle Change

As mentioned, the user can enter an exact value for the duty cycle between 0 and 1. This process does not allow entry of a duty cycle value for the pure sine wave, but all of the other waveshapes are affected by duty cycle changes. After a duty cycle update, the waveshape must be redrawn and the "Calculate Proximity Effects" process is called to update the optimum thickness and AC resistance values.

5.4.8.7   Change Frequency

On changing the frequency of the current waveshape, the skin depth (which is a function of frequency), R_{eff}/R_{dc} and the actual optimum thickness value in mm are recalculated and displayed.

5.4.8.8   Change Number of Layers

Changing the number of layers will also have an effect on the calculated optimum thickness value, and when the user chooses to modify the number of layers manually, the "Calculate Proximity Effects" process must be called to recalculate and update the displayed results.

5.4.8.9   Change Normalised Thickness

It was mentioned that the "Choose to Use Own Thickness Value" option allows modification of the normalised thickness value in order to see the effect on the AC resistance. If that option is on, this process allows the user to enter a value for the normalised thickness; else input of a value is disabled. Afterwards, the AC resistance must be recalculated using the "Calculate Proximity Effects" process.

5.4.8.10 Change Rise Time

The rise time variable applies to the variations on the square waveshape. Again, changing this value means that proximity effects must be recalculated.

5.4.9   Calculate Leakage Inductance

The user can manually change the percentage height of the window available for windings to be wound on (usually reduced due to the

presence of a bobbin). Leakage inductance is then automatically calculated, and expressed in µH.
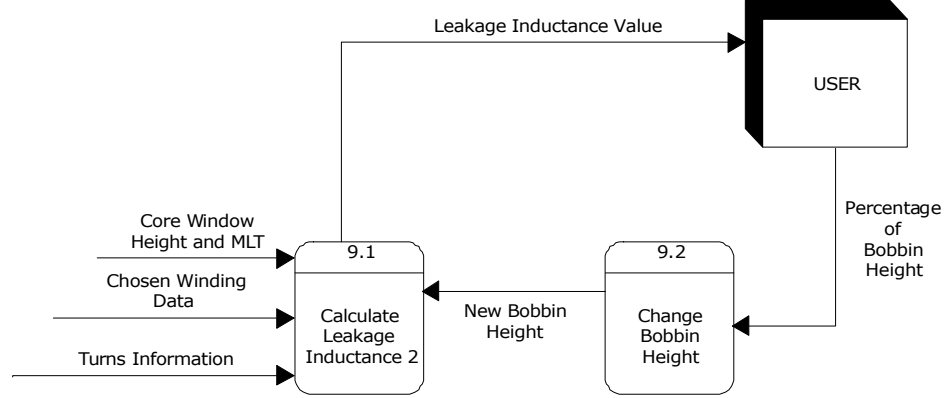
Figure 5.22. "Calculate Leakage Inductance" process DFD 9.

The total leakage is directly related to the total volume occupied by the windings. The greater the spread of windings along a core (increased width), the more reduced are the leakage effects. A simple expression for leakage inductance is used in the software, given by:

$$L_{\ell 1} + L_{\ell 2} = \frac{\mu_o N_p{}^2 MLTx}{3y},$$ (5.6)

where x and y are the total winding width and the winding height respectively [46]. Figure 5.22 is a data flow diagram showing the two subprocesses in the "Calculate Leakage Inductance" step. We will outline both of these subprocesses now.

5.4.9.1 Calculate Leakage Inductance

Firstly, the winding height is calculated by multiplying the chosen core window height with the percentage available for winding on a bobbin, as specified in the next subprocess. The number of primary or secondary layers is calculated from int((N/int(y/d)) + 1), where N is the number of winding turns, d is the winding diameter, y is the winding height, and int(z) returns the integer part of a real number z . The leakage inductance is a function of the winding height, the total winding width (the sum of

the products of winding thickness by number of layers for each winding), the number of primary turns and the mean length of a turn, and can be calculated using equation (5.6).

5.4.9.2 Change Bobbin Height

By default, the software sets the percentage of the core window height available for winding on a bobbin to 90%. The user can change this value manually if desired, and the leakage inductance value is then recalculated using the previous subprocess.

5.4.10 Custom Addition

If a particular core or winding is not available in the database supplied with the program, the user can add custom data. The layout of the folder for this step is shown in Figure 5.23.

Figure 5.23. Addition of new cores or windings into database.

The user begins by entering a customised or non-existent material. Then, after a new core or winding type is created, the data for a corresponding range of cores or windings are entered.
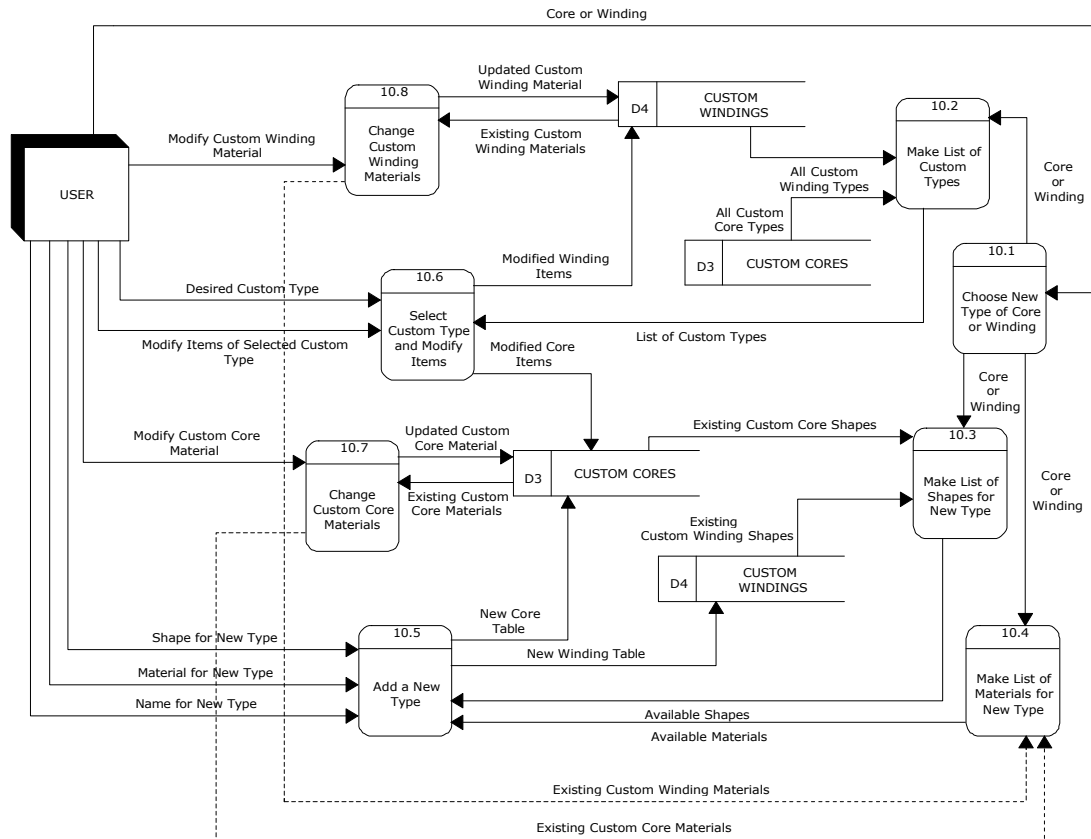
Figure 5.24. "Custom Addition" process DFD 10.

We will now give an overview of the subprocesses shown in the data flow diagram of Figure 5.24.

5.4.10.1 Choose New Type of Core or Winding

The user can choose whether to add a new type (i.e. a new group) of cores or of windings. When they choose to add a new type of core or winding, areas for entering data and material information specific to either cores or windings are displayed.

5.4.10.2 Make List of Custom Types

This process displays all the custom types that are available in the currently opened custom database file (of cores or windings, depending on which is selected). Each custom type has an associated table of data corresponding to a set of similar cores or windings.

5.4.10.3 Make List of Shapes for New Type

When the user decides to create a new type of winding or core, they must first select one of the available core or winding shapes. This process displays all the shapes that can be chosen for the new custom type: CC, EE, EI pot, toroidal or UU for cores, and round or layered for windings.

5.4.10.4 Make List of Materials for New Type

For a new type of winding or core, an associated material must be selected from the list of available materials. This list is generated from the "Material Attributes" table in the core or winding database, and the user can modify entries in this table through the "Change Custom Materials" subprocess.

5.4.10.5 Add a New Type

When the desired shape and material for the new type have been selected, and a name for the new type has been entered, a blank table for this type can then be created if the desired name does not already exist. Depending on whether a new type of core or winding is being created, the data fields that will be added to the new table will differ. When the new type has been successfully created, the list of available custom types must be updated by calling the "Make List of Custom Types" subprocess.

5.4.10.6 Select Custom Type and Change Items

This process allows the user to choose an entry from the list of available custom core or winding types, and then to make changes to individual cores or windings in the corresponding table of data.

5.4.10.7 Change Custom Core Materials

This process is described in section 5.4.10.8.

5.4.10.8 Change Custom Winding Materials

Two separate processes are required for changing custom materials because the material attributes are different for cores and windings. When the user makes changes to the materials, either by adding a new material or by modifying an existing one, the available materials list must be updated through the "Make List of Materials for New Type" procedure.

5.4.11 Show Circuit Diagram

This short step simply displays a diagram to the user, and consists of only one process (Figure 5.25).
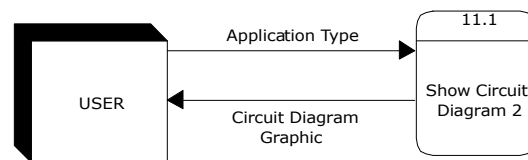
Figure 5.25. "Show Circuit Diagram" process DFD 11.

5.4.11.1 Show Circuit Diagram

Depending on the application chosen in the "Enter Specifications" step, a circuit diagram corresponding to the application is displayed to the user.

5.4.12 Navigation

As previously explained, it is important to be able to move back and forth through the design steps, but we must also make sure that we can not progress on to future steps without having completed all of the necessary steps so far. We will now describe the subprocesses shown in Figure 5.26 which control navigation.
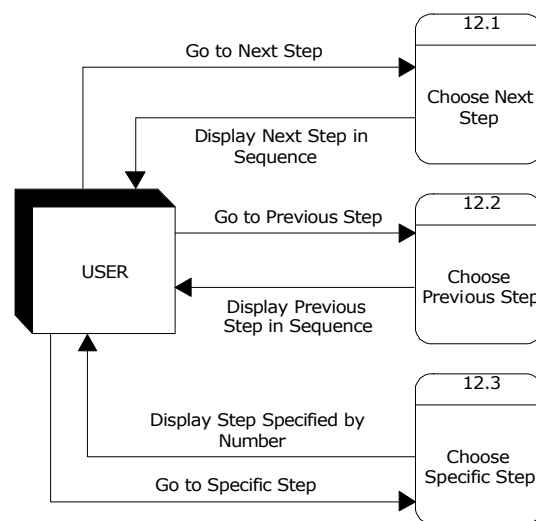
Figure 5.26. "Navigation" process DFD 12.

5.4.12.1 Choose Next Step

This process is described in section 5.4.12.2.

5.4.12.2 Choose Previous Step

The "Choose Next Step" subprocess moves on to the next step in the sequence, or, if we have reached the last possible step, returns to the first step. Similarly, the "Choose Previous Step" subprocess moves to either the previous step or the last step in the sequence if we were back at the first step. Both of these processes call the "Choose Specific Step" routine,

which will ensure that we cannot move to a step before we have completed all necessary information.

5.4.12.3 Choose Specific Step

We must keep track of the steps that have been completed so far before progressing any further in the design process. When the user attempts to navigate to a particular step, this process must first check that the required steps have been completed so far (if not, we could cause program failure by attempting to make calculations using variables that have not yet been set). Then, if the requisite number of steps have been carried out, this process will have to either set some default variables for the new step, or call some other processes to make calculations automatically. For example if we navigate to the leakage inductance step, the software will first set the initial bobbin size to 90% of the total height, and it will then calculate the leakage inductance values. If the user chooses to navigate to a step that they do not have access to yet, they will be informed of this and returned to the step they came from.

5.4.13 Split Flows

It can sometimes be difficult to show all data flows between entities, data stores and processes on higher-level data flow diagrams, and grouping of similar data flows is necessary. In the top level DFD of Figure 5.8, some of the data flows are split into two or more subflows or child flows on lower-level DFDs. All split data flows are listed at the end of Appendix C.

5.5   Summary

This chapter provided details of the software components of the developed system, from the design processes used and the resulting design to the four main software aspects of the system, namely: data base management

system; graphical user interface; optimisation techniques; and knowledge repository.

The main design stages were outlined with the aid of data flow diagrams and typical screenshots of user interaction. Finally, detailed descriptions of the underlying subprocesses were given.

Chapter 6

EXPERIMENTAL MEASUREMENTS

6.1   Introduction

The analysis thus far has focussed primarily on the reduction of total losses in transformers and the minimisation of AC resistance in layered transformer windings.   The former is the most commonly encountered in the majority of applications, and it offers excellent opportunities for optimising the design.

The first section of this chapter will deal with an experimental verification of the losses for a transformer designed using the method outlined in Chapter 3.

The remainder of the chapter will demonstrate the existence of the optimum design point, and the variation in losses for different cores and winding arrangements.

6.2   Total Loss from Temperature Rise

In section 3.2.5, we saw that the sum of the winding and core losses was related to the temperature rise of a transformer ΔT by

$$P = hA_t \Delta T , \qquad (6.1)$$

which is derived from Newton's equation of convection. h is the coefficient of heat transfer; typically $h = 10$ W/m²°C. A_t is the surface area of the transformer, given by

$$A_t = k_a A_p^{1/2}, \qquad\qquad\qquad (6.2)$$

where $k_a = 40$ and A_p is our familiar measure of core size.

In section 3.4.1, we designed a transformer for a push-pull converter application. This converter operates at 50 kHz, with an output power of 318.8 W. The push-pull application specifications also included a maximum temperature rise ΔT of 30 °C.

In the design example, the winding losses inclusive of high frequency effects were estimated at 0.953 W. The core losses were calculated to be 1.503 W. This yielded a total loss value of 2.456 W.

Measurements were taken on a push-pull converter constructed with the core and winding data selected in section 3.4.1. A photograph of this converter is given in Figure 6.1.
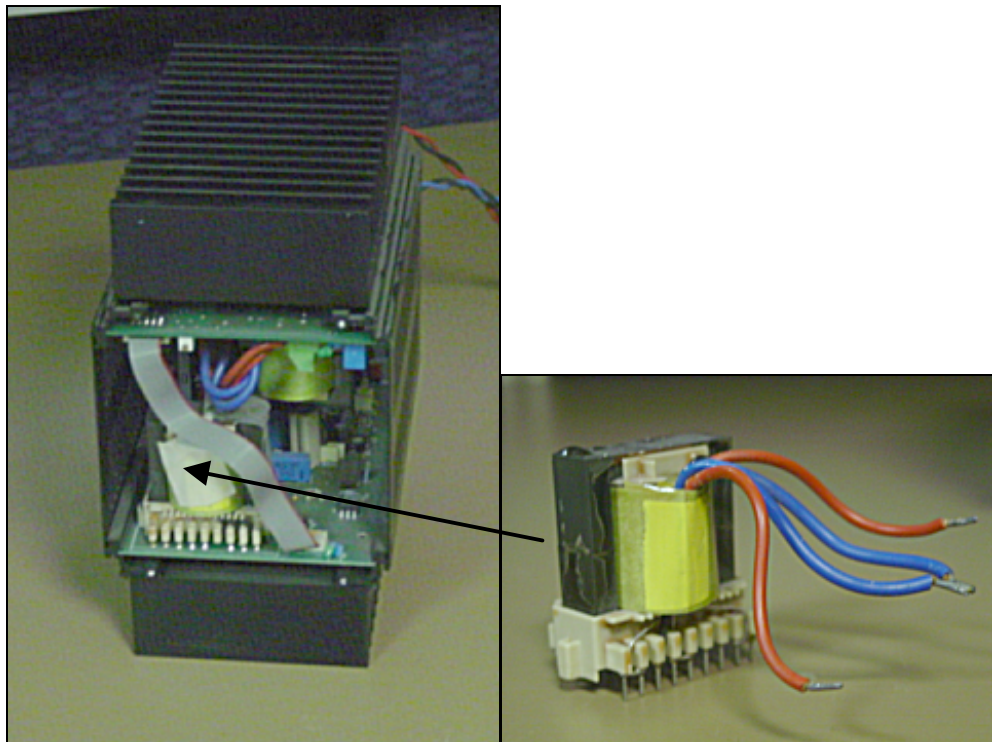
Figure 6.1. Constructed push-pull converter and transformer.

The transformer consists of an ETD44 core, with six turns of HF120 $\times$ 0.10 foil for each winding wound on an ETD44V bobbin. The area product value for this core is A_p = 4.81 cm^4.

Four separate temperature tests were carried out on the push-pull converter transformer for varying lengths of time and different initial transformer temperatures. All tests were carried out for an output voltage of 24 V. From these measurements, we will verify the loss predictions from the design example, and show that the temperature rise was maintained below the limit specified.

6.2.1   Test Results

We will examine one of the tests in detail, and then present a summary of the main results for all four of the tests.

Test C was carried out for 110 minutes, and was characterised by a gradual rise in temperature for about 60 minutes followed by a levelling-off period during the remainder of the test. The initial transformer temperature was 18.3 ^{o}C.

Test C (30-JUL)
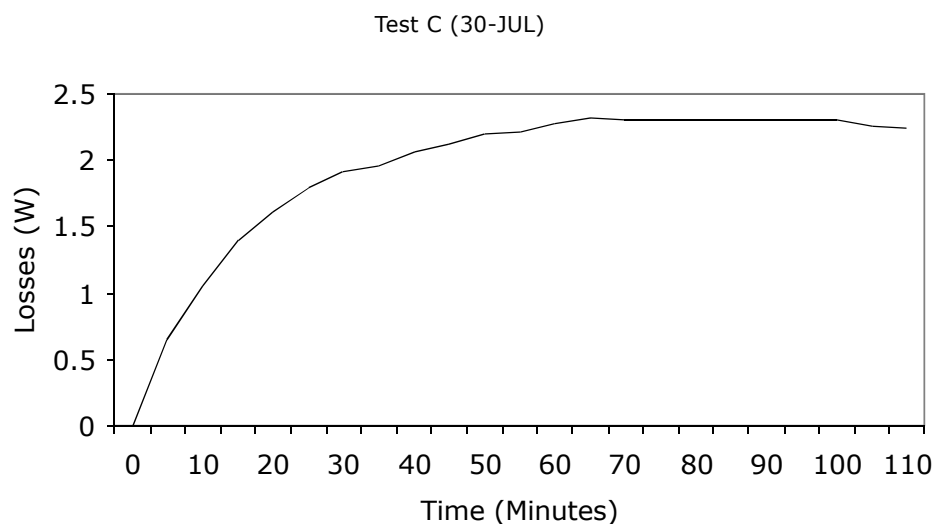
Figure 6.2. Test C total power loss versus time.

The total power loss is plotted in Figure 6.2, derived from the temperature measurements given in Table 6.1.

The power loss is calculated from (6.1), with h = 10 W/m²°C for natural convection and $A_t = 40 \times [4.81 \text{ cm}^4]^{0.5} = 87.727 \text{ cm}^2$ (6.2).

The temperature rise reached a peak value of 26.4 °C after 65 minutes, less than the 30 °C maximum set out initially in the design specifications. The corresponding losses at this point were 2.316 W, slightly less than the predicted value of 2.456 W.

TEST TIME (MINUTES)	TRANSFORMER TEMP. (°C)	TEMPERATURE RISE (°C)	TOTAL POWER LOSS (W)
0	18.3	0	0
5	25.6	7.3	0.64041
10	30.4	12.1	1.06149
15	34.2	15.9	1.39486
20	36.6	18.3	1.6054
25	38.7	20.4	1.78963
30	40.1	21.8	1.91245
35	40.7	22.4	1.96508
40	41.9	23.6	2.07035
45	42.5	24.2	2.12299
50	43.4	25.1	2.20194
55	43.6	25.3	2.21949
60	44.2	25.9	2.27213
65	44.7	26.4	2.31599
70	44.5	26.2	2.29844
75	44.5	26.2	2.29844
80	44.5	26.2	2.29844
85	44.5	26.2	2.29844
90	44.5	26.2	2.29844
95	44.5	26.2	2.29844
100	44.5	26.2	2.29844
105	44	25.7	2.25458
110	43.9	25.6	2.24581

Table 6.1. Test C temperature measurements.

Table 6.2 contains a summary of all the test results. In each case, the temperature rise never exceeded the maximum value of 30 °C in the initial design specifications for the push-pull converter. The maximum power loss was always just below the predicted total core and winding loss value of 2.456 W.

TEST NUMBER	DURATION (MINUTES)	MAXIMUM TEMP. RISE (°C)	MAXIMUM POWER LOSS (W)
A	75	25.7	2.25458
B	100	27.4	2.40372
C	110	26.4	2.31599
D	90	25.9	2.27213

Table 6.2. Temperature tests summary.

6.3   Core Loss for Varying Flux, Frequency

Loss measurements were carried out using two systems, designed for measuring magnetic characteristics at frequencies above and below the megahertz range respectively.

6.3.1   One-Port Measurements

Losses at high frequencies in the megahertz range were measured using a "one-port" measurement system as shown in Figure 6.3.   The main components of this system were a Hewlett Packard 4194A gain-phase impedance analyser with probes and an Amplifier Research 10A250 wideband power amplifier.   The small signal sinusoidal output of the impedance analyser – which is less than 1.2 V – is amplified to a large AC signal by the power amplifier, and then applied to the DUT (device under test) through the HP 4194A impedance probe.   The probe can withstand currents up to 0.5 A and voltages up to 150 V.   30 dB attenuators are required between the probe and the HP 4194A test and reference channels to reduce the measured voltage and current from the DUT.

Figure 6.3. One-port measurement system.

The analyser is interfaced with a personal computer running specialised core loss measurement software [41]. The impedance analyser can be controlled to test a given DUT using either a constant flux density at a variety of test frequencies or a set frequency for a range of flux density values. The software sets the voltage across the DUT, V_{DUT}, according to the required flux density, B_m, and frequency, f. Whichever test is chosen, the equipment must be calibrated with respect to the DUT, and this can be done in one of several ways. First, the HP4194A itself should be calibrated through the standard impedance probe calibration procedure. In this calibration step, the open circuit (0 siemens), short circuit (0 Ω) and reference impedance (50 Ω) fixtures are used to calibrate the probe-plus-amplifier configuration. Secondly, the winding resistance and stray inductance of the core can be compensated for by performing an open-circuit and short-circuit calibration in place of the DUT. The open-circuit test simply leaves the probe open, and the short-circuit calibration uses a winding similar to that used on the DUT but wound on a non-magnetic structure (for example, cardboard).

A number of specifications on the core are then inputted to the software: the number of turns, the cross sectional area, the magnetic path length, and the maximum core loss density. Using the measurements obtained from the analyser over the interface bus, the program produces data on a number of core characteristics including the real and imaginary parts of the complex permeability and the magnetic loss densities. This data is saved for plotting in mathematical packages later. We will examine some typical plots of power loss and permeability in section 6.3.1.3.

Measurements were performed at various flux density levels and over a range of frequencies from 100 kHz up to 3 MHz. Often these tests stop short of reaching the end of the frequency range due to saturation and the maximum input voltage for the analyser's input channels being exceeded (since the maximum voltage specified in the test channel of the HP 4194A is 1 V, the maximum voltage which can be applied to the DUT is 30 dBV or $1 \text{ V} \times 10^{30/20} = 31.62 \text{ V}$). Once V_{DUT} reaches 30 dBV, the software shuts down the measurement automatically.

6.3.1.1   Toroidal Cores Under Test

Commercial ferrite toroidal cores typically have a ratio of outside diameter to inside diameter in the range of 1.5 to 2.0. This means that the flux density, non-uniform in thicker cross sections, can be significantly higher on the inner edge of the core than on the outer portion of the toroid. This variation of flux density is compensated in the inductance calculations through the use of effective core geometries: A_e, the cross sectional area, l_e, the magnetic path length and V_e, the volume of the core.

In order to minimise any adverse effects that variations in flux density within the core have on the measurement of the material constants, we will use some very thin cores that minimise the ratio of the outer diameter to the inner diameter. The dependence of flux density and radius is related to eddy current loss. In such thin cores, the eddy current is

negligibly small and assumed to be zero, and the flux density is almost constant along a cross section.

The cores range in size from about 2 cm to 8 cm in diameter. The thin-walled samples listed as cores 1 to 3 in Table 6.3 have outer to inner diameter ratio values of approximately 1.1 (e.g. a 2 mm wall thickness for a 2 cm outer diameter).

CORE NUMBER, NAME	CROSS SECTIONAL AREA (m²), A_e	MAGNETIC PATH LENGTH (m), l_e	VOLUME OF CORE (m³), V_e	OUTER/INNER DIAMETER
1, MN80 #1a	1.08×10^{-5}	1.33×10^{-1}	1.44×10^{-6}	1.106
2, BE2 #2b	9.25×10^{-6}	1.18×10^{-1}	1.09×10^{-6}	1.105
3, BE2 #4b	5.06×10^{-6}	6.65×10^{-2}	3.31×10^{-7}	1.099
4, MN80 #3a	2.63×10^{-5}	2.89×10^{-2}	7.60×10^{-7}	2.259
5, BE2 #7	4.55×10^{-4}	1.91×10^{-1}	8.69×10^{-5}	1.775
6, BE2 #8	3.44×10^{-4}	2.78×10^{-1}	9.56×10^{-5}	1.354

Table 6.3. Toroidal core geometries.

MATERIAL	SATURATION FLUX DENSITY (mT)	RELATIVE PERMEABILITY	RESISTIVITY (Ω-cm)
Ceramic Magnetics MN80	500	2400	200
Thomson BE2 (B2)	190	1900	-

Table 6.4. Toroidal core material properties.

6.3.1.2 Winding Arrangements

Using data obtained from the one-port measurements, the core loss densities for a number of winding configurations for core 1 were compared to see the effect of the winding location on the resultant core losses. The windings on the test cores should ideally wrap fully around the circumference of the toroid. This uniform winding reduces the amount of leakage flux from the core, and thus provides for a more uniform flux density. However, the maximum number of turns allowed on the core is limited by the restrictions on the maximum value of the test voltage. When this is the case, a multistranded winding with fewer turns

can be used to provide the desired uniform flux density. Figure 6.4 shows how a multistranded winding with four conductors per turn results in a fully wound structure. Three arrangements are shown in this figure: six single-strand turns concentrated in one section of the core, six multi-strand turns that wrap around the entire circumference, and 25 single-strand turns that wrap around the circumference.

Localised Winding Core   Fully Wound Core

Multistranded Fully Wound Core
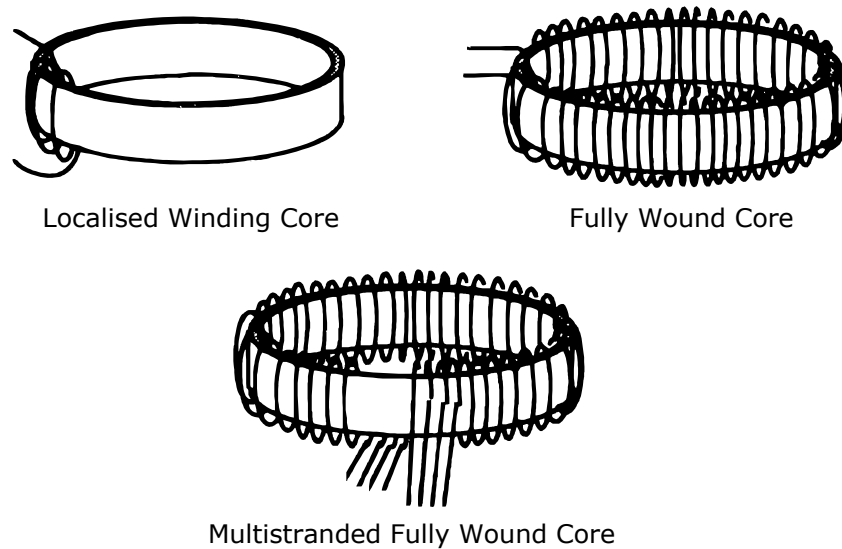
Figure 6.4. Winding arrangements for toroidal cores.

Figure 6.5 shows that the loss density values measured using the multistranded six-turn winding correlate well with the fully-wound 25-turn winding; a six-turn winding that is localised in only a small section of the core, however, produces a drop in the core loss of approximately 20 percent. The results in Figure 6.5 show that while the location of the winding may introduce only a small difference in flux density in the different parts of the core (on the order of 5 to 10%), this relatively small change in flux density can introduce a significant error in the measured losses since the loss density is a string function of the flux density; typically, the loss density in ferrites depends on the flux density to the power of 2.2 to 2.5 which means a 10% error in flux leads to a 20 to 25% error in loss. We will use FEA to illustrate this in section 6.3.3.1.
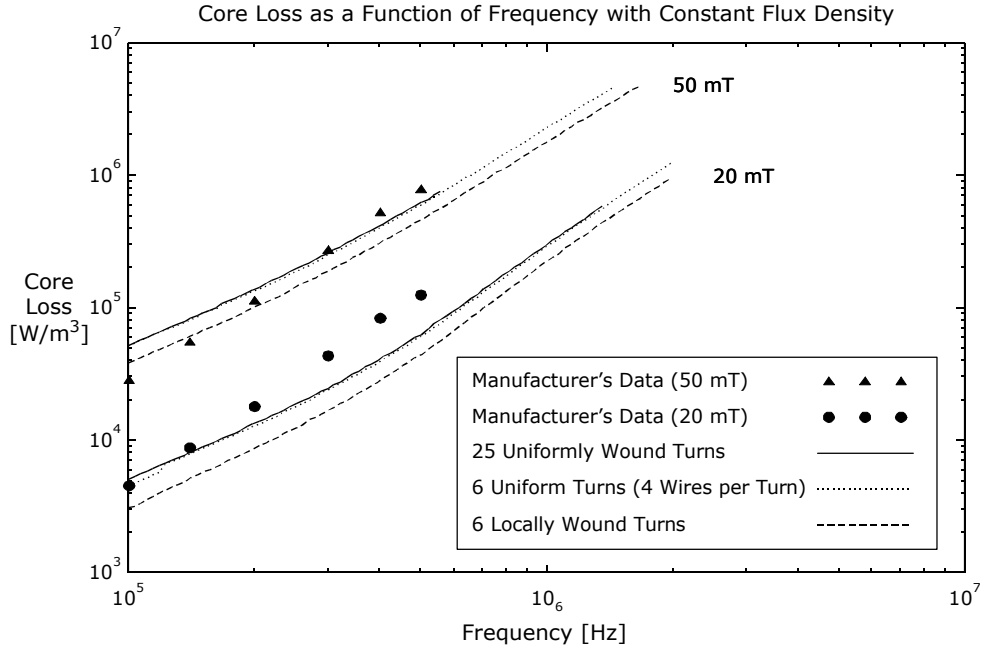
Figure 6.5. Measured loss density for different winding arrangements.

Core losses calculated using (3.13) do not take account of winding location, and as can be seen from these plots, core losses for the same core and material and flux density can vary significantly for different winding configurations.

Due to a shortage of available manufacturer's data for losses at various flux density levels and temperatures, the data for both 20 mT and 50 mT at 25 °C were extrapolated. Manufacturer's power loss plots for 100 mT and 125 °C were used along with power loss versus temperature curves. Power loss plots for 200 mT and 300 mT were also available, but these were less suited to extrapolation due to their truncated frequency ranges.

Firstly, the loss plots were decreased by the ratio $P_{fe1}/P_{fe2} = (B_{m1}/B_{m2})^\beta = (100 \text{ mT}/20 \text{ mT})^\beta = 25$ with $\beta \approx 2$ for ferrite materials such as MN80. Secondly, a temperature loss factor was taken into account; the manufacturer's power loss versus temperature curves illustrated a 100% increase in losses from 125 to 25 °C at 100 mT (the corresponding increases at 200 mT and 300 mT were around 60% and 20% respectively).

6.3.1.3 Effects of Core Size

Figure 6.6 shows the real part of the measured series permeability as a function of frequency for various toroidal core structures constructed from BE2 material. Their geometries are given in Table 6.3. The flux density for each of these tests was set to 15 mT. For the thicker walled toroids (cores 5 and 6), the bandwidth of the permeability is less than that of the thinner walled toroids (cores 2 and 3). The thicker cores have the lowest roll-off frequency since they suffer the most significant dimensional effects.
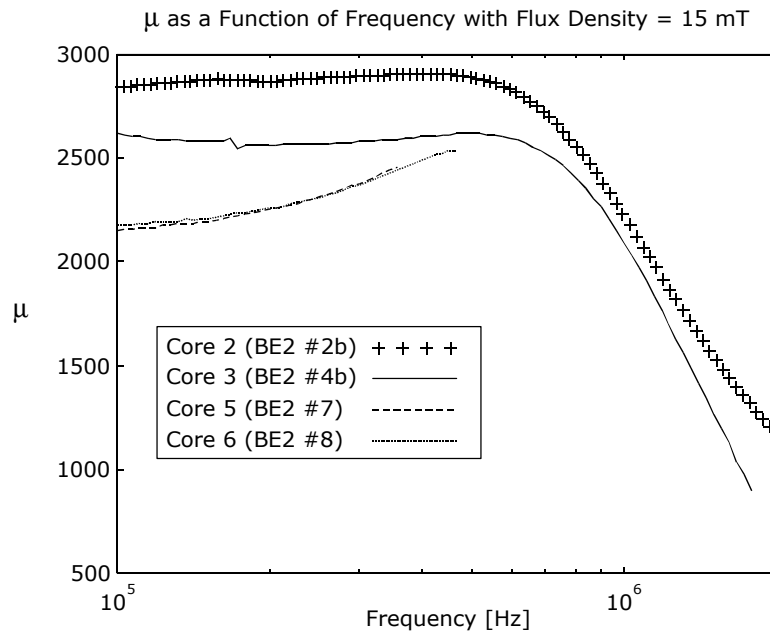
Figure 6.6. Real part of series permeability against frequency for BE2 material cores at 15 mT.

Figure 6.7 shows the core loss density for each of the BE2 material cores with a flux density of 15 mT. Here again, the thicker walled toroids (cores 5 and 6) have more significant changes from the baseline material data, and in each case the loss density in the core is higher than that predicted by published material data (e.g. around 1×10^3 W/m^3 at a frequency of 100 kHz and flux density levels less than 100 mT).

Core Loss as a Function of Frequency with Flux Density = 15 mT
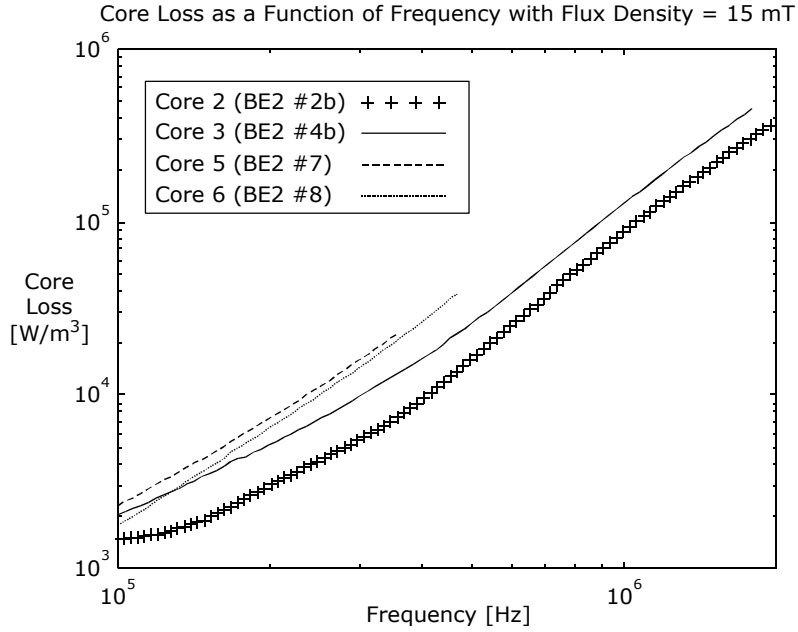
Figure 6.7. Core loss density at 15 mT for BE2 material cores.

6.3.1.4 Optimum Loss Curves

The experimental core data from the one-port measurement system described in section 6.3.1 was combined with calculated winding data to validate the characteristics of the optimum loss curve as presented in section 3.2.6.1. Figure 6.8 shows a selection of loss curves with various frequency values for the MN80 material core 1. All of the experimental data was taken at flux densities well below the material's saturation flux density constraint, which for MN80 is 500 mT.

The data was obtained by varying the frequency for fixed flux density values. However, a sufficient number of flux values were used such that it was possible to invert the data matrix and plot the losses as a function of flux for fixed frequency values (instead of as a function of frequency for fixed flux values). MATLAB's "polyfit" and "polyval" functions were used to predict extra loss values between data points where necessary.
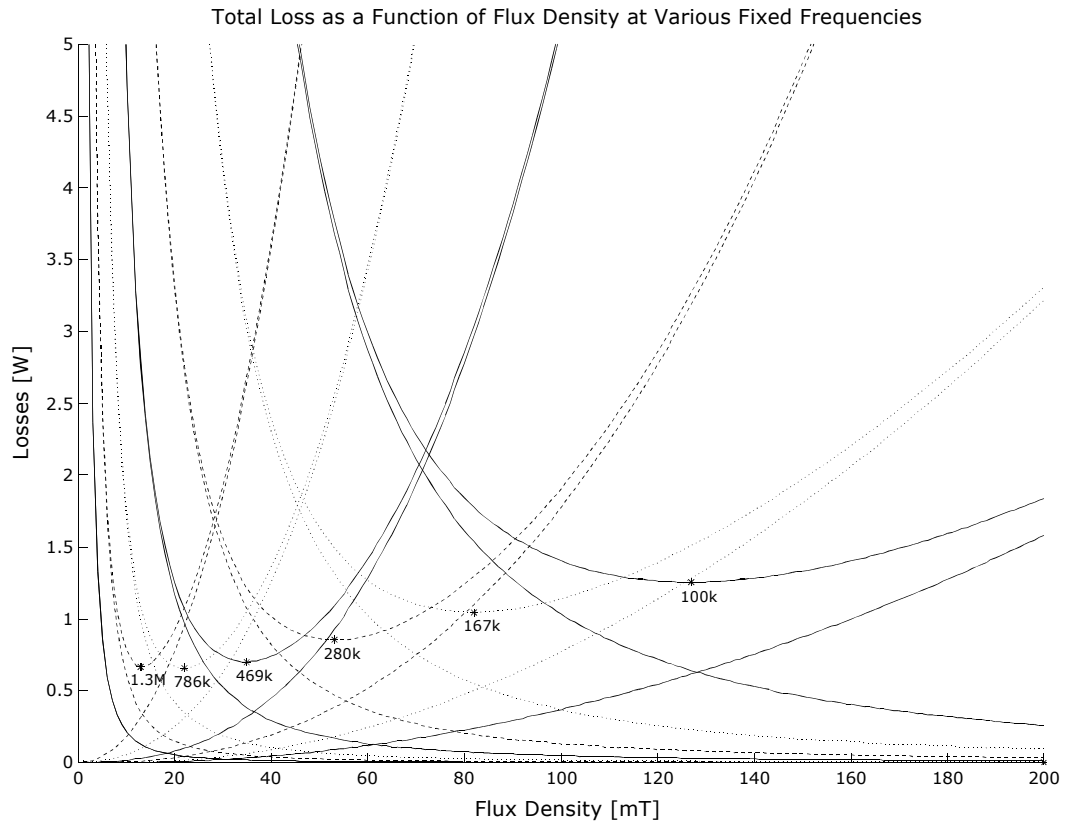
Figure 6.8. Loss plots for core 1 with various frequency values.

Figure 6.9 shows the optimum loss curve as a function of optimum flux density and frequency. For each optimum flux density value shown on the left hand side plot, there is a corresponding optimum frequency value on the right hand side plot (and vice versa). As we saw in Figure 3.6, the value of the total loss at the optimum design point increases with increasing flux density, but decreases with increasing frequency.
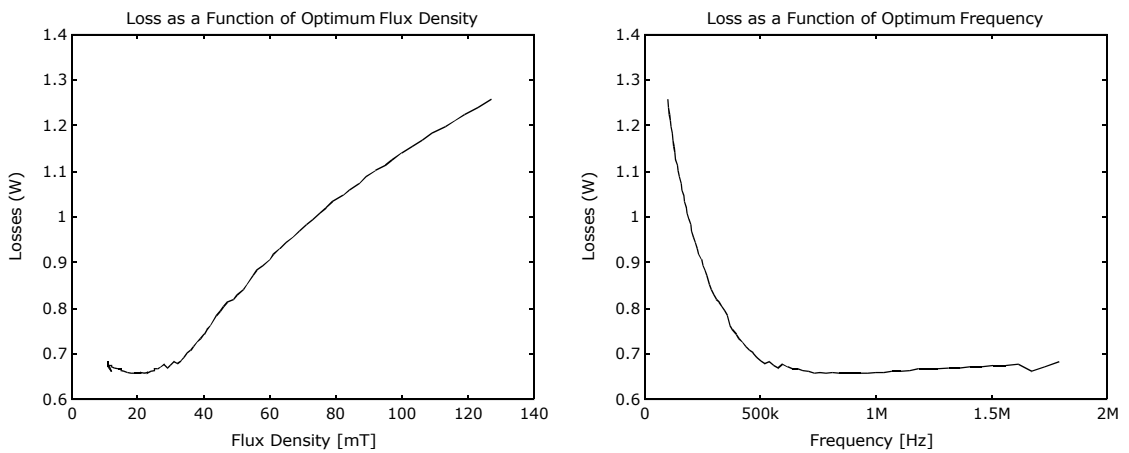
Figure 6.9. Experimental verification of optimum curve characteristics.

In 3-D, the optimum loss curve for this MN80 core 1 configuration moves from its maximum point at large B_m and low f to its minimum point at low B_m and large f. As we move from large B_m and low f to low B_m and large f, the B_m^β term in the core losses equation (3.16) decreases by a larger factor than the corresponding increase in the f^α term, resulting in an overall decrease in core losses. Similarly, in the winding losses equation (3.18), the $1/f^2$ term decreases by a larger factor than the $1/B_m^2$ term increases by, also resulting in an overall drop in winding losses. Since the core and winding losses are approximately equal along the optimum curve (at high frequencies with the core flux density is not saturated), then the reduction factors in the winding or core losses can be made equal by scaling by a or b from (3.20) as appropriate. These results agree with the theoretical curves presented in Figure 3.6, section 3.2.6.1.

6.3.2   Two-Port Measurements

The one-port measurement impedance probe setup and calibration procedures outlined above are generally adequate for small cores without air gaps. For such devices the magnetising current and leakage inductance are kept relatively small. However, at low frequencies the blocking capacitors of the impedance probe present significant series impedance, and an alternative test strategy that uses two separate windings such as shown in Figure 6.10 is more suitable. This two-winding test approach [119] uses one winding to excite the device under test (the core) and a separate winding to sense the flux induced in the core.

There are several advantages to using separate excitation and sensing windings including the elimination of voltage drops due to winding resistance and the ability to sense the flux in several regions of the core through the use of additional voltage pick-up windings. However, errors in the pickup winding, phase errors between the different probe channels and errors introduced in processing the measured data can limit the accuracy of such measurements to frequencies below the megahertz range [41].
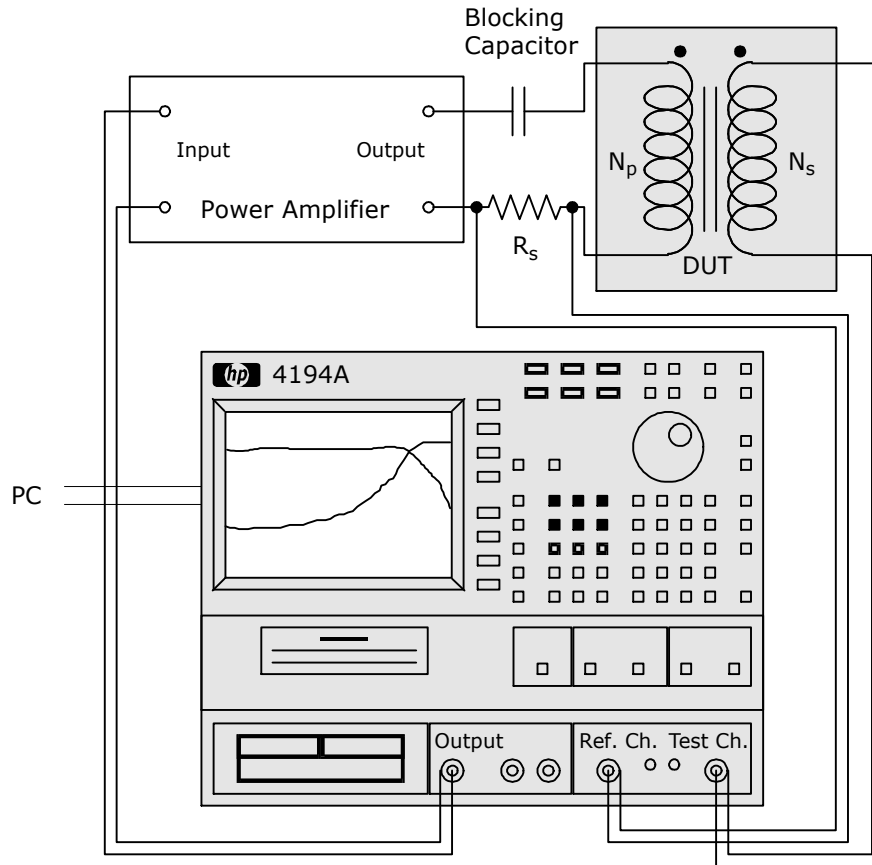
Figure 6.10. Two-port measurement system.

The setup shown in Figure 6.10 eliminates some of these problems by using the impedance analyser in its gain/phase mode to derive the impedance of the DUT. This setup is limited by the maximum input voltage of 2.42 V (RMS) for the impedance analyser's test and reference channels; only relatively small voltages can be sensed with such a setup, but this is not a significant restriction for measuring the small core samples of Table 6.3 at frequencies of approximately 10 kHz. The attenuators from the one-port measurement system cannot be used in this case, as they would place a 50 Ω load on the output of the DUT.

The low-frequency measurements obtained using the two-port test strategy are useful for determining the baseline hysteresis losses for the material. Since eddy current losses may be neglected at low frequencies, a plot of the measured losses normalised to frequency gives the residual losses (as well as any eddy current or other dimensional loss effects) for the material.

6.3.2.1 Combined Results

We will now apply the two-port measurement method to core 1 with a fully wound 25-turn winding (as used in the one-port measurements of section 6.3.1.2).

Since the core loss densities and permeabilities are not read in to a computer, these have to be calculated manually by first measuring the complex impedance of the sensing winding using the test and reference channels of the gain-phase analyser. This measurement was repeated for three different flux densities (achieved by varying the voltage exciting the winding according to V = $kfNB_mA_c$), and for each flux density three readings of impedance were taken at frequencies of 5, 10 and 15 kHz.
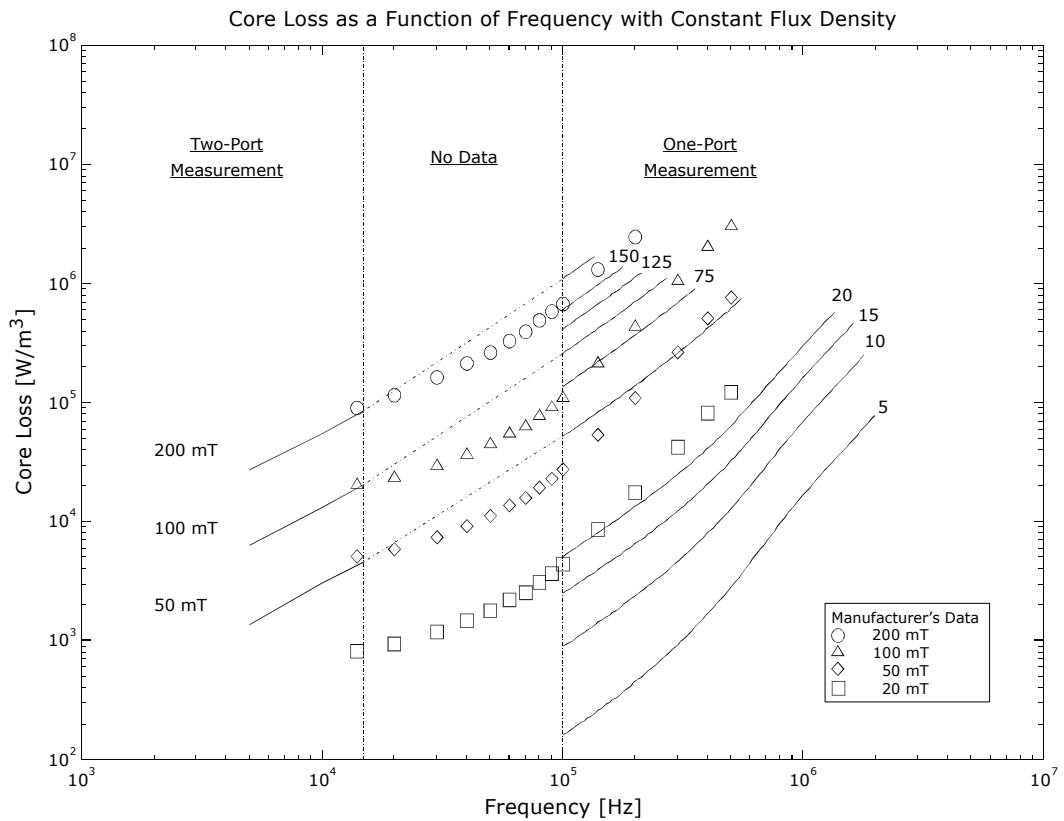
Figure 6.11. Comparison of low and high frequency (one-port and two-port) results.

A MATLAB program takes the impedances as read from the analyser in gain-phase format, converts them to R + $j\omega L$ (real and imaginary), and then scales these values by the turns ratio of the excitation to sensing

windings. These R and L values can then be used to calculate the power loss or permeability values respectively.

Both sets of measurement results (one-port and two-port) were combined to give a graph of the core loss densities over the range 5 kHz to 3 MHz as shown in Figure 6.11. Even though the measurements were taken from two very different setups, it was interesting to note that they matched up perfectly when combined on the same graph. Manufacturer's data was extrapolated as described in section 6.3.1.2.

6.3.3   Finite Element Analysis

With the finite element analysis (FEA) package Maxwell 2-D Simulator by Ansoft, some analyses were carried out on a model of core 1. In the first test, the effect of varying the core permeability on the percentage flux that reaches the side of the core furthest from a localised winding was analysed. In the second, the flux density levels in different regions of the same core with a localised winding were examined. These tests are detailed below.

6.3.3.1   Varying Permeability

While the use of a fully-wound device - whether it be wound with only a small number of multi-stranded turns or with many single-strand turns - provides a more uniform flux density, it is not well documented what impact a "non-ideal" winding has on the measured characteristics of the material. For high-permeability ferrite cores, the difference in flux density in the core due to leakage is relatively small. This is illustrated in Figure 6.12 which shows the results of an FEA simulation of the flux in core 1 from Table 6.3.

A diagram of the core and the lines normal to which fluxes were calculated is shown in the panel on Figure 6.12. These fluxes were normalised relative to the flux that links the excitation winding (point 1), and thus can be described as the percentage of source flux that links

points 2 and 4 ($\beta = \phi_2/\phi_1 = \phi_4/\phi_1$) and the percentage of source flux that reaches the opposite side of the toroid at point 3 ($\zeta = \phi_3/\phi_1$).
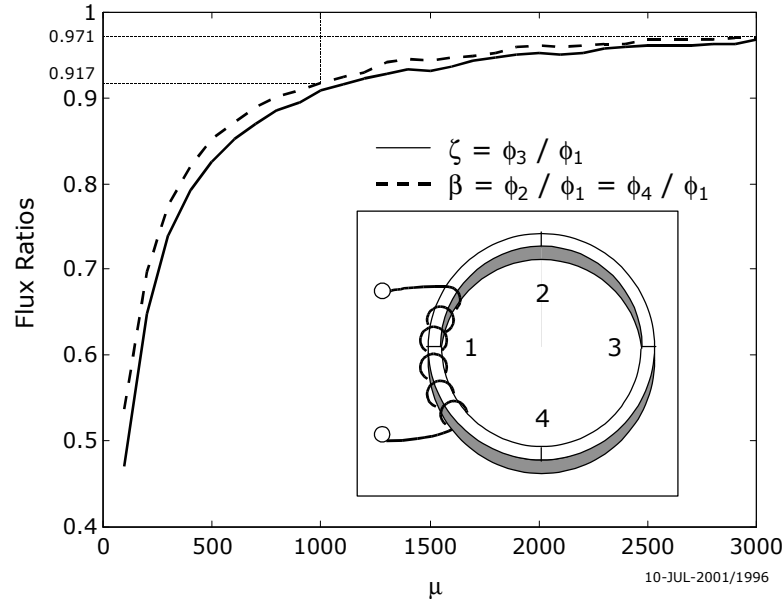
Figure 6.12. Ratio of flux densities at different locations within core 1 as a function of the core permeability.
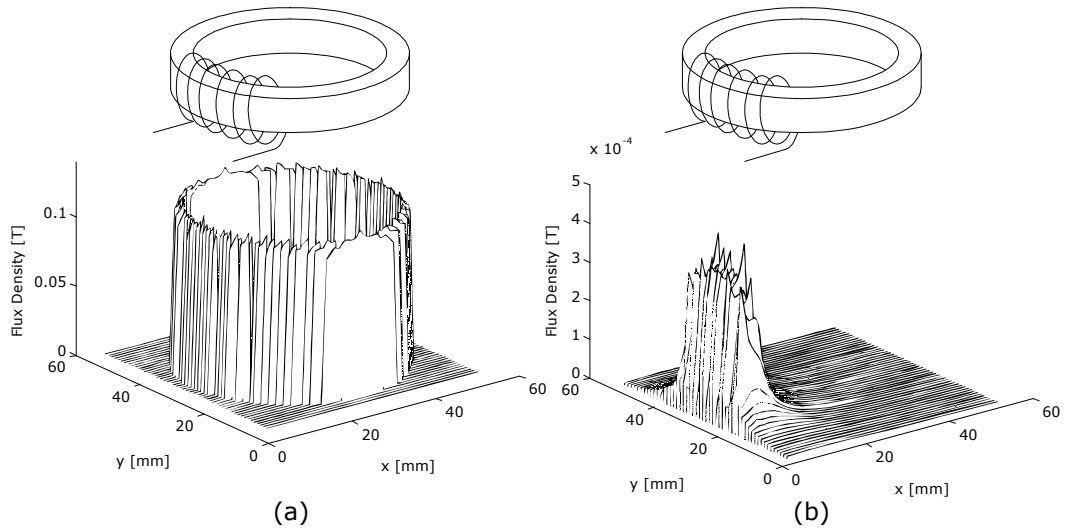
Figure 6.13. Flux density plots for a six-turn localised winding on core 1 with (a) μ = 1000, (b) μ = 100.

The flux that links all parts of the core is approximately 90% of the source flux for core permeability values above 1000. When the relative permeability is 3000, approximately 97% of the flux remains within the core and reaches the opposite end of the toroid from the winding. At the other end of the scale, if we drop below 1000, the flux ratios drops

considerably. This is as expected for low permeabilities and is demonstrated by the FEA flux plots in Figure 6.13.

6.3.3.2 Flux Density Variations

Another FEA analysis was performed to compare the flux levels at different points around the same locally wound core. The relative permeability was fixed at 2500 in this case. Figure 6.14 shows the flux plotted along the lines 1, 2, 3 and 4 (as marked in Figure 6.12) where the distance is directed outwards from the centre of the core.
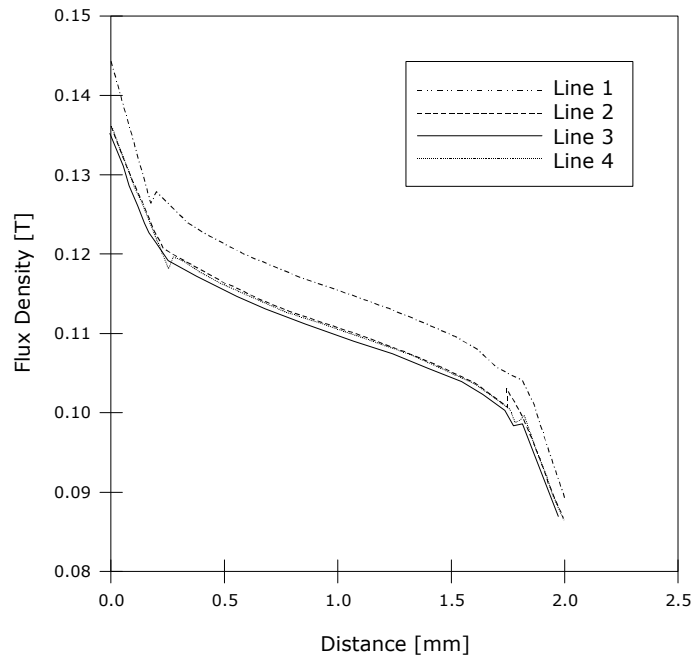
Figure 6.14. Flux levels at various points on simulated core 1 with a six-turn locally wound winding.

It can be seen that the flux density levels at lines 2, 3 and 4 are lower than those at line 1 by around 7%. The flux density along line 3 in the core is the lowest since it is furthest away from the winding. A 7% flux density drop would correspond to a reduction in core loss of around 20%, confirming the measurements on the locally wound core in section 6.3.1.2.

Core 1 was also simulated in FEA using fully wound 25-turn and six-turn (4 wires per turn) windings, and as expected showed no such flux density variations.

6.4 Summary

In this chapter, an experimental verification of the calculated losses for a push-pull converter was presented. For each of four tests, the temperature rise in the constructed transformer remained below the maximum value specified in the initial design.

The characteristics of the optimum design curve were also confirmed. The effect of varying both the size of the core and the location of the winding on core losses was then examined. Finally, an FEA analysis of the flux levels in a toroidal core with a localised winding was given.

Chapter 7

CONCLUSIONS

7.1   Problem Area

Transformer design is a well-developed electrical engineering subject, and there are many existing references that treat it. It is important to not simply design a transformer that will work, but to design one that is economical, efficient, and makes the best use of available materials. As in all design processes, there are numerous trade-offs between competing requirements, and some sort of optimum is sought. However, the properties of available materials can rigidly limit the design possibilities.

As discussed in Chapter 1, traditional transformer design methodologies often assume that the optimum design point in terms of maximum efficiency (with minimum total losses) occurs when both the core and winding losses are equal. This assumption can result in some "optimum" designs becoming saturation limited when flux density levels in the core exceed the manufacturer's saturation specifications. The problem is that the optimum flux density is calculated near to or greater than the saturation flux density of the core material. This saturation issue has been acknowledged in previous work, and a robust design methodology is required that will take this problem into account. Alternate paths to optimised transformer designs may be necessary based on certain initial conditions.

Another issue in transformer design is that of optimising the thickness of a layer in a constant thickness multilayered transformer winding. This thickness value was traditionally found by calculating harmonic AC winding loss summations repeatedly for a range of thickness values, and then reading the optimum layer thickness from a graph of total AC winding loss versus layer thickness. This process could involve loss

calculations at up to 30 harmonics for 10 or more thickness values in order to find the optimum thickness value for a single winding configuration. In addition, Fourier coefficients are requisite for the initial harmonic calculations, and these are usually only available for approximate versions of waveforms encountered in practice. A method is required that can yield quick but accurate formulas for the optimum thickness of each layer in a multilayered winding carrying an arbitrary periodic current waveshape.

In the past, the design of magnetic components was largely based on following empirical rules and reading values from design graphs. This was often quite time consuming, involving a one-way process which had to be repeated from the very beginning if one of the initial parameters, such as the desired output voltage for example, needed to be changed. Also, a number of different catalogues would often have to be referenced with wire size tables, data sheets for various cores, and other graphs for the properties of the available core materials. Now that computer aided design packages are becoming more pervasive, tools can be developed to carry out designs of magnetic components and also to allow evaluation of high-frequency effects on the induced losses in these components.

7.2   Solutions Presented

This thesis endeavours to provide solutions to the aforementioned issues by developing a robust transformer design methodology which is the basis for a computer package that also incorporates high frequency layered winding optimisation routines. We will now review these solutions as described in this thesis.

Chapter 3 describes a new methodology for transformer design which leads to optimised core and winding selection from the design specifications at both high and low frequencies. The selection of the core has been optimised to minimise both core and winding losses where possible. It was shown that for any transformer core there is a critical frequency. When designing below this frequency value, the flux density

cannot exceed the core material's saturation limit, and the winding losses may far exceed the core losses in such a design. Above the critical frequency, the total transformer losses are minimised by designing at an optimum flux density level for which the core and winding losses are approximately equal.

The model takes account of switching type waveforms encountered in switching mode power supplies, inclusive of any high frequency skin or proximity effects. Accurate approximations have been provided to facilitate calculations. A number of worked examples were also given in Chapter 3 to illustrate the generality of the methodology. These ranged from a 75 W forward converter operating at 25 kHz and incorporating winding skin effects, to a 1000 W centre-tapped rectified transformer operating at 50 Hz with a high winding to core loss ratio of 8:1.

With the inclusion of non-sinusoidal waveforms in the transformer design algorithm, the emphasis in Chapter 4 shifted to procedures for minimising AC foil resistances (and hence power dissipation) by optimising the layer thickness in a multilayer winding. The AC resistance of a layered winding was derived from first principles in Chapter 2 for use here.

Two new methods were described in Chapter 4 which ultimately yield useful formulas for the optimum layer thickness. These are based on RMS values and regression analysis respectively. The RMS values method may be easily applied to other waveforms once their RMS characteristics are known. The regression analysis method requires knowledge of the Fourier coefficients for a new waveform, but is even more accurate.

For bipolar rectangular, triangular and sinusoidal waveforms, and their rectified equivalents, simple and accurate approximations for the optimum layer thickness are established. This thickness may be found from knowledge of the number of layers, the rise time if applicable, and the duty cycle. One of the important features of this thesis is the extension of prior work for fixed duty cycles to a variable duty cycle.

The new transformer design methodology has been implemented in a computer application in conjunction with a database of core and winding

materials, as detailed in Chapter 5. This Windows-based package eliminates the time and effort previously required in traditional design methods by allowing the magnetics designer to step through designs for various applications with the ability to jump back and make certain changes as desired. After being guided by the program through the various stages, a full design may be prepared along with all of the core and wire size information required. The proximity effect formulas have also been implemented as part of the winding selection process.

In Chapter 6, measurements on various core samples at different frequencies using one-port and two-port core loss measurement systems were carried out to compare the effect of winding location and configuration on measured loss and flux density values. Using a finite element package, an analysis on a model of one of the sample cores was performed to show the effect of varying the permeability of the core on the percentage flux that reaches the side of the core furthest from a localised winding. Also, the characteristics of the optimum loss point from Chapter 3 were verified with experimental results.

7.3   Summary of Results

To test the methodologies, a number of validations were performed.

With respect to the transformer design methodology presented in Chapter 3, the example designs included a push-pull converter that was designed to operate at 50 kHz and 318.8 W power output. This converter was built according to the specifications and core/winding geometries resulting from the design example using the presented methodology. It was shown with experimental verification in Chapter 6 that the converter operated within the loss and temperature limits specified by the design.

A comparison was presented in Chapter 4 of the optimum thickness in a multilayered transformer winding obtained using the traditional Fourier analysis method with the thicknesses obtained using the RMS values and regression analysis methods, and the new methodologies were found to be

accurate to within a few percent. It was also shown that waveforms used for Fourier analysis are often approximations to the actual waveforms and can give rise to errors that are of the same order as the proposed formulas.

The theoretical nature of the optimum loss curve with respect to flux density and frequency was also collaborated in Chapter 6 with experimental measurements performed on toroidal cores.

7.4   Research Merits

A new procedure has been outlined for optimising the design of transformers with arbitrary waveforms that also takes into account high frequency AC loss effects in the transformer winding.

Some of the key aspects of this thesis include:

- Poynting vector method for finding the effective AC resistance.

- New methodology for transformer design which takes different paths above and below a critical frequency.

- Two new methods that yield optimum thickness formulas for any current waveshape.

- A software package that implements these methodologies.

An optimal (in terms of losses) transformer design methodology has been developed which leads to optimised core and winding selection from the design specifications at both high and low frequencies, and that has been adapted as a computer package to aid in designing transformers for a number of common applications; because of the generality the methodology can easily be adapted to other transformer applications. The unique transformer design system has been developed to manage all the

information associated with the methodology in an efficient but clear manner.

While the core and winding losses are not always equal (i.e. total losses minimised), they are as optimal as physically realisable with the core material flux constraint taken into account.

Procedures for minimising AC foil resistances (and hence power losses) by optimising the layer thickness for a multilayered winding have been presented. These procedures yield simple formulas for the optimum thickness for any waveshape, and can be used to obtain thickness formulas that account for varying duty cycles in non-sinusoidal waveshapes or for non-standard waveshapes in new transformer applications.

A multi-application transformer design package was presented, suitable for use by both novices and experts. The Windows-standard GUI allows the user to experiment through try-it-and-see design iterations. As well as incorporated design knowledge, the system allows high frequency winding optimisation and customisable transformer geometries. Calculation times are instantaneous, and a full design can be prepared in minutes once the specifications entry stage has been completed.

The contributions to knowledge can be summarised as follows:

- The robust transformer design methodology can be applied to other transformer applications once a number of factors unique to that application are derived.

- The optimum thickness methods yield quick formulas for any waveform encountered in future SMPS designs once either the RMS values or the Fourier coefficients are known or can be derived.

- The software system implementing both methods can be further developed for more transformer applications and can be updated to incorporate inductors and integrated magnetics.

214

With the current trend towards miniaturisation in power converters, the magnetics designer should now expect accurate computer aided techniques that will allow the design of any magnetic component while incorporating the latest advances in the area of high frequency optimisation. The contribution of this work was to present techniques, for optimising transformer designs and minimising layered winding losses, that will provide this new functionality to magnetics designers. The design techniques can also be easily extended to planar magnetic components.

Appendix A

WIRE DATA

Most wire tables list diameter, area and weight data for the AWG (American Wire Gauge) sizes as used in our examples. However, some information for the smaller wire sizes used to combat skin effects at higher frequencies (from AWG #41 upwards) was unavailable: number of turns per cm², current in amps at 5 A/mm², overall diameter in mm, resistance in mΩ/m at 20 °C. These values were derived as detailed in the following sections. Table A.1 lists the wire data used in the examples in section 3.4. Shaded areas contain derived data.

AWG NUMBER	IEC BARE DIA. (mm)	AWG BARE DIA. (mm)	RESIST-ANCE @ 20 °C (mΩ/m)	WEIGHT (g/m)	OVERALL DIA. (mm) *	CURRENT @ 5 A/mm² (A)	TURNS PER cm²
10		2.588	3.270	46.76	2.721	26.30	12
	2.5		3.480	43.64	2.631	24.54	12
11		2.308	4.111	37.19	2.435	20.92	14
	2.24		4.340	38.14	2.366	19.70	14
12		2.05	5.211	29.34	2.171	16.50	20
	2.0		5.440	27.93	2.120	15.71	20
13		1.83	6.539	23.38	1.947	13.15	23
	1.8		6.720	22.62	1.916	12.72	23
14		1.63	8.243	18.55	1.742	10.43	30
	1.6		8.500	17.87	1.711	10.38	30
15		1.45	10.42	14.68	1.557	8.256	39
	1.4		11.10	13.69	1.506	7.700	42
16		1.29	13.16	11.62	1.392	6.535	52
	1.25		13.90	10.91	1.351	6.140	52
17		1.15	16.56	9.234	1.248	5.193	68
	1.12		17.40	8.758	1.217	4.930	68
18		1.02	21.05	7.264	1.114	4.086	80
	1.0		21.80	6.982	1.093	3.930	85
19		0.912	26.33	5.807	1.002	3.266	99
	0.9		26.90	5.656	0.9900	3.180	105
20		0.813	33.13	4.615	0.8985	2.596	126
	0.8		34.00	4.469	0.8850	2.510	126
21		0.724	41.78	3.660	0.8012	2.058	161
	0.71		43.20	3.520	0.7900	1.980	168
22		0.643	52.97	2.887	0.7197	1.624	195
	0.63		54.80	2.771	0.7060	1.559	216
23		0.574	66.47	2.300	0.6468	1.294	247
	0.56		69.40	2.190	0.6320	1.232	270

AWG NUMBER	IEC BARE DIA. (mm)	AWG BARE DIA. (mm)	RESIST-ANCE @ 20 °C (mΩ/m)	WEIGHT (g/m)	OVERALL DIA. (mm) *	CURRENT @ 5 A/mm² (A)	TURNS PER cm²
24		0.511	83.87	1.823	0.5806	1.025	314
	0.5		87.10	1.746	0.5690	0.982	340
25		0.455	105.8	1.445	0.5213	0.813	389
	0.45		108.0	1.414	0.5160	0.795	407
26		0.404	134.2	1.114	0.4663	0.6409	492
	0.4		136.0	1.117	0.4620	0.6280	504
27		0.361	168.0	0.9099	0.4204	0.5118	621
	0.355		173.0	0.8800	0.4140	0.4950	635
28		0.32	213.9	0.7150	0.3764	0.4021	780
	0.315		219.0	0.6930	0.3710	0.3900	780
29		0.287	265.9	0.5751	0.3494	0.3235	896
	0.28		278.0	0.5470	0.3340	0.3080	941
30		0.254	339.4	0.4505	0.3054	0.2534	1184
	0.25		348.0	0.4360	0.3010	0.2450	1235
31		0.226	428.8	0.3566	0.2742	0.2006	1456
	0.224		434.0	0.3500	0.2720	0.1970	1512
32		0.203	531.4	0.2877	0.2484	0.1618	1817
	0.2		554.0	0.2790	0.2450	0.1570	1840
33		0.18	675.9	0.2262	0.2220	0.1272	2314
	0.18		672.0	0.2270	0.2220	0.1270	2314
34		0.16	855.5	0.1787	0.1990	0.1005	2822
	0.16		850.0	0.1790	0.1990	0.1010	2822
35		0.142	1086	0.1408	0.1783	0.0792	3552
	0.14		1110	0.1370	0.1760	0.0770	3640
36		0.127	1358	0.1126	0.1613	0.0633	4331
	0.125		1393	0.1100	0.1590	0.0610	4465
37		0.114	1685	0.0907	0.1455	0.0510	5372
	0.112		1735	0.0880	0.1430	0.0490	5520
38		0.102	2105	0.0726	0.1313	0.0409	6569
	0.1		2176	0.0700	0.1290	0.0390	6853
39		0.0889	2771	0.0552	0.1160	0.0310	8465
	0.09		2687	0.0570	0.1170	0.0320	8281
40		0.0787	3536	0.0433	0.1036	0.0243	10660
	0.08		3401	0.0450	0.1050	0.0250	10300
41		0.0711	4328	0.0353	0.0951	0.0199	12645
	0.071		4318	0.0350	0.0950	0.0200	12645
42		0.0635	5443	0.0282	0.0855	0.0158	15544
	0.063		5484	0.0280	0.0850	0.0160	15795
43		0.0559	7016	0.0218	0.0739	0.0123	20982
	0.05		8706	0.0170	0.0680	0.0098	24759

* Grade 2 or medium insulation.

Table A.1. AWG and IEC wire data.

A.1 Turns Density

The maximum number of turns per cm² is calculated by finding the number of turns in layer 1, the number of turns in layer 2, and the total number of layers (N) as shown in Figure A.1.
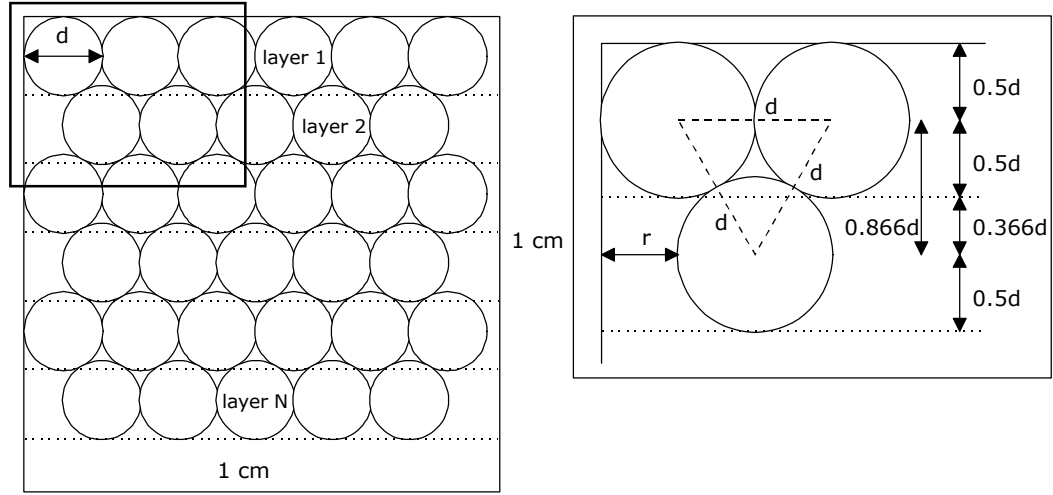
Figure A.1. Maximum turns of wire per cm².

The number of turns in layer 1 is given by

$$T_1 = \text{int}\left(\frac{1}{d}\right), \tag{A.1}$$

where d is the overall diameter of the copper wire in cm, and int(x) is a function rounding a number x down to the nearest integer.

In layer 2, the number of turns can be expressed as

$$T_2 = \text{int}\left(\frac{1 - d/2}{d}\right). \tag{A.2}$$

The number of turns in layer 1 is always greater than or equal to the number in layer 2.

The total number of layers, N, is calculated by assigning a height of d to the first horizontal layer, and a nominal height of $\sqrt{(0.75)}d = 0.866d$ to every layer after that. This yields

$$N = \text{int}\left(\frac{1-d}{0.866d}\right) + 1.$$ (A.3)

If N is an *even number*, it is then simply halved and multiplied by the sum of the number of turns in layer 1 and the number in layer 2 to yield the maximum number of turns per cm^2, T_m.

If N is an *odd number*, the maximum number of turns is obtained by dividing N into two sets of layers, with one set of layers being equal to the other set plus one. Then, the larger number of layers is multiplied by the number of turns in layer 1, and added to the product of the smaller number of layers with the number of turns in layer 2. This gives the maximum number of turns per cm^2, T_m.

In equation form, this may be written as:

$$T_m = T_1 \times \left(N - \text{int}\left(\frac{N}{2}\right)\right) + T_2 \times \text{int}\left(\frac{N}{2}\right).$$ (A.4)

NAME	OVERALL DIA. (cm)	TURNS IN LAYER 1	TURNS IN LAYER 2	NUMBER OF LAYERS	TURNS PER cm2
AWG #34	0.01990	50	49	57	2822
IEC 0.16	0.01990	50	49	57	2822
AWG #35	0.01783	56	55	64	3552
IEC 0.14	0.01760	56	56	65	3640
AWG #36	0.01613	61	61	71	4331
IEC 0.125	0.01590	62	62	72	4464
AWG #37	0.01455	68	68	79	5372
IEC 0.112	0.01430	69	69	80	5520
AWG #38	0.01313	76	75	87	6569
IEC 0.1	0.01290	77	77	89	6853
AWG #39	0.01160	86	85	99	8465
IEC 0.09	0.01170	85	84	98	8281
AWG #40	0.01036	96	96	111	10656
IEC 0.08	0.01050	95	94	109	10301
AWG #41	0.00951	105	104	121	12645
IEC 0.071	0.00950	105	104	121	12645
AWG #42	0.00855	116	116	134	15544
IEC 0.063	0.00850	117	117	135	15795
AWG #43	0.00739	135	134	156	20982
IEC 0.05	0.00680	147	146	169	24759

Table A.2. Turns density information for small AWG and IEC wire sizes.

A.2   Current Capability

The current handling capability in amps for a density of 5 A/mm² is simply calculated from $5\pi \times (\text{bare\_diameter}/2)^2$.

NAME	BARE DIA. (mm)	CURRENT @ 5A/mm² (A)
AWG #38	0.1020	0.040856
AWG #39	0.0889	0.031035
AWG #40	0.0787	0.024322
AWG #41	0.0711	0.019851
AWG #42	0.0635	0.015834
AWG #43	0.0559	0.012271

Table A.3. Current capability for small AWG wire sizes.

A.3   Overall Diameter

NAME	BARE DIA. (mm)	OVERALL DIA. (mm)	OVERALL − BARE DIFF.	ESTIMATED OVERALL (mm)
AWG #34	0.160	0.1990	0.0390	-
IEC 0.16	0.160	0.1990	0.0390	-
AWG #35	0.142	0.1783	0.0363	-
IEC 0.14	0.140	0.1760	0.0360	-
AWG #36	0.127	0.1613	0.0343	-
IEC 0.125	0.125	0.1590	0.0340	-
AWG #37	0.114	0.1455	0.0315	-
IEC 0.112	0.112	0.1430	0.0310	-
AWG #38	0.102	0.1313	0.0293	-
IEC 0.1	0.100	0.1290	0.0290	-
AWG #39	0.0889	0.1160	0.0271	-
IEC 0.09	0.0900	0.1170	0.0270	-
AWG #40	0.0787	0.1036	0.0249	-
IEC 0.08	0.0800	0.1050	0.0250	-
AWG #41	0.0711	-	-	0.0711 + 0.0240 = 0.0951
IEC 0.071	0.0710	0.0950	0.0240	-
AWG #42	0.0635	-	-	0.0635 + 0.0220 = 0.0855
IEC 0.063	0.0630	0.0850	0.0220	-
AWG #43	0.0559	-	-	0.0559 + 0.0180 = 0.0739
IEC 0.05	0.0500	0.0680	0.0180	-

Table A.4. Overall diameters for small AWG and IEC wire sizes.

Taking the difference between the overall and bare diameters of an IEC wire size, and adding it to the nearest equivalent AWG bare wire size gave us an approximation for the AWG overall diameters. This is a good estimate as can be seen from the IEC/AWG comparisons from #34 to #40.

A.4   Resistance per Length

Resistance values had to be converted from values given in Ω/1000 feet to $m\Omega$/m. 1 Ω/1000 feet is equivalent to 1 $m\Omega$/foot, and so we simply had to divide by the foot to metre conversion factor of 0.305. The resistance values for AWG #38 to #40 are for comparison, and they are similar to those in our original wire data table (Table A.1).

NAME	Ω/1000 ft.	$m\Omega$/m
AWG #38	648	2125
AWG #39	847	2777
AWG #40	1080	3540
AWG #41	1320	4328
AWG #42	1660	5443
AWG #43	2140	7016

Table A.5. Resistance per length for small AWG wire sizes.

Resistance values given in Table A.5 are for soft copper wire at 20 °C. For hard and medium copper wires, around 4% should be added to the corresponding soft wire value.

Appendix B

FOURIER ANALYSIS

This appendix contains Fourier analyses for nine different current waveforms.

Expressions for the average value of current, I_{dc}, the RMS value of the waveform, I_{rms}, and the RMS value of the nth harmonic, I_n, are derived in each case.

These expressions are related to the Fourier coefficients.

B.1   Sine Wave
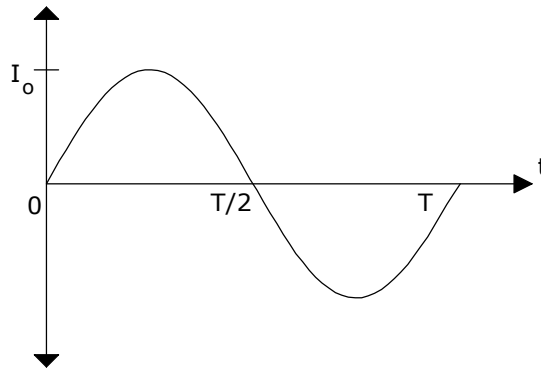
Figure B.1. Sine wave.

It is not necessary to derive a Fourier series in this case, the current is simply given by the expression

$$i(t) = I_o Sin(\omega t). \qquad (B.1)$$

Also, $I_{dc} = 0$, and $I_{rms} = I_o/\sqrt{2}$.

B.2 Duty Cycle Varying Rectified Sine Wave
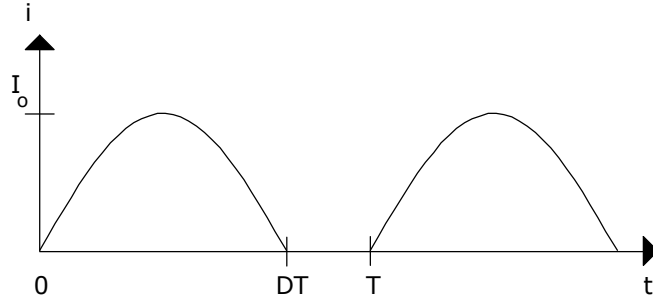
Figure B.2. Rectified sine wave with duty cycle D.

Figure B.2 shows a rectified or unipolar sine wave. It can be taken as an even function about 0 as shown in Figure B.3. We shall take one period T (from $-T/2$ to $T/2$) to calculate the Fourier series of i.
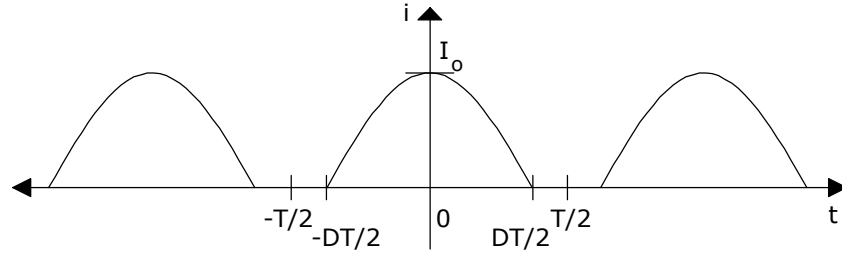
Figure B.3. Rectified sine wave taken as an even function.

For a range (-l, l), an even function has a Fourier series of the type f(x),

$$f(x) = \frac{a_o}{2} + \sum_{n=1}^{\infty} a_n \mathrm{Cos}\frac{n\pi x}{l}. \qquad (B.2)$$

In our case, $l = T/2$, $x = t$ and $f(x) = i(t)$. Also, since $\omega = 2\pi/T$, $n\pi x/l = n\pi t 2/T = n\omega t$. Therefore,

$$i(t) = \frac{a_o}{2} + \sum_{n=1}^{\infty} a_n \mathrm{Cos}(n\omega t). \qquad (B.3)$$

Also, $I_{dc} = a_o/2$, and $I_n = a_n/\sqrt{2}$.

Calculating the Fourier coefficients a_o and a_n yields

$$a_o = \frac{2}{l}\int_0^l f(x)dx = \frac{4}{T}\int_0^{\frac{T}{2}} i(t)dt$$

$$= \frac{4}{T}\left[\int_0^{\frac{DT}{2}} Sin\left(\frac{\pi}{DT}\left[t+\frac{DT}{2}\right]\right)dt\right] = \frac{4DI_o}{\pi} \qquad \text{(B.4)}$$

$$a_n = \frac{2}{l}\int_0^l f(x)Cos\frac{n\pi x}{l}dx = \frac{4}{T}\int_0^{\frac{T}{2}} i(t)Cos(n\omega t)dt$$

$$= \frac{4}{T}\left[\int_0^{\frac{DT}{2}} Cos\left(\frac{\omega t}{2D}\right)Cos(n\omega t)dt\right] = \frac{4DI_o}{\pi}\frac{Cos(n\pi D)}{(1-4n^2D^2)} \qquad \text{(B.5)}$$

A special instance of a_n arises when the frequency of the sine waveshape is a multiple of the frequency at which it is occurring, i.e. $n = k = 1/2D$ where $k \in \mathbf{N}$. If the expression in (B.5) were used for this case, $1/(1 - 4n^2D^2) \to \infty$. Therefore, a new formula is used where n is set to k and the frequency of the waveshape is now $k\omega$.

$$a_k = \frac{4}{T}\int_0^{\frac{T}{2}} i(t)Cos(k\omega t)dt$$

$$= \frac{4}{T}I_o\left[\int_0^{\frac{DT}{2}} Cos(k\omega t)Cos(k\omega t)dt\right] \qquad \text{(B.6)}$$

$$= \frac{2}{T}I_o\left[\int_0^{\frac{\pi}{2k\omega}} Cos(2k\omega t)+Cos(o)dt\right] = \frac{I_o}{2k}$$

Depending on the duty cycle, the waveform falls into one of two cases:

    I. $1/2D = k \notin \mathbf{N}$, or $1/2D = k \in \mathbf{N}$ with $k > N$, the total number of harmonics.

    II. $1/2D = k \in \mathbf{N}$ with $k < N$, the total number of harmonics.

If we limit the total number of harmonics to N, then these two cases are distinct because in the first, all a_n terms are of the form given in (B.5), whereas in the second, the kth term is given by (B.6) and the rest by (B.5).

B.2.1 Case I

The average value of current is $a_o/2$ (B.4), or

$$I_{dc} = \frac{2DI_o}{\pi}. \tag{B.7}$$

The RMS value of current is

$$I_{rms} = I_o \sqrt{\frac{D}{2}}. \tag{B.8}$$

The RMS value of the nth harmonic is $a_n/\sqrt{2}$ (B.5) or

$$I_n = \frac{2\sqrt{2}DI_o}{\pi} \frac{Cos(\pi nD)}{\left(1 - 4n^2D^2\right)}. \tag{B.9}$$

B.2.2 Case II

I_{dc} and I_{rms} are the same as in case I. The RMS value of the nth harmonic for $n \neq k$ is

$$I_n = \frac{2\sqrt{2}DI_o}{\pi} \frac{Cos(\pi nD)}{\left(1 - 4n^2D^2\right)}, \tag{B.10}$$

and for $n = k$ is

$$I_k = \frac{I_o}{2\sqrt{2}k}. \tag{B.11}$$

B.3   Duty Cycle Varying Bipolar Sine Wave

The case of the duty cycle varying sine wave in Figure B.4 is now examined. When D is 1, the waveform becomes a pure sine wave.
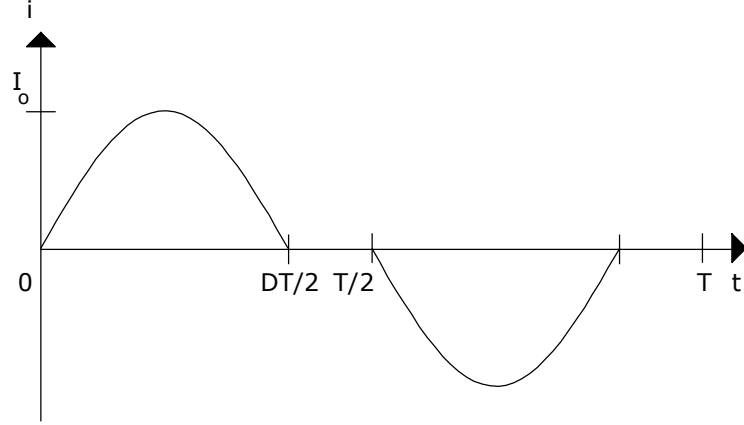
Figure B.4. Bipolar sine wave with duty cycle D.

An even function may be taken by moving the above waveform to the left by DT/4. The Fourier coefficients a_o and a_n are calculated over one period T of the even function (from -T/2 to T/2):

$$a_n = \frac{4}{T} \int_0^{\frac{T}{2}} i(t) \cos(n\omega t) dt$$

$$= \frac{4}{T} \left[\begin{array}{l} \int_0^{\frac{DT}{4}} I_o \cos\left(\frac{2\pi}{DT} t\right) \cos(n\omega t) dt + \\[2em] \int_{\frac{2T-DT}{4}}^{\frac{T}{2}} -I_o \cos\left(\frac{2\pi}{DT}\left[t - \frac{T}{2}\right]\right) dt \cos(n\omega t) dt \end{array} \right]$$

$$= \frac{4DI_o}{\pi(1-n^2D^2)} \left[\cos\left(\frac{nD\pi}{2}\right) - \cos(n\pi)\cos\left(\frac{nD\pi}{2}\right) \right], \qquad (B.12)$$

$$= \frac{4DI_o}{\pi(1-n^2D^2)} \cos\left(\frac{nD\pi}{2}\right) \dots \text{n odd}$$

$$= 0 \dots \text{n even}$$

$$a_o = \frac{4}{T}\int_0^{\frac{T}{2}} i(t)dt = \frac{4}{T}\left[\begin{array}{l} \int_0^{\frac{DT}{4}} I_o Cos\left(\frac{2\pi}{DT}t\right)dt + \\ \\ \int_{\frac{2T-DT}{4}}^{\frac{T}{2}} -I_o Cos\left(\frac{2\pi}{DT}\left[t - \frac{T}{2}\right]\right)dt \end{array}\right] = 0. \qquad (B.13)$$

As in section B.2, a special instance of a_n arises when the frequency of the sine waveshape is a multiple of the frequency at which it is occurring, i.e. $n = k = 1/D$ where $k \in \mathbf{N}$. If the expression in (B.12) were used for this case, $1/(1 - n^2D^2) \rightarrow \infty$. Therefore, a new formula is used where n is set to k and the frequency of the waveshape is now $k\omega$.

$$a_k = \frac{4}{T}\int_0^{\frac{T}{2}} i(t)Cos(k\omega t)dt$$

$$= \frac{4}{T}I_o\left[\begin{array}{l} \int_0^{\frac{DT}{4}} Cos(k\omega t)Cos(k\omega t)dt + \\ \\ \int_{\frac{2T-DT}{4}}^{\frac{T}{2}} -Cos\left(k\omega\left[t - \frac{\pi}{\omega}\right]\right)Cos(k\omega t)dt \end{array}\right]. \qquad (B.14)$$

$$= \frac{I_o}{2k}(1 - Cos(k\pi))$$

The kth harmonic is therefore zero when k is an even number. Depending on the duty cycle, the waveform falls into one of two cases:

I. $1/D = k \notin \mathbf{N}$, or $1/D = k \in \mathbf{N}$ with $k > N$, the total number of harmonics

II. $1/D = k \in \mathbf{N}$ with $k < N$, the total number of harmonics

If we limit the total number of harmonics to N, then these two cases are distinct because in the first, all a_n terms are of the form given in (B.12), whereas in the second, the kth term is given by (B.14) and the rest by (B.12).

B.3.1   Case I

The average value of current is $I_{dc} = 0$, the RMS value of the current is $I_{rms} = I_o\sqrt{(D/2)}$, and the RMS value of the nth harmonic is

$$I_n = \frac{2\sqrt{2}DI_o}{\pi(1-n^2D^2)}\text{Cos}\left(\frac{nD\pi}{2}\right).$$

(B.15)

B.3.2   Case II

As before, the average value of current is $I_{dc} = 0$, the RMS value of the current is $I_{rms} = I_o\sqrt{(D/2)}$, and the RMS value of the nth harmonic for $n \neq k$ is

$$I_n = \frac{2\sqrt{2}DI_o}{\pi(1-n^2D^2)}\text{Cos}\left(\frac{nD\pi}{2}\right),$$

(B.16)

and for $n = k$ is

$$I_k = \frac{I_o}{2\sqrt{2}k}(1-\text{Cos}(k\pi)).$$

(B.17)

B.4   Duty Cycle Varying Square Wave

B.4.1   Version I

Now we take the case of a duty cycle varying square wave. A finite number of N harmonics will produce a fixed rise and fall time in this waveform, and as N goes to infinity, the rise and fall times will go to zero.
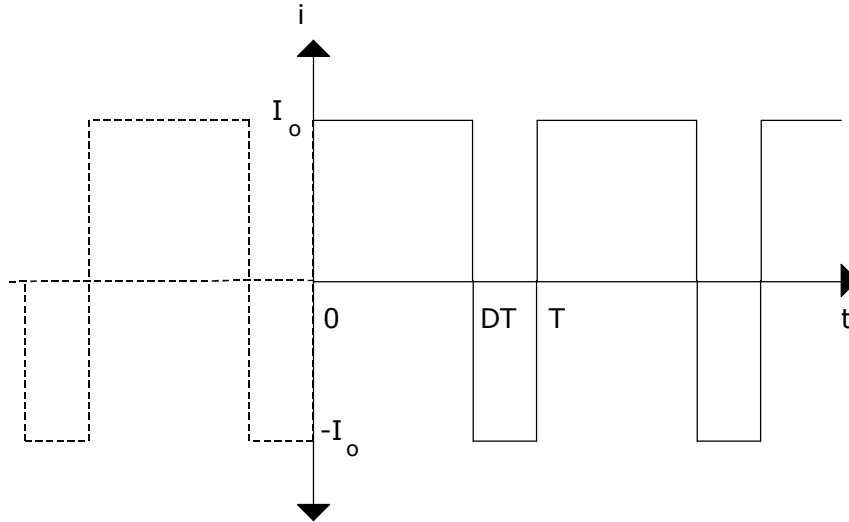
Figure B.5. Square wave with duty cycle D.
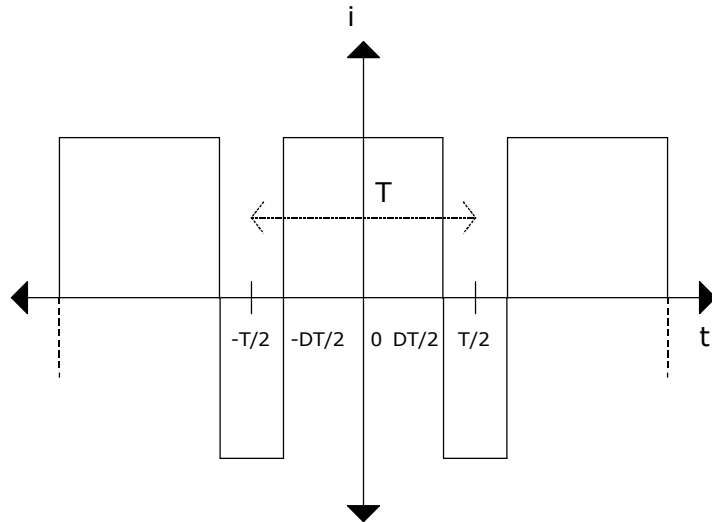
Figure B.6. Square wave taken as an even function.

Figure B.5 can be taken as an even function about 0 as shown in Figure B.6. We shall take one period T (marked by dashed arrow) to calculate the Fourier series of i. The Fourier coefficients a_n and a_o are calculated as follows:

$$
a_o = \frac{4}{T} \int_0^{\frac{T}{2}} i(t)dt
$$

$$
= \frac{4}{T} \left[\int_0^{\frac{DT}{2}} I_o dt + \int_{\frac{DT}{2}}^{\frac{T}{2}} -I_o dt \right] = 2I_o(2D-1)
$$

, (B.18)

$$a_n = \frac{4}{T} \int_0^{\frac{T}{2}} i(t) \text{Cos}(n\omega t) dt$$

$$= \frac{4}{T} \left[\int_0^{\frac{DT}{2}} I_o \text{Cos}(n\omega t) dt + \int_{\frac{DT}{2}}^{\frac{T}{2}} -I_o \text{Cos}(n\omega t) dt \right]. \qquad \text{(B.19)}$$

$$= \frac{4I_o}{n\pi} \text{Sin}(n\pi D)$$

The average value of current is $I_{dc} = I_o(2D - 1)$. The RMS value of current is I_o.

The RMS value of the nth harmonic is

$$I_n = \frac{1}{\sqrt{2}} \left[\frac{4I_o}{n\pi} \text{Sin}(n\pi D) \right] = \frac{2\sqrt{2}I_o}{n\pi} \text{Sin}(n\pi D). \qquad \text{(B.20)}$$

B.4.2 Version II
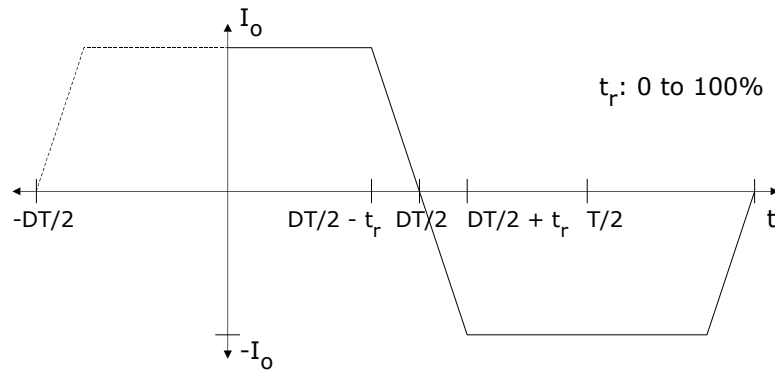
Figure B.7. Square wave with duty cycle D and rise time t_r.

Unlike waveform 4 version I, the square waveform as shown in Figure B.7 has a predefined rise and fall time, t_r, measured from 0 to 100% of the peak current.

If we centre the first half of the waveform about the current axis as shown, there are three sections to the waveform between t = 0 and t = T/2 for Fourier analysis:

i(t)	t
I_o	0 to $DT/2 - t_r$
$-\dfrac{I_o}{t_r}t + \dfrac{I_o DT}{2t_r}$	$DT/2 - t_r$ to $DT/2 + t_r$
$-I_o$	$DT/2 + t_r$ to $T/2$

Table B.1. Sections of square wave.

The Fourier coefficients are evaluated over these three segments, and yield

$$I_n = \frac{a_n}{2} = \frac{2\sqrt{2}I_o Sin(n\pi D)}{n\pi}\frac{Sin\left(nt_r\,\dfrac{2\pi}{T}\right)}{nt_r\,\dfrac{2\pi}{T}}, \tag{B.21}$$

$$I_{dc} = \frac{a_o}{2} = 2I_o D - I_o, \tag{B.22}$$

$$I_{rms} = I_o\sqrt{1 - \frac{8t_r}{3T}}. \tag{B.23}$$

B.5 Duty Cycle Varying Rectified Square Wave

B.5.1 Version I

Consider a duty cycle varying rectified square (or pulsed) wave as shown in Figure B.8. This is representative of the current in a push-pull winding. I_o is related to the DC output current; for a 1:1 turns ratio, it is equal to the DC output current for a 100% duty cycle.
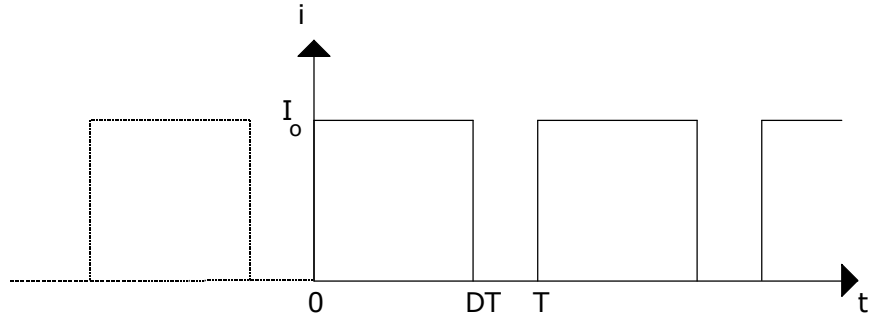
Figure B.8. Rectified square wave with duty cycle D.
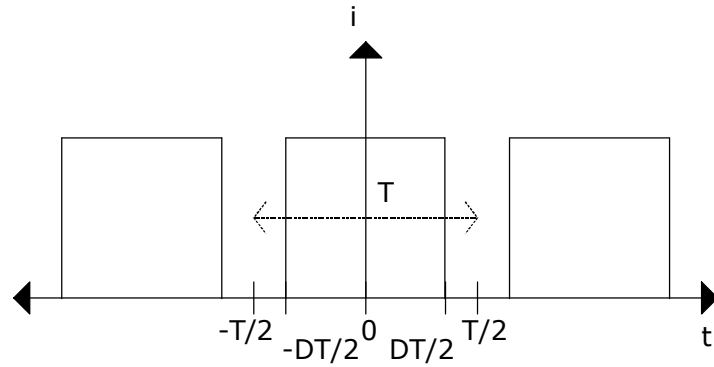
Figure B.9. Rectified square wave taken as an even function.

The Fourier coefficients a_o and a_n are calculated over one period T of the even function shown in Figure B.9 (from -T/2 to T/2).

$$a_o = \frac{4}{T} \int_o^{\frac{T}{2}} i(t)dt$$

$$= \frac{4}{T} \left[\int_o^{\frac{DT}{2}} I_o dt + \int_{\frac{DT}{2}}^{\frac{T}{2}} o dt \right] = 2I_o D \qquad \text{(B.24)}$$

$$a_n = \frac{4}{T} \int_o^{\frac{T}{2}} i(t)Cos(n\omega t)dt$$

$$= \frac{4}{T} \left[\int_o^{\frac{DT}{2}} I_o Cos(n\omega t)dt + \int_{\frac{DT}{2}}^{\frac{T}{2}} oCos(n\omega t)dt \right]. \qquad \text{(B.25)}$$

$$= \frac{2I_o}{n\pi} Sin(n\pi D)$$

232

The average value of current is $I_{dc} = I_o D$. The RMS value of current is $I_{rms} = I_o\sqrt{D}$. The RMS value of the nth harmonic is

$$I_n = \frac{1}{\sqrt{2}}\left[\frac{2I_o}{n\pi}Sin(n\pi D)\right] = \frac{\sqrt{2}I_o}{n\pi}Sin(n\pi D).$$

(B.26)

B.5.2   Version II

This version has a predefined rise and fall time, t_r.
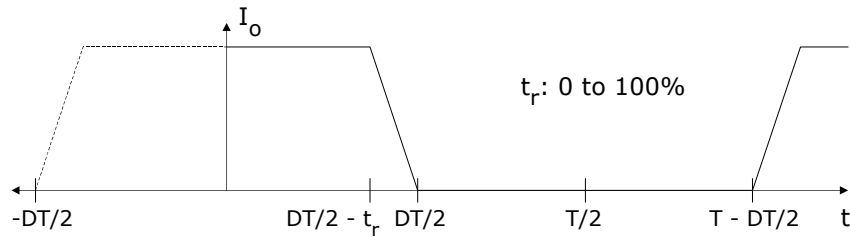
Figure B.10. Rectified square wave with duty cycle D and rise time t_r.

If we centre the pulse of the waveform about the current axis as shown, there are two sections to the waveform between t = 0 and t = T/2 for Fourier analysis:

i(t)	t
I_o	0 to DT/2 - t_r
$-\dfrac{I_o}{t_r}t + \dfrac{I_oDT}{2t_r}$	DT/2 - t_r to DT/2

Table B.2. Sections of rectified square wave.

The Fourier coefficients are evaluated over these two segments, and yield

$$I_n = \frac{a_n}{2} = \frac{\sqrt{2}I_o}{n\pi}Sin\left(n\pi D - \frac{n\pi t_r}{T}\right)\frac{Sin\left(\dfrac{n\pi t_r}{T}\right)}{\dfrac{n\pi t_r}{T}},$$

(B.27)

$$I_{dc} = \frac{a_o}{2} = I_o\left(D - \frac{t_r}{T}\right), \qquad\qquad (B.28)$$

$$I_{rms} = I_o\sqrt{D - \frac{4t_r}{3T}} \,. \qquad\qquad (B.29)$$

This waveform is not just a version of waveform 4 version II with a different DC value. This is due to our interpretation of the duty cycles as shown below. Let us define waveform 4 and 5 with the same duty cycle, rise time and peak current value. When waveform 5 is centred about the x-axis to correspond to waveform 4, we see that the rise time is halved, and the duty cycle is reduced to $D - t_r/T$.
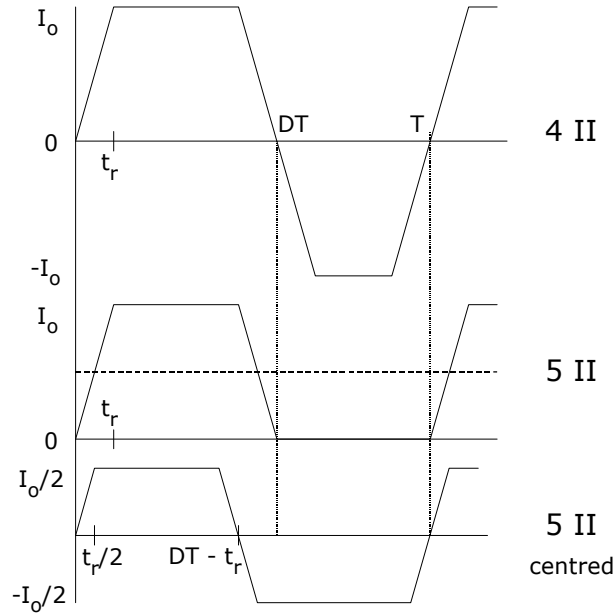
Figure B.11. Comparison of waveforms 4 and 5.

B.6   Duty Cycle Varying Bipolar Square Wave

B.6.1   Version I

Consider the duty cycle varying bipolar square wave as shown in Figure B.12. If D = 1, this waveform becomes a full square wave.
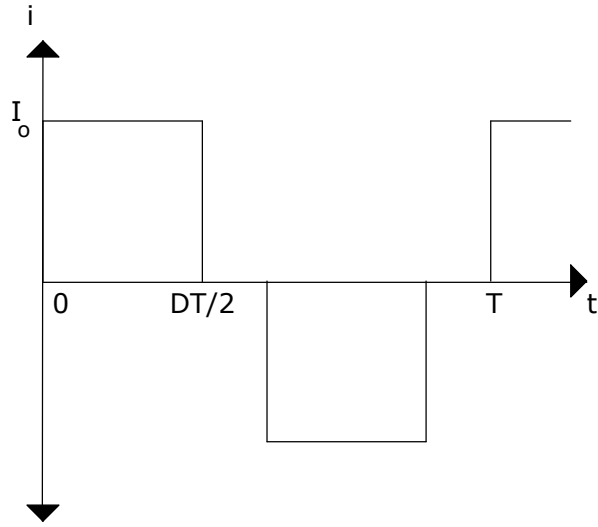
Figure B.12. Bipolar square wave with duty cycle D.
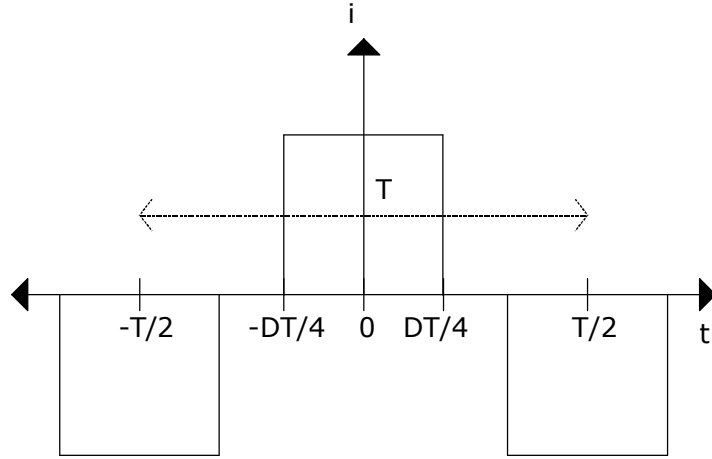
Figure B.13. Bipolar square wave taken as an even function.

Figure B.12 can be taken as an even function about 0 as shown in Figure B.13. We shall take one period T (marked by dashed arrow) to calculate the Fourier series of i. Calculating the Fourier coefficients a_n and a_0 yields

$$a_0 = \frac{4}{T} \int_0^{\frac{T}{2}} i(t)dt = \frac{4}{T}\left[\int_0^{\frac{DT}{4}} I_0 dt + \int_{\frac{2T-DT}{4}}^{\frac{T}{2}} -I_0 dt \right] = 0, \qquad (B.30)$$

$$a_n = \frac{4}{T} \int_0^{\frac{T}{2}} i(t) \cos(n\omega t) dt$$

$$= \frac{4}{T} \left[\int_0^{\frac{DT}{4}} I_o \cos(n\omega t) dt + \int_{\frac{2T-DT}{4}}^{\frac{T}{2}} -I_o \cos(n\omega t) dt \right]$$

$$= \frac{2I_o}{n\pi} \left[\sin\left(\frac{n\pi D}{2}\right) - \cos(n\pi)\sin\left(\frac{n\pi D}{2}\right) \right] \qquad . \qquad \text{(B.31)}$$

$$= \frac{4I_o}{n\pi} \sin\left(\frac{n\pi D}{2}\right) \dots n \text{ odd}$$

$$= 0 \dots n \text{ even}$$

The DC component is zero as expected from the even areas above and below the axis, and the RMS value of the nth harmonic (with n odd) is

$$I_n = \frac{2\sqrt{2}I_o}{n\pi} \sin\left(\frac{n\pi D}{2}\right). \qquad \text{(B.32)}$$

The RMS value of the waveform is $I_o\sqrt{(D)}$.

B.6.2   Version II
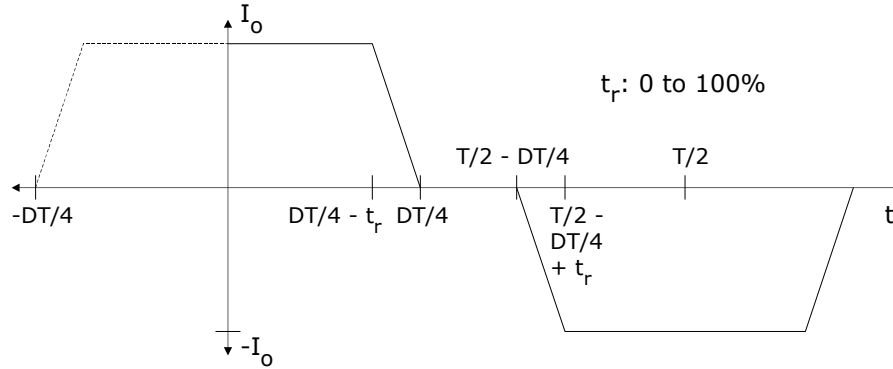
Figure B.14. Bipolar square wave with duty cycle D.

The bipolar square waveform as shown in Figure B.14 has a predefined rise and fall time, t_r, measured from 0 to 100% of the peak current. If we centre the first half of the waveform about the current axis as shown,

there are four non-zero valued sections to the waveform between t = 0 and t = T/2 for Fourier analysis:

i(t)	t
I_o	0 to DT/4 - t_r
$-\dfrac{I_o}{t_r}t + \dfrac{I_o DT}{4t_r}$	DT/4 - t_r to DT/4
$-\dfrac{I_o}{t_r}t + \dfrac{I_o T}{2t_r} - \dfrac{I_o DT}{4t_r}$	T/2 − DT/4 to T/2 −DT/4 + t_r
-I_o	T/2 −DT/4 + t_r to T/2

Table B.3. Sections of bipolar square wave.

The Fourier coefficients are evaluated over these four segments, and yield

$$I_n = \frac{a_n}{2} = \frac{2\sqrt{2}I_o}{n\pi} \mathrm{Sin}\left(n\pi\left(\frac{D}{2} - \frac{t_r}{T}\right)\right) \frac{\mathrm{Sin}\left(n\pi\frac{t_r}{T}\right)}{n\pi\frac{t_r}{T}}, \tag{B.33}$$

for n odd, and

$$I_{dc} = \frac{a_o}{2} = 0. \tag{B.34}$$

The RMS value of the waveform is

$$I_{rms} = I_o\sqrt{D - \frac{8t_r}{3T}}. \tag{B.35}$$

B.7   Duty Cycle Varying Triangle Wave

The average value of the triangle wave current shown in Figure B.15 is I_{dc} = 0.
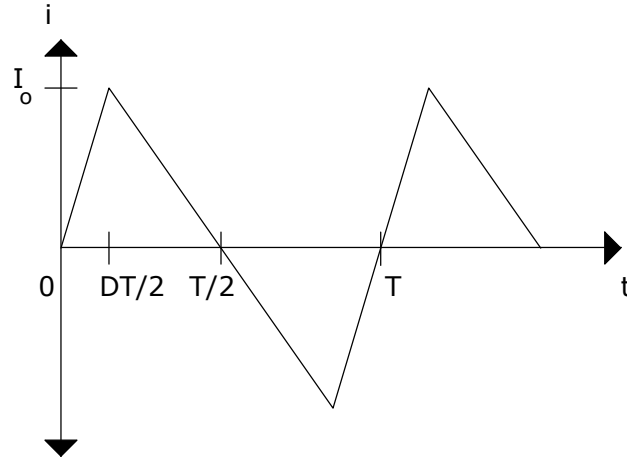
Figure B.15. Triangle wave with duty cycle D.

The RMS value of current is given by $I_{rms} = I_o \sqrt{\dfrac{1}{3}}$. The RMS value of the nth harmonic is

$$I_n = \frac{\sqrt{2}I_o(DSin(n\pi) - Sin(n\pi D))}{\pi^2 n^2 D(D-1)} = \frac{\sqrt{2}I_o Sin(n\pi D))}{\pi^2 n^2 D(1-D)} . \qquad (B.36)$$

B.8 Duty Cycle Varying Rectified Triangle Wave

The next waveform to be considered is the rectified triangle shown below.
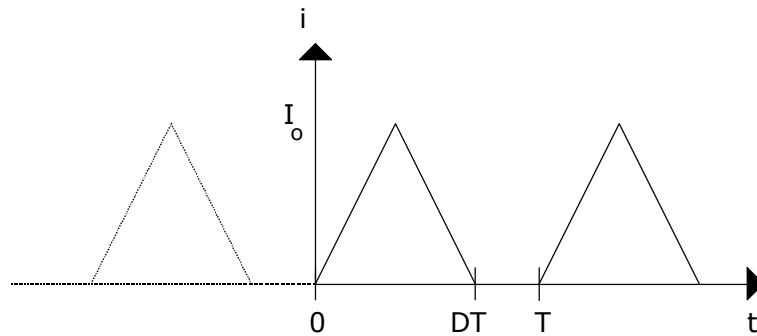
Figure B.16. Rectified triangle wave with duty cycle D.
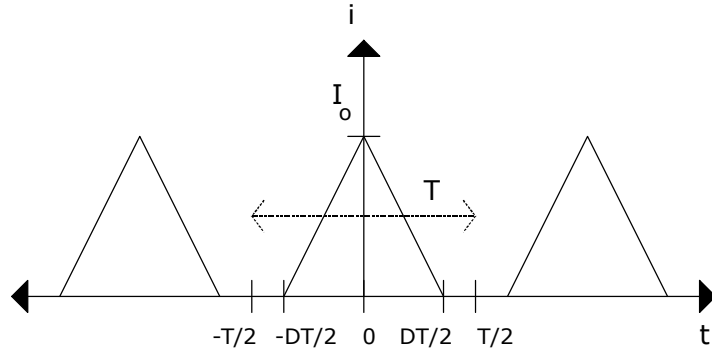
Figure B.17. Rectified triangle wave taken as an even function.

Taking one period T (marked by dashed arrow) of the even function shown in Figure B.17, we can calculate the Fourier coefficients of i as follows:

$$
\begin{aligned}
a_n &= \frac{4}{T}\int_0^{\frac{T}{2}} i(t)\mathrm{Cos}(n\omega t)dt \\
&= \frac{4}{T}I_o\left[\int_0^{\frac{DT}{2}}\left(2-\frac{2(t+DT/2)}{DT}\right)\mathrm{Cos}(n\omega t)dt\right] \\
&= \frac{2I_o}{\pi^2 n^2 D}[1-\mathrm{Cos}(n\pi D)] = \frac{4I_o}{\pi^2 n^2 D}\mathrm{Sin}^2\left(\frac{n\pi D}{2}\right)
\end{aligned}
\qquad , \qquad \text{(B.37)}
$$

$$
\begin{aligned}
a_o &= \frac{4}{T}\int_0^{\frac{T}{2}} i(t)dt \\
&= \frac{4}{T}I_o\left[\int_0^{\frac{DT}{2}}\left(2-\frac{2(t+DT/2)}{DT}\right)dt\right] = I_o D
\end{aligned}
\qquad . \qquad \text{(B.38)}
$$

The average value of current is $I_{dc} = I_o D/2$. The RMS value of current is $I_{rms} = I_o\sqrt{D/3}$. The RMS value of the nth harmonic is

$$
I_n = \frac{1}{\sqrt{2}}\left[\frac{4I_o}{\pi^2 n^2 D}\mathrm{Sin}^2\left(\frac{n\pi D}{2}\right)\right] = \frac{2\sqrt{2}I_o}{\pi^2 n^2 D}\mathrm{Sin}^2\left(\frac{n\pi D}{2}\right). \qquad \text{(B.39)}
$$

B.9   Duty Cycle Varying Bipolar Triangle Wave

The last waveform to be considered is the bipolar triangle wave shown in Figure B.18.
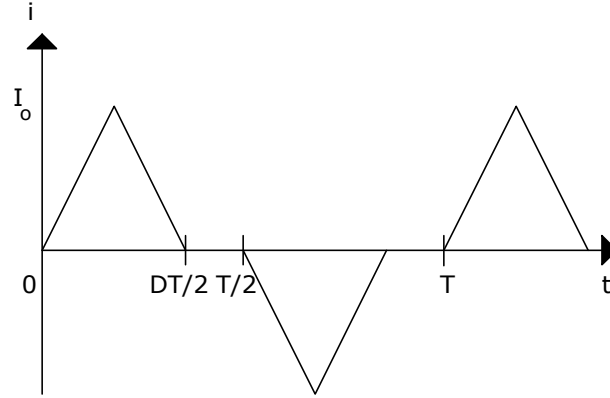
Figure B.18. Bipolar triangle wave with duty cycle D.

After taking one period T of the even function shown above by moving it to the left by DT/4, we can calculate the Fourier coefficients of i as follows:

$$
\begin{aligned}
a_n &= \frac{4}{T} \int_0^{\frac{T}{2}} i(t) \cos(n\omega t) dt \\
&= \frac{4}{T} I_o \left[\begin{array}{l} \displaystyle\int_0^{\frac{DT}{4}} \left(1 - \frac{4t}{DT} \right) \cos(n\omega t) dt + \\[4mm] \displaystyle\int_{\frac{2T-DT}{4}}^{\frac{T}{2}} \left(-\frac{4t}{DT} + \frac{2}{D} - 1 \right) \cos(n\omega t) dt \end{array} \right], \\[4mm]
&= \frac{8 I_o}{\pi^2 n^2 D} \left[1 - \cos\left(\frac{n D \pi}{2} \right) \right] \dots \text{n odd} \\
&= 0 \dots \text{n even}
\end{aligned}
\tag{B.40}
$$

$$a_o = \frac{4}{T} \int_0^{\frac{T}{2}} i(t)dt$$

$$= \frac{4}{T} I_o \left[\int_0^{\frac{DT}{4}} \left(1 - \frac{4t}{DT} \right) dt + \int_{\frac{2T-DT}{4}}^{\frac{T}{2}} \left(-\frac{4t}{DT} + \frac{2}{D} - 1 \right) dt \right]. \qquad \text{(B.41)}$$

$$= 0$$

The average value of current is zero. The RMS value of current is $I_{rms} = I_o \sqrt{D/3}$. The RMS value of the nth harmonic for n odd is

$$I_n = \frac{a_n}{\sqrt{2}} = \frac{4\sqrt{2}I_o}{\pi^2 n^2 D} \left(1 - Cos\left(\frac{nD\pi}{2} \right) \right). \qquad \text{(B.42)}$$

Appendix C

STRUCTURED ENGLISH CODE

This appendix includes structured English program code for the system processes outlined in section 5.4.

Also, a list of variables used in the subprocesses is included as well as details of the split data flows from the data flow diagrams of section 5.4.

C.1   Enter Specifications

NUMBER	NAME/DESCRIPTION
1.1	Choose an Application Type
1.2	Rectify Transformer Output
1.3	Display Custom Core Materials
1.4	Display Custom Winding Materials
1.5	Select One of the Core Materials
1.6	Select One of the Winding Materials
1.7	Calculate Area Product
1.8	Change Variable Values

Table C.1. "Enter Specifications" subprocesses.

C.1.1   Choose an Application Type

Choose from the available applications (centre-tapped transformer, forward converter, push-pull converter) and call the function to calculate the area product for the chosen application (in the case of all specifications already entered):

Call (Calculate Area Product, 1.7)

C.1.2   Rectify Transformer Output

Update the area product calculations after a change in the rectify transformer output status for a centre-tapped transformer only:

Call (Calculate Area Product, 1.7)

C.1.3   Display Custom Core Materials

If (custom core materials are not required) **Then**
        Open the regular cores database
Else
        Open the custom cores database
End If

Display the list of core materials (custom or regular)

C.1.4   Display Custom Winding Materials

If (custom winding materials are not required) **Then**
        Open the regular windings database
Else
        Open the custom windings database
End If

Display the list of winding materials (custom or regular)

C.1.5   Select One of the Core Materials

On selecting a core material from the list of available materials, we have to call the area product calculation routine since the specifications have changed:

Call (Calculate Area Product, 1.7)

C.1.6   Select One of the Winding Materials

On selecting a winding material from the list of available materials, we have to call the area product calculation routine since the specifications have changed:

Call (Calculate Area Product, 1.7)

C.1.7   Calculate Area Product

Read the specifications into variables: OutputVoltage, OutputCurrent, InputVoltageLower, InputVoltageUpper, Frequency1, TemperatureRise, AmbientTemperature, Efficiency1, TurnsRatio1.

Get core material data (CoreMaterialName, CoreDensity, SaturationFluxDensity, Kc, alpha, beta), winding material data (WindingMaterialName, WindingResistivity, alpha20), and expert options or constants (TemperatureFactor, WindowUtilisationFactor, StackingFactor, CoreVolumeConstant, WindingVolumeConstant, SurfaceAreaConstant, HeatTransferCoefficient).

Exit if any of the specifications are missing.

Check if have (centre-tapped transformer or forward converter or push-pull converter), calculating appropriate values for DutyCycle1, WaveformFactor, PrimaryPowerFactor, OutputPower, SecondaryPowerFactor, VARating as follows:

> **If** (centre-tapped transformer) **Then**
>   DutyCycle1 = -1
>   WaveformFactor = 4.44
>   PrimaryPowerFactor = 1
>
>   **If** (transformer is rectified) **Then**
>   OutputPower = (OutputVoltage + 1) * OutputCurrent
>   SecondaryPowerFactor = 1 / (2) ^ 0.5
>   **Else If** (transformer is not rectified) **Then**
>   OutputPower = OutputVoltage * OutputCurrent
>   SecondaryPowerFactor = 1
>   **End If**
>
>   VARating = (1 / ((Efficiency1 / 100) * PrimaryPowerFactor) …
>   … 1 / SecondaryPowerFactor) * OutputPower
> **Else If** (forward converter) **Then**
>   DutyCycle1 = (OutputVoltage / InputVoltageLower) * …
>   … (TurnsRatio1)
>   WaveformFactor = 1 / (DutyCycle1 * (1 - DutyCycle1)) ^ 0.5
>   PrimaryPowerFactor = (1 - DutyCycle1) ^ 0.5
>   OutputPower = (OutputVoltage + 1) * OutputCurrent
>   SecondaryPowerFactor = (1 - DutyCycle1) ^ 0.5
>   VARating = ((1 / ((Efficiency1 / 100) * PrimaryPowerFactor) …
>   … 1 / SecondaryPowerFactor) * OutputPower) *1.05)
> **Else If** (push-pull converter) **Then**
>   DutyCycle1 = (OutputVoltage / InputVoltageLower) * …
>   … (TurnsRatio1)
>   WaveformFactor = 4 / (DutyCycle1) ^ 0.5
>   PrimaryPowerFactor = 1 / (2) ^ 0.5
>   OutputPower = (OutputVoltage + 1.5) * OutputCurrent
>   SecondaryPowerFactor = (DutyCycle1 / (1 + DutyCycle1)) ^ 0.5
>   VARating = (1 / ((Efficiency1 / 100) * PrimaryPowerFactor) …
>   … + 1 / SecondaryPowerFactor) * OutputPower
> **End If**
>
> **If** (DutyCycle1 > 1) **Then**
>   **Output** ("The current specifications give a duty cycle greater …
>   … than the possible maximum of 1.0. Please change the turns …
>   … ratio or input/output voltages to more appropriate values.")
> **End If**

Calculate OptimumConstant, TemperatureFactor, CurrentDensityConstant, OptimumFluxDensity as follows:

OptimumConstant = ((4 * WindingResistivity * CoreVolumeConstant …
… * WindingVolumeConstant) / ((StackingFactor ^ 2) * …
… WindowUtilisationFactor * (HeatTransferCoefficient ^ 2) * …
… (SurfaceAreaConstant ^ 2))) ^ (2 / 3)

TemperatureFactor = ((HeatTransferCoefficient * …
… SurfaceAreaConstant) / (2 * WindingResistivity * …
… WindowUtilisationFactor * WindingVolumeConstant)) ^ (1 / 2)

CurrentDensityConstant = CoreVolumeConstant / (WindingResistivity …
… * WindowUtilisationFactor * WindingVolumeConstant)

OptimumFluxDensity = (1 / ((OptimumConstant ^ (7 / 8)) * …
… TemperatureFactor)) * ((TemperatureRise)^ (1 / 2) / …
… (StackingFactor * WindowUtilisationFactor)) * (((WaveformFactor …
… * Frequency1 * TemperatureRise) / VARating) ^ (1 / 6)) * (1 / …
… ((CoreDensity * Kc * (Frequency1 ^ alpha)) ^ (7 / 12)))

Calculate MaximumFluxDensity1 and AreaProduct1:

If (OptimumFluxDensity < SaturationFluxDensity) **Then**
    MaximumFluxDensity1 = OptimumFluxDensity
    AreaProduct1 = OptimumConstant * ((VARating / …
    … (WaveformFactor * Frequency1 * TemperatureRise)) ^ (4 / …
    … 3)) * ((CoreDensity * Kc * (Frequency1 ^ alpha)) ^ (2 / 3))
Else
    MaximumFluxDensity1 = SaturationFluxDensity
    a0 = CurrentDensityConstant * CoreDensity * Kc * …
    … (Frequency1 ^ alpha) * (MaximumFluxDensity1^ beta)
    a1 = 2 * (TemperatureFactor ^ 2) * TemperatureRise
    a2 = (VARating / (WaveformFactor * Frequency1 * …
    … MaximumFluxDensity1 * StackingFactor * …
    … WindowUtilisationFactor) ^ 2)
    AreaProduct1 = (VARating / (WaveformFactor * Frequency1 …
    … * MaximumFluxDensity1 * StackingFactor * …
    … WindowUtilisationFactor * TemperatureFactor * …
    … (TemperatureRise ^ 0.5))) ^ (8 / 7)
    AreaProduct1 = AreaProduct1 - ((a0 * (AreaProduct1 ^ 2)) - …
    … (a1 * (AreaProduct1 ^ (7 / 4))) + a2) / ((2 * a0 * …
    … AreaProduct1) - ((7 / 4) * a1 * (AreaProduct1 ^ (3 / 4))))
End If

If the DutyCycle1 variable is set to −1 (as set by the centre-tapped transformer), then we do not display a value for it.

Write results to appropriate text boxes: AreaProduct1 and AreaProduct2 (for step 2), MaximumFluxDensity1 and MaximumFluxDensity2 (for step 2), PrimaryPowerFactor, SecondaryPowerFactor, OutputPower, VARating, DutyCycle1, WaveformFactor, OptimumConstant, CurrentDensityConstant, TemperatureFactor, TurnsRatio2 (for step 3).

Set StepsTaken to 1 to show that we have completed the first stage and can progress to the next:

StepsTaken = 1

C.1.8   Change Variable Values

For any variable x, where x = {AmbientTemperature, CoreVolumeConstant, Efficiency1, Frequency1, HeatTransferCoefficient, InputVoltageLower, InputVoltageUpper, OutputCurrent, OutputVoltage, StackingFactor, SurfaceAreaConstant, TemperatureFactor, TemperatureRise, TurnsRatio1, WindingVolumeConstant, WindowUtilisationFactor}:

> **Get Input** (x)
> **If** (x is a valid number) **Then**
>   **Call** (Calculate Area Product, 1.7)

C.2   Choose Core Data

NUMBER	NAME/DESCRIPTION
2.1	Select Appropriate Core
2.2	Choose a Different Core
2.3	Choose a Core Type
2.4	Choose a Core Shape

Table C.2. "Choose Core Data" subprocesses.

C.2.1   Select Appropriate Core

Open the core group table corresponding to the name currently selected in the core types list, then iterate through the entries in the table until a core with an area product greater than or equal to that calculated is found:

> Open the core table matching the group currently selected in the list
>
> **Do While** (we have not reached the end of the core table)
>
>   **If** (the area product from the table in cm^4 >= AreaProduct1 * …
> … 10 ^ 8) **Then**
>   Obtain values for ChosenCoreWeight, ChosenCoreMLT, …
>   … ChosenCoreAreaProduct, ChosenCoreWindowArea, …
>   … ChosenCoreCrossSectionalArea, …
>   … ChosenCoreWindowHeight, ChosenCoreWindowWidth …
>   … from the currently selected record in the table
>
>   **If** (the currently selected MLT value in table = 0) **Then**
>   ChosenCoreMLT = 5 * (ChosenCoreAreaProduct …
>   … ^ 0.25)
>   **End If**
>
>   StepsTaken = 2
>   Exit this routine
>   **End If**

Move to the next record in the table
End Do

Choose last core in table anyway by stepping back one record (since …
… after iterating through the loop we have moved on to the end of …
… the table)

Output ("There is no core with a larger A$_p$ value. Now selecting last …
… core in the group.")

StepsTaken = 2

C.2.2   Choose a Different Core

The user clicks on a new record in the table of cores currently displayed, so
as to override the record chosen automatically:

If (StepsTaken < 2) Then
    We have not chosen a core shape or type yet, so …
    … exit this routine
End If

Obtain new values for ChosenCoreWeight, ChosenCoreMLT, …
… ChosenCoreAreaProduct, ChosenCoreWindowArea, …
… ChosenCoreCrossSectionalArea, …
… ChosenCoreWindowHeight, ChosenCoreWindowWidth …
… from the currently selected record in the table

If (the currently selected MLT value in table = 0) **Then**
    ChosenCoreMLT = 5 * (ChosenCoreAreaProduct …
    … ^ 0.25)
End If

StepsTaken = 2

C.2.3   Choose a Core Type

After choosing a new core type from the list of available core groups, we need
to update the displayed core table and choose the most appropriate core from
the list (i.e. the one with an area product greater than or equal to the one
calculated):

Call (Select Appropriate Core, 2.1)

C.2.4   Choose a Core Shape

If (custom cores are not chosen) **Then**

Open the cores database for the material attributes and all …
… other core data

Clear the currently displayed list of core types

For (every core table in the database)

If (the core material in the current table matches that …
… selected in the "Enter Specifications" step, i.e. …
… CoreMaterialName) **Then**

If (core shape y is chosen, where y is either CC, …
… EE, EI, pot, toroidal or UU) **Then**

If (core shape in current table is y) **Then**
Add the current group name to the …
… list of available core types
End If

Else If (all core shapes option is chosen) **Then**
Add the current group name to the list of …
… available core types
End If

End If

Next (core table)

Else If (custom cores are chosen) **Then**

Open the custom cores database for the material attributes …
… and all other custom core data

Clear the currently displayed list of core types

For (every custom core table in the database)

If (the core shape in the current table is CC, EE, EI, …
… pot, toroidal or UU) **Then**

If (the custom core material in the current table …
… matches that selected in the "Enter …
… Specifications" step, i.e. …
… CoreMaterialName) **Then**
Add the current group name to the list of …
… available core types
End If

End If

Next (custom core table)

End If

C.3 Calculate Turns Information

NUMBER	NAME/DESCRIPTION
3.1	Calculate Turns
3.2	Use Own Turns Values
3.3	Change Reset Turns
3.4	Change Primary Turns
3.5	Change Secondary Turns

Table C.3. "Calculate Turns Information" subprocesses.

C.3.1 Calculate Turns

The core is too large if ChosenCoreWeight * Kc * (Frequency1 ^ alpha) * (MaximumFluxDensity1 ^ beta)) > 400 * ((ChosenCoreAreaProduct * 10 ^ -8) ^ 0.5) * TemperatureRise. If so, display a warning message:

> **If** (core is too large) **Then**
> > **Output** ("Please check that you have chosen a small core type …
> > … for this application. Large cores are not suitable for high f.")

Check which transformer application was chosen and calculate the appropriate values for RMSInputVoltage, PrimaryWindingTurns, OutputVoltage, and SecondaryWindingTurns:

> **If** (centre-tapped transformer) **Then**
> > RMSInputVoltage = InputVoltageLower / (2) ^ 0.5
> >
> > **If** (transformer is rectified) **Then**
> > > OutputVoltage = OutputVoltage + 1
> >
> > **End If**
> >
> > PrimaryWindingTurns = Int((RMSInputVoltage) / …
> > … (WaveformFactor * MaximumFluxDensity1 * …
> > … ChosenCoreCrossSectionalArea * 10 ^ -4 * Frequency1) …
> > … + 0.5)
> > SecondaryWindingTurns = Int((OutputVoltage / …
> > … RMSInputVoltage) * PrimaryWindingTurns + 0.5)
>
> **Else If** (forward converter) **Then**
> > RMSInputVoltage = ((DutyCycle1 / (1 - DutyCycle1)) ^ 0.5) …
> > … * InputVoltageLower
> > PrimaryWindingTurns = Int((RMSInputVoltage) / …
> > … (WaveformFactor * MaximumFluxDensity1 * …
> > … ChosenCoreCrossSectionalArea * 10 ^ -4 * Frequency1) …
> > … + 0.5)
> > SecondaryWindingTurns = Int(PrimaryWindingTurns / …
> > … TurnsRatio1 + 0.5)
> > ResetWindingTurns = Int(PrimaryWindingTurns * (1 - …
> > … DutyCycle1) / DutyCycle1 + 0.5)
>
> **Else If** (push-pull converter) **Then**
> > RMSInputVoltage = (DutyCycle1 ^ 0.5) * InputVoltageLower
> > PrimaryWindingTurns = Int((RMSInputVoltage) / …

249

```
            … (WaveformFactor * MaximumFluxDensity1 * …
            … ChosenCoreCrossSectionalArea * 10 ^ -4 * Frequency1) …
            … + 0.5)
            SecondaryWindingTurns = Int(PrimaryWindingTurns / …
            … TurnsRatio1 + 0.5)
        End If
```

Calculate TemperatureCorrectedWindingResistivity and CurrentDensity:

```
        TemperatureCorrectedWindingResistivity = WindingResistivity * (1 …
        … + alpha20 * (TemperatureRise + AmbientTemperature - 20))
        CurrentDensity = ((400 * ((ChosenCoreAreaProduct * 10 ^ -8) …
        … ^ 0.5) * TemperatureRise - (ChosenCoreWeight * Kc * …
        … (Frequency1 ^ alpha) * (MaximumFluxDensity1 ^ beta))) / …
        … (TemperatureCorrectedWindingResistivity * (ChosenCoreMLT * …
        … 10 ^ -2) * WindowUtilisationFactor * (ChosenCoreWindowArea * …
        … 10 ^ -4))) ^ 0.5
```

Display the RMSInputVoltage, PrimaryWindingTurns, SecondaryWindingTurns, ResetWindingTurns for the forward converter application, and the CurrentDensity.

```
        StepsTaken = 3
```

C.3.2   Use Own Turns Values

```
        If (use own turns values is false) Then
```

```
            Disable entry of primary, secondary and reset winding turns
```

Recalculate turns automatically, checking if the user has selected a core yet as we cannot calculate turns without knowing the core dimensions:

```
            If (StepsTaken > 1) Then
                Call (CalculateTurns, 3.1)
            End If
```

```
        Else If (use own turns values is true) Then
```

In this part, turns values will not be calculated until any of the primary, secondary or reset turns values are modified:

```
            Enable entry of primary, secondary and reset winding turns
```

```
        End If
```

C.3.3   Change Reset Turns

```
        If (reset winding turns entry is disabled) Then
            Ignore any keys pressed
        Else
            Ensure that the value entered is a valid number
        End If
```

Set the ResetWindingTurns variable to the numeric value entered

C.3.4   Change Primary Turns

If (primary winding turns entry is disabled) **Then**
        Ignore any keys pressed
Else
        Ensure that the value entered is a valid number
End If

Set the PrimaryWindingTurns variable to the numeric value entered

C.3.5   Change Secondary Turns

If (secondary winding turns entry is disabled) **Then**
        Ignore any keys pressed
Else
        Ensure that the value entered is a valid number
End If

Set the SecondaryWindingTurns variable to the numeric value entered

C.4   Choose Winding Data

NUMBER	NAME/DESCRIPTION
4.1	Calculate Winding Sizes
4.2	Choose a Winding Shape
4.3	Select Primary Winding
4.4	Select Secondary Winding
4.5	Calculate Primary Optimum Thickness
4.6	Calculate Secondary Optimum Thickness
4.7	Choose a Different Primary Winding
4.8	Choose a Different Secondary Winding
4.9	Choose a Winding Type

Table C.4. "Choose Winding Data" subprocesses.

C.4.1 Calculate Winding Sizes

Check the transformer type and calculate the appropriate PrimaryCurrent and SecondaryCurrent:

> **If** (centre-tapped transformer) **Then**
> > PrimaryCurrent = OutputPower / ((Efficiency1 / 100) * …
> > … PrimaryPowerFactor * RMSInputVoltage)
> > **If** (transformer is rectified) **Then**
> > > SecondaryCurrent = OutputCurrent / (2 ^ 0.5)
> > **Else**
> > > SecondaryCurrent = OutputCurrent
> > **End If**
> **Else If** (forward converter) **Then**
> > PrimaryCurrent = OutputPower / ((Efficiency1 / 100) * …
> > … PrimaryPowerFactor * RMSInputVoltage)
> > SecondaryCurrent = ((DutyCycle1) ^ 0.5) * OutputCurrent
> **Else If** (push-pull converter) **Then**
> > PrimaryCurrent = (OutputPower / 2) / ((Efficiency1 / 100) …
> > … * PrimaryPowerFactor * RMSInputVoltage)
> > SecondaryCurrent = (OutputCurrent / 2) * (1 + DutyCycle1) …
> > … ^ 0.5
> **End If**

Calculate PrimaryWindingArea, CalculatedPrimaryWindingDiameter, SecondaryWindingArea, CalculatedSecondaryWindingDiameter:

> PrimaryWindingArea = PrimaryCurrent / (CurrentDensity * 10 ^ 6)
> CalculatedPrimaryWindingDiameter = 2 * (PrimaryWindingArea …
> … / PI) ^ 0.5
> SecondaryWindingArea = SecondaryCurrent / (CurrentDensity …
> … * 10 ^ 6)
> CalculatedSecondaryWindingDiameter = 2 * (SecondaryWindingArea …
> … / PI) ^ 0.5

Display the PrimaryCurrent, PrimaryWindingArea, CalculatedPrimaryWindingDiameter, PrimaryWindingThickness (multiply the diameter by 0.886), SecondaryCurrent, SecondaryWindingArea, CalculatedSecondaryWindingDiameter, and SecondaryWindingThickness.

Call the functions to choose actual winding sizes:

> **Call** (Select Primary Winding, 4.3)
> **Call** (Select Secondary Winding, 4.4)

and refresh the displayed tables of primary and secondary winding data.

> StepsTaken = 4

C.4.2 Choose a Winding Shape

> **If** (custom windings are not chosen) **Then**
>
> > Open the windings database for the material attributes and …
> > … all other winding data

Clear the currently displayed list of winding types

For (every winding table in the database)

    If (the winding material in the current table matches …
    … that selected in the "Enter Specifications" step, i.e. …
    … WindingMaterialName) **Then**

        If (round winding shape is chosen) **Then**

            If (shape in current table is round) **Then**
                Add the current group name to the …
                … list of available winding types
            End If

        Else If (layered winding shape is chosen) **Then**

            If (shape in current table is layered) **Then**
                Add the current group name to the …
                … list of available winding types
            End If

        Else If (all winding shapes option is chosen) **Then**
            Add the current group name to the list of …
            … available winding types
        End If

    End If

Next (winding table)

Else If (custom windings are chosen) **Then**

    Open the custom windings database for the material attributes …
    … and all other custom winding data

    Clear the currently displayed list of winding types

    For (every custom winding table in the database)

        If (the winding shape in the current table is round or …
        … layered) **Then**

            If (the custom winding material in the current …
            … table matches that selected in the "Enter …
            … Specifications" step, i.e. …
            … WindingMaterialName) **Then**
                Add the current group name to the list of …
                … available winding types
            End If

        End If

    Next (custom winding table)

End If

C.4.3   Select Primary Winding

For the primary winding, open the data table corresponding to the …
… name currently selected in the available winding types list

Do While (we have not reached the end of the primary winding table)
    If (CalculatedPrimaryWindingDiameter >= the bare diameter …
    … value in the current record) **Then**
        Exit this do loop the next time around
    End If
    Move to the next record in the current table
End Do

Move to the previous record

Set the ChosenPrimaryWindingDiameter value equal to the bare …
… diameter field in the current record, and the set the …
… ChosenPrimaryWindingResistivity value to the resistance at …
… 20 °C field

C.4.4   Select Secondary Winding

For the secondary winding, open the data table corresponding to the …
… name currently selected in the available winding types list

Do While (we have not reached end of the secondary winding table)
    If (CalculatedSecondaryWindingDiameter >= the bare …
    … diameter value in the current record) **Then**
        Exit this do loop the next time around
    End If
    Move to the next record in the current table
End Do

Move to the previous record

Set the ChosenSecondaryWindingDiameter value equal to the bare …
… diameter field in the current record, and the set the …
… ChosenSecondaryWindingResistivity value to the resistance at …
… 20 °C field

C.4.5   Calculate Primary Optimum Thickness

If (no value has been calculated for primary winding thickness) **Then**
    Exit this subroutine
End If

Select the primary winding option in the winding details specification …
… area of the "Calculate Optimum Thickness" step

Call (Calculate Proximity Effects, 8.1)

Set the primary optimum thickness to the OptimumThickness …
… value returned by the called function, and display this value

C.4.6   Calculate Secondary Optimum Thickness

If (no value was calculated for the secondary winding thickness) **Then**
        Exit this subroutine
End If

Select secondary winding option in the winding details specification …
… area of the "Calculate Optimum Thickness" step

Call (Calculate Proximity Effects, 8.1)

Set the secondary optimum thickness to the OptimumThickness …
… value returned by the called function, and display this value

C.4.7   Choose a Different Primary Winding

If (StepsTaken < 4) Then
        We have not chosen a winding shape or type yet, so …
        … exit this routine
End If

Obtain new values for ChosenPrimaryWindingDiameter (the bare …
… diameter in mm) and ChosenPrimaryWindingResistivity (the …
… resistance at 20 °C in mohm/m) from the current table record

C.4.8   Choose a Different Secondary Winding

If (StepsTaken < 4) Then
        We have not chosen a winding shape or type yet, so …
        … exit this routine
End If

Obtain new values for ChosenSecondaryWindingDiameter (the bare …
… diameter in mm) and ChosenSecondaryWindingResistivity (the …
… resistance at 20 °C in mohm/m) from the current table record

C.4.9   Choose a Winding Type

After selecting a new winding group from the list of available types, we need
to recalculate winding sizes using the new group as our source of available
windings:

Call (Calculate Winding Sizes, 4.1)

C.5 Calculate Winding Losses

NUMBER	NAME/DESCRIPTION
5.1	Calculate Winding Losses
5.2	Calculate Skin Effects
5.3	Calculate Proximity Effects (8.1)
5.4	Choose Winding Loss Type

Table C.5. "Calculate Winding Losses" subprocesses.

C.5.1 Calculate Winding Losses

Calculate the skin effect and proximity effect losses:

> **Call** (Calculate Skin Effects, 5.2)
> **Call** (Calculate Proximity Effects, 8.1) for the primary winding
> **Call** (Calculate Proximity Effects, 8.1) for the secondary winding

Display SkinEffect1, Frequency2, PrimarySkinEffectFactor, SecondarySkinEffectFactor, PrimaryRadius, SecondaryRadius, PrimaryProximityEffectFactor, SecondaryProximityEffectFactor.

Calculate PrimaryWindingResistance and SecondaryWindingResistance:

> **If** (dc losses only) **Then**
>   PrimaryWindingResistance = ChosenCoreMLT * (10 ^ (-2)) * …
>   … PrimaryWindingTurns * (10 ^ -3) * …
>   … (ChosenPrimaryWindingResistivity) * (1 + 0.00393 * …
>   … (AmbientTemperature + TemperatureRise - 20))
>   SecondaryWindingResistance = ChosenCoreMLT * (10 ^ (-2)) …
>   … * SecondaryWindingTurns * (10 ^ -3) * …
>   … (ChosenSecondaryWindingResistivity) * (1 + 0.00393 * …
>   … (AmbientTemperature + TemperatureRise - 20))
> **Else If** (skin effect losses only) **Then**
>   PrimaryWindingResistance = ChosenCoreMLT * (10 ^ (-2)) * …
>   … PrimaryWindingTurns * (10 ^ -3) * …
>   … (ChosenPrimaryWindingResistivity) * (1 + 0.00393 * …
>   … (AmbientTemperature + TemperatureRise - 20)) * …
>   … (PrimarySkinEffectFactor - 1)
>   SecondaryWindingResistance = ChosenCoreMLT * (10 ^ (-2)) …
>   … * SecondaryWindingTurns * (10 ^ -3) * …
>   … (ChosenSecondaryWindingResistivity) * (1 + 0.00393 * …
>   … (AmbientTemperature + TemperatureRise - 20)) * …
>   … (SecondarySkinEffectFactor - 1)
> **Else If** (proximity effect losses only) **Then**
>   PrimaryWindingResistance = ChosenCoreMLT * (10 ^ (-2)) * …
>   … PrimaryWindingTurns * (10 ^ -3) * …
>   … (ChosenPrimaryWindingResistivity) * (1 + 0.00393 * …
>   … (AmbientTemperature + TemperatureRise - 20)) * …

256

… (PrimaryProximityEffectFactor - 1)
                    SecondaryWindingResistance = ChosenCoreMLT * (10 ^ (-2)) …
                    … * SecondaryWindingTurns * (10 ^ -3) * …
                    … (ChosenSecondaryWindingResistivity) * (1 + 0.00393 * …
                    … (AmbientTemperature + TemperatureRise - 20)) * …
                    … (SecondaryProximityEffectFactor - 1)
          Else If (dc losses plus skin effect and proximity effect losses) **Then**
                    PrimaryWindingResistance = ChosenCoreMLT * (10 ^ (-2)) * …
                    … PrimaryWindingTurns * (10 ^ -3) * …
                    … (ChosenPrimaryWindingResistivity) * (1 + 0.00393 * …
                    … (AmbientTemperature + TemperatureRise - 20)) * …
                    … PrimarySkinEffectFactor * PrimaryProximityEffectFactor
                    SecondaryWindingResistance = ChosenCoreMLT * (10 ^ (-2)) …
                    … * SecondaryWindingTurns * (10 ^ -3) …
                    … *(ChosenSecondaryWindingResistivity) * (1 + 0.00393 * …
                    … (AmbientTemperature + TemperatureRise - 20)) * …
                    … SecondarySkinEffectFactor * SecondaryProximityEffectFactor
          End If

Calculate PrimaryWindingLosses, SecondaryWindingLosses,
TotalWindingLosses1:

          PrimaryWindingLosses = (PrimaryCurrent ^ 2) * …
          … PrimaryWindingResistance
          SecondaryWindingLosses = (SecondaryCurrent ^ 2) * …
          … SecondaryWindingResistance
          TotalWindingLosses1 = PrimaryWindingLosses + …
          … SecondaryWindingLosses

Display the PrimaryWindingResistance, SecondaryWindingResistance,
PrimaryWindingLosses, SecondaryWindingLosses, TotalWindingLosses1.

C.5.2   Calculate Skin Effects

Calculate SkinDepth1 (in mm):

          SkinDepth1 = (10 ^ 3) / (PI * Frequency1 * (4 * PI * (10 ^ -7)) …
          … / WindingResistivity) ^ 0.5

Set the PrimarySkinEffectFactor and SecondarySkinEffectFactor to double real
numbers, with initial value 1.

Calculate PrimarySkinEffectFactor:

          If (SkinDepth1 < (ChosenPrimaryWindingDiameter / 2)) **Then**
                    If (((ChosenPrimaryWindingDiameter / 2) / SkinDepth1) …
                    … < 1.7) **Then**
                              PrimarySkinEffectFactor = (1 + …
                              … (((ChosenPrimaryWindingDiameter / 2) / SkinDepth1) …
                              … ^ 4) / (48 + 0.8 * ((ChosenPrimaryWindingDiameter …
                              … / 2) / SkinDepth1) ^ 4))
                    Else
                              PrimarySkinEffectFactor = 0.25 + 0.5 * …
                              … ((ChosenPrimaryWindingDiameter / 2) / SkinDepth1) …
                              … + (3 / 32) * (SkinDepth1 / …
                              … (ChosenPrimaryWindingDiameter / 2))
                    End If
          End If

Calculate SecondarySkinEffectFactor:

```
    If (SkinDepth1 < (ChosenSecondaryWindingDiameter / 2)) Then
        If (((ChosenSecondaryWindingDiameter / 2) / …
        … SkinDepth1) < 1.7) Then
            SecondarySkinEffectFactor = (1 + …
            … (((ChosenSecondaryWindingDiameter / 2) / …
            … SkinDepth1) ^ 4) / (48 + 0.8 * …
            … ((ChosenSecondaryWindingDiameter / 2) / …
            … SkinDepth1) ^ 4))
        Else
            SecondarySkinEffectFactor = 0.25 + 0.5 * …
            … ((ChosenSecondaryWindingDiameter / 2) / …
            … SkinDepth1) + (3 / 32) * (SkinDepth1 / …
            … (ChosenSecondaryWindingDiameter / 2))
        End If
    End If
```

C.5.3   Calculate Proximity Effects

Call (Calculate Proximity Effects, 8.1)

C.5.4   Choose Winding Loss Type

If we change the desired winding loss type, for example from just DC to combined AC and DC losses, we need to recalculate the winding losses while informing the routine to calculate these losses of the new loss type. The available loss types are DC, AC proximity effect, AC skin effect, and all AC and DC losses:

Call (Calculate Winding Losses, 5.1)

C.6   Calculate Core Losses

NUMBER	NAME/DESCRIPTION
6.1	Calculate Core Losses

Table C.6. "Calculate Core Losses" subprocesses.

C.6.1   Calculate Core Losses

Calculate the core losses from the following equation:

CoreLosses = Kc * (Frequency1 ^ alpha) * …

```
    … (MaximumFluxDensity1 ^ beta)
      TotalCoreLosses1 = CoreLosses * ChosenCoreWeight
```

Display the following: Frequency3 (same as Frequency1 but for this step), MaximumFluxDensity3 (same again), CoreWeight, CoreLosses, TotalCoreLosses1, and the material constants Kc, alpha and beta.

C.7   Calculate Total Losses

NUMBER	NAME/DESCRIPTION
7.1	Calculate Total Losses

Table C.7. "Calculate Total Losses" subprocesses.

C.7.1   Calculate Total Losses

Calculate the total losses and efficiency:

```
      TotalLosses = TotalWindingLosses1 + TotalCoreLosses1
      Efficiency2 = OutputPower / (OutputPower + TotalLosses) * 100
```

Display Efficiency2, TotalWindingLosses2 (the same as TotalWindingLosses1), TotalCoreLosses2 (same again) and TotalLosses.

C.8   Calculate Optimum Winding Thickness

NUMBER	NAME/DESCRIPTION
8.1	Calculate Proximity Effects
8.2	Choose and Draw Waveshape
8.3	Choose to Use Own Thickness Value
8.4	Choose Primary or Secondary Winding
8.5	Rough Duty Cycle Change
8.6	Exact Duty Cycle Change
8.7	Change Frequency
8.8	Change Number of Layers
8.9	Change Normalised Thickness
8.10	Change Rise Time

Table C.8. "Calculate Optimum Winding Thickness" subprocesses.

C.8.1   Calculate Proximity Effects

If a frequency value (Frequency4) is not explicitly defined in this step, use the value Frequency1 from the "Specifications" step.

If a rise time is not specified, use an initial value of RiseTime = 5.

Calculate the total number of harmonics, and force this number to be odd:

    TotalNumberHarmonics = Int(35 / RiseTime)

    If (TotalNumberHarmonics Mod 2 = 0) **Then**
            TotalNumberHarmonics = TotalNumberHarmonics – 1
    End If

Also, if the number of layers (NumberLayers) is not specified, calculate it from the core and winding details of previous steps as follows:

    WindingHeight = ChosenCoreWindowHeight * Val(txtBobbinHeight) …
    … / 100
    NumberPrimaryLayers = Int((PrimaryWindingTurns / …
    … (Int(WindingHeight / CalculatedPrimaryWindingDiameter))) + 1)
    NumberSecondaryLayers = Int((SecondaryWindingTurns / …
    … (Int(WindingHeight / CalculatedSecondaryWindingDiameter))) + 1)
    If (primary winding) **Then**
            NumberLayers = NumberPrimaryLayers
    Else If (secondary winding) Then
            NumberLayers = NumberSecondaryLayers
    End If

If the duty cycle (DutyCycle2) is not specified by the user, take it to be equal to DutyCycle1 calculated in the "Specifications" step. The duty cycle slider is moved to a position corresponding to the value of DutyCycle2. If a sine waveshape is chosen by the user, the DutyCycle2 value is not set and the text "(none)" is displayed.

Calculate the skin depth:

    SkinDepth2 = (10 ^ 3) / (PI * Frequency4 * (4 * PI * (10 ^ -7)) / …
    … WindingResistivity) ^ 0.5

TopSummation = 0
BottomSummation = 0
FullSummation = 0

Calculate the normalised thickness and effective resistance for the chosen waveshape (note that NormalisedThickness is calculated using the regression analysis method, and NormalisedThickness2 using the RMS values method):

    If (sine wave) **Then**

            NormalisedThickness = (1 / ((2 / b) * NumberLayers ^ 2 + …
            … 3 / a - 2 / b)) ^ 0.25
            *NormalisedThickness2 = (1 / ((5 * (NumberLayers ^ 2) - 1) …
            … / 15)) ^ 0.25*

            If (using own thickness) **Then**
                    NormalisedThickness = OptimumThickness (as specified …

   … by the user in mm) / SkinDepth2
  End If

  ReffRdelta = ((Sinh(2 * NormalisedThickness) + Sine(2 * …
  … NormalisedThickness)) / (Cosh(2 * NormalisedThickness) - …
  … Cosine(2 * NormalisedThickness)) + (2 * ((NumberLayers) …
  … ^ 2 - 1) / 3) * (Sinh(NormalisedThickness) - …
  … Sine(NormalisedThickness)) / (Cosh(NormalisedThickness) …
  … + Cosine(NormalisedThickness)))

Else If (rectified sine wave) **Then**

  If (1 / (2 * DutyCycle2) Mod 1 = 0) **Then**
   DutyCycle2 = DutyCycle2 + 0.00001
  End If

  For (CurrentHarmonic = 1 To TotalNumberHarmonics)
   TopSummation = TopSummation + 2 * …
   … ((Cosine(CurrentHarmonic * PI * DutyCycle2)) ^ 2) …
   … / (1 - 4 * (CurrentHarmonic ^ 2) * …
   … (DutyCycle2 ^ 2)) ^ 2
   BottomSummation = BottomSummation + 2 * …
   … (CurrentHarmonic ^ 2) * ((Cosine(CurrentHarmonic * …
   … PI * DutyCycle2)) ^ 2) / (1 - 4 * (CurrentHarmonic …
   … ^ 2) * (DutyCycle2 ^ 2)) ^ 2
  Next (CurrentHarmonic)

  NormalisedThickness = ((1 + TopSummation) / …
  … (BottomSummation * ((2 / b) * …
  … NumberLayers ^ 2 + 3 / a - 2 / b))) ^ 0.25
  *NormalisedThickness2 = ((4 * (DutyCycle2 ^ 2)) / …*
  *… ((5 * (NumberLayers ^ 2) - 1) / 15)) ^ 0.25*

  If (using own thickness) **Then**
   NormalisedThickness = OptimumThickness (as specified …
   … by the user in mm) / SkinDepth2
  End If

  For (CurrentHarmonic = 1 To TotalNumberHarmonics)
   FullSummation = FullSummation + …
   … (((Cosine(CurrentHarmonic * PI * DutyCycle2)) ^ 2) …
   … / ((1 - 4 * (CurrentHarmonic ^ 2) * (DutyCycle2 …
   … ^ 2)) …^ 2)) * (CurrentHarmonic ^ 0.5) * …
   … NormalisedThickness * ((Sinh(2 * (CurrentHarmonic …
   … ^ 0.5) * NormalisedThickness) + Sine(2 * …
   … (CurrentHarmonic ^ 0.5) * NormalisedThickness)) / …
   … (Cosh(2 * (CurrentHarmonic ^ 0.5) * …
   … NormalisedThickness) - Cosine(2 * (CurrentHarmonic …
   … ^ 0.5) * NormalisedThickness)) + (2 * …
   … ((NumberLayers) ^ 2 - 1) / 3) * …
   … (Sinh((CurrentHarmonic ^ 0.5) * …
   … NormalisedThickness) - Sine((CurrentHarmonic …
   … ^ 0.5) * NormalisedThickness)) / …
   … (Cosh((CurrentHarmonic ^ 0.5) * …
   … NormalisedThickness) + Cosine((CurrentHarmonic …
   … ^ 0.5) * NormalisedThickness)))
  Next (CurrentHarmonic)

  ReffRdelta = ((8 * DutyCycle2) / ((PI ^ 2) * …
  … NormalisedThickness)) + ((16 * DutyCycle2) / ((PI ^ 2) …
  … * NormalisedThickness)) * FullSummation

Else If (bipolar sine wave) **Then**

```
If (1 / DutyCycle2 Mod 1 = 0) Then
      DutyCycle2 = DutyCycle2 + 0.00001
End If

For (CurrentHarmonic = 1 To TotalNumberHarmonics Step 2)
      TopSummation = TopSummation + …
      … ((Cosine(CurrentHarmonic * PI * DutyCycle2 / 2)) …
      … ^ 2) / (1 - (CurrentHarmonic ^ 2) * (DutyCycle2 …
      … ^ 2)) ^ 2
      BottomSummation = BottomSummation + …
      … (CurrentHarmonic ^ 2) * ((Cosine(CurrentHarmonic …
      … * PI * DutyCycle2 / 2)) ^ 2) / (1 - (CurrentHarmonic …
      … ^ 2) * (DutyCycle2 ^ 2)) ^ 2
Next (CurrentHarmonic)

NormalisedThickness = ((TopSummation) / (BottomSummation …
… * ((2 / b) * NumberLayers ^ 2 + 3 / a - 2 / b))) ^ 0.25
NormalisedThickness2 = ((DutyCycle2 ^ 2) / ((5 * …
… (NumberLayers ^ 2) - 1) / 15)) ^ 0.25

If (using own thickness) Then
      NormalisedThickness = OptimumThickness (as specified …
      … by the user in mm) / SkinDepth2
End If

For (CurrentHarmonic = 1 To TotalNumberHarmonics Step 2)
      FullSummation = FullSummation + …
      … (((Cosine(CurrentHarmonic * PI * DutyCycle2 / 2)) …
      … ^ 2) / ((1 - (CurrentHarmonic ^ 2) * (DutyCycle2 ^ …
      … 2)) ^ 2)) * (CurrentHarmonic ^ 0.5) * …
      … NormalisedThickness * ((Sinh(2 * (CurrentHarmonic …
      … ^ 0.5) * NormalisedThickness) + Sine(2 * …
      … (CurrentHarmonic ^ 0.5) * NormalisedThickness)) / …
      … (Cosh(2 * (CurrentHarmonic ^ 0.5) * …
      … NormalisedThickness) - Cosine(2 * (CurrentHarmonic …
      … ^ 0.5) * NormalisedThickness)) + (2 * …
      … ((NumberLayers) ^ 2 - 1) / 3) * …
      … (Sinh((CurrentHarmonic ^ 0.5) * …
      … NormalisedThickness) - Sine((CurrentHarmonic …
      … ^ 0.5) * NormalisedThickness)) / …
      … (Cosh((CurrentHarmonic ^ 0.5) * …
      … NormalisedThickness) +Cosine((CurrentHarmonic …
      … ^ 0.5) * NormalisedThickness)))
Next (CurrentHarmonic)

ReffRdelta = ((16 * DutyCycle2) / ((PI ^ 2) * …
… NormalisedThickness)) * FullSummation

Else If (square wave) Then

For (CurrentHarmonic = 1 To TotalNumberHarmonics)
      TopSummation = TopSummation + …
      … ((Sine(CurrentHarmonic * PI * DutyCycle2)) ^ 2) / …
      … (CurrentHarmonic ^ 2)
      BottomSummation = BottomSummation + …
      … (Sine(CurrentHarmonic * PI * DutyCycle2)) ^ 2
Next (CurrentHarmonic)

NormalisedThickness = (((2 * DutyCycle2 - 1) ^ 2 + (8 / PI ^ …
… 2) * TopSummation) / ((8 / PI ^ 2) * BottomSummation * …
… ((2 / b) * NumberLayers ^ 2 + 3 / a - 2 / b))) ^ 0.25
NormalisedThickness2 = (((1 - (8 * RiseTime) / (3 * 100)) * …
```

… (PI ^ 2) * ((RiseTime) / (100))) / ((5 * (NumberLayers …
… ^ 2) - 1) / 15)) ^ 0.25

If (using own thickness) **Then**
      NormalisedThickness = OptimumThickness (as specified …
      … by the user in mm) / SkinDepth2
End If

For (CurrentHarmonic = 1 To TotalNumberHarmonics)
      FullSummation = FullSummation + …
      … (((Sine(CurrentHarmonic * PI * DutyCycle2)) ^ 2) / …
      … (CurrentHarmonic ^ 1.5)) * ((Sinh(2 * …
      … (CurrentHarmonic ^ 0.5) * NormalisedThickness) + …
      … Sine(2 * (CurrentHarmonic ^ 0.5) * …
      … NormalisedThickness)) / (Cosh(2 * (CurrentHarmonic …
      … ^ 0.5) * NormalisedThickness) - Cosine(2 * …
      … (CurrentHarmonic ^ 0.5) * NormalisedThickness)) + …
      … (2 * ((NumberLayers) ^ 2 - 1) / 3) * …
      … (Sinh((CurrentHarmonic ^ 0.5) * …
      … NormalisedThickness) - Sine((CurrentHarmonic ^ …
      … 0.5) * NormalisedThickness)) / …
      … (Cosh((CurrentHarmonic ^ 0.5) * …
      … NormalisedThickness) + Cosine((CurrentHarmonic …
      … ^ 0.5) * NormalisedThickness)))
Next (CurrentHarmonic)

ReffRdelta = ((2 * DutyCycle2 - 1) ^ 2) / …
… NormalisedThickness + ((8 / PI ^ 2) * FullSummation)

Else If (rectified square wave) **Then**

For (CurrentHarmonic = 1 To TotalNumberHarmonics)
      TopSummation = TopSummation + …
      … ((Sine(CurrentHarmonic * PI * DutyCycle2)) ^ 2) / …
      … (CurrentHarmonic ^ 2)
      BottomSummation = BottomSummation + …
      … (Sine(CurrentHarmonic * PI * DutyCycle2)) ^ 2
Next (CurrentHarmonic)

NormalisedThickness = ((DutyCycle2 + (2 / ((PI ^ 2) * …
… DutyCycle2)) * TopSummation) / ((2 / ((PI ^ 2) * …
… DutyCycle2)) * BottomSummation * ((2 / b) * …
… NumberLayers ^ 2 + 3 / a - 2 / b))) ^ 0.25
NormalisedThickness2 = (((DutyCycle2 - (4 * RiseTime) / (3 * …
… 100)) * 2 * (PI ^ 2) * ((RiseTime) / (100))) / ((5 * …
… (NumberLayers ^ 2) - 1) / 15)) ^ 0.25

If (using own thickness) **Then**
      NormalisedThickness = OptimumThickness (as specified …
      … by the user in mm) / SkinDepth2
End If

For (CurrentHarmonic = 1 To TotalNumberHarmonics)
      FullSummation = FullSummation + …
      … (((Sine(CurrentHarmonic * PI * DutyCycle2)) ^ 2) / …
      … (CurrentHarmonic ^ 1.5)) * ((Sinh(2 * …
      … (CurrentHarmonic ^ 0.5) * NormalisedThickness) + …
      … Sine(2 * (CurrentHarmonic ^ 0.5) * …
      … NormalisedThickness)) / (Cosh(2 * (CurrentHarmonic …
      … ^ 0.5) * NormalisedThickness) - Cosine(2 * …
      … (CurrentHarmonic ^ 0.5) * NormalisedThickness)) + …
      … (2 * ((NumberLayers) ^ 2 - 1) / 3) * …
      … (Sinh((CurrentHarmonic ^ 0.5) * …

… NormalisedThickness) - Sine((CurrentHarmonic ^ …
… 0.5) * NormalisedThickness)) / …
… (Cosh((CurrentHarmonic ^ 0.5) * …
… NormalisedThickness) + Cosine((CurrentHarmonic ^ …
… 0.5) * NormalisedThickness)))
   Next (CurrentHarmonic)

   ReffRdelta = (DutyCycle2) / NormalisedThickness + ((2 / ((PI …
   … ^ 2) * DutyCycle2)) * FullSummation)

Else If (bipolar square wave) **Then**

   For (CurrentHarmonic = 1 To TotalNumberHarmonics Step 2)
      TopSummation = TopSummation + …
      … ((Sine(CurrentHarmonic * PI * DutyCycle2 / 2)) ^ 2) …
      … / (CurrentHarmonic ^ 2)
      BottomSummation = BottomSummation + …
      … (Sine(CurrentHarmonic * PI * DutyCycle2 / 2)) ^ 2
   Next (CurrentHarmonic)

   NormalisedThickness = ((TopSummation) / (BottomSummation …
   … * ((2 / b) * NumberLayers ^ 2 + 3 / a - 2 / b))) ^ 0.25
   *NormalisedThickness2 = (((DutyCycle2 - (8 * RiseTime) / (3 * …*
   *… 100)) * (PI ^ 2) * ((RiseTime) / (100))) / ((5 * …*
   … (NumberLayers ^ 2) - 1) / 15)) ^ 0.25

   If (using own thickness) **Then**
      NormalisedThickness = OptimumThickness (as specified …
      … by the user in mm) / SkinDepth2
   End If

   For (CurrentHarmonic = 1 To TotalNumberHarmonics Step 2)
      FullSummation = FullSummation + …
      … (((Sine(CurrentHarmonic * PI * DutyCycle2 / 2)) …
      … ^ 2) / (CurrentHarmonic ^ 1.5)) * ((Sinh(2 * …
      … (CurrentHarmonic ^ 0.5) * NormalisedThickness) + …
      … Sine(2 * (CurrentHarmonic ^ 0.5) * …
      … NormalisedThickness)) / (Cosh(2 * (CurrentHarmonic …
      … ^ 0.5) * NormalisedThickness) - Cosine(2 * …
      … (CurrentHarmonic ^ 0.5) * NormalisedThickness)) + …
      … (2 * ((NumberLayers) ^ 2 - 1) / 3) * …
      … (Sinh((CurrentHarmonic ^ 0.5) * …
      … NormalisedThickness) - Sine((CurrentHarmonic ^ …
      … 0.5) * NormalisedThickness)) / …
      … (Cosh((CurrentHarmonic ^ 0.5) * …
      … NormalisedThickness) + Cosine((CurrentHarmonic ^ …
      … 0.5) * NormalisedThickness)))
   Next (CurrentHarmonic)

   ReffRdelta = ((8 / ((PI ^ 2) * DutyCycle2)) * FullSummation)

Else If (triangle wave) **Then**

   For (CurrentHarmonic = 1 To TotalNumberHarmonics Step 2)
      TopSummation = TopSummation + 1 / …
      … CurrentHarmonic ^ 4
      BottomSummation = BottomSummation + 1 / …
      … CurrentHarmonic ^ 2
   Next (CurrentHarmonic)

   NormalisedThickness = (((96 / (PI ^ 4)) * TopSummation) / …
   … ((96 / (PI ^ 4)) * BottomSummation * ((2 / b) * …
   … NumberLayers ^ 2 + 3 / a - 2 / b))) ^ 0.25

*NormalisedThickness2 = (((PI ^ 2) * DutyCycle2 * (1 - …*
*… DutyCycle2) * (1 / 3)) / ((5 * (NumberLayers ^ 2) - 1) / …*
… 15)) ^ 0.25

If (using own thickness) **Then**
  NormalisedThickness = OptimumThickness (as specified …
  … by the user in mm) / SkinDepth2
End If

For (CurrentHarmonic = 1 To TotalNumberHarmonics Step 2)
  FullSummation = FullSummation + (1 / …
  … (CurrentHarmonic ^ 4)) * (CurrentHarmonic ^ 0.5) …
  … * ((Sinh(2 * (CurrentHarmonic ^ 0.5) * …
  … NormalisedThickness) + Sine(2 * (CurrentHarmonic …
  … ^ 0.5) * NormalisedThickness)) / (Cosh(2 * …
  … (CurrentHarmonic ^ 0.5) * NormalisedThickness) - …
  … Cosine(2 * (CurrentHarmonic ^ 0.5) * …
  … NormalisedThickness)) + (2 * ((NumberLayers) ^ 2 - …
  … 1) / 3) * (Sinh((CurrentHarmonic ^ 0.5) * …
  … NormalisedThickness) - Sine((CurrentHarmonic ^ …
  … 0.5) * NormalisedThickness)) / …
  … (Cosh((CurrentHarmonic ^ 0.5) * …
  … NormalisedThickness) + Cosine((CurrentHarmonic ^ …
  … 0.5) * NormalisedThickness)))
Next (CurrentHarmonic)

ReffRdelta = (96 / (PI ^ 4)) * FullSummation

Else If (rectified triangle wave) **Then**

For (CurrentHarmonic = 1 To TotalNumberHarmonics)
  TopSummation = TopSummation + …
  … ((Sine(CurrentHarmonic * PI * DutyCycle2 / 2)) ^ 4) …
  … / (CurrentHarmonic ^ 4)
  BottomSummation = BottomSummation + …
  … ((Sine(CurrentHarmonic * PI * DutyCycle2 / 2)) ^ 4) …
  … / (CurrentHarmonic ^ 2)
Next (CurrentHarmonic)

NormalisedThickness = ((1 + (32 / ((PI ^ 4) * (DutyCycle2 ^ …
… 4))) * TopSummation) / ((32 / ((PI ^ 4) * …
… (DutyCycle2 ^ 4))) * BottomSummation * ((2 / b) * …
… NumberLayers ^ 2 + 3 / a - 2 / b))) ^ 0.25
*NormalisedThickness2 = (((PI ^ 2) * (DutyCycle2 ^ 2) * (1 / …*
*… 3)) / ((5 * (NumberLayers ^ 2) - 1) / 15)) ^ 0.25*

If (using own thickness) **Then**
  NormalisedThickness = OptimumThickness (as specified …
  … by the user in mm) / SkinDepth2
End If

For (CurrentHarmonic = 1 To TotalNumberHarmonics)
  FullSummation = FullSummation + …
  … (((Sine(CurrentHarmonic * PI * DutyCycle2 / 2)) ^ …
  … 4) / (CurrentHarmonic ^ 4)) * (CurrentHarmonic ^ …
  … 0.5) * NormalisedThickness * ((Sinh(2 * …
  … (CurrentHarmonic ^ 0.5) * NormalisedThickness) + …
  … Sine(2 * (CurrentHarmonic ^ 0.5) * …
  … NormalisedThickness)) / (Cosh(2 * (CurrentHarmonic …
  … ^ 0.5) * NormalisedThickness) - Cosine(2 * …
  … (CurrentHarmonic ^ 0.5) * NormalisedThickness)) + …
  … (2 * ((NumberLayers) ^ 2 - 1) / 3) * …
  … (Sinh((CurrentHarmonic ^ 0.5) * …

… NormalisedThickness) - Sine((CurrentHarmonic ^ …
… 0.5) * NormalisedThickness)) / …
… (Cosh((CurrentHarmonic ^ 0.5) * …
… NormalisedThickness) + Cosine((CurrentHarmonic …
… ^ 0.5) * NormalisedThickness)))
        Next (CurrentHarmonic)

    ReffRdelta = ((3 * DutyCycle2) / (4 * NormalisedThickness)) …
    … + (24 / (NormalisedThickness * (PI ^ 4) * (DutyCycle2 ^ …
    … 3))) * FullSummation

Else If (bipolar triangle wave) **Then**

    For (CurrentHarmonic = 1 To TotalNumberHarmonics Step 2)
        TopSummation = TopSummation + ((1 - …
        … Cosine(CurrentHarmonic * PI * DutyCycle2 / 2)) ^ 2) …
        … / (CurrentHarmonic ^ 4)
        BottomSummation = BottomSummation + ((1 - …
        … Cosine(CurrentHarmonic * PI * DutyCycle2 / 2)) ^ 2) …
        … / (CurrentHarmonic ^ 2)
    Next (CurrentHarmonic)

    NormalisedThickness = ((TopSummation) / (BottomSummation …
    … * ((2 / b) * NumberLayers ^ 2 + 3 / a - 2 / b))) ^ 0.25
    *NormalisedThickness2 = (((PI ^ 2) * (DutyCycle2 ^ 2) * (1 / …*
    *… 12)) / ((5 * (NumberLayers ^ 2) - 1) / 15)) ^ 0.25*

    If (using own thickness) **Then**
        NormalisedThickness = OptimumThickness (as specified …
        … by the user in mm) / SkinDepth2
    End If

    For (CurrentHarmonic = 1 To TotalNumberHarmonics Step 2)
        FullSummation = FullSummation + (((1 - …
        … Cosine(CurrentHarmonic * PI * DutyCycle2 / 2)) ^ 2) …
        … / (CurrentHarmonic ^ 4)) * (CurrentHarmonic ^ 0.5) …
        … * NormalisedThickness * ((Sinh(2 * …
        … (CurrentHarmonic ^ 0.5) * NormalisedThickness) + …
        … Sine(2 * (CurrentHarmonic ^ 0.5) * …
        … NormalisedThickness)) / (Cosh(2 * (CurrentHarmonic …
        … ^ 0.5) * NormalisedThickness) - Cosine(2 * …
        … (CurrentHarmonic ^ 0.5) * NormalisedThickness)) + …
        … (2 * ((NumberLayers) ^ 2 - 1) / 3) * …
        … (Sinh((CurrentHarmonic ^ 0.5) * …
        … NormalisedThickness) - Sine((CurrentHarmonic ^ …
        … 0.5) * NormalisedThickness)) / …
        … (Cosh((CurrentHarmonic ^ 0.5) * …
        … NormalisedThickness) + Cosine((CurrentHarmonic ^ …
        … 0.5) * NormalisedThickness)))
    Next (CurrentHarmonic)

    ReffRdelta = (96 / (NormalisedThickness * (PI ^ 4) * …
    … (DutyCycle2 ^ 3))) * FullSummation
End If

Calculate ReffRdc and OptimumThickness in mm:

    ReffRdc = ReffRdelta * NormalisedThickness
    OptimumThickness = NormalisedThickness * SkinDepth2

Display values for SkinDepth2, OptimumThickness, NormalisedThickness,
ReffRdelta, and ReffRdc.

C.8.2   Choose and Draw Waveshape

This procedure will draw a graph for each of the available waveshapes in a boxed area of dimensions BoxWidth and BoxHeight.

The line function is used to draw a line between two points on the box; all coordinates are relative to the top left corner. If only one coordinate is specified, the line is drawn from the coordinate of the end of the previous line to the single new coordinate:

> Set a variable WaveshapeIndex equal to the number corresponding …
> … to the currently selected waveshape, this will be available for use …
> … by other procedures
>
> **If** (the "Calculate Optimum Winding Thickness" step is currently …
> … being displayed) **Then**
>> **Call** (Calculate Proximity Effects, 8.1)
> **End If**
>
> Clear the box if any data has already been plotted in it

Draw an x-axis and a y-axis:

> **Line From** (0, BoxHeight / 2) **To** (BoxWidth, BoxHeight / 2)
> **Line From** (0, 0) **To** (0, BoxHeight)

Divide the width of the box into 160 standard units for most waveshapes:

> UnitWidth = BoxWidth / 160
>
> Set the initial coordinates to 0, BoxHeight / 2, the first line will …
> … therefore begin at this point
>
> **If** (sine wave is chosen) **Then**
>
>> UnitWidth = BoxWidth / 40
>> **For** (i = 0 To 39)
>>> XValue = i * UnitWidth
>>> YValue = BoxHeight / 2 * (1 - Sin((PI / 8) * i))
>>> **Line To** (XValue, YValue)
>> **Next** (i)
>
> **Else If** (rectified sine wave is chosen) **Then**
>
>> **For** (i = 0 To 159)

The period of the sine wave used to plot the rectified function is 60, and after i = 60 we must subtract 60 and after i = 120 we must subtract 120:

>>> **If** (i >= 60) **And** (i < 120) **Then**
>>>> j = i - 60
>>> **Else If** (i >= 120) **Then**
>>>> j = i - 120
>>> **Else**
>>>> j = i
>>> **End If**

For x values during the duty cycle 'on' period, we plot the line segments using the sine function, else we draw our lines along the x-axis:

>>> **If** (i < 60 * DutyCycle2) **Or** ((i > 60) **And** (i < (60 + …

267

```
        … 60 * DutyCycle2))) Or ((i > 120) And (i < (120 + 60 …
        … * DutyCycle2))) Then
                YValue = BoxHeight / 2 * (1 - Sin((PI * j) / (60 …
                … * DutyCycle2)))
        Else
                YValue = BoxHeight / 2
        End If

        XValue = i * UnitWidth
        Line To (XValue, YValue)

    Next (i)

Else If (bipolar sine wave is chosen) Then

    For (i = 0 To 159)

        If (i >= 60) And (i < 120) Then
                j = i - 60
        Else If (i >= 120) Then
                j = i - 120
        Else
                j = i
        End If
```

For x values during the positive and negative duty cycle 'on' periods, we plot the line segments using positive or negative halves of the sine function, else we draw our lines along the x-axis:

```
        If (i < 60 * DutyCycle2) Or ((i > 120) And (i < (120 + …
        … 60 * DutyCycle2))) Then
                YValue = BoxHeight / 2 * (1 - Sin((PI * j) / (60 …
                … * DutyCycle2)))
        Else If (i > 60) And (i < (60 + 60 * DutyCycle2)) Then
                YValue = BoxHeight / 2 * (1 + Sin((PI * j) / (60 …
                … * DutyCycle2)))
        Else
                YValue = BoxHeight / 2
        End If

        XValue = i * UnitWidth
        Line To (XValue, YValue)

    Next (i)

Else If (square wave is chosen) Then

    For (i = 1 To 160)

        If (i < 60 * DutyCycle2) Or ((i > 60) And (i < (60 + …
        … 60 * DutyCycle2))) Or ((i > 120) And (i < (120 + 60 …
        … * DutyCycle2))) Then
                YValue = 0
        Else If ((i > 60 * DutyCycle2) And (i < 60)) Or ((i > …
        … (60 + 60 * DutyCycle2)) And (i < 120)) Or (i > (120 …
        … + 60 * DutyCycle2)) Then
                YValue = BoxHeight - 10
        Else
                If (DutyCycle2 = 0) Then
                        YValue = BoxHeight - 10
                Else If (DutyCycle2 = 1) Then
                        YValue = 0
                Else
```

```
                        YValue = BoxHeight / 2
                    End If
                End If

                XValue = i * UnitWidth
                Line To (XValue, YValue)

        Next (i)

Else If (rectified square wave is chosen) Then

        For (i = 1 To 160)

                If (i < 60 * DutyCycle2) Or ((i > 60) And (i < (60 + …
                … 60 * DutyCycle2))) Or ((i > 120) And (i < (120 + 60 …
                … * DutyCycle2))) Then
                    YValue = 0
                Else
                    If (DutyCycle2 <> 1) Then
                            YValue = BoxHeight / 2
                    Else
                            YValue = 0
                    End If
                End If

                XValue = i * UnitWidth
                Line To (XValue, YValue)

        Next (i)

Else If (bipolar square wave is chosen) Then

        For (i = 1 To 160)

                If (i < 60 * DutyCycle2) Or ((i > 120) And (i < (120 + …
                … 60 * DutyCycle2))) Then
                    YValue = 0
                Else If (i > 60) And (i < (60 + 60 * DutyCycle2)) Then
                    YValue = BoxHeight - 10
                Else
                    If (DutyCycle2 <> 1) Then
                            YValue = BoxHeight / 2
                    Else
                            YValue = 0
                    End If
                End If

                XValue = i * UnitWidth
                Line To (XValue, YValue)

        Next (i)

Else If (triangle wave is chosen) Then

        For (i = 0 To 159)

                If (i <= (60 * DutyCycle2)) Then
                    YValue = BoxHeight / 2 * (1 - i / (60 * …
                    … DutyCycle2))
                Else If (i > (DutyCycle2 * 60)) And (i <= (120 - 60 * …
                … DutyCycle2)) Then
                    YValue = BoxHeight / 2 * (1 - (1 - i / (60)) / (1 …
                    … - DutyCycle2))
```

269

Else If (i > (120 - (60 * DutyCycle2))) **And** (i <= (120 …
… + (60 * DutyCycle2))) **Then**
      YValue = BoxHeight / 2 * (1 - (i - 120) / (60 * …
      … DutyCycle2))
Else If (i > (120 + (60 * DutyCycle2))) **And** (i <= …
… 159) **Then**
      YValue = BoxHeight / 2 * (1 - (i / 60 - 3) / …
      … (DutyCycle2 - 1))
End If

XValue = i * UnitWidth
Line To (XValue, YValue)

    Next (i)

Else If (rectified triangle wave is chosen) **Then**

    For (i = 0 To 159)

        If (i >= 60) **And** (i < 120) **Then**
            j = i - 60
        Else If (i >= 120) **Then**
            j = i - 120
        Else
            j = i
        End If

        If (i <= (60 * DutyCycle2) / 2) **Or** ((i > 60) And (i …
        … <= (60 + (60 * DutyCycle2) / 2))) **Or** ((i > 120) …
        … **And** (i <= (120 + (60 * DutyCycle2) / 2))) **Then**
            YValue = BoxHeight / 2 * (1 - (2 * j) / …
            … (DutyCycle2 * 60))
        Else If ((i > (DutyCycle2 * 60) / 2) **And** (i < (60 * …
        … DutyCycle2))) **Or** ((i > (60 + (60 * DutyCycle2) / …
        … 2)) **And** (i < (60 + 60 * DutyCycle2))) **Or** ((i > (120 …
        … + (60 * DutyCycle2) / 2)) **And** (i < (120 + 60 * …
        … DutyCycle2))) **Then**
            YValue = BoxHeight / 2 * (1 - (2 - (2 * j) / …
            … (DutyCycle2 * 60)))
        Else
            YValue = BoxHeight / 2
        End If

        XValue = i * UnitWidth
        Line To (XValue, YValue)

    Next (i)

Else If (bipolar triangle wave is chosen) **Then**

    For (i = 0 To 159)

        If (i >= 60) **And** (i < 120) **Then**
            j = i - 60
        Else If (i >= 120) **Then**
            j = i - 120
        Else
            j = i
        End If

        If (i <= (60 * DutyCycle2) / 2) **Or** ((i > 120) **And** (i …
        … <= (120 + (60 * DutyCycle2) / 2))) **Then**
            YValue = BoxHeight / 2 * (1 - (2 * j) / …

```
                         … (DutyCycle2 * 60))
             Else If ((i > (DutyCycle2 * 60) / 2) And (i < (60 * …
             … DutyCycle2))) Or ((i > (120 + (60 * DutyCycle2) / …
             … 2)) And (i < (120 + 60 * DutyCycle2))) Then
                    YValue = BoxHeight / 2 * (1 - (2 - (2 * j) / …
                    … (DutyCycle2 * 60)))
             Else If (i > 60) And (i <= (60 + (60 * DutyCycle2) / …
             … 2)) Then
                    YValue = BoxHeight / 2 * (1 - (-2 * j) / …
                    … (DutyCycle2 * 60))
             Else If (i > (60 + (60 * DutyCycle2) / 2)) And (i < (60 …
             … + 60 * DutyCycle2)) Then
                    YValue = BoxHeight / 2 * (1 - (-2 + (2 * j) / …
                    … (DutyCycle2 * 60)))
             Else
                    YValue = BoxHeight / 2
             End If

             XValue = i * UnitWidth
             Line To (XValue, YValue)

         Next (i)

    End If
```

C.8.3   Choose to Use Own Thickness Value

```
    If (we choose not to use own normalised thickness value) Then
         Disable entry of value for normalised thickness and …
         … force calculation of optimum normalised thickness
    Else If (we choose to use own normalised thickness value) Then
         Enable entry of value for normalised thickness
    End If

    Call (Choose and Draw Waveshape, 8.2, with parameter …
    … WaveshapeIndex)
```

C.8.4   Choose Primary or Secondary Winding

By selecting the primary or secondary winding using option buttons we need to redraw our waveshape and also recalculate proximity effects (since there may be differing numbers of layers from primary to secondary); both can be achieved by calling this function:

```
    Call (Choose and Draw Waveshape, 8.2, with parameter …
    … WaveshapeIndex)
```

C.8.5 Rough Duty Cycle Change

This procedure uses a slider to change the duty cycle between 0 and 1 in steps of 0.1, a quick way of seeing the effect on the optimum thickness since it is recalculated after every move of the slider:

> **If** (waveshape is a sine wave) **Then**
>   Exit this subroutine
> **End If**

To avoid any problems with duty cycles of 0 or 1, we add or subtract 1/1000:

> **If** (the user sets the duty cycle to 0) **Then**
>   Set the duty cycle value to 0.001
> **Else If** (they set it to 1) **Then**
>   Set the duty cycle value to 0.999
> **Else**
>   Set the duty cycle to the value selected by the slider control
> **End If**

Redraw the waveshape with the new duty cycle, this will in turn call the function to recalculate proximity effects:

> **Call** (Choose and Draw Waveshape, 8.2, with parameter …
> … WaveshapeIndex)

C.8.6 Exact Duty Cycle Change

> **If** (waveshape is a sine wave) **Then**
>   Do not allow the user to enter a duty cycle value
> **End If**
>
> Ensure that the value entered is a valid number
>
> **If** (the value entered is greater than 0.999) **Then**
>   **Output** ("Duty cycle must be between 0.001 and 0.999.")
>   Set the duty cycle value to 0.999
> **Else If** (the value entered is less than 0.001) **Then**
>   **Output** ("Duty cycle must be between 0.001 and 0.999.")
>   Set the duty cycle value to 0.001
> **End If**
>
> **Call** (Choose and Draw Waveshape, 8.2, with parameter …
> … WaveshapeIndex)

C.8.7 Change Frequency

After entering a new frequency value, we redraw the waveshape which in turn calls the function to recalculate the proximity effects:

> Ensure that the frequency entered is a valid number

272

Call (Choose and Draw Waveshape, 8.2, with parameter …
… WaveshapeIndex)

C.8.8   Change Number of Layers

If the number of layers in the layered winding is changed manually, it is necessary to recalculate proximity effects since the optimum thickness is a function of the number of layers:

Ensure that the number of layers entered is a numeric value

Call (Choose and Draw Waveshape, 8.2, with parameter …
… WaveshapeIndex)

C.8.9   Change Normalised Thickness

If (we are not allowed to enter new normalised thickness values) **Then**
    Ignore any input from the user
Else
    Ensure that the normalised thickness value entered is numeric
End If

Call (Choose and Draw Waveshape, 8.2, with parameter …
… WaveshapeIndex)

C.8.10 Change Rise Time

For square wave variations, the rise time will affect the optimum thickness:

Ensure that the rise time value entered is numeric

Call (Choose and Draw Waveshape, 8.2, with parameter …
… WaveshapeIndex)

C.9   Calculate Leakage Inductance

NUMBER	NAME/DESCRIPTION
9.1	Calculate Leakage Inductance
9.2	Change Bobbin Height

Table C.9. "Calculate Leakage Inductance" subprocesses.

C.9.1 Calculate Leakage Inductance

Calculate WindingHeight, NumberPrimaryLayers, NumberSecondaryLayers, TotalWindingWidth, TotalLeakageInductance:

    WindingHeight = ChosenCoreWindowHeight * …
    … Val(txtBobbinHeight) / 100
    NumberPrimaryLayers = Int((PrimaryWindingTurns / …
    … (Int(WindingHeight / CalculatedPrimaryWindingDiameter))) + 1)
    NumberSecondaryLayers = Int((SecondaryWindingTurns / …
    … (Int(WindingHeight / CalculatedSecondaryWindingDiameter))) + 1)
    TotalWindingWidth = Val(txtPrimaryWindingThickness) * …
    … NumberPrimaryLayers + Val(txtSecondaryWindingThickness) * …
    … NumberSecondaryLayers
    TotalLeakageInductance = (4 * PI * (10 ^ -7) * …
    … (PrimaryWindingTurns ^ 2) * ChosenCoreMLT * (10 ^ -2) * …
    … TotalWindingWidth * (10 ^ -2)) / (3 * WindingHeight * (10 ^ -2))

Display the WindowHeight, WindowWidth, WindingHeight, NumberPrimaryLayers, NumberSecondaryLayers, TotalWindingWidth, and TotalLeakageInductance.

C.9.2 Change Bobbin Height

After making a change to the percentage of the total core window height available for winding on a bobbin, we need to recalculate the leakage inductance:

    Ensure that the bobbin height entered is a numeric value
    Call (Calculate Leakage Inductance, 9.1)

C.10 Custom Addition

NUMBER	NAME/DESCRIPTION
10.1	Choose New Type of Core or Winding
10.2	Make List of Custom Types
10.3	Make List of Shapes for New Type
10.4	Make List of Materials for New Type
10.5	Add a New Type
10.6	Select Custom Type and Change Items
10.7	Change Custom Core Materials
10.8	Change Custom Winding Materials

Table C.10. "Custom Addition" subprocesses.

C.10.1 Choose New Type of Core or Winding

Display the appropriate data entry areas depending on the new type required:

> **If** (a new type of core is desired) **Then**
> > Display grids for custom core data and custom core materials
> > Hide grids for custom winding data and custom winding …
> > … materials
>
> **Else If** (a new type of winding is desired) **Then**
> > Hide grids for custom core data and custom core materials
> > Display grids for custom winding data and custom winding …
> > … materials
>
> **End If**
>
> **Call** (Make List of Custom Types, 10.2)
> **Call** (Make List of Shapes for New Type, 10.3)
> **Call** (Make List of Materials for New Type, 10.4)

C.10.2 Make List of Custom Types

Create a drop down list of available custom types to choose from using the tables in the custom core or winding databases:

> **If** (new type of core is chosen) **Then**
> > Open the custom cores database
> > Clear the list of available custom types (CustomType)
> > **For** (each of the tables in the custom cores database)
> > > **If** (the table is a valid core table, i.e. contains cores …
> > > … of shape "CC", "EE", "EI", "POT", "TOR" or "UU") **Then**
> > > > Add the core group name, shape and material …
> > > > … from the current table to the list of available …
> > > > … custom core types
> > >
> > > **End If**
> >
> > **Next** (custom core table)
>
> **Else If** (new type of winding is chosen) **Then**
> > Open the custom windings database
> > Clear the list of available custom types (CustomType)
> > **For** (each of the tables in the custom windings database)
> > > **If** (the table is a valid winding table, i.e. contains …
> > > … windings of shape "RND" or "LYR") **Then**
> > > > Add the winding group name, shape and material …
> > > > … from the current table to the list of available …
> > > > … custom winding types
> > >
> > > **End If**
> >
> > **Next** (custom winding table)
>
> **End If**

C.10.3 Make List of Shapes for New Type

Update the list of shapes available for a new type of core or winding:

    If (new type of core is chosen) **Then**
        Clear the NewTypeShape list currently displayed (in …
        … case new type of winding was previously chosen)
        Add "CC", "EE", "EI", "POT", "TOR", and "UU" …
        … to the list of available shapes (NewTypeShape)
    Else If (new type of winding is chosen) **Then**
        Clear the NewTypeShape list currently displayed (in …
        … case new type of core was previously chosen)
        Add "RND", "LYR" to the list of available shapes …
        … (NewTypeShape)
    End If

C.10.4 Make List of Materials for New Type

Update the list of materials available for a new type from the corresponding custom databases:

    If (new type of core is chosen) **Then**
        Open the "Material Attributes" table in custom cores database
        Clear the NewTypeMaterial list currently displayed (in case …
        … new type of winding was previously chosen, or new …
        … materials were added)

        Do While (we have not reached the end of the table)
            Add the name of the current material in the table …
            … to the list of available materials (NewTypeMaterial)
            Move to the next entry in the table
        End Do
    Else If (new type of winding is chosen) **Then**
        Open the "Material Attributes" table in the custom windings …
        … database
        Clear the NewTypeMaterial list currently displayed (in case …
        … new type of core was previously chosen, or new materials …
        … were added)

        Do While (we have not reached the end of the table)
            Add the name of the current material in the table …
            … to the list of available materials (NewTypeMaterial)
            Move to the next entry in the table
        End Do
    End If

C.10.5 Add a New Type

    If (no text values are entered for the new type name, shape or …
    … material) **Then**
        Output ("Please fill in the name, shape and material boxes.")

```
                Exit this subroutine
        End If

        If (a new type of core is chosen) Then

                Open the custom cores database
                Create a name (TableName) for a new table by combining the …
                … name, shape and material of the new type in a text string
                For (every existing table in the custom cores database)

                        If (the current table has same name as TableName) Then
                                Output ("Core type of this name already exists.")
                                Exit this subroutine
                        End If

                Next (custom cores table)

                Create a new table with name TableName
                Add these fields to the table: name, $A_c$ (cm$^2$), $W_a$ (cm²), $A_p$ …
                … (cm$^4$), window width (mm), window height (mm), $A_L$ value …
                … (nH), $\mu_e$ value, material, g value (mm), MPL (cm), core …
                … weight (kg), manufacturer, MLT (cm)
                Output ("New core type created.")

        Else If (a new type of winding is chosen) Then

                Open the custom windings database
                Create a name (TableName) for a new table by combining the …
                … name, shape and material of the new type in a text string
                For (every existing table in the custom windings database)

                        If (the current table has same name as TableName) Then
                                Output ("Winding type of this name already …
                                … exists.")
                                Exit this subroutine
                        End If

                Next (custom windings table)

                Create a new table with name TableName
                Add these fields to the table: name, bare diameter (mm), …
                … resistance at 20 °C (mohm/m), weight (g/m), overall …
                … diameter (mm), current at 5A/mm², turns per cm²
                Output ("New winding type created.")

        End If

        Call (Make List of Custom Types, 10.2)
```

C.10.6 Select Custom Type and Change Items

This routine enables the user to alternate between displaying custom core or custom winding data from a particular table:

```
        If (desired new type is core) Then
                Open the custom core details table corresponding to the name …
                … selected from the available custom core types list
        Else If (desired new type is winding) Then
                Open the custom winding details table corresponding to the …
```

… name selected from the available custom winding types list
        End If

The user is also allowed to make changes to the data in the table opened for the current custom type, which are automatically reflected in the database.

C.10.7 Change Custom Core Materials

If we make changes to the custom core material data, we must update the list of available materials:

        Call (Make List of Materials for New Type, 10.4)

C.10.8 Change Custom Winding Materials

If we make changes to the custom winding material data, we must also update the list of available materials:

        Call (Make List of Materials for New Type, 10.4)

C.11   Show Circuit Diagram

NUMBER	NAME/DESCRIPTION
11.1	Show Circuit Diagram

Table C.11. "Show Circuit Diagram" subprocesses.

C.11.1 Show Circuit Diagram

Display the appropriate circuit diagram:

        If (centre-tapped transformer) **Then**
                Hide the push-pull and forward converter diagrams and show …
                … the centre-tapped transformer diagram
        Else If (forward converter) **Then**
                Hide the centre-tapped transformer and push-pull converter …
                … diagrams and show the forward converter diagram
        Else If (push-pull converter) **Then**
                Hide the centre-tapped transformer and forward converter …
                … diagrams and show the push-pull converter diagram
        End If

C.12 Navigation

NUMBER	NAME/DESCRIPTION
12.1	Choose Next Step
12.2	Choose Previous Step
12.3	Choose Specific Step

Table C.12. "Navigation" subprocesses.

C.12.1 Choose Next Step

If (the current folder corresponds to the last step in the sequence, …
… i.e. the step number is equal to the total number of folders) **Then**
    Display the first folder in the sequence
Else
    Move on to the next folder in the sequence
End If

Call (Choose Specific Step, 12.3)

C.12.2 Choose Previous Step

If (the current folder corresponds to the first step in the …
… sequence) **Then**
    Display the last folder in the sequence
Else
    Move on to the previous folder in the sequence
End If

Call (Choose Specific Step, 12.3)

C.12.3 Choose Specific Step

If (the user chooses to display the "Choose Core Data" step) **Then**

    If (StepsTaken < 1) **Then**
        Output ("Please enter specifications before progressing …
        … on to the next step.")
        Go back to the previous step
    Else

Reset the option to use custom turns values in case the user had previously chosen to enter their own turns values and this option was not reset for the current design:

           Call (Use Own Turns Values, 3.2, with parameter false)
           Set the use own turns option button to off
           Call (Choose Core Shape, 2.4, with the "all cores" …
           … option selected as an initial default setting)
       End If

     Else If (the user chooses to display the "Calculate Turns …
… Information" step) **Then**

       If (StepsTaken < 2) **Then**
           Output ("Please choose a core shape and type before …
           … progressing on to the next step.")
           Go back to the previous step
       Else

If the option to use custom turns values is off, then we want to calculate the
turns information as normal:

           If (the use own turns option is off) Then
             Call (Calculate Turns, 3.1)
           End If

       End If

     Else If (the user chooses to display the "Choose Winding Data" …
… step) **Then**

       If (StepsTaken < 3) **Then**
           Output ("Please calculate the number of turns before …
           … progressing on to the next step.")
           Go back to the previous step
       Else
           Call (Choose a Winding Shape, 4.2, with the "all …
           … windings" option selected as an initial setting)
       End If

     Else If (the user chooses to display the "Calculate Winding Losses" …
… step) **Then**

       If (StepsTaken < 4) **Then**
           Output ("Please select a winding type before …
           … progressing on to the next step.")
           Go back to the previous step
       Else
           Call (Choose Winding Loss Type, 5.4, with the "dc …
           … losses" option selected as an initial setting)
       End If

     Else If (the user chooses to display the "Calculate Core Losses" …
… step) **Then**

       If (StepsTaken < 4) **Then**
           Output ("Please select a core and winding before …
           … progressing on to subsequent steps.")
           Go back to the previous step
       Else
           Call (Calculate Core Losses, 6.1)
       End If

     Else If (the user chooses to display the "Calculate Total Losses" …
… step) **Then**

If (StepsTaken < 4) **Then**
    Output ("Please select a core and winding before …
    … progressing on to subsequent steps.")
    Go back to the previous step
Else
    Call (Calculate Total Losses, 7.1)
End If

Else If (the user chooses to display the "Calculate Optimum …
… Winding Thickness" step) **Then**

If (StepsTaken < 4) **Then**
    Output ("Please select a core and winding before …
    … progressing on to subsequent steps.")
    Go back to the previous step
Else
    Clear any previous values displayed for Frequency4, …
    … RiseTime, NumberLayers or DutyCycle2
    Call (Choose and Draw Waveshape, 8.2, with …
    … parameter WaveshapeIndex, initially a sine wave)
End If

Else If (the user chooses to display the "Calculate Leakage …
… Inductance" step) **Then**

If (StepsTaken < 4) **Then**
    Output ("Please select a core and winding before …
    … progressing on to subsequent steps.")
    Go back to the previous step
Else
    Set bobbin height in this step to an initial value of 90%
    Call (Calculate Leakage Inductance, 9.1)
End If

Else If (the user chooses to "Show Circuit Diagram") **Then**

    Call (Show Circuit Diagram, 11.1)

End If

C.13   Variables

C.13.1   Real Numbers

Initial values of variables are shown in brackets where applicable.

a0, a1, a2, alpha, AmbientTemperature (25), AreaProduct1, beta,
BottomSummation, CalculatedPrimaryWindingDiameter,
CalculatedSecondaryWindingDiameter, ChosenCoreAreaProduct,
ChosenCoreCrossSectionalArea, ChosenCoreMLT, ChosenCoreWeight,
ChosenCoreWindowArea, ChosenCoreWindowHeight, ChosenCoreWindowWidth,
ChosenPrimaryWindingDiameter, ChosenPrimaryWindingResistivity,
ChosenSecondaryWindingDiameter, ChosenSecondaryWindingResistivity,
CoreDensity, CoreLosses, CoreVolumeConstant (5.6), CurrentDensity,
CurrentDensityConstant, DutyCycle1, DutyCycle2, Efficiency1, Frequency1,

Frequency4, FullSummation, HeatTransferCoefficient (10), InputVoltageLower, InputVoltageUpper, Kc, MaximumFluxDensity1, NominalDutyCycle, NominalInputVoltage, NormalisedThickness, OptimumConstant, OptimumCurrentDensity, OptimumFluxDensity, OptimumThickness, OutputCurrent, OutputPower, OutputVoltage, PrimaryCurrent, PrimaryPowerFactor, PrimarySkinEffectFactor, PrimaryWindingArea, PrimaryWindingLosses, PrimaryWindingResistance, PrimaryWindingTurns, ReffRdc, ReffRdelta, ResetWindingTurns, RiseTime, RMSInputVoltage, SaturationFluxDensity, SecondaryCurrent, SecondaryPowerFactor, SecondarySkinEffectFactor, SecondaryWindingArea, SecondaryWindingLosses, SecondaryWindingResistance, SecondaryWindingTurns, SkinDepth1, StackingFactor (1), SurfaceAreaConstant (40), TemperatureCorrectedWindingResistivity, TemperatureFactor (5.39E+04), TemperatureRise, TopSummation, TotalCoreLosses1, TotalLeakageInductance, TotalLosses, TotalWindingLosses1, TotalWindingWidth, TurnsRatio1 (1), UnitWidth, VARating, WaveformFactor, WindingHeight, WindingResistivity, WindingVolumeConstant (10), WindowUtilisationFactor (0.4), XValue, YValue

C.13.2 Constants

a = 11.571, b = 6.182, PI = 3.141593

C.13.3 Integers

CurrentHarmonic, i, j, NumberLayers, NumberPrimaryLayers, NumberSecondaryLayers, StepsTaken, TotalNumberHarmonics, WaveshapeIndex

C.13.4 Text Strings

CoreMaterialName, TableName, WindingMaterialName

C.14 Split Data Flows

As mentioned in section 5.4.13, it is sometimes necessary to combine multiple data flows from a lower-level data flow diagram (DFD) into a single flow on a higher-level DFD. A full list of split data flows from DFD numbers 0 to 12 is given in Table C.13, where the left column shows the parent flow and the right shows the corresponding child flows.

PARENT	CHILD
MaCoDe (DFD 0)	**Choose Core Data (DFD 2)**
Core Shape and Type	Core Type
	Core Shape
Core Data	Cores Matching Chosen Type
	Core Types Matching Chosen Shape
Custom Core Data	Custom Cores Matching Chosen Type
	Custom Core Types Matching Chosen Shape
MaCoDe (DFD 0)	**Calculate Turns Information (DFD 3)**
Custom Turns Values	Custom Reset Turns Value
	Custom Primary Turns Value
	Custom Secondary Turns Value
MaCoDe (DFD 0)	**Choose Winding Data (DFD 4)**
Custom Winding Data	Custom Windings Matching Chosen Type
	Custom Winding Types Matching Chosen Shape
Winding Shape and Type	Winding Type
	Winding Shape
Winding Data	Windings Matching Chosen Type
	Winding Types Matching Chosen Shape
Select New Windings	Select New Primary Winding
	Select New Secondary Winding
Chosen Winding Data	Chosen Secondary Winding Data
	Chosen Primary Winding Data
Optimum Thicknesses	Secondary Optimum Thickness
	Primary Optimum Thickness
Which Winding	Get Optimum for Secondary Winding
	Get Optimum for Primary Winding
MaCoDe (DFD 0)	**Calculate Winding Losses (DFD 5)**
Total Winding Losses	Secondary Winding Resistance and Losses
	Primary Winding Resistance and Losses
MaCoDe (DFD 0)	**Calculate Optimum Winding Thickness (DFD 8)**
Waveshape and Winding Parameters	New Duty Cycle
	Desired Waveshape
	Desired Winding
	Use Own Thickness
	New Thickness
	New Rise Time
	New Number of Layers
	New Frequency
MaCoDe (DFD 0)	**Allow Custom Addition (DFD 10)**
New Core Data	Updated Custom Core Material
	New Core Table
	Modified Core Items
New Winding Data	Updated Custom Winding Material
	New Winding Table
	Modified Winding Items
New Core or Winding Materials and Geometries	Material for New Type
	Shape for New Type
	Name for New Type
	Modify Custom Winding Material
	Modify Custom Core Material
	Core or Winding
	Desired Custom Type
	Modify Items of Selected Custom Type
Existing Winding Data	All Custom Winding Types
	Existing Custom Winding Materials
Existing Core Data	All Custom Core Types
	Existing Custom Core Materials

PARENT	CHILD
MaCoDe (DFD 0)	**Navigation (DFD 12)**
Desired Step Number	Go to Specific Step
	Go to Next Step
	Go to Previous Step
Displayed Step	Display Step Specified by Number
	Display Next Step in Sequence
	Display Previous Step in Sequence

Table C.13. Data flows split from DFD 0 to lower level DFDs 1 to 12.

C.15   Database Table Fields

TABLE	FIELD	FORMAT
Cores	Name	Text
	A_c (cm^2)	Number
	W_a (cm^2)	Number
	A_p (cm^4)	Number
	Window Width (mm)	Number
	Window Height (mm)	Number
	A_L Value (nH)	Text
	μ_e Value	Number
	Material	Text
	g Value (mm)	Text
	MPL (cm)	Number
	Core Weight (kg)	Number
	Manufacturer	Text
	MLT (cm)	Number
Core Materials	Name	Text
	Manufacturer	Text
	Saturation Flux Density (T)	Number
	K_c	Number
	α	Number
	β	Number
	Density (kg/m^3)	Number
Windings	Name	Text
	Bare Diameter (mm)	Number
	Resistance @ 20 °C (mΩ/m)	Number
	Weight (g/m)	Number
	Overall Diameter (mm)	Number
	Current @ 5 A/mm^2 (A)	Number
	Turns per cm^2	Number
Winding Materials	Name	Text
	Resistivity (Ω/m)	Number
	α_{20}	Number

Table C.14. Core and winding database table fields.

REFERENCES

[1]   Amar, M., Kaczmarek, R., "A General Formula for Prediction of Iron Losses Under Nonsinusoidal Voltage Waveforms", *IEEE Transactions on Magnetics*, vol. 31, no. 5, pp. 2504-2509, September, 1995.

[2]   Asensi, R., Cobos, J.A., Garcia, O., Prieto, R., Uceda, J., "A Full Procedure to Model High Frequency Transformer Windings", *PESC '94 Proceedings*, vol. 2, pp. 856-863, 1994.

[3]   Balakrishnan, A., Joines, W.T., Wilson, T.G., "Air-Gap Reluctance and Inductance Calculations for Magnetic Circuits Using a Schwarz-Christoffel Transformation", *PESC '95 Proceedings*, vol. 2, pp. 1050-1056, 1995.

[4]   Bartoli, M., Noferi, N., Reatti, A., Kazimierczuk, M.K., "Modelling Litz-Wire Winding Losses in High-Frequency Power Inductors", *PESC '96 Proceedings*, vol. 2, pp. 1690-1696, June, 1996.

[5]   Bennett, E., Larson, S.C., "Effective Resistance to Alternating Currents of Multilayer Windings", *AIEE Transactions*, vol. 59, pp. 1010-1016, 1940.

[6]   Boillot, M.H., Gleason, G.M., Horn, L.W., *Essentials of Flowcharting*, Iowa: WCB, 1975.

[7]   Brown, D.C., *Intelligent Computer Aided Design*, Amsterdam: North-Holland, 1992.

[8]   Carsten, B., "High Frequency Conductor Losses in Switchmode Magnetics", *HFPC Proceedings*, pp. 155-176, May, 1986.

[9]   Cheng, K.W.E., Evans, P.D., "Calculation of Winding Losses in High-Frequency Toroidal Inductors Using Single Strand Conductors", *IEE Proceedings on Electr. Power Appl.*, vol. 141, no. 2, pp. 52-62, March, 1994.

[10]   Cheng, K.W.E., Evans, P.D., "Calculation of Winding Losses in High-Frequency Toroidal Inductors Using Multistrand Conductors", *IEE Proceedings on Electr. Power Appl.*, vol. 142, no. 5, pp. 313-322, 1995.

[11]   Chryssis, G., *High-Frequency Switching Power Supplies: Theory and Design*, 2nd ed., New York: McGraw-Hill, 1989.

[12] Chung, H.Y., Poon, F.N.K., Liu, C.P., Pong, M.H., "Analysis of Buck-Boost Converter Inductor Loss Using a Simple Online B-H Curve Tracer", *APEC '00 Proceedings*, vol. 2, pp. 640-646, 2000.

[13] Codd, E.F., "Relational Completeness of Database Sublanguages", *Database Systems: A Prentice Hall and IBM Research Report*, no. RJ-987, pp. 65-98, Editor: Rustin, R., 1972.

[14] Coonrod, N.R., "Transformer Computer Design Aid for Higher Frequency Switching Power Supplies", *PESC '84 Proceedings*, pp. 257-267, 1984.

[15] Crepaz, S., "Eddy-Current Losses in Rectifier Transformers", *IEEE Transactions on Power Apparatus and Systems*, vol. 89, no. 7, pp. 1651-1656, 1970.

[16] Dai, N., Lee, F.C., "Design of a High Density Low-Profile Transformer", *APEC '96 Proceedings*, vol. 1, pp. 434-440, 1996.

[17] de Beer, A.S., Ferreira, J.A., van Wyk, J.D., "Considerations in the Design of High Frequency, High Power Nonlinear Magnetic Components", *IAS '92 Proceedings*, vol. 1, pp. 1105-1112, 1992.

[18] Dhawan, R.K., Davis, P., Naik, R., "An Experto-Fuzzy Approach to Core Geometry Selection for High Frequency Power Transformers", *HFPC Proceedings*, pp. 132-146, September, 1994.

[19] Dixon, Jr., L.H., "Eddy Current Losses in Transformer Windings and Circuit Wiring", *Unitrode Switching Regulated Power Supply Design Seminar Manual*, vol. M-9, pp. 1-10, New Hampshire: Unitrode, 1988.

[20] Dowell, P.L., "Effects of Eddy Currents in Transformer Windings", *IEE Proceedings*, vol. 113, no. 8, pp. 1387-1394, 1966.

[21] Draper, N.R., Smith, H., *Applied Regression Analysis*, New York: Wiley, 1966.

[22] Edwards, P., Broadwell, B., *Flowcharting and Basic*, Florida: Harcourt Brace Jovanovich, 1974.

[23] Evans, P.D., Chew, W.M., "Reduction of Proximity Losses in Coupled Inductors", *IEE Proceedings, Part B*, vol. 138, no. 2, pp. 51-58, 1991.

[24] Evans, P.D., Heffernan, W.J.B., "Transformer for Multimegahertz Power Applications", *IEE Proceedings on Electr. Power Appl.*, vol. 142, no. 6, pp. 379-389, November, 1995.

[25] Ferch, M.F., "Light Transformers for High Power", *PCIM Magazine*, no. 4, pp. 236-238, 1997.

[26] Ferreira, J.A., *Electromagnetic Modelling of Power Electronic Converters*, Boston: Kluwer, 1989.

[27] Ferreira, J.A., van Wyk, J.D., "Experimental Evaluation of Losses in Magnetic Components for Power Converters", *IEEE Transactions on Industrial Applications*, vol. 27, no. 2, pp. 335-338, March/April, 1991.

[28] Ferreira, J.A., "Analytical Computation of AC Resistance of Round and Rectangular Litz Wire Windings", *IEE Proceedings*, vol. 139, no. 1, pp. 21-25, January, 1992.

[29] Ferreira, J.A., "Improved Analytical Modeling of Conductive Losses in Magnetic Components", *IEEE Transactions on Power Electronics*, vol. 9, no. 1, pp. 127-131, January, 1994.

[30] Flanagan, W.M., *Handbook of Transformer Design and Applications*, 2nd ed., New York: McGraw-Hill, 1993.

[31] Frohleke, N., Becker, B., Wallmeier, P., Grotstollen, H., "Computer Aided Optimization of Multi-Winding Transformers for SMPS Considering HF Effects", *IAS '94 Proceedings*, vol. 2, pp. 1043-1048, 1994.

[32] Gane, C., Sarson, T., *Structured Systems Analysis: Tools and Techniques*, New Jersey: Prentice Hall, 1979.

[33] Garcia, M.A.P., Viejo, C.J.B., Secades, M.R., Gonzalez, J.D., "Design Criteria for Transformers in High Voltage Output, High Frequency Power Converter Applications", *EPE Journal*, vol. 4, no. 4, pp. 37-40, December, 1994.

[34] Goad, S.R., *The Theory and Design of Switched-Mode Power Transformers for Minimum Conductor Loss*, PhD Dissertation: Virginia Tech, 1985.

[35] Goldberg, A.F., Kassakian, J.G., Schlecht, M.F., "Issues Related to 1-10 MHz Transformer Design", *IEEE Transactions on Power Electronics*, vol. 4, no. 1, pp. 113-123, January, 1989.

[36] Gradzki, P.M., Lee, F.C., "Power Test of Ferrite Materials in 1 to 20 MHz Frequency Range", *VPEC Seminar Proceedings*, pp. 175-780, September/October, 1989.

[37]   Gradzki, P.M., Jovanovic, M.M., Lee, F.C., "Computer-Aided Design for High-Frequency Power Transformers", *APEC '90 Proceedings*, pp. 336-343, March, 1990.

[38]   Gradzki, P.M., Lee, F.C., "Domain Wall Resonance and Its Effect on Losses in Ferrites", *PESC '91 Proceedings*, pp. 627-632, 1991.

[39]   Gradzki, P.M., Lee, F.C., "High-Frequency Core Loss Characterization Technique Based on Impedance Measurement", *VPEC Seminar Proceedings*, pp. 1-8, September, 1991.

[40]   Gradzki, P.M., Lee, F.C., "Magnetostriction and Its Effects on Losses in Ferrites", *VPEC Seminar Proceedings*, pp. 9-14, September, 1991.

[41]   Gradzki, P.M., *Core Loss Characterization and Design Optimization of High-Frequency Power Ferrite Devices in Power Electronics Applications*, PhD Dissertation: Virginia Tech, 1992.

[42]   Gu, W.J., Liu, R., "A Study of Volume and Weight Versus Frequency for High-Frequency Transformers", *PESC '93 Proceedings*, pp. 1123-1129, 1993.

[43]   Hanselman, D.C., Peake, W.H., "Eddy-Current Effects in Slot-Bound Conductors", *IEE Proceedings on Electr. Power Appl.*, vol. 142, no. 2, pp. 131-136, 1995.

[44]   Heinemann, L.H., Helfrich, J., "Modeling and Accurate Determination of Winding Losses of High Frequency Transformers in Various Power Electronics Applications", *APEC '00 Proceedings*, vol. 2, pp. 647-653, 2000.

[45]   Hess, J., "Trends of Power Applications: New Ferrite Materials and Optimized Core Shapes", *EEIC/ICWA '93 Proceedings*, pp. 359-367, 1993.

[46]   Hurley, W.G., Wilcox, D.J., McNamara, P.S., "Calculation of Short Circuit Impedance and Leakage Inductance in Transformer Windings", *PESC '91 Proceedings*, pp. 651-658, 1991.

[47]   Hurley, W.G., Wölfle, W., "Optimizing the Design of Transformers at High Frequencies", *UPEC '92 Proceedings*, vol. 1, pp. 282-285, 1992.

[48]   Hurley, W.G., Wilcox, D.J., "Calculation of Leakage Inductance in Transformer Windings", *IEEE Transactions on Power Electronics*, vol. 9, no. 1, pp. 121-126, January, 1994.

[49]   Ingram, G.L., "CAE Aids Optimum Inductor/Transformer Design", *PCIM Magazine*, pp. 26-30, September, 1993.

[50]   Jiles, D.C., Atherton, D.L., "Theory of Ferromagnetic Hysteresis", *Journal of Magnetism and Magnetic Materials*, vol. 61, pp. 48-60, Amsterdam: North-Holland, 1986.

[51]   Jongsma, J., "Minimum Loss Transformer Windings for Ultrasonic Frequencies", *Philips Electronics Applications Bulletin*, no. 35, pp. 146-163 and 211-226, The Netherlands: Philips, 1978.

[52]   Jongsma, J., "High-Frequency Ferrite Power Transformer and Choke Design, Part 3: Transformer Winding Design", *Philips Technical Publications*, no. 207, pp. 63-90, The Netherlands: Philips, 1986.

[53]   Judd, F.F., Kressler, D.R., "Design Optimization of Small Low-Frequency Power Transformers", *IEEE Transactions on Magnetics*, vol. 13, no. 4, pp. 1058-1069, 1977.

[54]   Kassakian, J.G., Schlecht, M.F., "High-Frequency High-Density Converters for Distributed Power Systems", *IEEE Proceedings*, vol. 76, no. 4, pp. 362-376, 1988.

[55]   Katane, T., Nohgi, H., Sakaki, Y., "Optimum Core Dimensions of Transformer for Switching Power Supplies", *PESC '94 Proceedings*, vol. 1, pp. 24-28, 1994.

[56]   Krishnamoorthy, C.S., Rajeev, S., *Computer Aided Design: Software and Analytical Tools*, New Delhi: Narosa Publishing, 1991.

[57]   Kusko, A., Wroblewski, T., *Computer Aided Design of Magnetic Circuits*, Cambridge: MIT Press, 1969.

[58]   Kutkut, N.H., Divan, D.M., "Optimal Air-Gap Design in High-Frequency Foil Windings", *IEEE Transactions on Power Electronics*, vol. 13, no. 5, pp. 942-948, September, 1998.

[59]   Kutkut, N.H., "A Simple Technique to Evaluate Winding Losses Including Two-Dimensional Edge Effects", *IEEE Transactions on Power Electronics*, vol. 13, no. 5, pp. 950-958, September, 1998.

[60]   Lammeraner, J., Safl, M., Toombs, G.A., *Eddy Currents*, Florida: CRC Press, 1966.

[61]   Lavers, J.D., Bolborici, V., "Loss Comparison in the Design of High Frequency Inductors and Transformers", *IEEE Transactions on Magnetics*, vol. 35, no. 5, pp. 3541-3543, September, 1999.

[62] Lewis, T., "The Big Software Chill", *IEEE Computer Magazine*, pp. 12-14, March, 1996.

[63] Linkous, R., Kelley, A.W., Armstrong, K.C., "An Improved Calorimeter for Measuring the Core Loss of Magnetic Materials", *APEC '00 Proceedings*, vol. 2, pp. 633-639, 2000.

[64] Lotfi, A.W., Gradzki, P.M., Lee, F.C., "Proximity Effects in Coils for High Frequency Power Applications", *IEEE Transactions on Magnetics*, vol. 28, no. 5, pp. 2169-2171, September, 1992.

[65] Lotfi, A.W., Chen, Q., Lee, F.C., "Nonlinear Optimisation Tool for the Full-Bridge Zero-Voltage-Switched DC-DC Converter", *IEE Proceedings, Part B*, vol. 140, no. 5, pp. 289-296, September, 1993.

[66] Lotfi, A.W., Lee, F.C., "A High Frequency Model for Litz Wire for Switch-Mode Magnetics", *IAS '93 Proceedings*, vol. 2, pp. 1169-1175, October, 1993.

[67] Lotfi, A.W., Lee, F.C., "Two Dimensional Skin Effect in Power Coils for High Frequency Applications", *IEEE Transactions on Magnetics*, vol. 31, no. 2, pp. 1003-1006, March, 1995.

[68] Lowther, D.A., Silvester, P.P., *Computer Aided Design in Magnetics*, New York: Springer-Verlag, 1986.

[69] Marquadt, D.W., "An Algorithm for Least Squares Estimation of Nonlinear Parameters", *Journal of the Society for Industrial and Applied Mathematics*, vol. 2, pp. 431-441, 1963.

[70] McAdams, W.H., *Heat Transmission*, 3rd ed., New York: McGraw-Hill, 1954.

[71] McLachlan, N.W., *Bessel Functions for Engineers*, 2nd ed., Oxford: Clarendon Press, 1961.

[72] McLyman, W.T., *Transformer and Inductor Design Handbook*, New York: Marcel Dekker, 1978.

[73] McLyman, W.T., *Magnetic Core Selection for Transformers and Inductors*, California: KG Magnetics, 1982.

[74] McLyman, W.T., *Designing Magnetic Components for High Frequency DC-DC Converters*, New York: Marcel Dekker, 1993.

[75] Meares, L.G., Hymowitz, C., "Improved Spice Model Simulates Transformer's Physical Processes", *EDN Magazine*, August, 1993.

[76] Medland, A.J., *The Computer-Based Design Process*, 2nd ed., London: Chapman and Hall, 1992.

[77]   Mitchell, T.M., Mahadevan, S., Steinberg, L.I., "LEAP: A Learning Apprentice System for VLSI Design", *Machine Learning: An Artificial Intelligence Approach*, vol. 3, pp. 271-289, Editors: Kodratoff, Y., Michalski, R.S., San Francisco: Morgan Kaufmann Press, 1990.

[78]   Mulder, S.A., *Application Note on the Design of Low Profile High Frequency Transformers*, The Netherlands: Philips, 1990.

[79]   Mulder, S.A., *Loss Formulas for Power Ferrites and Their Use in Transformer Design*, The Netherlands: Philips, 1994.

[80]   Muldoon, W.J., "Analytical Design Optimization of Electronic Power Transformers", *PESC '78 Proceedings*, pp. 216-225, 1978.

[81]   Ngo, K.D.T., Lai, R.S., "Effect of Height on Power Density in High-Frequency Transformers", *PESC '91 Proceedings*, pp. 667-672, 1991.

[82]   Niemela, V.A., Skutt, G.R., Urling, A.M., Chang, Y., Wilson, T.G., "Calculating the Short-Circuit Impedances of a Multiwinding Transformer from Its Geometry", *PESC '89 Proceedings*, vol. 2, pp. 607-617, 1989.

[83]   Nowacki, H., "Modelling of Design Decisions for CAD", *Computer Aided Design: Modelling, Systems Engineering, CAD Systems*, Editors: Goos, G., Hartmanis, J., New York: Springer-Verlag, 1980.

[84]   Pauly, D.E., "Power Supply Magnetics Part I: Selecting Transformer/Inductor Core Material", *PCIM Magazine*, pp. 23-38, January, 1996.

[85]   Perry, M.P., "Multiple Layer Series Connected Winding Design for Minimum Losses", *IEEE Transactions on Power Apparatus and Systems*, vol. 98, no. 1, pp. 116-123, January, 1979.

[86]   Petkov, R., "Optimum Design of a High-Power High-Frequency Transformer", *IEEE Transactions on Power Electronics*, vol. 11, no. 1, pp. 33-42, 1996.

[87]   Prieto, R., Garcia, O., Asensi, R., Cobos, J.A., Uceda, J., "Optimizing the Performance of Planar Transformers", *APEC '96 Proceedings*, vol. 1, pp. 415-421, 1996.

[88]   Prigozy, S., "PSPICE Computer Modeling of Hysteresis Effects", *IEEE Transactions on Education*, vol. 36, no. 1, pp. 2-5, 1993.

[89]   Ramo, S., Whinnery, J.R., Van Duzer, T., *Fields and Waves in Communications Electronics*, New York: Wiley, 1965.

[90]   Richter, A.N., "Litz Wire Use in High-Frequency Power Conversion Magnetics", *Powertechnics Magazine*, pp. 31-33, April, 1987.

[91]   Robert, F., Mathys, P., Schauwers, J.P., "Ohmic Losses Calculations in SMPS Transformers: Numerical Study of Dowell's Approach Accuracy", *IEEE Transactions on Magnetics*, vol. 34, no. 4, pp. 1255-1257, July, 1998.

[92]   Robert, F., Mathys, P., Schauwers, J.P., "A Closed-Form Formula for 2-D Ohmic Losses Calculation in SMPS Transformer Foils", *IEEE Transactions on Power Electronics*, vol. 16, no. 3, pp. 437-444, May, 2001.

[93]   Robinson, E.A., *Least Squares Regression Analysis in Terms of Linear Algebra*, Houston: Goose Pond Press, 1981.

[94]   Sabin, M.A., *Programming Techniques in Computer Aided Design*, London: NCC Publications, 1974.

[95]   Smit, M.C., Ferreira, J.A., Wyk, V., Ehsani, M., "An Ultrasonic Series Resonant Converter with Integrated L-C-T", *IEEE Transactions on Power Electronics*, vol. 10, no. 1, pp. 25-31, January, 1995.

[96]   Smith, S.I., *Magnetic Components*, New York: Van Nostrand Reinhold, 1985.

[97]   Snelling, E.C., *Soft Ferrites: Properties and Applications*, 2nd ed., London: Butterworths, 1988.

[98]   Spiegel, M.R., *Mathematical Handbook of Formulas and Tables*, New York: McGraw-Hill, 1992.

[99]   Sullivan, C.R., Sanders, S.R., "Design of Microfabricated Transformers and Inductors for High-Frequency Power Conversion", *IEEE Transactions on Power Electronics*, vol. 11, no. 2, pp. 228-238, 1996.

[100] Sullivan, C.R., "Optimal Choice for Number of Strands in a Litz-Wire Transformer Winding", *PESC '97 Proceedings*, pp. 28-35, 1997.

[101] Sullivan, C.R., "Computationally Efficient Winding Loss Calculation with Multiple Windings, Arbitrary Waveforms, and Two-Dimensional or Three-Dimensional Field Geometry", *IEEE Transactions on Power Electronics*, vol. 16, no. 1, pp. 142-150, January, 2001.

[102] Undeland, T.M., Lode, J., Nilssen, R., Robbins, W.P., Mohan, N., "A Single-Pass Design Method For High-Frequency Inductors", *IEEE Industrial Applications Magazine*, pp. 44-51, September/October, 1996.

[103] Urling, A.M., Niemela, V.A., Skutt, G.R., Wilson, T.G., "Characterizing High-Frequency Effects in Transformer Windings - A Guide to Several Significant Articles", *APEC' 89 Proceedings*, pp. 373-385, March, 1989.

[104] Vandelac, J., Ziogas, P.D., "A Novel Approach for Minimizing High-Frequency Transformer Copper Losses", *IEEE Transactions on Power Electronics*, vol. 3, no. 3, pp. 266-276, 1988.

[105] Various, *Pulse Engineering Design Manual for SMPS Power Transformers*, no. 824, San Diego: Pulse, 1982.

[106] Various, *Salford Electrical Instruments Magnetic Components Catalogue*, Oldham: Hirst, Kidd and Rennie, 1986.

[107] Various, *Philips Components Soft Ferrites Catalogue*, vol. MA01, The Netherlands: Philips, 1993.

[108] Various, *Ceramic Magnetics Inc. Engineered Ferrites Catalogue*, New Jersey: CMI, 1994.

[109] Various, *Siemens Matsushita Components Ferrites and Accessories Catalogue*, Germany: Siemens, 1994.

[110] Various, *Linton and Hirst Laminations Catalogue*, Swindon: EJW, 1994.

[111] Various, *Magnetics (Spang and Company) Ferrite Cores Catalogue*, Pennsylvania: Magnetics, 1995.

[112] Venkatraman, P.S., "Winding Eddy Current Losses in Switch Mode Power Transformers Due to Rectangular Currents", *Powercon 11 Proceedings*, vol. A-1, pp. 1-11, 1984.

[113] Wallace, I.T., Kutkut, N.H., Bhattacharya, S., Divan, D.M., Novotny, D.W., "Inductor Design for High-Power Applications with Broad-Spectrum Excitation", *IEEE Transactions on Power Electronics*, vol. 13, no. 1, pp. 202-208, January, 1998.

[114] Waseem, A.R., "Analysis of Planar Sandwich Inductors by Current Images", *IEEE Transactions on Magnetics*, vol. 26, no. 5, pp. 2880-2887, September, 1990.

[115] Whitten, J.L., Bentley, L.D., *Using Excelerator for Systems Analysis and Design*, St. Louis: Times Mirror, 1987.

[116] Wilcox, D.J., Conlon, M., Hurley, W.G., "Calculation of Self and Mutual Impedances for Coils on Ferromagnetic Cores", *IEE Proceedings, Part A*, vol. 135, no. 7, pp. 470-476, September, 1988.

[117] Williams, R., Grant, D.A., Gowar, J., "Multielement Transformers for Switched-Mode Power-Supplies: Toroidal Designs", *IEE Proceedings, Part B*, vol. 140, no. 2, pp. 152-160, 1993.

[118] Wilson, Jr., T.G., Wilson, T.G., Owen, Jr., H.A., "Coupling of Magnetic Design Choices to DC-to-DC Converter Electrical Performance", *IEEE Transactions on Power Electronics*, vol. 13, no. 1, pp. 3-10, January, 1998.

[119] Zhang, J., Skutt, G.R., Lee, F.C., "Some Practical Issues Related to Core Loss Measurement Using Impedance Analyzer", *APEC '95 Proceedings*, pp. 547-554, 1995.

Twinkle, twinkle little star, P equates to I squared R.
Twinkle, twinkle in the sky, P is also E times I.

Twinkle, twinkle can you see, P equals R neath the square of E.
E is the same as I times R, But E over I is also R.

E over R comes up with I, This law is Ohm's, I wonder why?
R is in ohms, E is in volts, I is in amperes like lightning bolts.

So starkle, starkle, little twink, My mind's too muddled now to think.
All these equations may be true, But it's pie in the sky, lest you know what to do.

- Walter Bartelt

PUBLICATIONS

A list of publications on the research work carried out in this thesis follows.

Journal Papers

- W.G. Hurley, E. Gath, J.G. Breslin, "Optimizing the AC Resistance of Multilayer Transformer Windings with Arbitrary Current Waveforms", *IEEE Trans. on Power Electronics*, vol. 15, no. 2, pp. 369-376, March 2000 [IEEE Power Electronics Society 2000 Transactions Prize Paper Award].

- W.G. Hurley, W. Wölfle, J.G. Breslin, "Optimized Transformer Design: Inclusive of High Frequency Effects", *IEEE Trans. on Power Electronics*, vol. 13, no. 4, pp. 651-659, July 1998.

Refereed Conference Proceedings

- J.G. Breslin, W.G. Hurley, "Computer Aided High Frequency Transformer Design Using an Optimized Methodology", *IEEE Computers in Power Electronics Conference*, Virginia Polytechnic Institute, July 2000.

- W.G. Hurley, E. Gath, J.G. Breslin, "Optimizing the AC Resistance of Multilayer Transformer Windings with Arbitrary Current Waveforms", *Proc. of the IEEE Power Electronics Specialists Conference: PESC '99*, Charleston SC, pp. 580-585, June 1999.

- J.G. Breslin, W.G. Hurley, "Derivation of Optimum Winding Thickness for Duty Cycle Modulated Current Waveshapes", *Proc. of the IEEE Power Electronics Specialists Conference: PESC '97*, St. Louis MO, pp. 655-661, June 1997.

- G. Skutt, J.G. Breslin, F.C. Lee, "Measurement Issues in the Characterization of Ferrite Magnetic Material", *Virginia Power Electronics Center Seminar*, Virginia Polytechnic Institute, 1996.

- J.G. Breslin, W.G. Hurley, "A Novel Optimisation Scheme for Designing High Frequency Transformer Windings", *Proc. of the 31st Universities Power Engineering Conference: UPEC 31*, Crete, vol. 1, pp. 465-468, September 1996.

- J.G. Breslin, W.G. Hurley, "Design of Magnetic Components Using a Graphical Interface: Inclusive of High Frequency Effects", *Proc. of the 30th Universities Power Engineering Conference: UPEC 30*, University of Greenwich, vol. 1, pp. 347-350, September 1995.